The University Of Sheffield.

Developing a Mouse Preparation to Study Neurovascular Coupling in Health & Ageing

By:

Kira Shaw

A thesis submitted in partial fulfilment of the requirements for the degree of Doctor of Philosophy

The University of Sheffield
Faculty of Science
School of Psychology

Submission Date: September 2016

Acknowledgements

Thank you to Jason, whose honesty, passion, and never-ending enthusiasm for research was both motivating and inspiring. Your guidance and advice throughout the PhD has been a 10 (10 10). My thanks also to Luke, I wouldn't have been able to get through this PhD without all the things you have taught me. I will be forever grateful for the many hours you have dedicated to helping me with my code, experiments and writing. Sorry for the long chapters though… maybe you taught me too much. I most definitely owe you a Fozzy in Glozzy. Cheers as well to Myles for his insightful comments on the analysis and the chapters, but mostly for bringing the office banter. Your visits, and our (at times slightly inappropriate) lunchtime conversations, provided a welcome distraction on gloomy thesis-heavy afternoons.

To my Sheffield NeuroGirls, Rebecca and Priya, I will miss your unwavering loyalty and support. Despite the many hours spent together in our small office, we could always find something to talk about. Rebecca you've helped me to grow in confidence, and you will always be someone I turn to for advice. Priya you're so kind and warm-hearted, I'm not sure I could have finished this thesis without your company in them long (long, long, long) Pot Noodle-filled hours. I feel so lucky that we were all able to go through the PhD experience together, and I am truly happy that I found two best friends for life.

Thanks to my other office buddy Tim… I know you think that we always forget you, but I'll never forget your homemade sausage rolls. I would like to thank Paul for training me on the surgical skills. I was lucky to learn from the mouse master. I'm also grateful to Sam, you were always available to give me advice on my code or thesis, or just to reminisce about all things Singapore with. Cheers as well to Clare, you helped brighten up those many hours spent in a dark lab. Your drive and your success are truly inspiring. Thank you to Mike too, those early days of the PhD spent teasing you really helped me to settle in, and you were always on side to give some friendly advice. My thanks also to Aneurin, as the NeuroGirls and Magnetic Dr K we pioneered a great public engagement team. I would also like to extend my thanks to the rest of the Alfred Denny team – for there was always a friendly face on hand to offer advice (or snacks) in the meeting room. Thanks also to Michael Port, and the technical support staff.

My time in Sheffield and Singapore wouldn't have been complete without the friends that I've made along the way. My Sheffield buddies: Chip and Nat – you've been like sisters to me. Your good cop/bad cop advice has helped me to deal with any situation life has to throw at me (can you guess who is who?). Leon, you're always good for a rant or two on the way home, you've been a great housemate and gym buddy (*Leon's Fitness Boutique*©) over the years. Chloe & Will, you're a constant support, thanks so much for being there through the trash (West St Live) and the class (BBC Proms). My Singapore crew: Jess, Tom, Jon, Al, Josie, etc., you were my family in Asia, and I'll forever miss those times we spent in the sun, on the beach, and of course in the Prince of Wales and Attica!

Thanks finally to my family: to my parents and my sister Lian, who have provided unrelenting support throughout my many years in education. What student doesn't need to get away and visit home with their dirty laundry bundled into a suitcase from time-to-time? It is your relentless and unwavering pride in me, which has truly helped me to believe in myself. Finally, I'd like to thank Mark. You have always supported my goals, relocating to Singapore with me, and spending many hours quietly playing Football Manager whilst I worked on my thesis. Thanks for being my rock, but mostly for buying me cheese in times of need.

Acronyms

2D-OIS	Two-Dimensional Optical Imaging Spectroscopy
20-HETE	20-Hydroxyeicosatetraenoic Acid
AA	Arachidonic Acid
ATP	Adenosine Triphosphate
BOLD	Blood Oxygen Level Dependent
CBF	Cerebral Blood Flow
CBV	Cerebral Blood Volume
cGMP	Cyclic Guanosine Monophosphate
Ca^{2+}	Calcium
ChR2	Channel Rhodopsin-2
CO_2	Carbon Dioxide
COX-2	Cyclooxygenase-2
EETs	Epoxyeicosatrienoic Acid
fMRI	Functional Magnetic Resonance Imaging
GABA	Gamma-Amino Butyric Acid
HbO_2	Oxygenated Haemoglobin
Hbr	Deoxygenated Haemoglobin
Hbt	Total Haemoglobin
IGF-1	Insulin-Like Growth Factor-1
K^+	Potassium
LDF	Laser Doppler Flowmetry
LFP	Local Field Potential

M	Mean
mGLuR	Metabotropic Glutamate Receptor
MUA	Multi-Unit Activity
NADPH	Nicotinamide Adenine Dinucleotide Phosphate
NMDAR	N-Methyl-D-Aspartate Receptor
nNOS	Nitric Oxide Synthase
NO	Nitric Oxide
NVC	Neurovascular Coupling
O_2	Oxygen
PGE2	Prostaglandin E2
PLA_2	Phospholipases A2
ROS	Reactive Oxygen Species
S1	Somatosensory Cortex
SEM	Standard Error Mean
SD	Standard Deviation
SST	Somatostatin Interneurons
V1	Visual Cortex
VIP	Vasoactive Intestinal Peptide-Expressing Interneurons

Contents

Abstract

The aim of this research was to develop a mouse preparation suitable for studying neurovascular coupling in health, development and ageing. Neurovascular coupling is the process linking increases in neuronal activity with corresponding increases in local cerebral blood flow. Exactly how these processes are linked is still a matter of debate, although a range of cellular mechanisms, including astrocytes, pericytes, and interneurons, have been proposed to play a role. The study of neurovascular coupling is of prime importance, as haemodynamic changes are used in blood oxygen level dependent (BOLD) functional magnetic resonance imaging (fMRI), to make inferences about underlying neuronal responses. Further, it is thought that neurovascular coupling may be impaired in ageing, or in certain neurodegenerative diseases, e.g. Alzheimer's disease. Recent work has applied high spatiotemporal resolution, invasive techniques (e.g. two-dimensional optical imaging spectroscopy, and a multichannel electrode) to study neurovascular coupling in *in vivo* rodent preparations. Whilst the use of a rodent preparation allows for the detailed investigation of neurovascular responses, there are confounds associated with the effects of anaesthesia or behavioural state (i.e. active or passive) on cerebral physiology.

Here, neurovascular coupling was investigated in an *in vivo* mouse model using an awake, head-fixed preparation or an anaesthetised preparation, in health, development and ageing. The major findings indicated that: (1) haemodynamic responses could be measured in an awake, head-fixed mouse chronically for up to 3 months; (2) locomotion profoundly altered the haemodynamic responses recorded from awake subjects; (3) a balanced, modular anaesthesia regime could be administered which resulted in comparable haemodynamic responses between awake and anaesthetised subjects; and (4) neurovascular coupling was altered in development and old age. These findings provide important insights on how behaviour, anaesthesia and ageing may affect neurovascular responses in the widely-researched mouse model.

Chapter 1

Introduction

1.1 Abstract

Neurovascular coupling is the process by which neural activity evokes localised increases in cerebral blood flow (CBF). Whilst it is known that alterations in neural activity and metabolism are correlated with CBF changes, the exact mechanisms which bind these processes are currently still being debated. In fact blood oxygen level dependent (BOLD) functional magnetic resonance imaging (fMRI), widely applied in clinical studies, measures these CBF changes and makes inferences about underlying neuronal changes. As such, understanding the processes which link the neural and haemodynamic activity is of upmost importance. Numerous high spatiotemporal resolution methods have been applied to study the cerebral neural and haemodynamic responses directly, e.g. two-dimensional optical imaging spectroscopy (2D-OIS) and the insertion of a multichannel electrode. Due to the invasive nature of these methods, typically anaesthetised animal preparations are used. The rodent whisker barrel provides a suitable model to study neurovascular coupling as each individual whisker is topographically represented in the contralateral somatosensory cortex. Much of the previous work has employed anaesthesia to study neurovascular coupling in the rodent whisker barrel, but anaesthesia may alter neuronal and haemodynamic responses both temporally and spatially. In a move to overcome the confounds of anaesthesia, recent studies have favoured imaging an awake, head-fixed mouse. Whilst the awake preparation is not confounded by the effects of anaesthesia on the brain's physiology, there may be additional effects of behavioural state to consider. Studies of neurovascular coupling are further confounded when considering the developing or ageing brain. During both development and ageing there are changes to the components of the neurovascular unit, which may alter neurovascular responses and influence the interpretation of BOLD fMRI studies conducted in these populations. Clearly, more research is needed to investigate neurovascular coupling mechanisms in health, age and disease. This thesis aims to establish methods for imaging neurovascular coupling in high spatiotemporal detail in the mouse model.

1.2 Neurovascular Coupling

1.2.1 Brief history and Theory behind Neurovascular Coupling

The active brain is reliant on a constant source of oxygen and glucose which is supplied via cerebral blood flow (CBF). As cerebral energy demands are high, any increases in local neuronal activity have an associated rise in metabolic demand which alters the rate of oxygen consumption ($CMRO_2$), these changes in brain state are also matched with localised increases in haemodynamic signals (blood oxygen level dependent (BOLD) response, CBF or cerebral blood volume (CBV)). The increased influx of fresh blood has a high concentration of oxygenated haemoglobin (HbO_2), therefore marginally increasing the local oxygen supply to meet the increased demand. Neurovascular coupling (NVC) refers to such tight links between the changes in neural activity and the subsequent alterations to the magnitude and spatial spread of the blood flow. The existence of neurovascular coupling has been long-speculated since a study by Roy & Sherrington (1890) in which it was suggested that the

"*brain possesses an intrinsic mechanism by which its vascular supply can be varied locally in correspondence with local variations of functional activity*".

Many clinical brain imaging tools, such as functional magnetic resonance imaging (fMRI), use direct measures of the vascular changes to infer any underlying changes in neural activity and function. The wide-spread use of such brain imaging techniques emphasizes the importance of investigating the mechanisms which connect the cerebral neuronal and vascular changes.

Cellular, metabolic and vascular processes underlie brain activation (*Figure 1.1 B*), the fine details of which are currently still under investigation. The neurovascular unit is the term for the functional components of NVC which work together during brain activation: the neurons, blood vessels, pericytes, astrocytes and microglia (*Figure 1.1 A*). The numerous cellular processes of the neurons require an energy supply from adenosine triphosphate (ATP). ATP is anaerobically synthesized by glycolysis (which produces a small amount of ATP), and aerobically synthesized by oxidative glucose metabolism (which uses oxygen (O_2) to produce a large amount of ATP). In the brain most of the glucose is metabolised aerobically, meaning cerebral metabolism is dependent on a constant and reliable source of

both oxygen and glucose. This continuous supply of oxygen and glucose is maintained by the CBF, which delivers the energy substrates needed to the neural tissue using the vast supply of cerebral blood vessels. Waste products, like carbon dioxide (CO_2) and excessive heat, are then removed from the brain using this same intricate vascular system.

The exact mechanisms which bind neural, metabolic, and haemodynamic responses have still not been agreed upon. It was originally suggested that the energy demand directly controls the dilation or constriction of the vascular smooth muscle cells by feedback mechanisms dependent on variations in the concentrations of metabolic by-products, such as potassium (K+), nitric oxide (NO), adenosine, CO_2, and arachidonic acid metabolites (Roy & Sherrington, 1890). However, whilst intuitively appealing, a direct link between energy state and blood flow is not accepted. As this idea seems overly simplistic, a number of alternative explanations have since been offered. One possibility is that feedforward mechanisms occur in which astrocytes link neurotransmitter activity to the vasculature (Attwell & Iadecola, 2002; Lauritzen, 2005). Alternatively, there is also evidence that the vascular endothelium cells can capitalise on the same pathways as the astrocytes to alter vascular smooth muscle tone (Chen et al., 2014), or perhaps that neurons may directly innervate the smooth muscle cells to control blood flow (Hamel, 2004; Iadecola, 2004). In all likelihood NVC is controlled by multiple mechanisms, both feedforward and feedback, and elucidating and understanding these differing control mechanisms will be important in the study of both the healthy and the diseased brain. In order to comprehend these NVC control mechanisms, first one must have a good understanding of the basic components which make up the neurovascular unit (Cauli & Hamel, 2010).

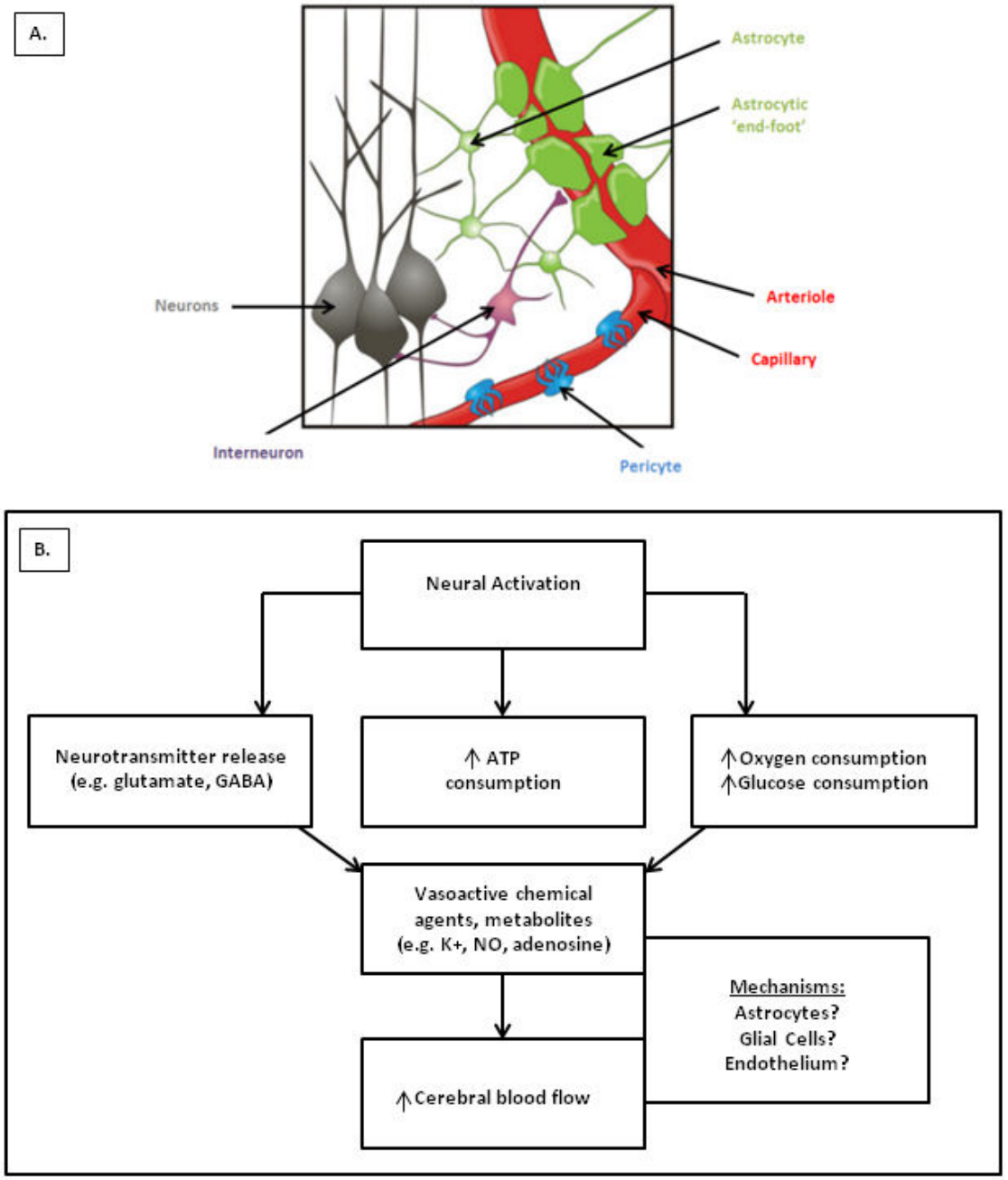

Figure 1.1 – Components of the Neurovascular Unit and Possible Mechanisms of Neurovascular Coupling

A. *The elements of the neurovascular unit (as adapted from: Gordon, Mulligan & MacVicar, 2007).* ***B.*** *The basic sequence of cellular, metabolic and vascular processes which comprise brain activation, and the possible mechanisms which link neuronal and haemodynamic activity.*

1.2.2 The Role of Neurons in Neurovascular Coupling

The driving force of neurovascular coupling is the cerebral neuronal system, whose activity requires the delivery of energy substrates. The central nervous system (CNS) is comprised of nerve tissues which control all activities of the body, and in vertebrates includes the brain and the spinal cord. The basic unit of the CNS is the neuron, which is an electrically excitable cell that processes and transmits information via electrical and chemical signals. There are different types of neurons across the cortex, but the pyramidal neuron is the most numerous excitatory cell, and thus serves as representative of the archetypal neuronal shape. The neuron is typically made up of the cell body (soma), and the dendrites and an axon (which extend from the soma). The soma and dendrites receive synaptic signals from other neurons, whereas the axon transmits synaptic signals to other neurons. The axon is usually ensheathed by myelin which is an electrically insulating substance essential for proper functioning. The signals between neurons occur via synapses, which are specialised connections with the other cells. This synaptic signalling process is the key to neuronal functioning, and is both an electrical and chemical process. As the neuron is electrically excitable, metabolically-driven ion pumps maintain voltage gradients, by permitting electrically charged ions or chemicals to flow across the membrane. If the net excitation received surpasses a certain threshold then the neuron generates a brief pulse named an action potential, which is a propagating electrical signal that fundamentally triggers the chemical release of neurotransmitters across a synapse to be received by the target neuron or cell via specialised receptors. Interneurons are one of the three classifications of neurons, and they're special because they create neural circuits which enable communication between sensory or motor neurons and the CNS. They typically function in reflexes or neuronal oscillations and can be local (i.e. form with nearby neurons to analyse small pieces of information) or relay (i.e. connecting one region of the brain with other regions). Interneurons allow the brain to perform complex functions such as learning and decision making.

Much effort has been invested into understanding the temporal dynamics of the nerve cells in fine detail. Activated neurons can either act directly on the receptors of local vasculature, or indirectly via astrocytes, which act as intermediaries (Cauli & Hamel, 2010). Direct vasoactive mediators released from neurons correspond respectively to COX-2 derivatives, whereas astrocytes are thought to act mainly by releasing dilatory epoxyeicosatrienoic

acids (EETs), which is a comparatively slower process than the release of PGE2 and NO (or other neutrally released vasoactive molecules) (Figure 1.2).

It is known that an increase in intracellular calcium (Ca^{2+}) is an initial requirement for the production and release of vasoactive messengers from the neurons (Lauritzen, 2005). Rapid Ca^{2+} release is attributed to a fast (10-12 milliseconds) spiking response of the neurons, and to activation of Ca^{2+} permeable ionotropic receptors (Peterson et al., 2003); whereas slower neural dynamics are thought to rely on metabotropic receptors, which cause the release of Ca^{2+} from intracellular stores (Perea & Araque, 2005). Takano and colleagues (2006) showed *in vivo* that arterioles started to dilate ~500 milliseconds after the onset of the Ca^{2+} increases, meaning the effects of the vasodilatory messengers must be achieved by this time. Haemodynamic responses are known to initiate ~600 milliseconds after the onset of sensory stimulations (Kleinfeld et al., 1998; Devor et al., 2003), and so the early phase of the haemodynamic response must be accounted for by cell types which express fast evoked Ca^{2+} events. Consistent with the idea that neuron-derived messengers are involved in the early phase of NVC, the blockade of NO synthesis (which links neurons with blood vessels) almost fully wiped out the haemodynamic responses produced by a brief sensory stimulation (Kitaura et al., 2007). On the other hand, the blockade of EET receptors (which link astrocytes and blood vessels) stopped about 50% of the blood flow response to a long-lasting stimulation (Liu et al., 2008).

1.2.3 Astrocytic Signalling – The Bridge between the Neurons and the Blood Vessels

The glial cells are non-neuronal cells which are important for healthy brain function and work closely with nerve cells by providing support and protection for the neurons, maintaining homeostasis, supplying nutrients and oxygen, and forming the myelin. The most widely studied glial cells in the area of neurovascular functioning are the astrocytes. Astrocytes physically connect the nerve cells to blood vessels as their “vascular endfeet” make contact with the capillary walls, making them an essential component in the understanding of NVC. Astrocytes have been implicated in many processes including: structural support; nervous system repair; the regulation of electrical impulses within the brain; the storage of glycogen to refuel neurons during periods of intense activity; metabolic support via the provision of nutrients to neurons; neurotransmitter uptake and release; the regulation of ion concentration in extracellular space (astrocytes express

potassium channels meaning they're permeable to potassium and clear excess accumulation); modulation of synaptic transmission (astrocytes can release ATP to suppress it); and astrocytes may serve as intermediaries in the neuronal regulation of blood flow (Cauli & Hamel, 2010; Howarth et al., 2014; Volterra & Meldolesi, 2005).

As the neurons are enwrapped by glial cells, and are connected to the cerebral blood vessels via glial cells, much effort has been invested into the understanding of the role of the astrocytes in NVC, leading to the concept of the neuronal-astrocytic-vascular tripartite functional unit (Vaucher & Hamel, 1995). Anatomically astrocytes are ideally suited as a bidirectional mediator between neurons and blood vessels; a single astrocyte contacts thousands of synapses, and has specialised astrocytic "endfeet" which cover about 99% of the surface of cerebral vessels. Structurally, astrocytes form non-overlapping domains, meaning a single astrocyte may be capable of executing multiple NVC functions; and they are coupled to gap junctions, ideally located to establish an electrical syncytium allowing for localised signals to be amplified across neural networks. Such unique astrocytic properties, so firmly integrated into the neurovascular coupling unit, led to speculation over the existence of specialised astrocytic subpopulations (e.g. astrocytes for detecting signals around the synapse/blood vessels, vs. astrocytes that spread information across the neural networks) (Filosa et al., 2016).

Some research suggests that astrocytes are involved in the regulation of cerebrovascular tone (Attwell et al., 2010; Carmignoto & Gomez-Gonzalo, 2010). Seminal work from Carmignoto's group demonstrated that neuronal stimulation can trigger a mGluR-dependent parenchymal arteriole vasodilator response which is preceded by astrocytic Ca^{2+} activation (Zonta et al., 2003). The mechanism proposed by the authors was changes in intracellular Ca^{2+} in astrocytes, which produce a vasodilatory signal via prostaglandin E_2 (PGE_2). Additionally, astrocytic Ca^{2+} increases are thought to contribute to the generation of other vasoactive signals such as NO, EETs, glutamate, adenosine and ATP (Carmignoto & Gomez-Gonzalo, 2010), all of which have the ability to modulate parenchymal arteriole vascular tone. K^+ signalling from astrocytes is another key mechanism contributing to NVC (Filosa et al., 2006). K^+ released during neuronal activation is taken up by astrocyte processes at the synapse and released at endfeet processes surrounding blood vessels, acting as a powerful vasodilatory signal of pial and parenchymal arterioles (Figure 1.2).

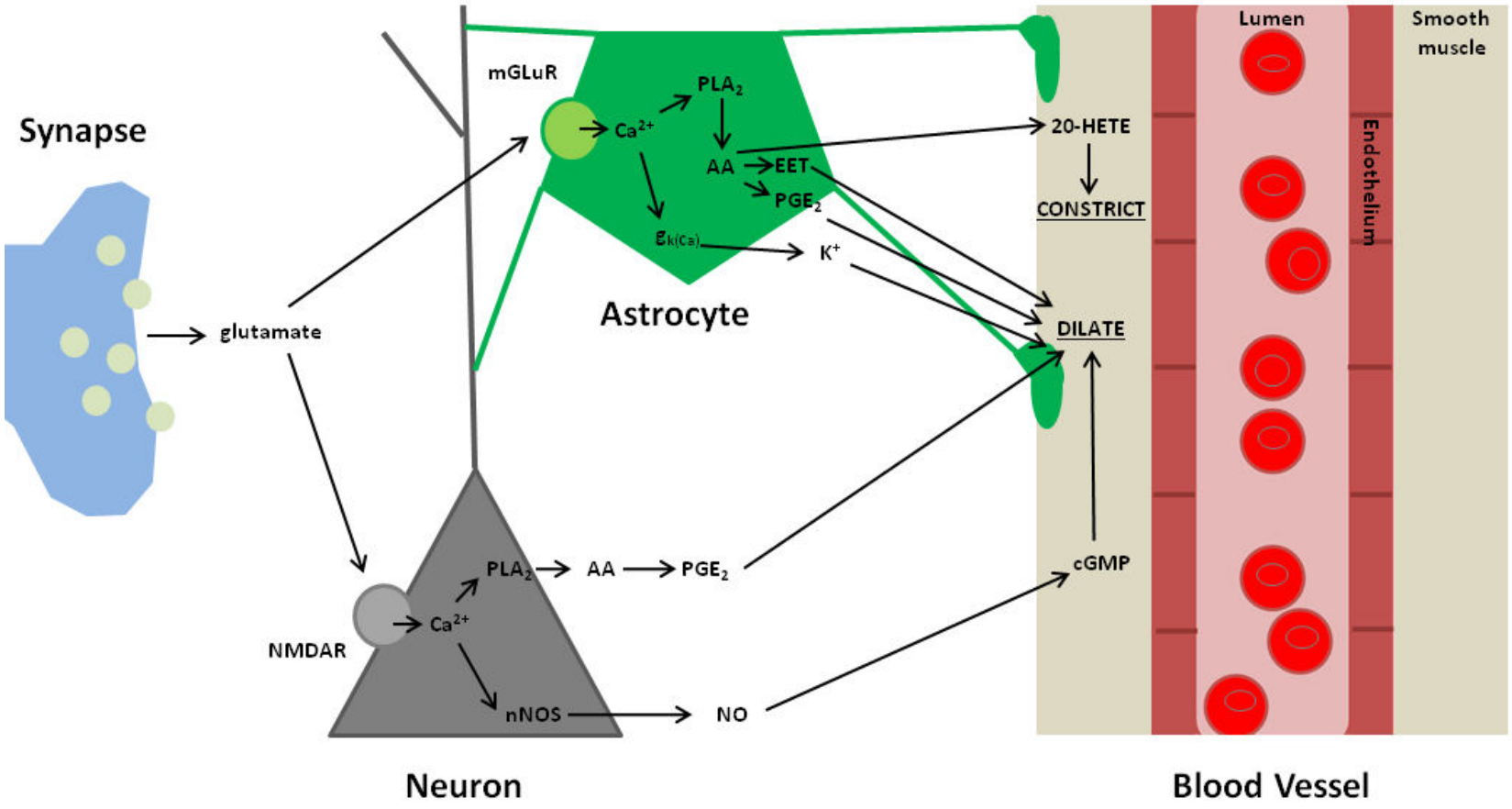

Figure 1.2 – Pathways from Astrocytes and Neurons to Blood Vessels

A simplified diagram showing the potential pathways from astrocytes and neurons, which regulate CBF by sending vasoactive messengers to influence the vasculature.

1.2.4 The role of the Blood Vessels in Neurovascular Coupling

Haemodynamic changes predominantly occur by the control of the vasculature at the arteriolar level (Hillman et al., 2007); from the pial surface, to the precapillary level, where vascular pericytes are located (Hall et al., 2014; Jones, 1970). As discussed, the neuronal control of the vascular energy supply is largely moderated by feedforward mechanisms in which the neurons signal directly to the blood vessels by changing the tone of the smooth muscle (which forms a continuous layer around the arterioles), or activate astrocytes to release vasoactive agents that act on the smooth muscle surrounding the vessels (Figure 1.2).

It has recently been shown than vessel dilation/constriction is not only modulated by changes in the tone of the smooth muscle surrounding arterioles, but also that pericytes may play a role (e.g. Hall et al., 2014). Pericytes are cells which are present at ~50μm intervals along capillaries (Figure 1.1 A), and which can alter capillary diameter (meaning they may regulate blood flow changes at the capillary level). They have been shown to constrict or dilate in response to neurotransmitters resulting from CA^{2+} alterations (Puro, 2007). Signals for contraction (depolarisation) and potentially for constriction (hyperpolarisation) can propagate from one pericyte to another, spreading through gap junctions between pericytes, or through gap junctions with endothelial cells (Puro, 2007). On average active neurons are located closer to pericytes than arterioles (Lovick et al., 1999), and this even raises the possibility that vascular responses to changes in neuronal activity may be initiated by pericytes before they're even propagated to upstream arterioles.

Recent evidence has also indicated that the vascular endothelium may be involved in NVC, as selective alterations to endothelial signalling blocked the stimulus-evoked dilation of pial arteries in the somatosensory cortex (Chen et al., 2014). The possible involvement of the endothelium means that the initiators and mediators of NVC could be located at the capillary bed level, not necessarily requiring contact with the surface of arteriole smooth muscle cells (Collins et al., 1998).

The fractional increase in cerebral blood flow in response to sustained neural activity is at least 4-fold greater than the increase in ATP consumed by the neurons (Lin et al., 2010).

This demonstrates that blood flow is mainly regulated by feedforward neurotransmitter-mediated mechanisms over a negative-feedback loop driven by energy-demand, as a negative-feedback system couldn't produce a sustained increase in energy supply larger than the increase in energy consumption. This disproportionate increase in blood flow forms the basis of blood-oxygen level dependent (BOLD) functional imaging. It is unclear why there is such a large increase in blood flow, but there are speculations that this large increase occurs as a by-product of a system which attempts to maintain blood flow and prevent cell death under pathological conditions in which energy use is raised (Attwell et al., 2010).

Given the complex nature of neurovascular coupling, a multitude of techniques have been applied to its investigation. Recent work has favoured the use of methods with high spatiotemporal resolution in order to gain a detailed understanding of the mechanisms contributing to NVC.

1.3 Experimental Techniques to Study Neurovascular Coupling

The following section introduces the techniques used for the experiments conducted within this thesis (i.e. two-dimensional optical imaging (2D-OIS), and the insertion of a multi-channel electrode). The techniques described and employed are invasive, necessitating the use of an animal model. The rodent somatosensory barrel cortex was chosen, and the details of the history of this animal model and its merits will be examined in section 1.4.

1.3.1 Electrophysiological Recordings

The placement of a multichannel electrode into the region of interest (e.g. rodent somatosensory cortex) provides a direct method of measuring neural activity (Figure 1.3 A). This electrophysiology technique allows researchers to study the live dynamics of neural networks across various spatial and temporal scales. The local field potential (LFP) and multi-unit activity (MUA) are the extracellularly recorded signals which describe local neuronal network dynamics. MUA and LFP measurements result from the dynamic interaction of the various synaptic and cellular mechanisms: the LFP represents the low frequency (<500Hz) content of the raw recording, and is thought to arise from membrane currents of the neurons near to (few mm) the recording electrode; the MUA represents the

high frequency (>1000Hz) part of the recording, and is thought to represent the spiking of local neurons (output of a neural population). For the purposes of this thesis, local field potentials (LFPs) were considered, as previous research indicates that LFPs correlate most closely with BOLD fMRI responses (Logothetis et al., 2001; Goense & Logothetis, 2008). The typical LFP response is characterised by large depolarisations to each stimulation, which gradually decrease in size (Figure 1.3 B). Logothetis et al. (2001) demonstrated that there was an increase in LFPs during stimulation which was significantly stronger than the stimulation-induced increases in MUA. MUA was shown to adapt to the stimulation, returning to baseline levels, whereas LFP activity remained elevated throughout the stimulus presentation. These findings imply that the haemodynamic response seems to be better correlated with the LFPs, indicating that activation in a cortical area is more likely to reflect the incoming input and the local processing, rather than the overall spiking activity. Note that these findings are still controversial however, as these conclusions are at odds with more recent work by Burns et al., (2010) who assessed LFP and MUA activity in response to fine (< 0.1s) and coarse (1-5s) stimulations. In this experiment both the MUA and LFP produced sustained responses to visual stimulations, this different finding was attributed to differences in the data analysis method and experimental set-up used. More detail of the theory and application of electrophysiological approaches is given in section 2.5.2.

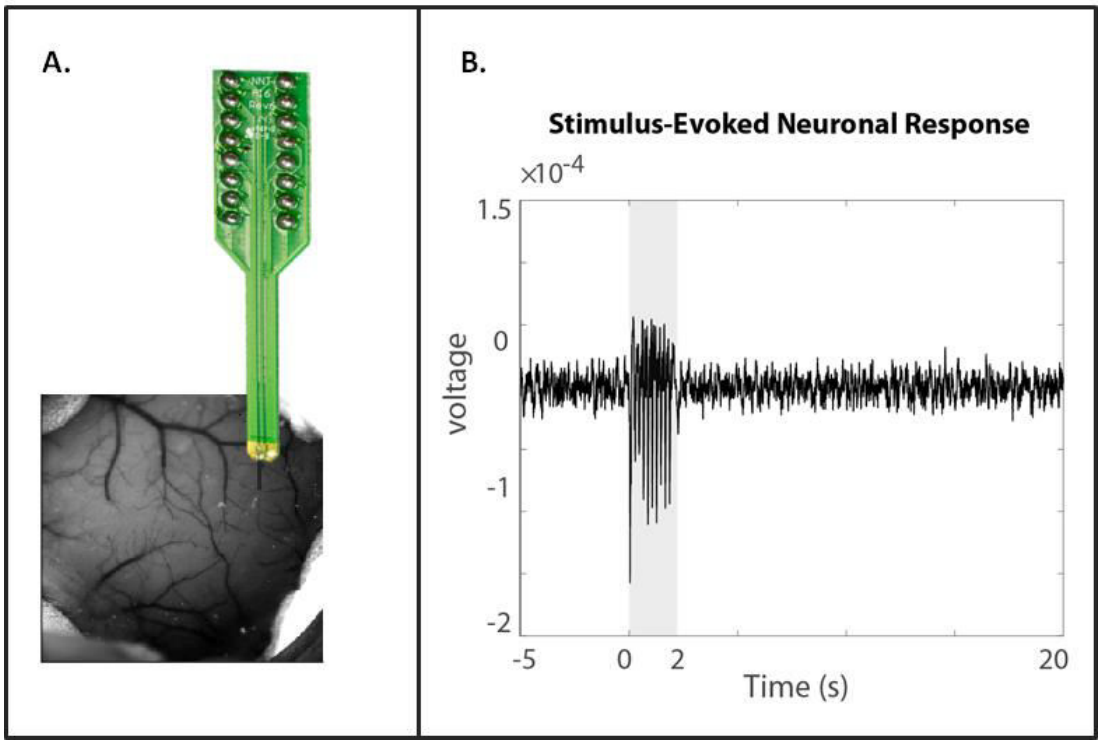

Figure 1.3 – Multichannel Electrode Experimental Set-Up

A. *A 16-channel electrode is inserted perpendicularly into the cortex to record neuronal activity.* ***B.*** *The typical local field potential changes observed within the cortex when a stimulus is presented. Stimulation causes an individual depolarisation to each stimulus (i.e. 2s whisker stimulation at 5Hz is 10 stimulus hits), with a profile of gradually decreasing responses to successive stimuli.*

1.3.2 Two-dimensional Optical Imaging Spectroscopy (2D-OIS)

Optical imaging is used to image intrinsic signals based on the optical properties (scattering/reflectance) of brain tissue. These are dependent on the localised blood volume and oxygen saturation, as HbO_2 and Hbr have different absorption and scattering properties for light in the visible wavelength band (see Figure 2.4). The 2D-OIS system developed within the Sheffield laboratory (Figure 1.4 A) uses four wavelengths sequentially applied to the brain surface. The wavelengths were chosen in two pairs, with a similar total absorption coefficient for each pair to sample the same tissue volume. The absorption coefficients for HbO_2 and Hbr were selected to be as different as possible to improve the signal to noise ratio (Figure 2.4). The remitted light was recorded by a camera synchronised to the application of each wavelength. Analysis of the recorded images involved multiple assumptions (i.e. about baseline saturation, and haemoglobin concentration), and the use

of models of photon path length produced using Monte Carlo simulations (see Kennerley et al., 2009). A description of the 2D-OIS method is given in more detail in section 2.5.1. Analysis of 2D-OIS recordings gives two-dimensional estimates of Hbt, HbO_2, and Hbr (Figure 1.4 B); whose responses can be visualised both temporally (i.e. time series) or spatially (i.e. spatial maps).

2D-OIS has previously been used in the Sheffield laboratory to explore the stimulus-evoked haemodynamic responses in the well-defined whisker barrel somatosensory cortex of the rodent (e.g. Berwick et al., 2005a; 2008; Boorman et al., 2010; 2015; Jones et al., 2004; Martin et al., 2002, 2006, 2013a, 2013b; Sharp, Shaw et al., 2015). In these studies the typical haemodynamic response to stimulation consists of a rapid increase in Hbt and HbO_2, with a concomitant decrease in Hbr in the corresponding contralateral whisker barrel region. This response corresponds with an overall increase in local CBF, and thus an increase in oxygenated blood in the region. Specifically, some studies have reported rapid dilation of the parenchyma, followed by the dilation of the pial arterioles, which then feed the deeper capillary beds of the cortex (Bouchard et al., 2009; Chen et al., 2011; Hillman et al., 2007). 2D-OIS is used in chapters 3, 4, 5 & 6, to locate the active whisker region and to investigate haemodynamic responses in the exposed somatosensory cortex.

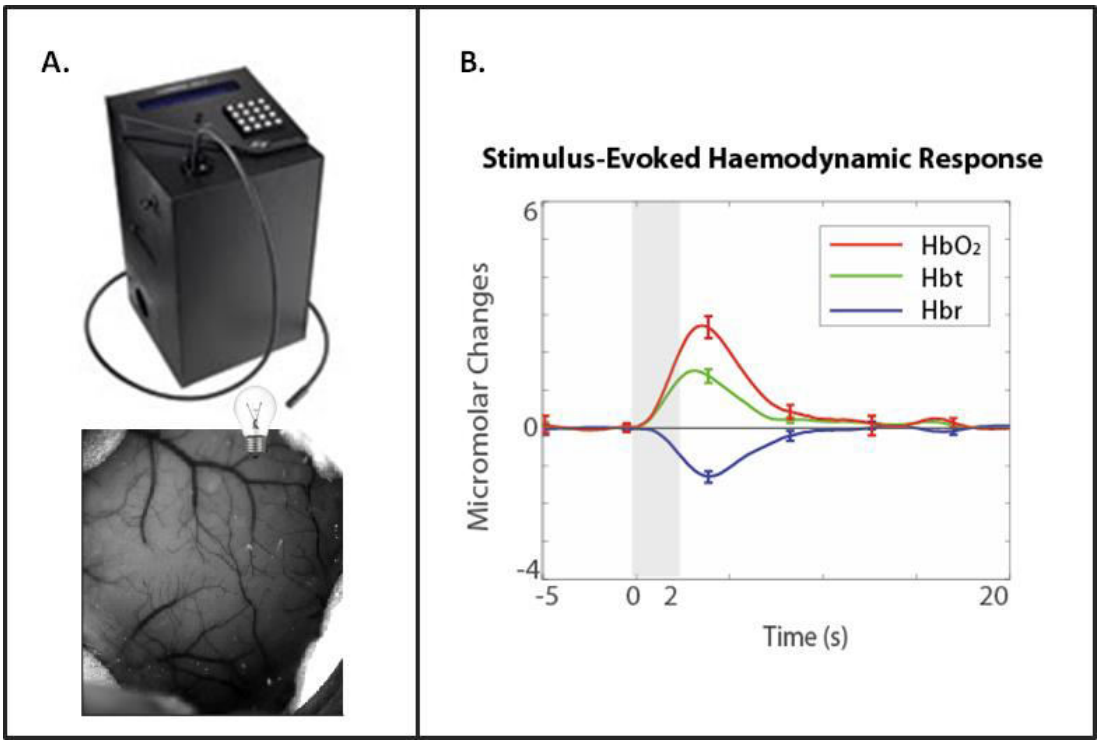

Figure 1.4 – Optical Imaging Spectroscopy Experimental Set-Up

A. *A four wavelength flasher illuminates the exposed cortex, which has been thinned to translucency so the underlying vasculature is visible.* ***B.*** *The typical haemodynamic changes observed within the cortex when a stimulus is presented. Stimulation causes an increase in total blood volume (Hbt) and oxyhaemoglobin (HbO_2), with a concomitant decrease in deoxygenated haemoglobin (Hbr).*

1.3.3 Concurrent Electrophysiology & 2D-OIS

These techniques (electrophysiological recordings and 2D-OIS) are not typically applied in isolation. In fact, they have previously been applied concurrently to measure the relationships between the magnitudes of local field potentials from cortical layer IV, and the accompanying surface haemodynamic responses (e.g. Berwick et al., 2008; Boorman et al., 2010; 2015; Jones et al., 2004).

When applying these methods, the neural activity is measured at infragranular depths, whereas the haemodynamic changes are measured from the surface of the cortex. Thus, it could be argued that the measure of neural activity is recorded from a different cortical layer than the haemodynamic changes. However, it has previously been stated that

stimulus-evoked neural and vascular responses show parallel increases in activity across all cortical layers (Huo et al., 2014), as seen in somatosensory (Di et al., 1990; Einevoll et al., 2007; Herman et al., 2013), auditory (Szymanski et al., 2011), and visual (Xing et al., 2012) cortices. These findings indicate that the deeper electrophysiological activity, recorded using the multichannel electrode, will likely be accompanied by a corresponding increase in neural activity in the superficial layers.

1.4 Animal Models of Neurovascular Coupling

The application of such techniques to discern the underlying components of fMRI is typically relatively invasive; as such animal models are often favoured in neurovascular coupling research. The rodent primary somatosensory cortex is the model often used for studying neurovascular coupling. The primary somatosensory cortex of the rodent contains a highly organised representation of the skin, hair, forepaw/hindpaw surface, and the vibrissae (whiskers) (Chapin & Lin, 1984; Figure 1.4). The whisker-barrel system provides an attractive model because of its elegant structural organisation. Each of the rodent's whiskers corresponds topographically to one-to-one cell groupings (referred to as barrels) in layer IV of the somatosensory cortex (Cox, Woolsey, & Rovainen, 1993; see Figure 1.5). This structure is the rodent's main sensory system for exploring the environment and collecting aesthetic information regarding the objects around it. Neurons in each of the individual barrels are strongly and selectively activated when the corresponding whisker makes contact with a surface and/or is stimulated (Bernardo et al., 1990; Berwick et al., 2008). Cox and colleagues conducted an experiment which provided evidence for these functionally linked cerebral vascular units providing focal regulation of cerebral blood flow in individual whisker barrels in rats (Cox et al., 1993). Precise histological work revealed dense capillary networks confined to single barrels; and the stimulation of specific whiskers led to increased blood flow into the arterioles which supplied these whiskers. Individual barrel representations within the somatosensory cortex are highly independent as neurons have high synaptic connectivity within each barrel and barrel column, and lower connectivity between individual barrels. This whisker-barrel model is also preserved in the mouse, which is growing increasingly popular in research due to the availability of transgenic disease models.

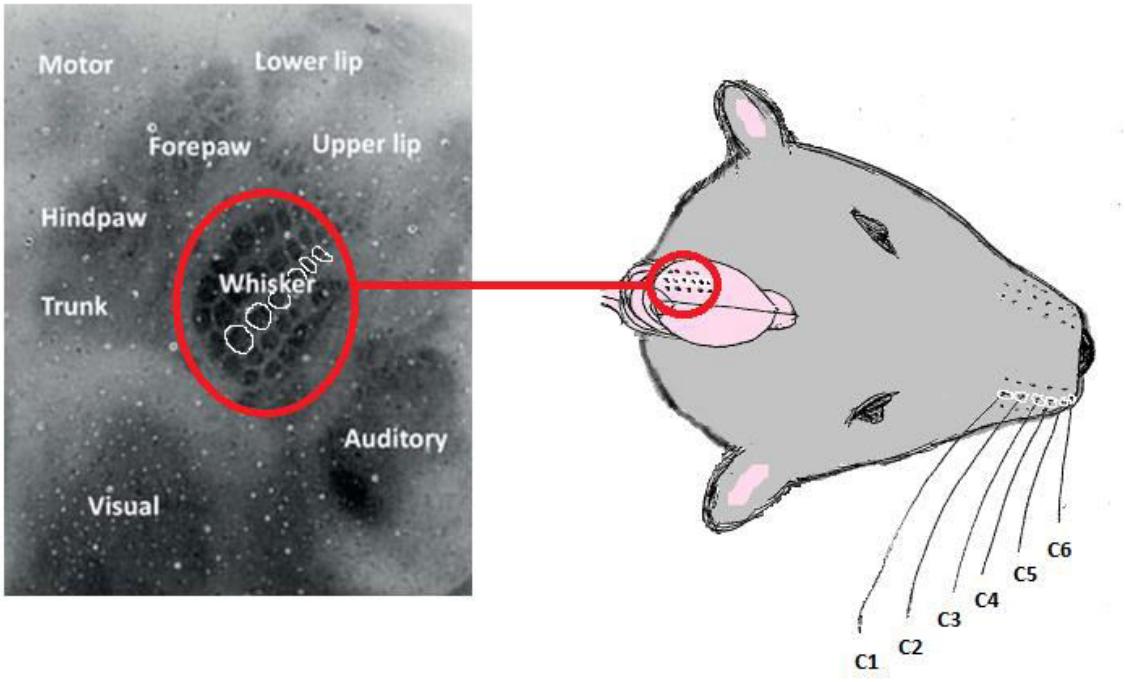

Figure 1.5 – The Structural Organisation of the Rodent Whisker-Barrel System

Illustration demonstrating the topographical organisation of each individual whisker barrel in layer IV of the somatosensory cortex. The greyscale image shows a post-mortem histological section of the rat somatosensory cortex centred on the S1 whisker barrel field and stained for cytochrome oxidase (section from the Sheffield laboratory, adapted from Boorman et al., 2015); the whisker barrels and surrounding anatomically mapped regions have been labelled.

1.5 The Bias of Anaesthetics

The use of anaesthesia has been widely applied in *in vivo* animal models (Vanzetta & Grinvald, 2008). Anaesthesia can have varied actions on the brains physiology, including changes to the neural processing and vascular reactivity (Masamoto & Kanno, 2012). Anaesthesia may thus be a confounder which interferes with the NVC relationship due to its modulatory effects on neural and vascular responses.

1.5.1 Anaesthetic Alterations of Neurovascular Coupling

Anaesthetics have different sites of action, potentially resulting in discrepancies in the interpretation of neurovascular coupling mechanisms between animal experiments. For

example, Du and colleagues showed differences in CBF alterations to intravenously infused cocaine in rats under alpha-chlorase (increase in CBF) versus isoflurane (decrease in CBF) (Du et al., 2009). Furthermore, the role of the vasoactive messenger nitric oxide in controlling stimulus-evoked CBF responses was shown to be dominant in anaesthetised rats (urethane, Gerrits et al., 2001), but play no major role in awake rats (Nakao et al., 2001). Such findings highlight the critical interference of anaesthesia in neurovascular coupling pathways. Knowing that anaesthesia can affect the major pathways of NVC, it seems likely that these may have an impact on the temporal dynamics and spatial coordination of neural and vascular responses (for review see Masamoto and Kanno, 2012).

1.5.1.1 Anaesthetic Alterations of the Temporal Dynamics of Neurovascular Coupling

Previous work has assessed the effects of four different anaesthetics on somatosensory-evoked potential after the electrical stimulation of rat paws (Hayton et al., 1999). The different anaesthetic conditions showed slightly altered onset latency times of somatosensory-evoked potential following forepaw stimulation. Dose-dependent increases in the latency of somatosensory-evoked potential have also been observed in human subjects (Sebel et al., 1986).

Prakash and colleagues (2007) compared the temporal profiles of haemoglobin somatosensory maps in the rat versus the mouse cortex. They used 2D-OIS to explore the differing haemodynamic volume changes in response to whisker stimulation across the two species. The rats showed the expected biphasic mirror-image stimulus-evoked changes in oxygenated (HbO_2) and deoxygenated (Hbr) haemoglobin; with an increase in HbO_2 and a decrease in Hbr. The haemodynamic profile of responses from the mouse was entirely different to that of the rat. The haemodynamic changes observed in the mouse were monophasic, with a prolonged increase in Hbr and a parallel decrease in HbO_2, which is contrast to that normally observed (e.g. Berwick et al., 2002; 2008; Boorman et al., 2010; Hillman et al., 2007; Martin et al., 2013; Nielsen & Lauritzen, 2001; Sharp, Shaw, et al., 2015; Takuwa et al., 2011; 2012; etc.). The authors speculated that these results highlight differing haemodynamic changes to physiological stimulation across the species. They reasoned that the mouse brain capillary density could be disproportionately low, resulting in a mismatch between oxygen consumption and functional hyperaemia. The findings are relatively controversial as other authors have been able to demonstrate a typical

haemodynamic profile to whisker stimulation in both the anaesthetised and the awake mouse (e.g. Neill & Stryker, 2008; Takuwa et al., 2011; 2012; Sharp, Shaw, et al., 2015). In fact, data from the laboratory in Sheffield has been able to replicate this reversed haemodynamic response profile shown by Prakash and colleagues, but only under very high levels of anaesthesia (Sharp, Shaw et al., 2015). Analysis of the arterial network demonstrated a failed dilation of the middle cerebral artery, which may explain the "inverted" haemodynamic response presented by Prakash and colleagues. When the anaesthetic regime was modified, the "normal" haemodynamic response profile returned; with a large increase in total haemoglobin (Hbt) and HbO_2, and a decrease in Hbr and arterial recruitment. These findings again highlight the variability and stability of the haemodynamic response when the animal is under anaesthesia, further emphasizing the importance of adopting a rigorous anaesthetic regime. In this case, anaesthesia completely altered the baseline physiology, changing the haemodynamic response profile drastically and so altering the interpretation of neurovascular coupling.

1.5.1.2 Anaesthetic Alterations of the Spatial Coordination of Neurovascular Coupling

Anaesthesia-dependent variations in the spatial extent of the haemodynamic response were observed by Chen et al. (2001), who mapped haemodynamic changes to finger pad stimulation in the monkey somatosensory cortex under pentothal and isoflurane. Pentothal produced localised haemodynamic changes, whereas haemodynamic responses obtained under isoflurane were much broader. Indeed, pentothal had suppressive actions on the cortical activity, likely due to the suppression of the neuronal excitability; whereas isoflurane enhanced surround inhibition (Chen et al., 2001). These variation in cortical mapping could depend on the actions of anaesthesia on both the neural and vascular components. For instance, anaesthesia may alter the balance between excitatory and inhibitory activity, or may change the vessel reactivity; although the mechanisms underlying this remain unknown.

1.5.1.3 Experimental Conditions which Necessitate the Use of Anaesthesia

Whilst anaesthesia has been shown to alter the NVC relationship, certain experimental imaging conditions require its usage (e.g. due to the application of invasive methods, or because of the population being studied). In conditions where the use of anaesthesia is

unavoidable, appropriate anaesthesia selection is vital. Choosing a suitable anaesthetic regime and adjusting the dosage are essential for achieving stable and reproducible experimental results. For instance, rats under urethane anaesthesia have been shown to be physiologically stable for 8-12 hours (Lincoln, 1969), whereas rats anaesthetised with medetomidine required the medetomidine infusion rate to be adjusted over time due to potential pharmacokinetic changes in long-term experiments exceeding 3 hours (Pawela et al., 2009). A study conducted by Sharp, Shaw, et al. (2015) (and in chapter 5 of this thesis) demonstrated that haemodynamic responses to whisker stimulation were preserved between the anaesthetised and awake state following the careful selection of a suitable 'balanced' anaesthetic regime.

1.5.1.4 Overcoming the Bias of Anaesthesia: a Move towards Awake Imaging

There has been a recent movement which favours awake neuroimaging of the cortex, to counter these known effects of anaesthesia on the NVC responses. For the purposes of this thesis (chapters 3, 4 & 5), the methodology of Carandini and colleagues was adapted (Ayaz et al., 2013; Haider et al., 2013; Pisauro et al., 2013). This preparation involves a mouse head-fixed atop of a spherical treadmill, free to engage in locomotion or rest. The movement of the spherical treadmill is detected using optical motion sensors, which provide information about the speed and direction of locomotion as the animal moves (more detail on this experimental set-up is covered in section 2.4.1 and in chapter 3). Awake preparations such as these have opened new avenues for studying NVC in a more naturalistic way without the influence of anaesthetics, and with the additional consideration of behavioural state.

1.5 Neurovascular Coupling across the Lifespan

The techniques described here (i.e. 2D-OIS and electrophysiology, with or without anaesthesia) have been applied to study NVC in fine spatiotemporal detail. It is essential to gain a comprehensive understanding of NVC in order to aid in the interpretation of widely used BOLD fMRI studies, and to provide possible diagnosis and treatment avenues for certain neurodegenerative diseases (in which NVC breaks down, e.g. Alzheimer's disease). Whilst many studies seek to characterise NVC for these reasons, the picture is further complicated by the fact that NVC changes during the life span, potentially confounding the interpretation of fMRI studies conducted with developmental or aged populations.

1.5.1 Neurovascular Coupling in the Developing Brain

During development the brain undergoes many changes which have the potential to alter neurovascular coupling; therefore, a constant relationship between BOLD signal and neural activity cannot be assumed (Harris et al., 2011).

1.5.1.1 Structural Changes to the Developing Brain

The following review of the developing brain will assess the structural changes to the components of the neurovascular unit: (1) the neurons; (2) the vasculature; and (3) the glial cells (i.e. astrocytes).

1.5.1.1.1 Neuronal Development

The brain undergoes dramatic changes in early life. For instance, there is an increase in cortical thickness during early development, followed by a slower thinning of the cortical grey matter between childhood and adolescence (Ostby et al., 2009; Paus et al., 2005; Shaw et al., 2008; Tamnes et al., 2010). This change in cortical thickness through development is thought to reflect the excessive formation and then selective deletion of synapses (Chan et al., 2002). Myelination also increases throughout development, which involves changes in axonal diameter and myelin wrap number and density (Fields, 2008; Harris et al., 2011).

There are changes to the balance of excitation and inhibition in the developing brain, critical for regulating firing rates and information flow across the neuronal network (Akerman & Cline, 2007). GABAergic interneurons develop at different times postnatally across different brain regions (Le Magueresse & Monyer, 2013). There is a developmental switch of the neurotransmitter GABA from depolarising to hyperpolarising (Ben-Ari, 2002), altering the excitatory to inhibitory balance of the brain, and sharpening the neural response to a stimulus (Sillito, 1975; Crook et al., 1998; Gabernet et al., 2005). Such changes may affect the spatiotemporal profile of haemodynamic activity within the brain, as it is thought that interneurons may play an essential role in neurovascular coupling (Cauli et al., 2004). Developmental changes have been observed in interneuron numbers, and in the vasoactive substances which they produce. Nitric oxide synthase (nNOS) containing

interneurons are found in increasingly higher densities during development, before decreasing with age (Downen et al., 1999; Eto et al., 2010; Ohyu & Takashima, 1998).

1.5.1.1.2 Vascular Development

Vascular development is incomplete at birth, with the vasculature maturing as the brain develops. Microvascular density will have a major impact upon brain oxygenation. Vascular volume increases have been shown in the primate (Risser et al., 2009) and rat (Keep & Jones, 1990) during development, with corresponding decreases in the mean distance between the tissue and the nearest vessel (Risser et al., 2009). These changes in blood volume fraction alone can produce proportional changes in BOLD signal across development (Ogawa et al., 1993; Buxton et al., 2004). The changes to the vasculature are highly plastic, and cortical regions which use more energy become more highly vascularised than less active areas (Weber et al., 2008; Tieman et al., 2004). It is likely that during these developmental changes to blood vessel density in the brain parenchyma, the neural activity may not be as efficiently coupled to the blood flow as when the vasculature is fully developed.

1.5.1.1.3 Astrocyte Development

As well as there being developmental changes to the structure of the neurons and the vasculature, there are also changes to the astrocytes. Astrocytes are an important mediator of neurovascular coupling (Cauli & Hamel, 2010), and so their development may alter neurovascular coupling in early life. Astrocytes increase in both size and number during development, not reaching their adult population density until around P24 in the rat hippocampus, and P50 in the rat cortex (Nixdorf-Bergweiler et al., 1994; Stichel et al., 1991). There are also accompanying morphological changes to astrocytes, such as to branching and orientation. Gap junctional coupling of astrocytes develops by P11 in rat visual cortex (Binmöller & Müller, 1992), which is essential for enlarging the area over which neuronal activity can influence blood flow. These differences in the size and connectivity of astrocytes may alter the blood flow responses caused by neuronal activation. Further, there are developmental changes in the expression of the metabotropic glutamate receptors (mGluR5; Romano et al., 1995). mGluR5 is highly expressed in the brain during early life (rat P1; Catania et al., 1994), but then decreases 3-fold within the cortex before adulthood (van den Pol et al., 1995). mGluR5 are involved in the astrocytic

pathway of neurovascular coupling, as they are responsible for raising astrocyte calcium levels during neuronal activity.

1.5.1.2 Functional Changes to the Developing Brain

Given the developmental changes to the mechanisms mediating neurovascular coupling described, it would be surprising if such changes did not contribute significantly to at least some of the BOLD signals observed experimentally. Such alterations to the BOLD signal during development may cause problems interpreting experimental results. As such, previous work has shown conflicting results regarding the haemodynamic and neuronal changes which occur in the developing brain (e.g. Colonnese, et al., 2008; Kozberg et al., 2013; Martin et al., 1999; Roche-Labarbe et al., 2014).

1.5.1.2.1 Clinical Investigations of Neurovascular Coupling in Development

Clinical imaging studies of infants and young children have used non-invasive techniques (e.g. EEG, BOLD fMRI, and near-infrared spectroscopy) to examine neurovascular coupling during development. Electrophysiological techniques, such as EEG, have consistently identified brain activity in response to peripheral somatosensory stimuli in both preterm and term neonates (Karniski, 1992; Karniski et al., 1992; Lauronen et al., 2006; Pike & Marlow, 2000; Vanhatalo & Lauronen, 2006); although, EEG patterns do not acquire adult-like temporal structure until later development (Marshall et al., 2002). However, developmental studies investigating haemodynamic responses have reported considerable variability (Arichi et al., 2012; Seghier et al., 2006), with the identification of both positive (Arichi et al., 2010; Cantlon et al., 2006; Liao et al., 2010; Marcar et al., 2004; Schapiro et al., 2004) and negative (Anderson et al., 2001; Born et al., 1998; 2000; Heep et al., 2009; Martin et al., 1999; Muramoto et al., 2002; Seghier et al., 2004; Yamada et al., 1997; 2000) BOLD signal responses within the same study population. Such discrepancies may arise from technical issues (e.g. with the stimulus paradigms used, or analysis techniques applied), differences in behavioural state, (i.e. natural sleep, sedation, awake), or may be due to genuine physiological differences within the developing brain (Arichi et al., 2010; Karen et al., 2008).

Arichi et al. (2010) believe many of the discrepancies seen in fMRI BOLD experiments (i.e. negative and positive signals) may be due to the data analysis techniques applied. By

encompassing a flexible characterisation of the haemodynamic response function, and by using a non-parametric group analysis to reduce the effects of between subject variance and noise, the authors were able to detect positive BOLD patterns of activation which were fully compatible with the data seen from adult subjects. Physiological factors must also be considered as an explanation of age-related changes in BOLD signal. During the first ~10 years of life there are major increases in synaptic density (Huttenlocher, 1990; Yamada et al., 1997), followed later in life by synaptic pruning. In line with these synaptic changes, oxygen use is found to rapidly increase with synapse development in children (Muramoto et al., 2002), before later decreasing (~0.5% per year) with ageing. Thus, this transition in oxygen use during development may be concerning for the interpretation of the BOLD signals. The BOLD signal is mainly related to the paramagnetic Hbr concentration, which depends upon the balance of oxygen use ($CMRO_2$) and blood flow (CBF) increase. The larger the increases in oxygen use relative to the increases in blood flow as evoked by neural activity, the smaller the positive BOLD response will be (Karen et al., 2008). Meek et al. (1998) used near-infrared spectroscopy to measure both HbO_2 and Hbr in the awake, newborn brain; they found increases in both HbO_2 and Hbr in response to visual stimulation, indicating that the increase in oxygen supply was insufficient to meet the oxygen demands of the developing brain. Blood pressure increases and heart rate decreases also occur throughout childhood (Chiang et al., 2000), again which could confound the BOLD signal (Kalisch et al., 2001). Analyses of neural circuit development using fMRI are thus limited by a lack of knowledge about which developmental stage the BOLD signal can first be reliably evoked, and about how the dynamics of CBF vary as a function of age (Colonnese et al., 2008).

The general lack of consistency in the clinical studies investigating neurovascular development have been difficult to reconcile (Kozberg et al., 2013). Due to the experimental inconsistencies, e.g. no follow-up studies, limited patient numbers, variable stimulation paradigms, etc., confusion still remains regarding neurovascular coupling in the developing brain. It will be of prime importance to resolve such discrepancies, and gain an improved understanding of brain development. Recent work has employed animal models to use more invasive, high-resolution techniques to systematically probe neurovascular coupling within the developing brain.

1.5.1.2.2 Animal Studies of Neurovascular Coupling in Development

Whilst the use of animal models has allowed for more detailed and invasive investigations of neurovascular coupling, there are still discrepancies in the findings (Colonnese et al., 2008; Kozberg et al., 2013; Zehender et al., 2013).

The BOLD fMRI technique was employed to study brain development in one study, which found only positive BOLD in response to a visual stimulation in infant macaques (Kourtzi et al., 2006). Colonnese and colleagues (2008) also found positive BOLD responses in the developing brain. They measured BOLD responses and made extracellular recordings in the rat somatosensory cortex at varying ages in response to electrical paw stimulation. BOLD responses were reliably detected in rat pups from 13 days postpartum (P13); after which age-dependent increases in the (uniformly positive) BOLD signal amplitude were observed. The time course of the haemodynamic response showed decreases in the onset latency and the time to peak. The haemodynamic results were correlated with the electrophysiological data, which indicated that the changes measured using fMRI were caused by the systematic growth and acceleration of the haemodynamic response, and by the maturation of cortical connectivity patterns.

In contrast, Kozberg et al. (2013) used optical imaging to measure haemodynamic responses to electrical hindpaw stimulation, and found an inverted haemodynamic response (i.e. negative BOLD signal) in newborn rats compared to adult rats (positive BOLD signal. The authors suggested that the discrepancy in these results may be due to certain electrical stimulation paradigms inducing alterations in systemic blood pressure, possibly confounding the developing brain and creating false positive BOLD signals in immature rodents.

Zehender and colleagues (2013) also measured neurovascular coupling in the immature rodent whisker barrel cortex during prolonged whisker stimulation. Multi-channel electrodes recorded local field potentials (LFPs) and multi-unit activity (MUA); and laser Doppler flowmetry (LDF) recorded blood flow responses *in vivo* in P7 and P30 mice. Neurovascular coupling was found to undergo a physiological shift during the first month of life. In P30 subjects, the MUA showed stable increases during whisker stimulation, with expected concurrent increases in CBF. In P7 subjects however, whilst the MUA increased to stimulation, the blood flow decreased. There were slight differences in the MUA between age groups, as MUA in P7 subjects showed fatigue compared P30 animals. Specifically, MUA decreased in the course of stimulation at both ages, but this effect was significantly higher

in P7 animals. There was also a delay in the maximum peak of LFP responses and MUA in P7 mice. These results indicate that the developing brain is not capable of maintaining prolonged neural processing on a stable level, which may be the reason for the concurrent decline in blood flow observed. The authors speculated that these discrepancies between ages were likely due to a reduced level of myelination at P7, meaning there would be reduced nerve conduction velocity.

An important factor in the findings of Kozberg et al. (2013) and Zehender et al. (2013) was the presence of delayed, global vasoconstriction to stimulation in the developing brain, which was present prior to the development of vasodilatory responses. These constrictions remained during development, causing biphasic haemodynamic responses, whereby stimulation evoked an increase in Hbt, followed by a prolonged decrease in Hbt. This global vasoconstriction effect could be caused by vascular steal (Harel et al., 2002; Shmuel et al., 2002), be an indicator of reduced or inhibitory neural activity (Boas et al., 2008; Devor et al., 2008); or could be linked to the haemomodulatory effects of noradrenergic or cholinergic systems (Bekar et al., 2012; Takata et al., 2013). Although speculative, Kozberg & Hillman (2016) suggest that this vasoconstriction during development may serve to limit the extent of hyperaemic responses to protect the fragile perinatal vasculature, which is particularly prone to haemorrhage in premature infants.

1.5.1.2.3 Implications

It is possible that these variations in response patterns seen across development reflect the progressive maturation of neurovascular coupling (Arichi et al., 2012; Kozberg & Hillman, 2016), since many of the components of the neurovascular unit are still developing postnatally (Harris et al., 2011). For the robust interpretation of developmental fMRI data, it is critical to gain a detailed understanding of the developmental changes to brain processes which may influence the BOLD signal. Whilst recent work has employed animal models to gain a more detailed understanding of the neurovascular mechanisms underlying the BOLD signal in development, there are still inconsistencies in the results which need to be resolved. Furthering the understanding of neurovascular coupling during development is important for improved understanding of neonatal brain development, and thus the diagnosis, treatment, and management of neonatal neurological conditions.

Neurovascular coupling may develop from infancy and early childhood into adulthood, but there are also profound changes associated with ageing (i.e. old age). To gain a complete understanding of the maturation of neurovascular responses, it will be important to assess how they change across the lifespan. Further, the ever-ageing population provides stark motivation to advance the understanding of neurovascular coupling in old age, in order to aid in the treatment and management of age-related neurological disorders (e.g. dementia) and cognitive decline.

1.5.2 Neurovascular Coupling in the Ageing Brain

Ageing has been associated with the decline of neurovascular coupling, which likely contributes to the impairment of cerebral function seen in elderly patients and aged laboratory animals (Fabiani et al., 2013; Park et al., 2007; Sorond et al., 2013; Stefanova et al., 2013; Topcuoglu et al., 2009; Toth et al., 2014a; 2015; Zaletel et al., 2005). Ageing has been associated with a breakdown in neurovascular coupling due to alterations in the structure and function of the components of the neurovascular unit (e.g. cerebral blood vessels, neurons, and astrocytes; e.g. Creasey & Rapoport, 1985; Huttenlocher, 1990; Jacobs & Scheibel, 1993; Masliah et al., 1993; Park et al., 2007; Peters et al., 2008; Sowell et al., 2003; Topcuoglu et al., 2009; Toth et al., 2014a; 2015).

1.5.2.1 Structural Changes to the Ageing Brain

This discussion of the ageing brain will begin by reviewing the known structural changes to these components of the neurovascular unit: (1) the neurons; (2) the vasculature; and (3) the glial cells (i.e. astrocytes).

1.5.2.1.1 Neuronal Changes during Ageing

Changes to neuronal structure and organisation have also been observed in the aged brain. Sowell and colleagues (2003) found reductions in both grey and white matter volume associated with ageing. Neuropathological evidence has also shown reductions in the neuron count (Creasey & Rapoport, 1985), dendrites (Jacobs & Scheibel, 1993), and synapses (Huttenlocher, 1990; Masliah et al., 1993; Peters et al., 2008) in the prefrontal cortex during ageing; and age-induced alterations in calcium regulation have been observed (Barnes & Burke, 2006). Reduction in neuron numbers and connections may have profound

functional effects on the brains processing efficiency. Ultimately neuronal firing and the ability to propagate action potentials will be affected, which in turn would affect the plasticity of the brain. Alterations in the mechanisms of plasticity in ageing include a decline in GABA projection neurons and interneurons (Madhusudan et al., 2009; Schmidt et al., 2010; McQuail et al., 2012; Stanley et al., 2012). GABA is thought to be involved in the selectivity of synaptic changes which occur during learning (Hayama et al., 2013); meaning the reduced pruning of non-active dendritic spines could lead to increased non-specific connectivity, thereby compromising learning.

1.5.2.1.2 Vascular Changes during Ageing

Cerebral blood vessels undergo profound changes associated with ageing (see Iadecola et al., 2009 for review). For instance, Farkas & Luiten (2001) showed that cerebral capillaries were thickened in the cortex and hippocampus; pericytes had degenerated; and endothelial cells were elongated with reduced numbers of mitochondria. Ageing has further been associated with increases in the stiffness of cerebral blood vessels, and tortuosity and narrowing of arterioles and capillaries (Park et al., 2007; Hajdu et al. 1990; Hutchins et al., 1996). Ageing is associated with an insulin-like growth factor-1 (IGF-1) deficiency (Toth et al., 2014b), which increases the production of NADPH oxidase-derived reactive oxygen species (ROS) in the cerebral vessels, contributing to compromised neurovascular coupling by decreasing nitric oxide (NO) levels, and promoting endothelial dysfunction (Girouard & Iadecola, 2006; Park et al., 2007; Topcuoglu et al., 2009; Toth et al., 2015a; 2015b; Zaletel et al., 2005). These profound structural and regulatory changes to the blood vessels during ageing have generally been associated with a reduction in resting CBF (Farkas & Luiten (2001); Kalaria, 2008), and with an attenuation of the stimulus-evoked CBF response (Iadecola et al., 2009; Panczel et al., 1999). This disruption of cerebral circulation alters the balance between the delivery of energy substrates and the clearance of metabolic waste, eventually leading to brain dysfunction (Gorelick et al., 2011; Iadecola et al., 2009).

1.5.2.1.3 Astrocyte Changes during Ageing

It is generally agreed that there is hypertrophy of astrocytes with age (Peters, 2007). They increase in size and become more filamentous; and so as nerve fibres are reduced in ageing, astrocytes fill up the vacated space (Sandell & Peters, 2002). However, it is thought that there is no significant increase in the number of astrocytes (Berciano et al., 1995;

Diamond et al., 1977; Hansen et al., 1987; Long et al., 1998; Pakenberg et al., 2003). It has been hypothesized that astrocytes switch from being neurotrophic to neurotoxic in ageing (Garcia-Matas et al., 2008; Jiang & Cadenas, 2014). For instance, astrocytes in the senescence-accelerated mouse (i.e. a model of age-related cognitive decline) showed elevated oxidative stress and reduced neuroprotective capacity (Garcia-Matas et al., 2008); and old mice have been shown to have increased mitochondrial aerobic metabolism and inflammatory responses (Jiang & Cadenas, 2014).

1.5.2.2 Functional Changes of NVC associated with Ageing

The profound changes to the mechanisms mediating neurovascular coupling in the aged brain likely contribute to the cognitive and functional deficits seen in elderly patients and lab animals. The pathologies which alter neurovascular coupling in ageing affect the interpretation of fMRI studies comparing the responses of elderly patients to those of healthy adult patients. Therefore, the interpretation of fMRI studies conducted in an aged population are constrained, as for example, comparing the aged population to healthy adults assumes that the two groups have comparable neurovascular coupling. Indeed, inconsistencies have been found between ageing fMRI studies (Ances et al., 2009; D'Esposito et al., 2003).

1.5.2.2.1 Clinical Investigations of Neurovascular Coupling in Ageing

Clinical investigations of neurovascular coupling in elderly patients employ non-invasive techniques (e.g. EEG and fMRI) to measure the underlying neuronal and haemodynamic responses. As cognitive impairments are associated with ageing, electrophysiological studies have mainly focused on the impairment of frontally mediated systems (e.g. prefrontal cortex) in older adults. EEG signals from elderly patients have shown a reduction in frequency and amplitude (Nitish & Tong, 2004; Purdon et al., 2005; Thompson et al., 2008; West & Covell, 2001), with a gradual slowing of the alpha rhythm which corresponds to mental deterioration. These findings support the notion that memory failure in older adults results from the functional impairment of a frontally mediated neural system. Whilst there is a general consensus that neural activity is attenuated in elderly patients, there have been inconsistencies reported across ageing fMRI studies. Cognitive, motor, and sensory tasks have been found to induce increases (Lee et al., 2011; Mattay et al., 2002); decreases (Buckner et al., 2000; Hesselman et al., 2001; Nyberg et al., 2010; Raemaekers et al., 2006;

Ross et al., 1999; Tekes et al., 2005); or cause no change (Aizenstein et al., 2004; Gazzeley & D'Esposito, 2005) in the size of the positive BOLD response between young adults and old adults.

Data analysis techniques may be causing some issues in the interpretation of these conflicting BOLD responses, as Aizenstein et al. (2004) found that altering the criteria for voxel selection to include negative peaking voxels resulted in a reduced fMRI signal. It is also possible that the differences found in the BOLD responses could be due to regionally-dependent changes associated with ageing. In support of this hypothesis, Bucker et al. (2000) found a visual-motor stimulus caused a reduced BOLD signal in the visual cortex of older adults compared to younger adults, but no differences in the BOLD response in the motor cortex. Interpretation of the effects of ageing by simply studying the magnitude of the BOLD signal may be problematic, as it reflects a complex interaction between changes in CBF, $CMRO_2$, and cerebral blood volume (CBV). The BOLD signal is not an absolute measure, it is a relative measure that uses resting CBF as a baseline (D'Esposito et al., 2003). As such, differences in resting CBF between populations may have important implications for fMRI comparisons (Ances et al., 2009). Conflicting results have found resting cerebral metabolism to be constant in old age (Goldstein & Reivich, 1991), or to decline with old age (Marchal et al., 1992; Yamaguchi et al., 1986). Again, the differences in baseline metabolism may be regionally specific (Loessner et al., 1995), which makes generalisations difficult. Ances et al. (2009) illustrate how a calibrated BOLD approach can be used to overcome these baseline differences in CBF & $CMRO_2$, providing a more quantitative assessment for comparisons between different subject populations. In order to understand the mixed results found in the fMRI studies of ageing, supplementary research is required which does not rely on the use of BOLD fMRI.

Zaletel et al. (2005) used concurrent transcranial Doppler to study haemodynamic responses and EEG to study neural responses in the occipital lobe of young and old adults in response to a visual stimulus. No differences were found in the evoked potential between the two groups, but CBF responses were found to be attenuated in the old participants. The findings of Topcuoglu et al. (2009) and Fabiani et al. (2013) are in line with these results, as they showed no age-related differences in evoked potential in the visual cortex (Fabiani et al. (2013); Topcuoglu et al. (2009)), but reduced haemodynamic changes (Fabiani et al. (2013)). These studies indicate that within the cortex there may be a reduction in CBF responses associated with ageing, but not in the neuronal activity, indicating that there

could be neurovascular uncoupling. These results further emphasize that issues may arise in ageing studies when using haemodynamic measures to study neuronal function.

1.5.2.2.2 Animal Studies of Neurovascular Coupling in Ageing

To gain an even more detailed understanding of the functional neurovascular changes underlying old age, supplementary animal studies have been conducted which employ invasive techniques to record neural and haemodynamic changes in fine spatiotemporal detail.

Some animal studies have found comparable results suggesting attenuation of the blood flow response in ageing (Park et al., 2007; Toth et al., 2014a; 2014b; Tucsek et al., 2014). For example, Park and colleagues (2007) examined the effect of ageing on neurovascular and endothelial mechanisms regulating cerebral microcirculation in mice at age 3, 12, and 24 months. Ageing was shown to have deleterious effects on endothelium-dependent vasodilation, and to disrupt the increases in CBF induced by whisker stimulation. The cerebrovascular effects of ageing were well developed at 12 months of age, except for the response to hypercapnia which was not significantly reduced until 24 months. Hypercapnia by inhalation of CO_2 is thought to induce nitric-oxide dependent vasodilation, which is impaired in ageing (Topcuoglu et al., 2009; Toth et al., 2015b; Zaletel et al., 2005).

Toth et al. (2014a) also found attenuated stimulation-evoked CBF responses in the whisker barrel cortex of young adult (3 months) and aged (24 months) mice. Resveratrol (3,4',5-trihydroxystilbene) was used to treat the aged rodents, as it is thought to have endothelial protective effects by increasing the levels of endothelium-derived nitric oxide (NO), and inhibiting NADPH oxidase. After 10 days of Resveratrol treatment, stimulus-evoked CBF responses in aged mice were restored to the levels seen in young adult subjects. A nNOS inhibitor was used to confirm that resveratrol treatment restored NO mediation of neurovascular coupling in aged animals. Work from the same lab by Tarantini et al. (2015) mimicked the effect of ageing on the brain by pharmacologically inhibiting the synthesis of epoxyeicosatrienoic acids (EETs), prostaglandins and NO. They found significant 'neurovascular uncoupling', characterised by intact evoked field responses and impaired CBF responses. A battery of behavioural tests confirmed that the neurovascular uncoupling

was associated with significant cognitive impairment, as performance in learning and memory tasks was compromised.

Balbi and colleagues (2015) found that cerebral vessels were structurally intact in old mice, but again found profound functional impairment. In their experiments CBF responses to forepaw stimulation were substantially reduced in 8 and 12 month old mice, demonstrating that cerebral vascular impairments may even be present in early adulthood. Although other studies showed age-related cerebral deficits were present from 12 months, Balbi et al. showed that the maintenance of CBF responses over time were compromised from 8 months old ('vascular fatigue') by presenting trains of repetitive stimuli. Immunohistochemistry was employed to quantify the neurovascular unit across age categories, i.e. capillary density, smooth muscle cell coverage of cerebral arterioles, pericyte and astrocytic endfeet coverage of capillaries, and blood brain barrier leakage. None of these structures were altered, suggesting neurovascular impairment occurs before any age-dependent microvasculature structural changes occur. Hypercapnia was induced through the inhalation of carbon dioxide (CO_2); but here there were no significant deficits found in the global increase of CBF in the aged mice.

The animal studies reviewed so far have emphasized the contribution of age-related cerebrovascular changes to cognitive decline; however other work has examined the contributions of local field potential (LFP) gamma activity and parvalbumin-positive (PV) interneurons to impaired neurovascular coupling in the ageing brain (Jessen et al., 2015). Jessen and colleagues (2015) tested the association between evoked PV interneuron activity, gamma power, CBF, and oxygen consumption in young adult (3-10 months) and old adult (16-24 months) mice. The stimulation-evoked changes in CBF were smaller, although $CMRO_2$ significantly increased, in old adult mice. Somatosensory stimulation-evoked gamma frequency was also reduced in the brains of old mice, and was linked to strong reductions in the Ca^{2+} activity of PV interneuronal perisomatic projections. The projections of PV interneurons innervate nearby pyramidal cells and interneurons; such interactions are critical to evoked neural responses, and may change the balance between excitation and inhibition. No changes were observed in LFP alpha or beta frequency bands, evoked neuronal spike activity, or Ca^{2+} responses in neurons and astrocytes. This study indicates that neurovascular coupling remained functional in old adult animals, and reduced blood flow responses were likely a result of altered network or vascular dynamics.

Whilst BOLD fMRI studies of ageing have shown mixed results regarding CBF changes in the elderly (Aizenstein et al., 2004; Buckner et al., 2000; Gazzeley & D'Esposito, 2005; Hesselman et al., 2001; Lee et al., 2011; Mattay et al., 2002; Nyberg et al., 2010; Raemaekers et al., 2006; Ross et al., 1999; Tekes et al., 2005), studies which employed alternative methods to gain more spatiotemporal detail have generally shown attenuated CBF responses in old adult subjects compared to young adult subjects (Balbi et al., 2015; Fabiani et al., 2013; Jessen et al., 2015; Park et al., 2007; Toth et al., 2014a; 2014b; Tucsek et al., 2014; Zaletel et al., 2005). The results regarding age-dependent changes to neuronal activity have shown inconsistencies, as some studies report no changes in evoked field responses (Fabiani et al., 2013; Topcuoglu et al., 2009; Zaletel et al., 2005), whereas others have shown attenuated evoked field responses (Nitish & Tong, 2004; Purdon et al., 2005; Thompson et al., 2008; West & Covell, 2001), or reductions in LFP gamma activity and PV interneuron CA^{2+} signalling (Jessen et al, 2015). Clearly, more research is needed to investigate neurovascular coupling mechanisms in ageing in more spatiotemporal detail. Such studies will be of prime importance in the treatment or even prevention of age-related cognitive deficits, and may even have implications for cerebrovascular disease (e.g. stroke and vascular dementia) research.

Here, the mouse was selected over the rat to study neurovascular coupling in health and ageing because of the higher availability of transgenic disease models in this species, the possibilities of applying optogenetic techniques, and the ability to head-fix the animals whilst allowing for the measurement of locomotion. It was of particular interest to study the effects of locomotion on the vascular responses in head-fixed mice as locomotion has previously been shown to effect neurovascular responses in the cortex (*visual cortex:* Ayaz et al., 2013; Neill & Stryker, 2010; Saleem et al., 2013; *somatosensory cortex:* Huo et al., 2014; 2015).

1.6 Aims

Overall, this thesis aims to investigate neurovascular coupling in the somatosensory cortex of the mouse. Previous work in the Sheffield laboratory has focused on using the rat model (e.g. Berwick et al., 2002; 2005; 2008; Boorman et al., 2010; 2015; Jones et al., 2004; Kennerley et al., 2009; Martin et al., 2002; 2006; 2013a; 2013b; Slack et al., 2015). First, the experimental set-up for imaging haemodynamic responses and tracking locomotion in the awake, head-fixed mouse are detailed (chapters 3 & 4). The anaesthetised mouse

preparation is also discussed (chapter 5), with the selection of a suitable anaesthetic regime applied in order to overcome the confounds associated with an awake preparation, and to employ the concurrent use of invasive electrophysiological techniques (chapter 6).

1.6.1 List of Aims

- To establish an experimental set-up for the concurrent measurement of haemodynamic responses and locomotion in the awake, head-fixed mouse (*chapter 3*).
- To investigate the effects of locomotion and/or whisker stimulation on the haemodynamic responses in awake, head-fixed mice (*chapter 4*). Hypothesis: whisker stimulation will cause the expected increase in Hbt and HbO_2, with concomitant decrease in Hbr, in awake mice (similar to the responses seen in rats, e.g. Berwick et al., 2002; 2005; 2008; Boorman et al., 2010; 2015; Jones et al., 2004; Kennerley et al., 2009; Martin et al., 2002; 2006; 2013a; 2013b). Locomotion will alter haemodynamic responses within the whisker barrel region (in line with previous work conducted in the cortex by Ayaz et al., 2013; Huo et al., 2014; 2015; Neill & Stryker, 2010; Saleem et al., 2013).
- To compare the stimulation-evoked haemodynamic responses of awake and anaesthetised mice under the selection of a suitable, novel anaesthetic preparation (*chapter 5;* Sharp, Shaw, et al., 2015). Hypothesis: the stimulus-evoked haemodynamic responses under this novel anaesthetic regime will be similar to those seen in the awake mouse, i.e. an increase in Hbt and HbO_2, with a concomitant decrease in Hbr (in contrast to the findings of Prakash et al., 2007).
- To investigate neurovascular coupling in healthy adult mice, and compare the responses to those seen in developing and aged mice (*chapter 6*). Hypothesis: neural and haemodynamic responses will be attenuated in developing (Colonnese et al., 2008; Kozberg et al., 2013; Zehender et al., 2013) and aged (Balbi et al., 2015; Jessen et al., 2015; Park et al., 2007; Toth et al., 2014a) mice in response to whisker stimulation as compared to responses seen in healthy adults.

Chapter 2

Materials and Methods

2.1 Abstract

This chapter details the materials and methods which were implemented to perform all the experimental procedures outlined within this thesis. All procedures were conducted in accordance with the Home Office regulations (Animals (Scientific Procedures) Act, 1986). The surgical techniques used are described in detail for an awake preparation (chapters 3, 4 & 5) and an anaesthetised preparation (chapter 5 & 6). Two-dimensional optical imaging spectroscopy (2D-OIS) was used to measure haemodynamic changes, and multi-channel electrophysiology to measure neural responses in somatosensory cortex (S1).

2D-OIS was used to measure haemodynamic responses for the awake and anaesthetised experiments (chapter 3, 4, 5 & 6). For the anaesthetised experiments performed in chapter 6 however, a second imaging session was conducted in which haemodynamic data and neural recordings were collected simultaneously via the concurrent application of two techniques (2D-OIS and multi-channel electrophysiological recordings).

Each of these experimental techniques will be discussed with a brief overview of the theoretical background, descriptions of the areas of application and the practical function of the equipment used, as well as the details of data analysis.

2.2 Animal Preparation

The following methods were developed and performed in line with the Animals (Scientific Procedures) Act 1986, under approval of the UK Home Office.

2.2.1 Pre-Surgery

Male and female C57/BL6 mice weighing between 18 and 45 g were used in all experiments (sourced from: Harlan Ltd or Charles River Ltd). For the awake animal imaging study (chapters 3, 4, & 5), mice ranged from 3-12 months in age. For the anaesthetised animal study conducted in chapter 5 mice were all 6 months in age. For the anaesthetised animal ageing study (chapter 6) mice were aged 8-12 weeks in condition 1 (n=5, young condition), 6 months old in condition 2 (n=5, adult condition) and >18 months old in condition 3 (n=5, old condition).

Prior to experimentation the animals were housed in a 12-hr dark/light cycle environment in an average temperature of 22°C, with food and water made freely available. Before surgery animals were anaesthetised with an anaesthetic mix consisting of 1 part fentanyl-fluanisone (trade name Hypnorm), 1 part midazolam (trade name Hypnovel), and 2 parts sterile H2O (1:1:2 by volume; 0.8 ml/kg, intraperitoneally (i.p.)). Anaesthetic depth was monitored throughout the surgical and anaesthetised experimental procedures through use of the toe-pinch reflex and the close monitoring of breathing state. Anaesthesia was maintained during surgical preparation and the experimental stage using isoflurane (0.25-0.8%) in 100% oxygen concentration for inhalation. The body temperature was maintained at 37°C throughout the procedures with the use of a homoeothermic blanket (Harvard Apparatus, UK) via rectal temperature measurement.

2.2.2 Surgery

The author was able to carry out all the aseptic surgical techniques described here and performed the majority of all surgeries. However, Dr Paul Sharp and Dr Clare Howarth

conducted and supervised some of surgeries for the purposes of training, and when multiple surgeries were carried out in a short period of time. Both the awake (chapters 3, 4, & 5) and the anaesthetised (chapters 5 & 6) studies required the subjects to recover from the surgical procedures for future imaging sessions (at a later time point).

Surgery was conducted under aseptic conditions to produce a thinned cranial window overlying the somatosensory cortex (S1). A thinned cranial window is a translucent area of the skull, which allows optical techniques to be performed over the cerebral cortex. To produce a thinned cranial window the mouse was placed on its front, and the hair on the top of the head was shaved from the back of the ears to behind the eyes using a scalpel. The mouse was then placed in a stereotaxic frame (Kopf Instruments, Inc.) to secure the head and administer gaseous anaesthesia (isoflurane) via a nose cone. A midline incision was made to remove the surface tissue and expose the skull. The barrel cortex was located within a region approximately 1mm posterior from bregma and 3.5mm lateral from the midline. The skull overlying the barrels on the right side of the head was thinned to translucency (bone approximately 100-200µm thick) to expose the underlying vasculature using a dental drill with a steel ball drill bit of 0.5mm in width (Pro-Lab Basic, Bein Air). During the drilling process saline was dripped over the area of thinning at regular intervals to increase depth visibility, to act as a coolant, and to reduce bruising. Once the desired area had been thinned, a layer of superglue (Loctite, Henkel Inc UK) was applied over the exposed cortex to enhance transparency and to act as an extra protective layer to seal and protect the now weakened skull (see Figure 2.1).

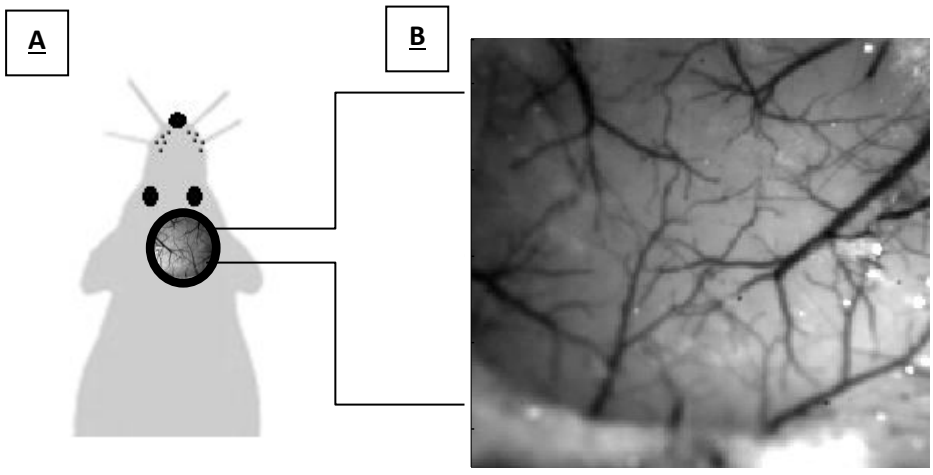

Figure 2.1 – Location of the Thinned Cranial Window

A. *The location of the thinned cranial window on the right hand side of the cerebral cortex overlaying the somatosensory region.* ***B.*** *A reference image, taken using the optical imaging*

camera, showing the thinned cranial window (illuminated at 575nm) and the underlying vasculature.

Following completion of the thinned cranial window, a metal headplate (centred over the right barrel cortex) was attached to the skull with dental cement (Super bond C&B; Sun Medical). The headplate was used to secure the head during imaging, reducing movement artefacts. Following headplate fixation, the animal was taken off the gaseous anaesthetic, and placed in an incubator (TLC eco, Brinsea) to be monitored during recovery. Once the animal was able to drink water and move freely, it was taken out of the incubator and placed in its own cage. The subjects were given at least 1 week to recover from the initial surgery. During this recovery period animals were housed individually, and checked regularly to ensure they were in good health.

2.3 Stimulation Paradigm

Mechanical whisker stimulation was used in all experiments. The mechanical whisker deflection was computer-controlled (1401plus, CED Ltd) running custom written script ('Spike2, CED Ltd'). The script allows control of the frequency, amplitude and duration of whisker stimulation. The stimulator arm was positioned ~1cm lateral and anterior to the mouse's nose, directed at the large caudal vibrissae. The whisker pad was mechanically deflected ~1cm at 5Hz in a caudal direction during the stimulus train, allowing the vibrissae to return passively to the resting position before the onset of the next stimulation. Various experimental paradigms were in place, with the whiskers being stimulated for 2 or 16 seconds (Figure 2.2). For the spontaneous (no whisker stimulation) experimental trials, the mechanical device was left in place, but no deflections were administered.

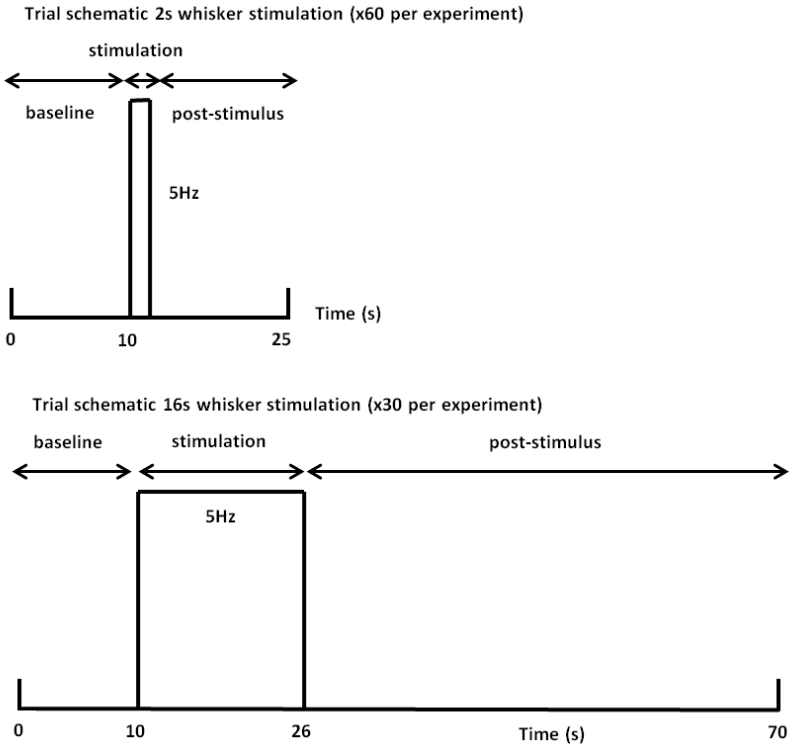

Figure 2.2- Mechanical Whisker Stimulation Experimental Paradigms

Whiskers were mechanically deflected at 5Hz for 2s or 16s, with a 10s baseline period before stimulus presentation, and a post-stimulus period of 13s or 44s respectively. This whisker stimulation format was repeated for a number of trials: 60 times for the 2s whisker stimulation paradigm (spanning a total of 25 minutes for the whole paradigm), and 30 times for the 16s whisker stimulation paradigm (spanning a total of 35 minutes for the whole paradigm). Spontaneous experiments, in which no whisker stimulation was presented, followed one of these timing formats, but with no 5Hz stimulation.

2.4 Experimental Imaging Set-Up

Two separate experimental imaging set-ups were used for the purpose of this thesis: awake imaging experiments (chapters 3, 4 & 5), and anaesthetised imaging experiments (chapters 5 & 6). These slight alterations to the experimental imaging set-up will be described in more detail in the following section.

2.4.1 Awake Animal Experiments

For awake animal experiments (chapters 3, 4 & 5), subjects were imaged multiple times (minimum 14 sessions per animal across multiple days). Only optical imaging was used, and no neural data were collected due to the invasive/acute nature of the electrophysiological techniques available.

Following the minimum 1 week post-surgery recovery period, a training period commenced in which the animal was habituated to the experimenter and the experimental set-up, with increasing exposure over 5 days. Once habituated, imaging sessions comprised of both 2s and 16s whisker stimulation experiments, and spontaneous (no whisker stimulation) experiments (lasting approximately 90 minutes).

The experimental equipment consisted of a spherical treadmill (Styrofoam floating ball, 20 cm diameter), secured to the imaging table by a magnetised steel holder; an optical motion sensor connected to a custom written MATLAB (The Mathworks Inc., USA) interface which was able to track rotations of the Styrofoam ball over time; a mechanical whisker stimulator; and a cranial head plate holder (placed over the ball to hold the mouse securely in place) (Figure 2.3).

2.4.2 Anaesthetised Animal Experiments

For the anaesthetised animal experiments (chapter 5 & 6), following the recovery period from the initial surgery, and then prior to each imaging session, the animal was injected with the anaesthetic mix containing 1 part fentanyl-fluanisone, 1 part midazolam, and 2 parts sterile H_2O (this time at a 70% dose per gram intraperitoneally). Following this injection, the animal was secured using a head plate holder, which was held in place with a flexible, mechanical arm fixed above the stereotaxic frame. The animal was further secured to the bite bar of the stereotaxic frame. Anaesthetic depth was maintained by adjusting the level of inspired isoflurane (0.25-0.75%) delivered under 100% oxygen concentration.

For the anaesthetised animal experiments conducted in chapter 5 subjects underwent one imaging session in which 2D-OIS was used to monitor haemodynamic changes only. For the

anaesthetised experiments in chapter 6 however, subjects underwent two imaging sessions: the first session consisted of 2D-OIS to monitor haemodynamic changes only; and the second imaging session combined 2D-OIS with the insertion of a multi-channel electrode into the active whisker region, to monitor concurrent haemodynamic responses and neural activity.

For these anaesthetised animal experiments, the experimental paradigm consisted of 2s and 16s mechanical whisker stimulation (at 5Hz frequency; Figure 2.2). The anaesthetised experiments conducted in chapter 6 also additionally included carbogen experiments, in which there was no whisker stimulation, but the temporary induction of 10% carbon dioxide under 100% oxygen.

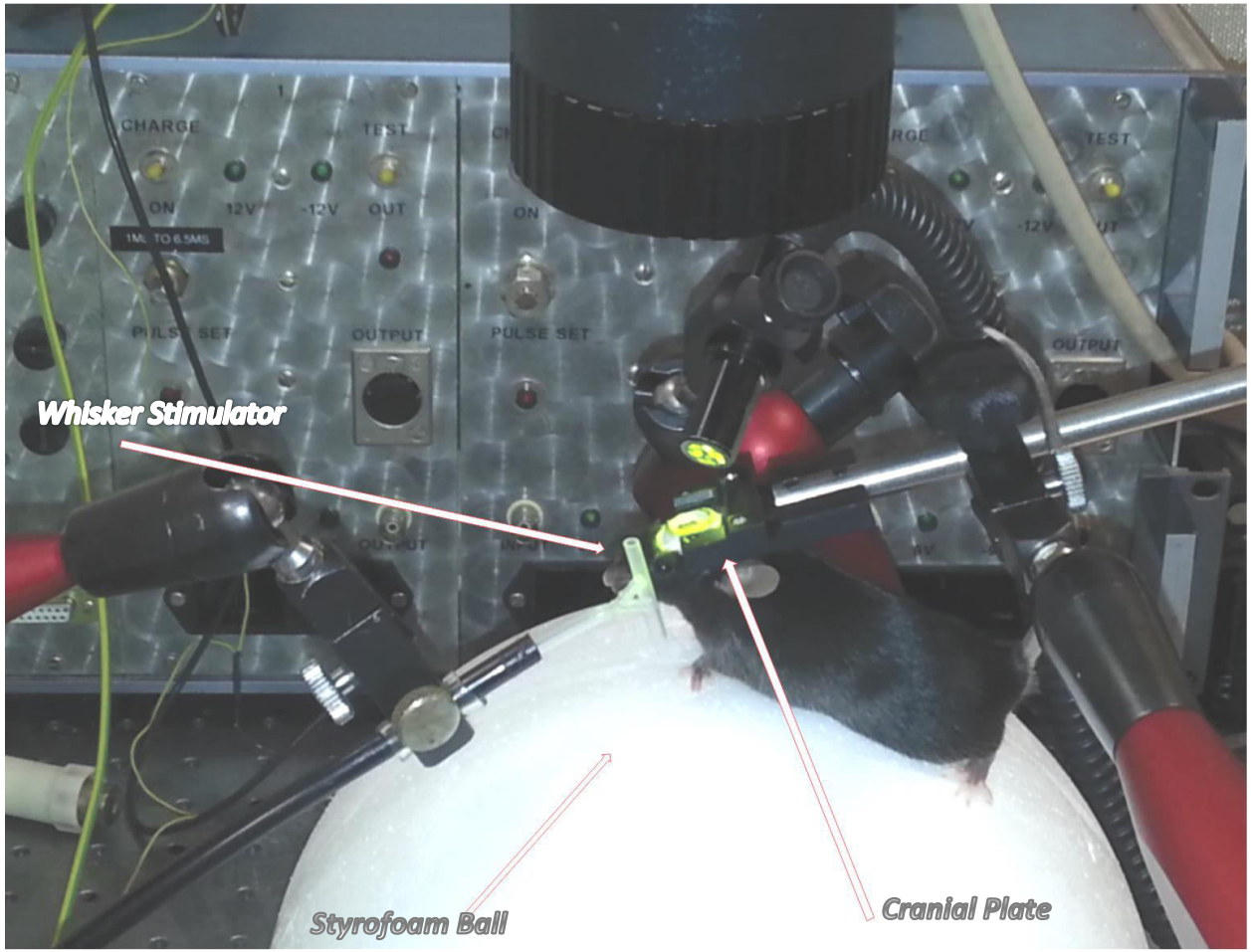

Figure 2.3 – The Experimental Set-Up for the Awake Mouse Preparation

2.5 Experimental Techniques

The theoretical background underlying the experimental techniques employed in this thesis is described, as well as explanations of the practicalities of implementing such methods.

2.5.1 Optical Imaging Spectroscopy: Study of Cerebral Blood Volume and Oxygenation

The aim of optical imaging spectroscopy (OIS) is to estimate concentration changes of total blood volume (Hbt), oxyhaemoglobin (HbO_2), and deoxyhaemoglobin (Hbr) in the cortex over a two dimensional plane using changes in the amount of reflected light. Previously, the optical imaging spectroscopy method has been described in detail (Mayhew, et al., 2000); and implemented in many studies conducted at the Sheffield laboratory (e.g. Berwick et al., 2005; 2008; Boorman et al., 2010; 2015; Harris et al., 2014).

2.5.1.1 Theory of Optical Imaging Spectroscopy

HbO_2 and Hbr have different absorption coefficients at different wavelengths of light (Figure 2.4). Optical imaging spectroscopy capitalises on these differences, in order to distinguish between oxygenated and deoxygenated blood. Clear differences can be seen in the absorption spectra between HbO_2 and Hbr in Figure 2.4.

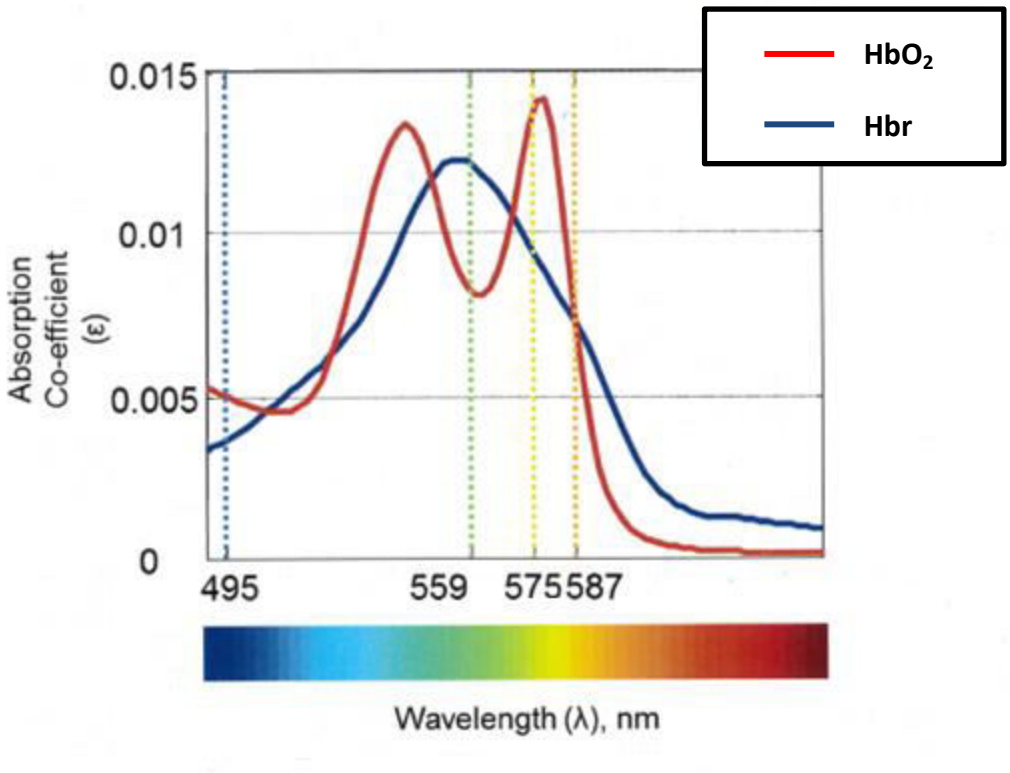

Figure 2.4 – Simplified HbO_2 and Hbr Absorption Spectra

(adapted from Bruyns-Haylett, 2013)

The absorption coefficient spectra (ε) for oxyhaemoglobin (HbO_2) and deoxyhaemoglobin (Hbr) are shown to follow a relatively similar path, although they have maximally different absorption co-efficiency at three distinct wavelength points (495nm, 559nm, & 575nm, plotted as coloured dotted lines), with a fourth (587nm) absorption spectra which is similar for both (isosbestic point).

If a white light of intensity I_0 is shone onto a sample (e.g. the cortex), some of this light will be absorbed, and the rest will be remitted at the (measurable) intensity *I*. This level of absorption (also referred to as attenuation) can be calculated, providing there is no scattering of the photons of light. However, in the brain tissue the photons of light will scatter, which creates longer path lengths than in a non-scattering medium, increasing the chance that the photons will be absorbed. A continuous measurement of the pathways through the brain tissue which the photons of light take is not possible. Instead, a Monte Carlo Simulation (MCS) is used to estimate the unknown differential path length (Δl) which a photon of light would take at different concentrations of absorbents (Δc), with consideration of the different scattering angles (u) and thus scattering coefficients (μ_s) which may occur. This can be related to the differential attenuation (ΔA) that occurs.

2.5.1.1.1 Monte Carlo Simulations of Path Length

Through the MCS, estimates are made of how many 'steps' a photon will take before it is remitted (if it is remitted at all, Figure 2.5). This is illustrated in the figure below, in which the green path length is shorter than the blue path length. As such, the scattering coefficients (μ_s) of the two path lengths will be different (i.e. the blue will be larger than the green). To calculate the path length estimations, the angle of scattering (u) and the scattering coefficient (μ_s), must be inputted into the MCS algorithm.

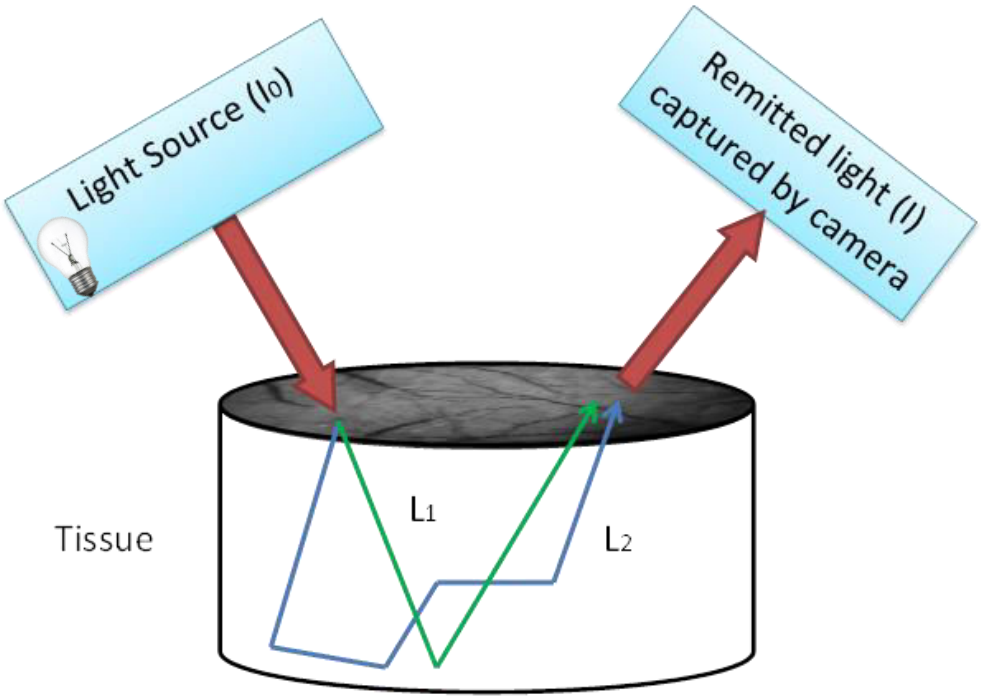

Figure 2.5 – Variable Path Length of Photons Scattering in Tissue

Upon passing through tissue, light may be scattered or absorbed. The paths (L1, L2) of two example photons travelling through the tissue are shown in blue and green. The green photon is subject to less scattering than the blue photon, and so will have a smaller scattering coefficient by comparison.

To estimate the angle of scattering (u), the Henyey-Greenstein probability function is used to create a weighting factor, g:

$$g = \int_0^{2\pi} \cos\vartheta . p(\vartheta) . d\vartheta \qquad (1)$$

Here, if g=0, random erratic movement is expected, if g=1, no scattering occurs, and if g=-1, the photon reverses its previous movement.

Here, a weighting factor of g=0.85 is assumed, which indicates a large degree of forward scattering (Cope & Delpy, 1988). This assumption was based on *in vivo* measurements made by Johns et al., 2005, where the scattering was largely found to be homogenous over the cortical surface (the top 2mm, which OIS records from).

The next equation is used to create the scattering angle (u), through the calculation of a randomised weighting (t) for each path length, in which s is a randomly generated number.

$$t = \frac{(1+g^2 - (\frac{1-g^2}{1+(g*s)})^2}{2*g} \quad (2)$$

$$\therefore u = \arccos(t) \quad (3)$$

From here, the scattering angle (u) can be used to create the reduced scattering co-efficient μ_s‘.

$$\mu_s' = \mu_s(1-u) \quad (4)$$

Following the definition of the scattering co-efficient, it can be used within the MCS to create a density function $\varphi(x)$ of path lengths, which is then binned into segments (x). Referring back to the example in Figure 2.5, L1 has 2 paths, and L2 has 5 paths. An exponential decay function is incorporated which includes the baseline attenuation coefficient (μ_a), meaning the density function can be used to calculate the differential path length:

$$\Delta l = \frac{\int_0^\infty \varphi(x)*x*e^{-x\mu_a}dx}{\int_0^\infty \varphi(x).dx} \quad (5)$$

The different wavelengths will have altered differential path lengths ($\Delta l(\lambda)$), which can then be applied in a modified Beer-Lambert equation:

$$\Delta A(\lambda) = \Delta l(\lambda).\left(\varepsilon_{HbO_2}(\lambda).\Delta[HbO2] + \varepsilon_{Hbr}(\lambda).\Delta[Hbr]\right) \quad (6)$$

Within this modified Beer-Lambert calculation, the change in attenuation is a measured variable for each wavelength of light used ($\Delta\tilde{A}(\lambda)$). The path lengths for the different wavelengths can be calculated as previously detailed ($\Delta l(\lambda)$) and the specific absorption coefficients (ε) for HbO_2 and Hbr are already known for each of the different wavelengths (Figure 2.4). As such, there are two unknowns remaining in equation 6: the change in the concentration of HbO_2 ($\Delta[HbO2]$), and Hbr ($\Delta[Hbr]$). The use of four wavelengths of light generates four equations.

2.5.1.1.2 The Tissue Model (Homogenous or Heterogeneous)

Previous 2D-OIS studies conducted in the Sheffield laboratory have employed a homogeneous tissue model (Berwick et al., 2005; Jones et al., 2005; Kennerley et al., 2005; Martindale et al., 2003), which assumes that the baseline levels and resultant changes of cerebral blood volume (Hbt_0) and oxygenation (Hbo_0) are the same throughout the different layers of cortex. However, as the brain is known to display a heterogeneous distribution of vascular structures (Pawlik, 1981), the model was updated to improve its accuracy (Kennerley et al., 2009).

As mentioned above, the scattering can be assumed to be homogeneous on the superficial 2mm of the cortex (Johns et al., 2005), and so in the updated heterogeneous model, the reduced scattering coefficient was given by the following equation (Van der Zee, 1992):

$$\mu_s'(\lambda) = 2.7 * \left(\frac{\lambda}{560}\right)^{-1} \quad (7)$$

As such, the coefficients which change across the different layers are given by:

- The coefficient of absorption (μ_a) is updated to include five values (each value for one of the previous five layers in the model).

$$\mu_a(\lambda) \propto (\varepsilon_{Hbo}(\lambda)HbO2 + \varepsilon_{Hbr}(\lambda)Hbr) \quad (8)$$

- Baseline values of total haemoglobin (Hbt_0).
- Baseline values of oxygen saturation (Hbo_0).

Further explanations of exactly how the layer coefficients for these parameters were calculated can be found in Kennerley et al. (2009). Briefly, the BOLD signal and other relevant fMRI measurements were used to inform the updated 2D-OIS algorithm.

The total blood volume/haemoglobin can thus be calculated by summing the values for the oxy and deoxy haemoglobin together:

$$\Delta[Hbt] = \Delta[HbO2] + \Delta[Hbr] \quad (9)$$

2.5.1.2 Application of the Optical Imaging Experimental Method

For this thesis, the imaging of animal subjects was conducted following the surgery (and additional recovery period), using two-dimensional optical imaging spectroscopy (2D-OIS). In the anaesthetised experiments, the animal was fixed in a stereotaxic frame (Kopf Instruments), and for the awake experiments the animal was head-fixed using a headplate holder. The stereotaxic frame was angled to reduce specularity when the animal was placed under the CCD camera (used to collect images during 2D-OIS). For the repeated imaging experiments conducted with the awake animal subjects, the animal was fixed on top of a Styrofoam ball which was placed directly under a CCD (charge-coupled device) camera (1M30P, Silicone Mounted Design; SMD, operating in 4x4 binning mode).

2D-OIS records the changes in the reflection spectra of imaged cortical tissue. The cortex was illuminated with a white light source (300watt halogen bulb) filtered through a switching galvanometer system (Lambda DG-4, Sutter Instruments Company). The high-speed filter changer used 4 different wavelengths of light (order *575, 559, 495* and *587* nm) to optimise the differences between oxygenated and deoxygenated haemoglobin, and the switching of the filters produced the spectrographic sequence necessary for optical imaging. Each filter was presented for 1/32 of a second (32Hz camera frame rate), which resulted in a frame rate of 8Hz for each wavelength (32/4). The remitted light passed through a lens (focal lens 100mm, Leica Inc/Ltd) followed by a microscope with magnification 0.63-6x (MX9.5 and MZ8 Leica), before reaching the CCD camera. The spatial resolution of the CCD camera approximately meant each pixel represented 75x75um of the cortex, with a temporal resolution of 125ms.

2.5.1.3 Optical Imaging Data Analysis

Data analysis was performed using MATLAB (Mathworks Inc, USA). The four wavelength data were processed using a simplified algorithm to provide haemodynamic information (as detailed in section 2.5.1.1). Optical imaging data were analysed in all experimental chapters within this thesis (chapters 3, 4, 5 & 6).

2.5.1.3.1 Analysis of Temporal Responses

An in-house software tool was used to visualise an image of the exposed somatosensory cortex and underlying vessels (middle cerebral artery, MCA, and draining veins). An initial fast mapping experiment was conducted in which the whiskers were mechanically stimulated, and the specific area of the cortex which showed the greatest magnitude response to the whisker stimulation was identified. To isolate the whisker barrel region, a pre-programmed design matrix (statistical parametric mapping, SPM), optimised for the typical haemodynamic response profile expected for specific whisker stimulation paradigms (e.g. stimulation onset of 10s and characteristic shape of the Hbt response programmed) was applied. This 'fast' analysis allowed the position of positive haemodynamic responses to be localised. Once the whisker barrel location was confirmed, the experimental paradigm commenced (e.g. no stimulation, 2s stimulation, or 16s). The area of interest was then selected and extracted, and the haemodynamic responses (Hbt, HbO_2 and Hbr) from these regions were then averaged across multiple experimental trials to reduce the size of the data for processing. The locations chosen using 2D-OIS to represent the whisker barrels were subsequently used for the placement of electrodes to record neural activity (for chapter 6).

2.5.1.3.2 Analysis of Spatial Responses

Haemodynamic response maps (Hbt, HbO_2 & Hbr) were generated by averaging spatial images of the haemodynamic activity during locomotion and/or whisker stimulation (0-5 seconds from onset). These response maps were used to visualise the spatial extent of the haemodynamic responses.

A 'pixel analysis' was also developed to capture the size (spatial extent) of the Hbt response during whisker stimulation (2s & 16s) and/or locomotion (Figure 2.6 & Figure 2.7). The

images of the Hbt responses over time (during locomotion or stimulation) were first subject to cropping (to remove the edges of the image, which were typically dental cement); and filtering and smoothing (to remove noise (pixels >10 standard deviations above the average), and individual vessel definition). The data were then split into time bins, whereby an average spatial image over 1 second was generated every 0.5 seconds (to create Hbt spatial map frames over time). Next, a threshold was defined: the minimum threshold was 2 standard deviations greater than the average pixel response (i.e. to locate the variance resulting from stimulation), and the maximum threshold was the 99^{th} percentile of the data (top 1% excluded in case there were still noise spikes). Once defined, the threshold was applied to the data (each frame over time), and the pixels within the pre-specified threshold were retained. The largest group of pixels (which had to be >100 pixels in total) was selected, and any holes were filled in, or spurs (i.e. spikes of noise) removed, from the object. Next a mask was drawn around the remaining response area, and the size of this mask was calculated as a percentage of the whole image over time (i.e. for each time bin).

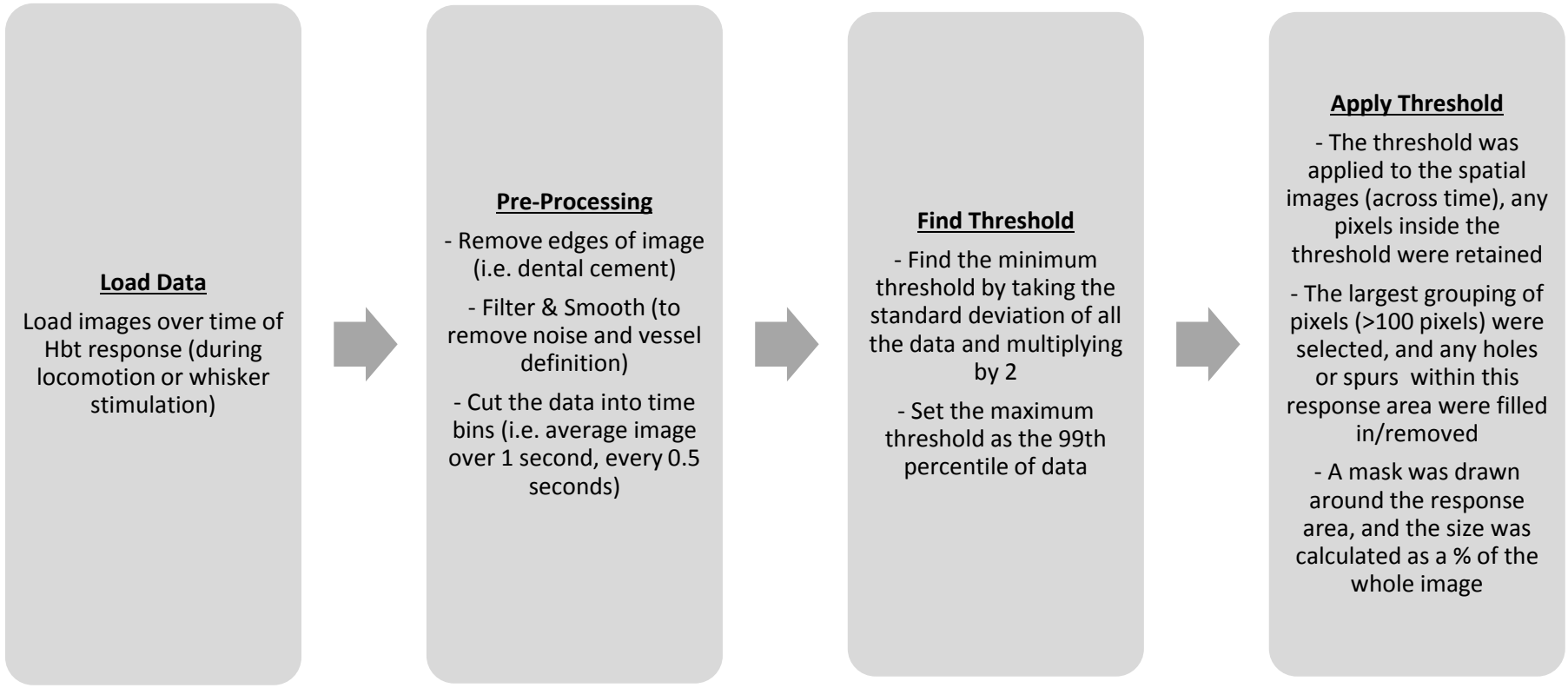

Figure 2.6 - Flow Chart demonstrating the Pixel Analysis Method for Assessing the Spatial Extent of Hbt Responses during Stimulation or Locomotion

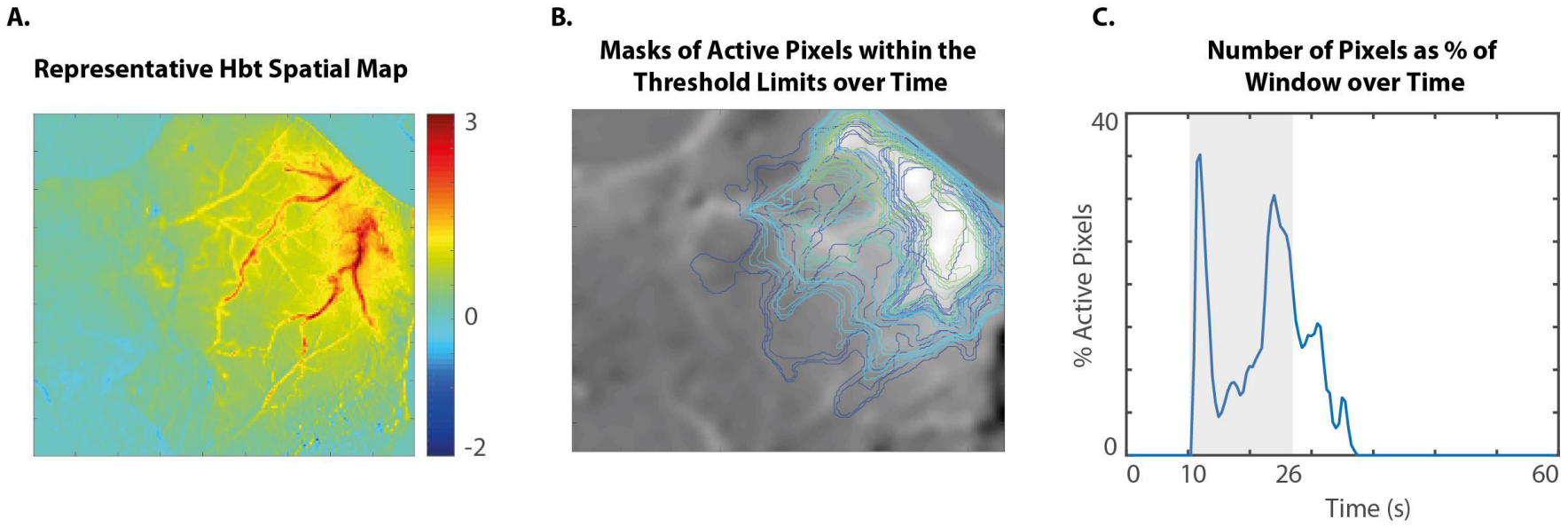

Figure 2.7 –Demonstration of the Selection of Active Pixels within the Cortical Image

A. *A representative spatial map which is loaded into the Pixel Analysis - each frame is averaged over 1 second, every 0.5 seconds.* ***B.*** *For each spatial map loaded over time, the largest group of active pixels (within the threshold limits) are detected, and a mask is drawn around the boundaries.* ***C.*** *The size of this mask (around the active pixels boundaries) is calculated as a percentage of the whole window over time.*

2.5.2 Multi-Channel Electrophysiology: Measures of Electrical Activity

2.5.2.1 Electrophysiology Theory

Electrophysiology concerns the study on the electrical properties of biological cells, such as neurons. It is necessary to measure neural activity alongside haemodynamic changes to aid in the interpretation and understanding of neurovascular coupling. Multi-channel electrodes were inserted perpendicularly into the cortical surface to record neural activity across the different layers of the cortex (Figure 2.8). The probes had 16 linearly arranged recording sites (100µm spacing), each with an area of 177µm² and an impedance of 1.5-7MΩ. The width of the probe tip was 33µm at the end point, and 123µm at the uppermost recording site (Neuronexus). Each of the 16 electrode sites was able to record a range of neural processes to a temporal resolution of 0.04ms at sampling rate of 24.414kHz. Multiple recording sites allowed for recording with a spatial dimension, however, the raw recorded signals are a complex combination of signal summation across the sites. The stimulation and resultant activation of various neurons and neural circuits within somatosensory cortex encompass a large range of detectable neural activity, with differing power, frequency and waveform shape. For the purpose of this thesis, and for simplification of neural recordings, there was a focus on local field potentials.

2.5.2.1.1 Local Field Potentials

The activation of neurons results in the flow of positive ions (e.g. Na^+) into specific active sites of the axons or dendrites. The in-flow of ions described creates an extracellular current sink. Other ions flow out of more distant inactive sites, producing a current source equivalent to the sink (Logothetis & Wandell, 2004). Low impedance extracellular electrodes detect changes in current flow by recording a weighted sum of all current sources and sinks. It is the weighted summation of sources and sinks that are referred to as local field potentials (LFPs). The LFP represents the low frequency integrated synaptic processes, which include potentials of somato-dendritic spikes and voltage gated membrane oscillations (Logothetis & Wandell, 2004). The signals recorded using the multichannel electrode are thought to be integrated to within 0.5-3mm of each electrode recording site (Mitzdorf, 1987). The magnitude of the detected LFP is linked to the size and topology of the dendritic field arrangement and has little to do with cell size. Dendrites which face in the opposite direction to the stomata of a nearby cell result in the production

of strong dendrite to stoma dipoles when activated by a synchronous synaptic input. This strong dipole relationship is commonly seen in pyramidal cells in the cerebral cortex. The pyramidal cells have most of their dendrites running vertically down through the cortex (perpendicular to the cortical surface), which means they provide a maximum LFP signal, due to this ideal 'open field' arrangement (Legatt et al., 1980; Logothetis & Wandell, 2004). The LFP signals, taken from the electrode recordings in this thesis, have been assumed to represent integrated sub-threshold dendrite and synaptic processing.

2.5.2.2 Measuring Neural Activity – Concurrent Electrophysiology and 2D-OIS recording

Neural activity was measured concurrently with haemodynamic changes for the chronic anaesthetised experiments only (chapter 6). 2D-OIS was used to locate the whisker barrel field in the right somatosensory cortex, informing the placement of the electrode for concurrent measurement of electrophysiological activity (Figure 2.8). The main challenge when simultaneously recording 2D-OIS and electrophysiology, was to ensure that the orientation of the electrode minimised any shadowing of the 2D-OIS light source and did not block the camera view.

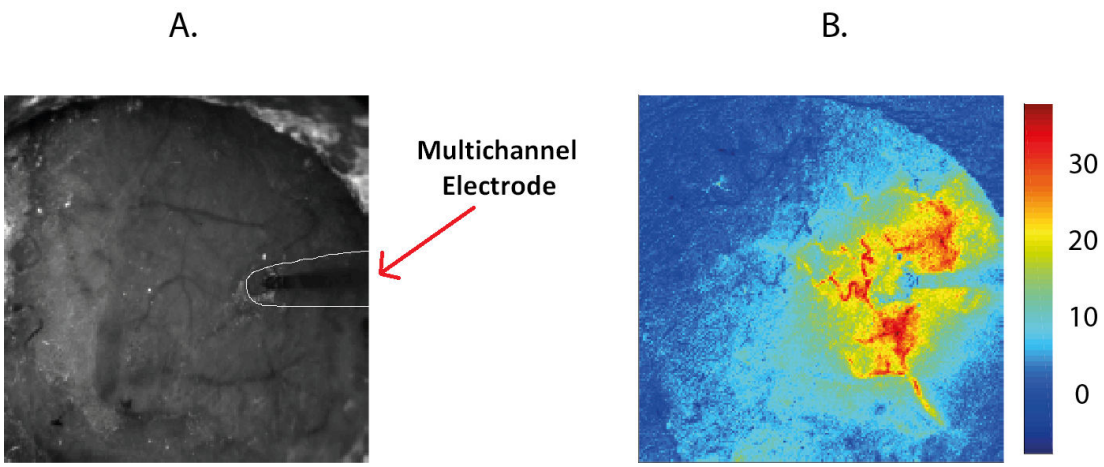

Figure 2.8 – Concurrent Electrophysiology and 2D-OIS

A. *Camera image taken during a representative experiment. The multi-channel electrode is inserted perpendicularly into the cortical surface, and is highlighted with a white outline.* ***B.*** *2D-OIS image of activation (Hbt). Mechanical stimulation of the whisker pad causes changes in the Hbt in the contralateral whisker barrel cortex.*

2.5.2.2.1 Electrophysiology Hardware

The subject was secured in a stereotaxic frame, and a single, multichannel electrode was used in all cases. A 'headstage' consisting of a 32pin D-sub socket (Tucker Davis Technologies; TDT) connected to an 18pin dual-in-line (DIL) socket was attached to the stereotaxic arm. A reference (indifferent) electrode was connected to the top left DIL socket. This reference electrode was a silver wire of 10cm in length and was inserted subcutaneously through the skin of the animal's neck. The DIL hole on the top right was grounded (in the faraday cage). The 16 channel electrode probe (NeuroNexus Technologies) was attached to the lower 16 pins. An isolated pre-amp device was also connected to the D-sub socket of the 'headstage', and this pre-amp was connected via a fibre optic lead to a modular data acquisition unit (TDT). A custom written MATLAB (The Mathworks Inc., USA) interface was used to collect data and perform basic processing. Electrophysiology experiments were always performed in a five sided faraday cage, with an open front to allow for access to the animal and the experimental set-up. The faraday cage was necessary to prevent unwanted radio frequency interference, for instance the 50Hz common mode signal arising from the electrical mains or the electrical noise from much of the surrounding lab equipment. Earth leads were used to ground any metal or electrical items present inside the faraday cage during the running of the experiments.

2.5.2.2.2 Electrode Placement

The electrode location was identified using 2D-OIS to locate the area of peak activity within the exposed S1 in response to mechanical stimulation of the whisker pad (see section 2.5.1.3). An activation map was generated from the haemodynamic recorded using 2D-OIS, which was spatially registered and overlaid onto a reference image of the cortex. This allowed the researcher to visualise the location within the exposed somatosensory cortex in which to insert the electrode. A small hole was then made into the thinned skull using a dental drill. The electrode was slowly lowered perpendicular to the cortical surface into the selected site, with great care taken to avoid any bruises, bone sutures, and major dural or cortical vessels. It was important to avoid such regions to prevent excessive bleeding, which could affect electrophysiological recordings as well as to prevent the blocking of light for the application of 2D-OIS. The exact positioning of the electrode was monitored using the microscope, and the probe was lowered until the tip made contact with the cortex,

equating to a cortical depth of around 1550µm (meaning the top recording site was 50µm above the cortical surface).

Following electrode placement the preparation was allowed to stabilise for up to an hour to minimise the effects of cortical spreading depression (Lauritzen et al., 1982; Ba et al., 2002). Electrode function was checked before continuing with the experiment, using the mechanical whisker device to stimulate the whisker pad (50 pulses, frequency 5Hz, duration 1s, inter-stimulus interval 2s). Experimental recordings were initiated once normal patterns of electrical field potentials were observed, and there was little observable noise in the data. If the neural data seemed distorted or particularly noisy, adjustments were made to the probe location and/or the earth connections.

The electrophysiological data acquisition equipment (RZ5, Tucker Davis Technologies) was set to record, and used the stimulation output trigger sent to the electromechanical whisker stimulator for temporal synchronisation with the other neuroimaging equipment. The data were recorded with a sampling frequency of 24K. Data were collected from a range of experimental stimulation paradigms (i.e. no stimulation, 2s whisker stimulation, or 16s whisker stimulation).

2.5.2.3 Analysis of Recorded Neural Activity

The electrophysiological data were first pre-processed by applying a band stop filter at 49-51Hz to remove the 50Hz common mode noise.

2.5.2.3.1 Local Field Potentials

For the purposes of this thesis (chapter 6), the time course of the LFP was plotted and assessed, and metrics were taken (i.e. the minima). For the analysis of this LFP data, the LFP responses from all 16 channels were plotted and visualised, and the 4 channels next to each other which were the most responsive to the stimulation, and did not look like stimulation-artefacts, were selected. The data from all 16 channels were not used, due to the size of the electrode compared to the size of the mouse brain. Likely, some of the deeper channels would be in subcortical regions, which goes beyond the scope of this thesis. An example of the 16 channel LFP output is shown in Figure 2.9 (C), with normalised baseline points

plotted in order of depth. An example of a stimulus-evoked LFP response (averaged across 4 channels) was shown in chapter 1 (Figure 1.3).

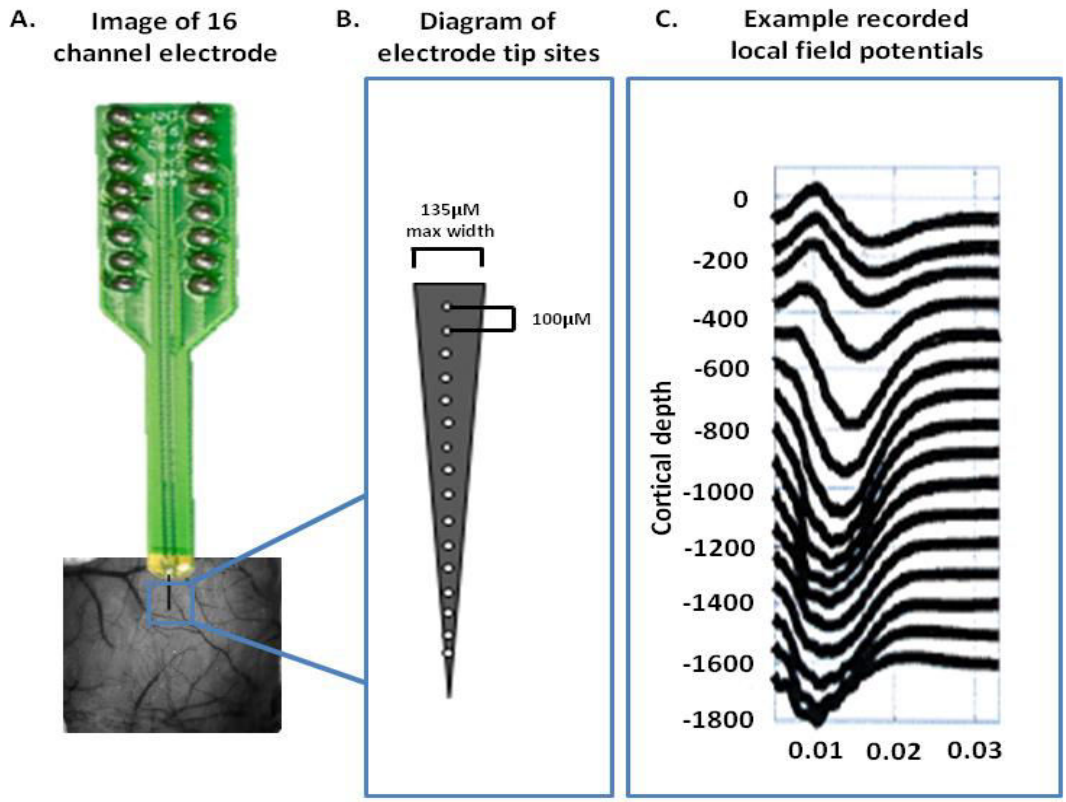

Figure 2.9 – Recording of the Electrophysiology with a Multi-Channel Electrode (adapted from Boorman, 2009)

A. *A 16 channel recording electrode is perpendicularly inserted into the whisker barrel cortex.* ***B.*** *Schematic diagram of the electrode tip, showing spacing and the maximum width.* ***C.*** *Example local field potentials plotted in order of spatial depth through the cortex.*

2.5.3 Statistical Analysis

Statistical tests will be applied throughout the experimental chapters (chapter 4, 5 & 6). The data were statistically analysed using two-tailed paired t-tests. Bonferonni-adjusted α was applied to correct for multiple comparisons, with p levels for significance set at 0.05 before Bonferroni's correction for multiple comparisons. Comparisons were made across the temporal response profiles of haemodynamic (area under the Hbt curve, and maximum peak of the Hbt curve) and neuronal (initial LFP depolarisation and overall average LFP

depolarisation during stimulation) responses. The number of active pixels in the spatial Hbt response maps over time were also compared across subjects.

Chapter 3

The development of a novel platform for multi-modal neuroimaging and behavioural monitoring of awake, head-fixed mice

3.1 Abstract

Assessing neurovascular coupling in the same mouse chronically without the need for anaesthetic is an important technique as it avoids the confounds of anaesthesia and reduces the number of animals needed at separate time points. However, an awake behaving mouse introduces its own complexities in terms of behaviour and locomotion that need to be controlled for. Here, a novel awake mouse preparation was developed in which subjects, with a thinned cranial window overlying the somatosensory cortex, were head-fixed atop of a spherical treadmill whilst haemodynamic activity and locomotion were measured during both sensory-evoked and spontaneous experimental paradigms (n=8). Novel methods were developed to detect locomotion both directly (using an optical motion sensor), and indirectly (using motion artefacts). Locomotion caused an increase in the total blood volume in the whisker barrel region compared to stationary periods. Image registration was applied to remove motion artefacts from the haemodynamic data. The novel imaging platform for imaging head-fixed awake mice was developed and tested in this chapter, and will be used in chapter 4 to assess haemodynamic responses.

3.2 Introduction

Neurovascular coupling is the process by which active regions of the brain are dynamically supplied with oxygen and glucose, via localised increases in cerebral blood flow (CBF). These haemodynamic changes drive the positive blood oxygenation level-dependent (BOLD) functional magnetic resonance imaging (fMRI), whose signal interpretation is often used to make inferences about underlying neural activity (Buxton & Frank, 1997; Buxton et al., 1998; Ogawa et al., 1990). Understanding the physiological mechanisms which form the basis of neurovascular coupling is thus a prerequisite for the accurate analysis and interpretation of fMRI signals (Hillman, 2014). In addition, there is mounting evidence that impaired neurovascular coupling occurs in a number of neurodegenerative diseases such as Alzheimer's, and so a more complete understanding of neurovascular coupling could lead to the possibilities of earlier diagnosis or more advanced therapeutic treatments for such diseases (Iadecola, 2013).

The use of *in vivo* animal models has advanced the understanding of the relationship between neural and vascular responses (Iadecola, 2004; Logothetis & Wandell, 2004) as they allow the use of invasive techniques that can measure both neural and haemodynamic responses at high temporal and spatial resolution. Previously the Sheffield laboratory has focused on investigating neurovascular coupling in the somatosensory cortex of the urethane anaesthetised rat (Berwick et al., 2008; Kennerley et al., 2009; Boorman et al., 2010, 2015). The rat was selected as a suitable model to study neurovascular coupling as the somatosensory pathway from the whiskers to the barrel cortex has a well-defined topography and a highly concomitant blood supply (Woolsey et al., 1975). The standard experimental procedure consisted of the electrical stimulation of the whisker pad, whilst optically imaging the haemodynamic changes through a thinned cranial window overlying the contralateral somatosensory cortex, and simultaneously measuring the corresponding neuronal changes via the insertion of multichannel electrodes into the whisker barrels (Berwick et al., 2008; Boorman et al., 2010).

Indeed *in vivo* experiments investigating neurovascular coupling in animals commonly use anaesthesia, as this allows for the use of invasive techniques with minimal interference from the motion of the subject. However anaesthesia can have direct effects on neurovascular coupling, altering neural and vascular physiology. Therefore the Sheffield

laboratory also compared results from anaesthetised rats with those from awake rats (Berwick et al., 2002; Martin et al., 2002, 2006, 2013a, 2013b). For these experiments the animals were placed into a harness which was suspended from a frame whilst haemodynamic changes evoked by a non-noxious stimulation of the whisker pad were recorded from the contralateral somatosensory cortex, again through a thinned cranial window (Martin et al., 2013b). While the animal was awake the animal was not fully mobile, and no attempt was made to measure any behavioural aspects of the animal.

An understanding of the relationship between neural activity and the associated haemodynamic changes is crucial, not only for the accurate interpretation of functional brain imaging data, but also because neurovascular coupling has been shown to breakdown in certain pathologies (e.g. Alzheimer's disease). The mouse is a well-placed model to investigate neurodegenerative diseases as recent developments have led to the creation of a number of transgenic models which replicate or mimic the symptoms of such diseases. The mouse somatosensory cortex mirrors the well-defined topography of the rat, thus also providing a useful model in the study of neurovascular coupling. However, a necessary prerequisite is to apply the same techniques that have been successful in exploring neurovascular coupling in the rat, to the mouse. Indeed several laboratories have successfully employed optical imaging techniques in the anaesthetised mouse (Cang et al., 2005; Neill & Stryker, 2008; Takuwa et al., 2012; Zhang & Murphy, 2007).

Whilst the anaesthetised mouse preparation facilitates the use of invasive optical techniques, there are confounds associated with the use of anaesthesia. These confounds may be particularly relevant for disease models, where baseline physiology is already impaired. Furthermore, the ability to chronically monitor the same subject is facilitated by awake behaving preparations, and this is especially important when monitoring disease progression. The awake preparation would also aid the use of paradigms with more complex behavioural tasks than just presenting somatosensory stimuli to probe underlying neural circuits. Thus it would desirable to establish an awake mouse optical imaging preparation.

Another possibility would be to adapt the available methodology of Martin and colleagues (*awake body-restricted rat experiments*; Berwick et al., 2002; Martin et al., 2002, 2006, 2013a, 2013b) to the mouse, however the mouse isn't as physically strong as the rat and so can be head-fixed without additional bodily restraint. Limiting the physical restraint reduces

stress from body restriction, permits more naturalistic behaviour, and allows for concurrent movement (locomotion) and whisking to be simultaneously tracked. For these reasons the methodology of Carandini and colleagues was adapted instead (Haider et al., 2013; Ayaz et al., 2013; Pisauro et al., 2013). This experimental set-up usually incorporates a head-fixed animal resting or walking atop of a Styrofoam ball, which was able to rotate as the animal moved. The movement of the floating ball is detected with optical motion sensors, providing information about the speed and direction of locomotion. The small mass of the mouse walking on the low-friction environment of the spherical treadmill minimises the force applied against the head holder, allowing for stable and long-term imaging. This has opened new avenues for studies on the effects of locomotion on mammalian cortical function, which has previously been limited in larger mammals (Chen et al., 2013). For the purposes of this experimental chapter, the skull overlying the somatosensory cortex was thinned to translucency (termed 'thin cranial window') during recovery anaesthesia. The efficacy of chronic thin cranial windows for repeated optical imaging experiments within the same mammalian subject has been previously demonstrated over time periods for up to 12 months (Holtmaat et al., 2009; Roome & Kuhn, 2014; Slovin et al., 2002).

3.2.1 Aims

Thus the aim of this chapter is to describe the building and testing of a novel platform for multi-modal, chronic imaging of awake head-fixed mice in Sheffield. Stimulation-evoked and spontaneously occurring cortical hemodynamic responses will be recorded. The development of the method will be described and illustrated with the preliminary data. Novel in house analysis was developed to track the locomotion of the animal, by measuring the displacements (rotation) of the spherical treadmill. In initial subjects treadmill displacement was not measured, and an alternative method for tracking locomotion was devised.

Data demonstrates the necessity of measuring subject locomotion to account for its effects on both the cortical haemodynamic signal, and its physical effects adding motion artefacts to recorded cortical images. A data analysis method was also devised to register images of the cortical surface to one another accounting for 'movement artefacts'. This novel method will allow for the subsequent investigation (in chapter 4) of the effects of locomotion interacting with stimulus-evoked and spontaneously occurring haemodynamic changes.

3.3 Methods

The methods detailed here build on those described in section 2.4.2, with specific additional information relating to the development of the locomotion detector.

3.3.1 Animal Subjects

Eight adult C57BL/6J mice were used for the experiments (24-40g, 2 male, 6 female; Harlan, UK). All animals were housed in a 12-h light/dark cycle in temperatures of 25°C. Food and water were available *ad libitum*.

3.3.2 Animal Surgery

All procedures were conducted in accordance with the guidelines and regulations of the UK Government, Animals (Scientific Procedures) Act 1986, the European directive 2010/63/EU, and approved by the University of Sheffield ethical review and licensing committee. Prior to aseptic surgery the mice were anaesthetised with fentanyl-fluanisone (Hypnorm, Vetapharm Ltd), midazolam (Hypnovel, Roche Ltd) and sterile water (1:1:2 by volume; 0.8ml/kg, i.p.). During surgery anaesthesia was maintained using isoflurane (0.5-0.8%) in 100% oxygen, and temperature was controlled using a homoeothermic blanket with a rectal probe (Harvard Apparatus) set at 37°C.

Mice were secured to a stereotaxic frame (Kopf Instruments) via ear bars and a bite bar, and the eyes were protected using viscotears® (Novartis). The hair covering the top of the head was shaved, and the skin beneath was treated with an iodine solution for disinfection purposes before being removed. The skull overlying the right somatosensory cortex was thinned until translucent using a dental drill to create the optical window (~3mm^2). The optical window was then coated with a thin layer of clear cyanoacrylate cement (Loctite, Henkel Inc UK), which added structural reinforcement and smoothed the window to reduce specular reflections from the skull surface during imaging. A stainless steel head plate, with a 5mm diameter hole in the centre, was fixed to the skull using dental cement (Super bond C&B; Sun Medical). Following the initial surgical procedure mice were removed from the isoflurane, placed into an incubator maintained at 28°C, and were closely monitored until

able to walk and groom independently, they were then housed individually and allowed at least 1-week to recover before any imaging commenced.

3.3.3 Awake Animal Imaging and Stimulation Acclimatisation

Following surgery and recovery, the mice were allowed to acclimatise to the experimenter, the imaging room, the experimental set-up, and head-fixation onto a spherical treadmill (Styrofoam ball, 20cm diameter) (Figure 3.2). Acclimatisation involved daily training sessions, which gradually increased their exposure time on the treadmill. During the first session mice were handled by the experimenter in the imaging room and allowed to move from hand to hand (~10 minutes), the mice were then allowed to explore the Styrofoam ball without head fixation for ~10 minutes while the handler manually controlled the ball's rotation. The second session followed the format of the first session, and the third session consisted of head-fixing the mouse to the ball with the room lights on for 10 minutes, followed by head-fixation to the ball for a further 20 minutes with the lights off. These 30 minute sessions were repeated daily with the lights switched off until the mice learnt to move freely and confidently on the Styrofoam ball, and showed natural grooming behaviour when stationary (usually after 2-3 sessions of head fixation to the spherical treadmill). Once natural grooming behaviour had been observed whilst head-fixed to the spherical treadmill, the final two training sessions (~30 minutes) consisted of head-fixation again but with the introduction of the mechanical whisker stimulator. The mechanical whisker stimulator consisted of a microprocessor (Arduino Inc) controlled stepper motor, remotely located with plastic tubing used to transfer movement to a vertical bar which made contact with the whiskers. A sweet popcorn reward was provided after every training and experimental imaging session (toffee popcorn, Sunkist).

3.3.4 Experimental Paradigms

For the experimental paradigms the whisker stimulator oscillated at 5Hz across the whiskers for 2 seconds every 25 seconds over 60 trials, or for 16 seconds every 70 seconds over 30 trials (Figure 2.2). In experiments in which there was no whisker stimulation (spontaneous activity), the trials followed the same format as those with the whisker stimulation (i.e. 25 seconds or 70 seconds), but the motor for the whisker stimulator was switched off meaning that the whiskers were not deflected.

3.3.5 Locomotion Tracking

Following initial 'pilot' experiments in the first two subjects (n=2), an optical motion sensor was later fixed next to a round disc attached to the side of spherical treadmill, so that locomotion could be concurrently tracked for all the remaining subjects (n=7) (Figure 3.1). An alternative method for detecting the locomotion events of the subjects in which no motion sensor was attached was later devised by selecting a region of interest on the edge of the exposed cortex which overlaid both the thinned skull and the dental cement. This allowed for large changes in motion to be detected in these initial sessions which did not have the treadmill data.

3.3.6 Two-Dimensional Optical Imaging Spectroscopy (2D-OIS)

2D-OIS was used to provide spatial estimates of changes in the cortical oxyhaemoglobin (HbO), deoxyhaemoglobin (Hbr), and total haemoglobin (Hbt) concentrations across the cortical surface. 2D-OIS uses a Lambda DG-4 high-speed galvanometer (Sutter Instrument Company, USA) to illuminate the exposed cortex with 4 wavelengths of light (495 ± 31 nm, 559 ± 16 nm, 575 ± 14 nm, and 587 ± 9 nm). A Dalsa 1M60 CCD camera was placed above the cortical window which collected remitted light with a frame rate of 32Hz, synchronised to filter switching essentially giving an effective frame rate of 8Hz. Images were acquired at a resolution of 184x184 pixels (individual pixel size on the cortical surface was ~75µm). Spectral analysis was used to estimate haemoglobin concentration changes, and was based on the path length scaling algorithm (PLSA) as described previously by Berwick and colleagues (2005). In brief, the algorithm utilises a modified Beer-Lambert Law with a path length correction factor. The concentration of haemoglobin in the tissue was estimated to be at 104µm based on previous measurements (Kennerley et al., 2005), and saturation approximated at 50% when breathing normal air. The spectral analysis provided two-dimensional images of the changes in HbO, Hbr and Hbt over time.

3.3.7 Data Analysis

All data analysis was performed using MATLAB® (MathWorks Inc, USA).

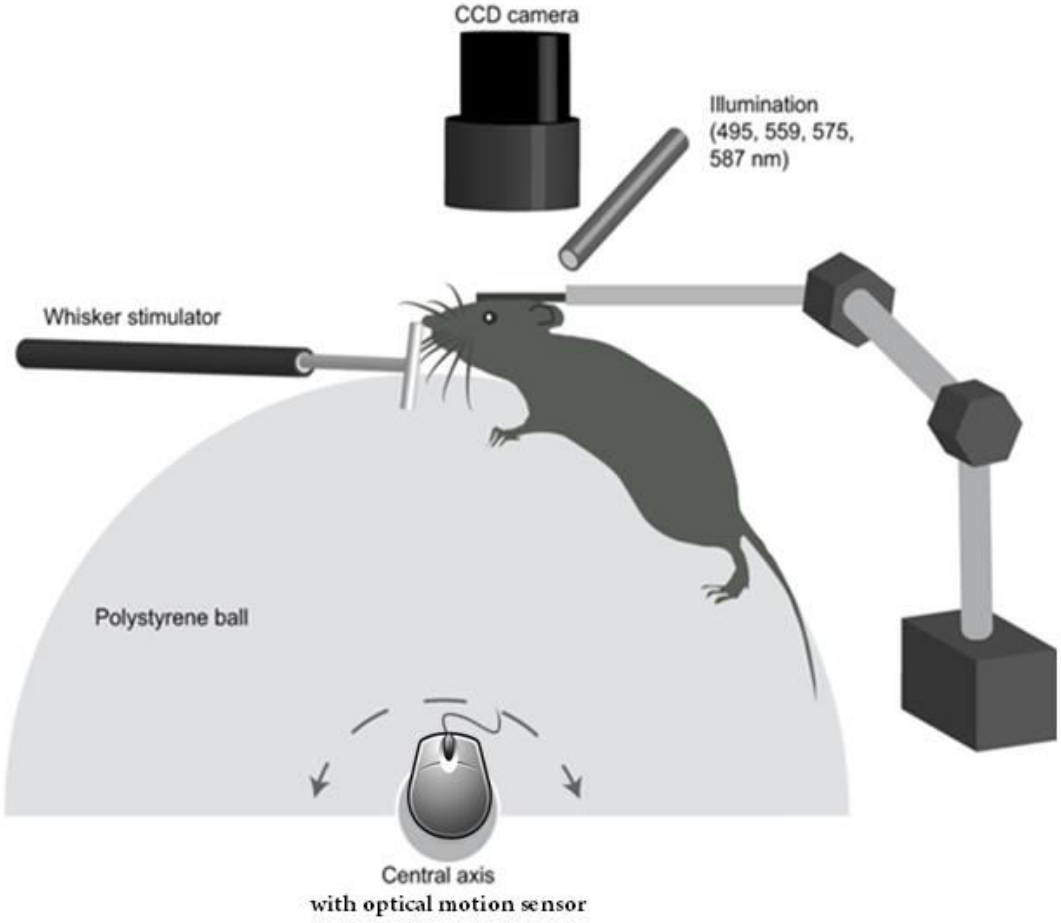

Figure 3.1 - Experimental Set-Up for Awake Mouse Imaging

(Image adapted from Sharp, Shaw, et al., 2015)

Haemodynamic changes were imaged using 2D-OIS through the thinned-cranial window of head-fixed mice. A four-wavelength flasher illuminated the thinned-skull preparation, and a CCD camera recorded the images. A vertical bar moved across the left whisker pad to evoke haemodynamic responses in the right whisker barrel cortex. Mice were able to move on a spherical treadmill which rotated in one dimension using a central axis. An optical sensor was fixed close to the central axis to detect changes in locomotion as the spherical treadmill rotated.

3.4 Initial Results, Observations & Subsequent Development of Analyses Tools

The following section describes the development of and the initial data obtained from the novel awake imaging platform.

3.4.1 Maintaining the Quality of the Thinned Cranial Window

Chronic imaging experiments involve multiple sessions in which the mouse is head-fixed atop of a spherical treadmill with the thinned cranial window uncovered. The window was covered with a thin layer of clear cyanoacrylate cement, to offer structural protection and allow the underlying vessels in the cortex to be seen clearly. To perform imaging over a long period of time the progressive quality of the thin window was assessed over a 3 month period (Figure 3.2).

Following initial surgery the subject required at least one week for recovery (Guo et al., 2014). During this recovery period no head-fixation took place, to avoid any bruising or unnecessary stress or pain to the animal, and the subjects were closely observed. After the recovery time, the underlying vessels were visible for imaging and there were no visible signs of inflammation. The quality of the thin cranial window, using the experimental set-up described with regular head-fixation over multiple sessions, was found to last up to 3 months, after which partial skull regrowth was typically observed (Figure 3.2 C). The skull regrowth usually started from the area of thinned skull nearest to Lambda (the suture line in the skull towards the back of the mouse's head), meaning the nearby 'active whisker region' was at risk of being obscured early into the regrowth period. After monitoring the first experimental subject for 3 months post-surgery, subsequent animals weren't imaged for longer than a 3 month time window to avoid skull regrowth covering the active region of interest. If necessary to image the animal over a longer time window, it is possible to extend the thinned cranial window so the active region of interest is in the centre and initial regrowth does not obscure the important vessels of interest.

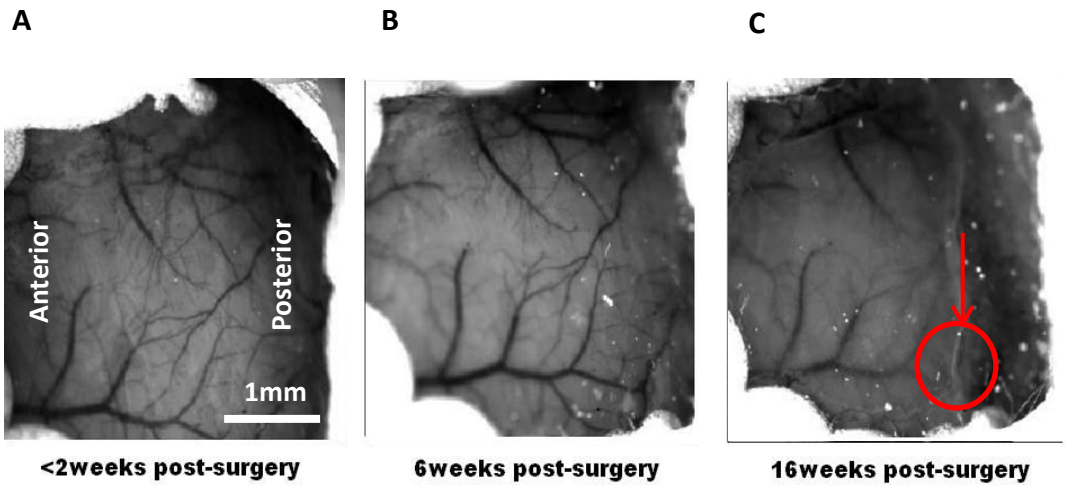

Figure 3.2 - Bone Regrowth over the Thinned Cranial Window Long-Term

A. *The thinned cranial window was allowed at least 1 week to recover post-surgery before any imaging took place. Imaging could begin once the thinned skull preparation was clear and showed no visible signs of inflammation.* ***B.*** *More than 1 month after the initial surgery had taken place the thinned cranial window was still clear, with underlying vasculature still visible for imaging.* ***C.*** *Repeated head-fixation and optical imaging was not ideal 3 months after the initial surgical procedure as skull regrowth occurred which partially obscured the region of interest. The red arrow marks the skull regrowth, and the red circle marks the 'active whisker region' which was localised using mechanical whisker stimulation.*

Note: all 1mm scale bars presented in this thesis are approximations (based on the fact the entire span of each cranial window was ~3mm).

3.4.2 Chronic Two-Dimensional Optical Imaging

Following the assessment of the sustained quality of the thinned cranial window long-term, the haemodynamic changes across the exposed cortex were investigated. Chronic imaging allows for multiple optical recordings to be taken over a period of days or months. To compare the neurovascular coupling response between multiple imaging sessions however, it is important to ensure that the same spatial area of exposed cortex is consistently imaged. Due to the laboratory facilities being shared by different teams of researchers, it was not possible to permanently fix the experimental set-up between imaging sessions. To ensure spatial consistency of the cortical images between multiple experimental sessions it was important to record external parameters such as the angle, orientation and zoom of

the CCD camera, and the exact location of the spherical treadmill set-up in the metal faraday cage (positioned below the CCD camera). A reference image was acquired during the first imaging session to visually check that the imaging plane was consistent across sessions. Spatial consistency between experiments was important for the later analysis of the spatial spread of the cerebral blood volume changes, which occurred both during whisker stimulation and periods of locomotion.

For each experimental session a region of interest were selected from the somatosensory cortex, and used to generate subsequent time-series to display the temporal blood volume changes. A mechanical whisker stimulation was used to evoke haemodynamic changes which were used to spatially localise the whisker barrels. A region was selected overlying the whisker barrels by regressing the time series for each pixel in the image of the cortex against a design matrix of a representative 'box car' haemodynamic response function. Subsequent 'activation' z-scores were then calculated on a pixel-by-pixel basis, and the 2000 pixels within 50% of the maximum z-score were selected to form the 'whisker barrel region' used in subsequent time-series analysis (Figure 3.3). It was essential to keep the whisker region selection consistent between experiments to allow for the comparison of the temporal blood volume changes in response to whisker stimulation and/or locomotion.

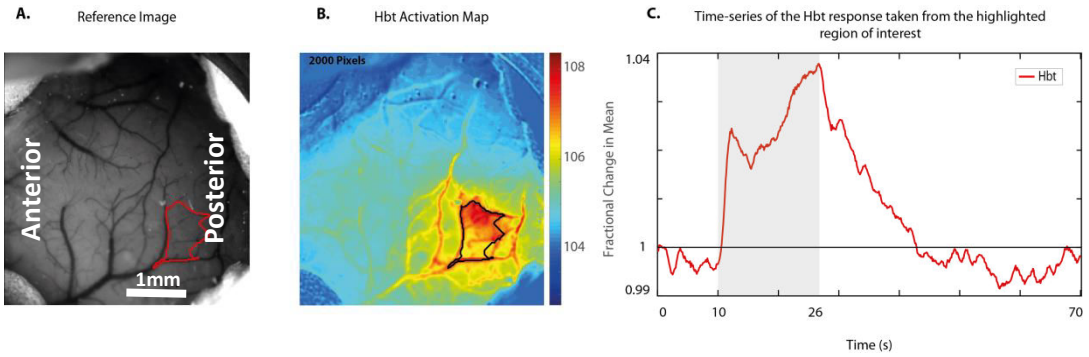

Figure 3.3 - An in vivo image of the surface vasculature and the averaged spatial and temporal activation maps during a 16s-mechanical whisker stimulation

A. *Representative in-vivo image of the thinned cranial window overlying the somatosensory cortex with the underlying surface vasculature visible.* ***B.*** *Image shows the Statistical Parametric Mapping (SPM) z-score map of the Hbt response to a 16s whisker stimulation. The black highlighted region shows the 2000 pixels selected which are within 50% of the maximum z-score used to form the active whisker region of interest.* ***C.*** *The corresponding time series of the average cortical haemodynamic response (Hbt) elicited by the 16s whisker*

stimulation in a representative subject (for the 2000 pixels which were selected to form the whisker region of interest).

3.4.3 The Detection of Locomotion using an Optical Motion Sensor

Following the selection of the regions of interest, the next step was to monitor locomotion as the subjects were allowed to move whilst head-fixed on a freely-rotating spherical treadmill. During the initial experiments it was observed that the subject had distinct temporal periods of locomotion or remaining stationary during experimental imaging sessions. In the absence of stimulation, spontaneously occurring haemodynamic changes were observed whilst the animal was running, and so locomotion was deemed an important factor to measure. Therefore, following initial pilot imaging, an optical motion sensor was then fixed to the spherical treadmill which detected movements of the ball and recorded locomotion directly into a custom-built MATLAB® locomotion tracker interface (The Mathworks Inc., USA).

The locomotion tracker recorded the movement of the spherical treadmill and generated a data file which contained: the locomotion data (a vector to show the ball rotation across each sample point, stationary periods were marked with zeros, with numerical integers reflecting the displacement of the spherical treadmill during the locomotion periods (i.e. the higher the number the faster the ball rotation)); the time vector (which corresponded with the walking data, and allowed for the measurement of locomotion across seconds); and the trigger points (which marked the onset of the whisker stimulation across all the trials, and could be used to temporally interpolate the locomotion data so that it was synchronised with the timing of the haemodynamic data for later comparison) (Figure 3.4 A).

This locomotion data (from the optical motion sensor) was then analysed to detect the onset of movement, and to extract the corresponding haemodynamic changes in the somatosensory cortex during these locomotion periods. The haemodynamic data were recorded using a CCD camera, before being sectioned into separate time blocks relating to distinct experimental trials. The locomotion data were pre-processed to remove noise using a median filter; a minimum threshold was then applied to further remove artefacts arising from system noise and very small subject movements (Figure 3.4 B). The filtered walking data were then temporally interpolated to match the sampling interval of the haemodynamic data (Figure 3.4 C). Haemodynamic and locomotion data were synchronised

using the onset of stimulation as a marker, to investigate the effects of locomotion on evoked and spontaneously occurring haemodynamic changes.

3.4.4 The Categorisation of Distinct Locomotion Events

To delineate locomotion events from stationary periods, walking data were analysed to categorise the onset and cessation of locomotion (see 'locomotion categorisation method', Figure 3.4). The temporal distance between separate locomotion events was subject to a minimum time threshold to ensure that each of the separate locomotion periods automatically selected were independent. Any locomotion events which fell within this minimum temporal period were classified as a single locomotion event (Figure 3.4 D). Locomotion and haemodynamic data were extracted for fixed periods before and after the onset of each locomotion event to assess the effect of locomotion on haemodynamic changes.

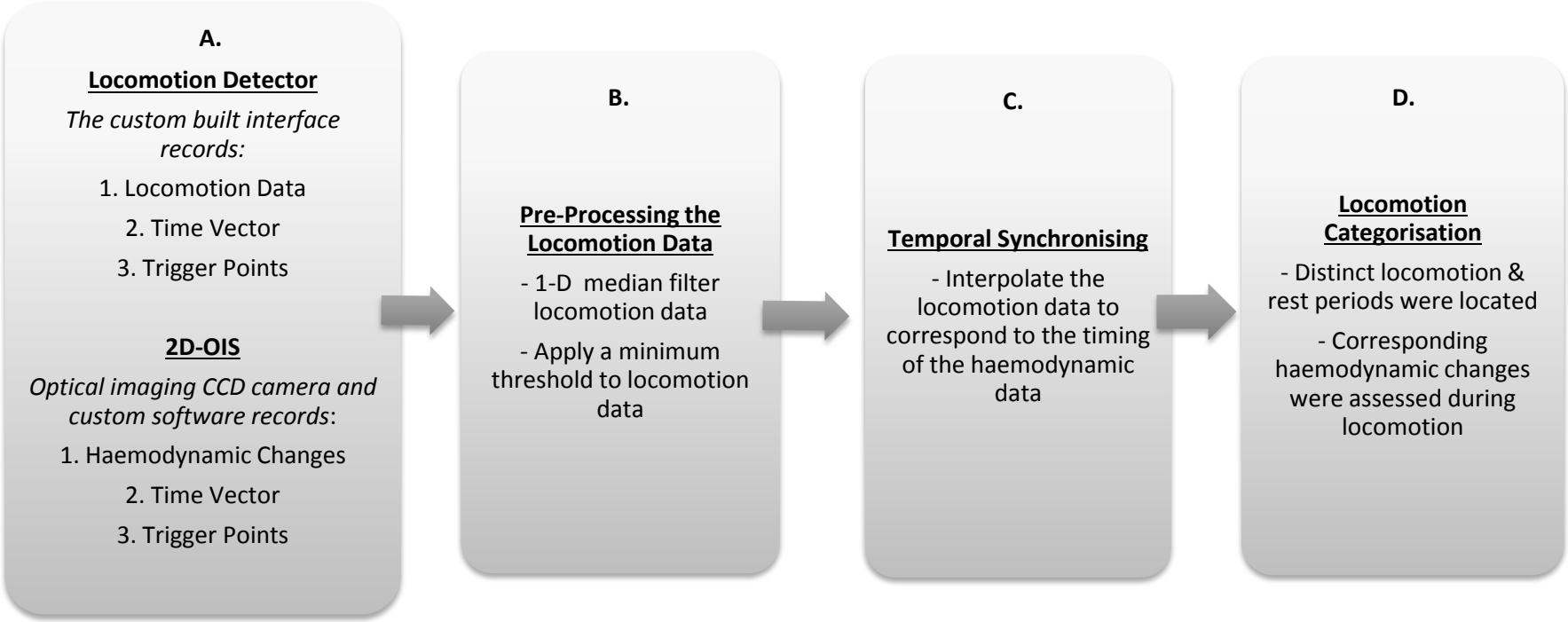

Figure 3.4 - Flow Chart demonstrating the Processing Steps for Acquisition, Pre-Processing, and Synchronisation of Locomotion Events and Haemodynamic Changes in the Somatosensory Cortex

A. *The locomotion detector records movement which is inputted into a custom-built interface to produce walking data (marked at each sample point with zeros for stationary periods and numerical integers when running); a time vector (in seconds); and trigger points (to mark the onset of stimulation). 2D-OIS is used to record haemodynamic changes in the somatosensory cortex; a time vector (in seconds); and the trigger points (to mark the onset of stimulation).* ***B.*** *The walking data is pre-processed to remove noise by applying a median filter, and then removing any small movements which fall beneath a minimum threshold. C. The walking data is temporally synchronised with the haemodynamic data so that the effect of locomotion on the blood volume in the somatosensory cortex can be later elucidated. D. Locomotion periods were located, the onset and cessation of locomotion was marked in time, and corresponding haemodynamic changes were assessed.*

3.4.5 The Extraction of Locomotion from Experiments with no Optical Motion Sensor

Preliminary analysis of discrete locomotion events demonstrated a potential relationship with cerebral blood volume changes. As locomotion was an important behaviour for consideration in the analysis of haemodynamic changes in the somatosensory cortex of the awake, head-fixed mouse, a method (intrinsic locomotion extraction) was devised to extract the locomotion information from recordings which did not include locomotion-specific recording equipment (i.e. optical motion sensor).

A small movement artefact was noted in the images of the cortex acquired during locomotion periods. The artefacts were found to be most prominent at the edge of the thin cranial window, and were most likely enhanced by the high contrast between the tissue and the metal head plate. The intrinsic locomotion extraction method developed here capitalised on these motion artefacts. A small region of interest was selected on the edge of the thinned cranial window (overlaying both the tissue and the metal head plate in both the x and y planes), and was used to detect the movements of the head, with the largest movement artefacts being attributed to the greatest changes in locomotion (Figure 3.5). Whilst this method was not reliable enough to distinguish locomotion speed, it was useful for assessing the onset and cessation of locomotion events. The time series, taken from the pixels contained within this edge region, were extracted and used in the place of the walking data arising from the locomotion detector (described above in section 3.4.3).

The data taken from this edge region was subjected to the same filtering and event extraction as above (sections 3.4.3 & 3.4.4). The reliability of the intrinsic locomotion extraction method for detecting locomotion events was tested using a subject in which the optical motion sensor was also in place during experimental sessions. The intrinsic locomotion extraction method was then applied to this subject, and compared to the locomotion periods detected using the locomotion detector method (from the optical motion sensor) (Figure 3.5). The two methods of detecting locomotion events in time were inputted into the locomotion categorisation script and were found to be comparable, meaning that the imaging data taken from the pilot subjects (n=2) across multiple sessions could be inputted into the later analysis of the effect of locomotion on haemodynamic changes in the somatosensory cortex (detailed in chapter 4). This locomotion extraction method was also useful for recovering locomotion information from subjects in whose experimental sessions the optical motion sensor was problematic.

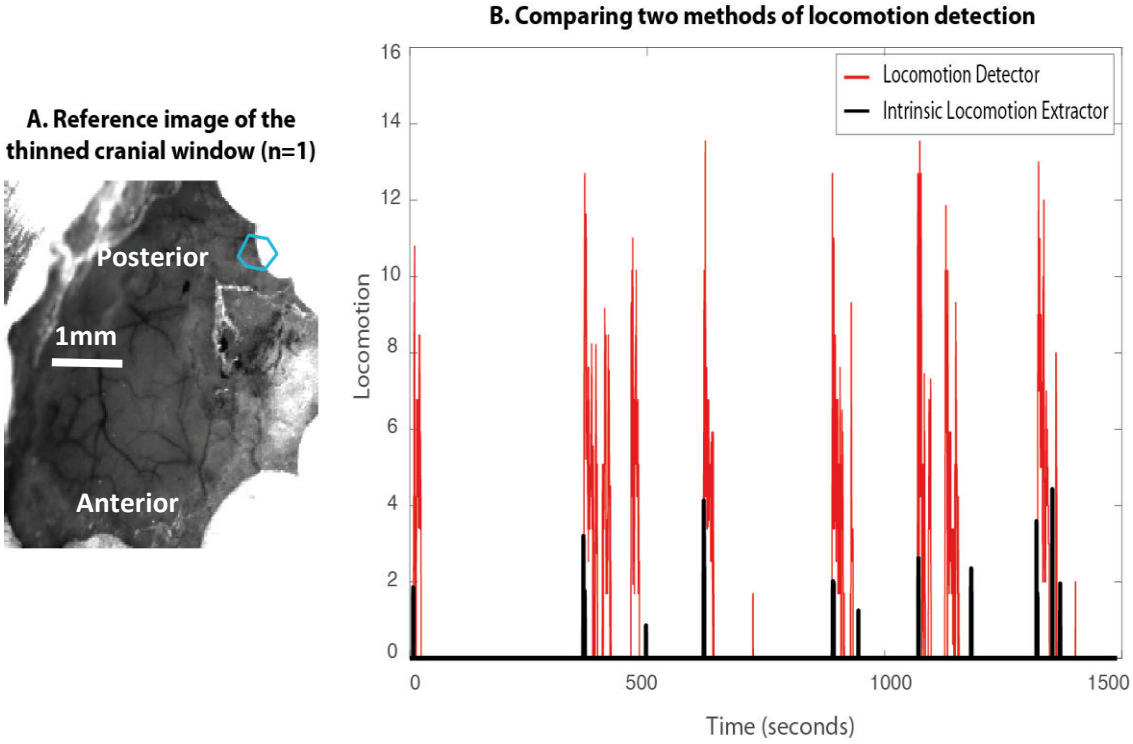

Figure 3.5 – Comparing the locomotion detector to an alternative method for categorising locomotion and stationary periods (when no optical motion sensor was fixed to the spherical treadmill)

A. *An image of the thinned cranial window with a region of interest centred over the edge of the thinned skull and the adjacent dental cement (region selected due to the high contrast between the tissue and the head plate). This region was used to extract locomotion when no optical sensor was in place. The alternative method of extracting locomotion aims to detect large movements of the head thought to occur during locomotion events.* ***B.*** *Red data were collected with the locomotion detector (i.e. optical motion sensor, n=1). Black data were collected using the intrinsic locomotion extraction method from the same representative subject (i.e. edge region of interest, n=1).*

3.4.6 Reducing the Effects of Motion on Recorded Haemodynamic Changes

The motion artefacts arising from movements of the head during locomotion were useful for extracting locomotion information in the absence of motion sensing equipment; however these motion artefacts also added noise to the 2D-OIS recordings of the haemodynamic changes. During each experimental session, whenever the animal engaged with locomotion the slight movements of the head which occurred were problematic when assessing the spatial extent of CBV changes across the somatosensory cortex over multiple

experimental trials. Head movement reduced the data quality and blurred the cortical images.

Two approaches were used to counteract these motion artefacts. The first approach was to fix the headplate holder with a second holding arm to add extra mechanical security to the set-up. The second approach used image registration techniques (MATLAB®, image processing toolbox) which were optimised for use with the data collected here. Image registration is the process of aligning multiple images, using geometric transformations to a single reference image. The image registration was applied to each individual experimental paradigm completed during a given session.

The image registration process required the raw data files which contained the multiple images of the cortex taken throughout each experiment. First a fixed image was selected by taking one image of the cortex (from the middle of each recorded sequence of images), and this image was then used as a reference point by which to co-align all the other images. Geometric transforms were applied to align each individual image of the cortex to the fixed image. As each image was aligned to a shared fixed point, motion artefacts were reduced throughout the experimental recording (Figure 3.6 B) when compared to the motion artefacts before image registration was applied (Figure 3.6 A). This made it possible to explore any spatial changes in the extent of the haemodynamic activity across the exposed cortex during whisker stimulation or locomotion.

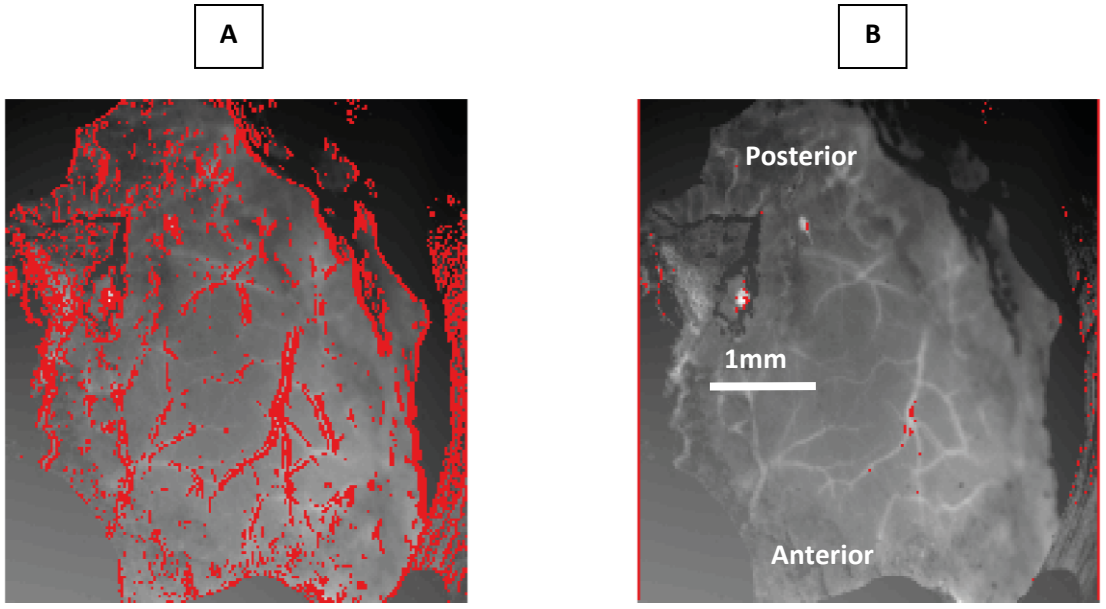

Figure 3.6– Example of the image registration technique applied to reduce motion artefacts in the spatial images taken of the cortex during experimental imaging sessions

Two images were taken from different time points within the same experimental recording session and were subtracted from each other, the difference pixels (marked in red) were then overlaid onto the first image of the cortex to show the movement. ***A.*** *Image of the cortex showing the subtraction before image registration was applied. The large number of red pixels indicates high levels of motion.* ***B.*** *An image of the cortex from the same experimental session, but showing the subtraction after image registration has been applied. There are fewer red pixels, indicating the image registration has reduced motion artefacts between images.*

The applicability of the awake mouse imaging platform developed here will be discussed in the following section (section 3.5), with reference to its advantages and disadvantages over existing experimental platforms.

3.5 Discussion

The awake mouse imaging platform provides a useful tool with which to study neurovascular coupling in the somatosensory cortex of the mouse, both chronically and without the influence of anaesthetics on the underlying brain physiology.

3.5.1 Quality & Stability of the Thinned Cranial Window over Time

It has been shown here that the quality and clarity of the thinned cranial window remains stable for a period of up to 3 months, after which skull regrowth occurred which partially obscured regions of interest. The 3 month period allowed for repeated, chronic imaging across multiple sessions. If longer than 3 months is needed for experimental imaging (for example to monitor long-term disease progression or aging), it is possible to extend the area of the thinned cranial window, while ensuring the active area of interest is within the centre of the window, so that initial regrowth does not cover vessels of interest.

3.5.2 Maintaining Spatial Consistency with Chronic 2D-OIS

It was important that the numerous images of the cortex taken over the multiple experimental imaging sessions were spatially consistent, to allow for between-session comparisons of the spatial extent of the haemodynamic changes across the somatosensory cortex. The experimental set-up used here was shared with other researchers and so equipment (i.e. the spherical treadmill, headplate fixation point, and CCD camera) was moved between imaging sessions. It was thus necessary to record all external parameters (such as spherical treadmill location points, CCD camera zoom and orientation); and also to use a reference image from a previous imaging session to try and replicate the image orientation and camera zoom between sessions. The whisker barrel region of interest selected for each experimental session was consistently placed by using standardised MATLAB code to select the local, large vasculature active during whisker stimulation, and by ensuring that the selected regions had the same number of pixels (2000).

3.5.3 Measuring Concurrent Locomotion with 2D-OIS

The head-fixed preparation developed here allowed for subject movement, which preliminary analysis showed produced substantial haemodynamic changes in the somatosensory cortex. Locomotion was therefore deemed an important factor to consider

when performing awake imaging and thus required direct measurement. Here an optical motion sensor was affixed to the spherical treadmill which measured the motion of the treadmill over time. A motion event detection- and categorisation- script were custom-built, which isolated locomotion and stationary periods. An alternative method for extracting locomotion information was devised which did not rely upon an optical motion sensor. This method was used to analyse the preliminary experimental sessions in which no motion sensor was present. A small region of interest was selected which encompassed the edge of the thinned cranial window and the surrounding dental cement. During locomotion the head was prone to motion which could be measured from this edge region. As the locomotion analysis primarily targeted locomotion versus stationary periods, this method of capturing the motion was deemed to be appropriate. The method was validated by comparing it to locomotion data collected from the same subject and experimental session, but using the optical motion sensor.

3.5.4 Reducing Motion Artefacts on Recorded Haemodynamic Changes

The motion artefacts, arising from subject movement, within the data were reduced to allow for fine scale analysis of the temporal profile and spatial spread of the haemodynamic responses across the somatosensory cortex (Bonin et al., 2011; Chen et al., 2013; Dombeck et al., 2007; Greenberg & Kerr, 2009; Thévenaz et al., 1998). A second holder arm was added to the set-up to increase mechanical stability. Image registration code was used to reduce motion artefacts by geometrically transforming all the images in space to a fixed reference image taken from the same experimental session.

While this experimental platform does have many advantages, especially over anaesthetised preparations, it does have some limitations which are described below.

3.5.5 Limitations of the Approach

Maintenance and potential for infection. For the long-term health of the thinned-cortical region it was essential to maintain aseptic conditions during surgical procedures (Ruiz et al., 2013). Before the skin was cut an iodine solution was used to disinfect and clean the skin, ensuring there were no later infections during the healing process. Once the thin cranial window had been created it was reinforced with superglue for protection, and dental cement was used to seal the gap between the skin and the exposed skull, again this helped

to ensure that there were no infections whilst the animal was recovering from surgery. Finally, between imaging sessions when the animal was housed in its own cage, a seal was created (made from sterile insulating tape with small holes to allow air through) to protect the thinned skull from any dust or damage caused by external pressures or collisions. These factors are essential for the long-term health of the thinned cortical preparation, however systematic tests have not been conducted to compare susceptibility to infection with and without these precautionary parameters in place. Inflammation responses are not necessarily always visible by eye. Thus, future work may benefit from assessing possible immune-inflammation responses resulting from the surgery, by conducting post-imaging immunohistochemistry experiments in which activated astrocytes and microglia are stained for in the brain tissue under the thin window.

Target depth. Most of the advantages of using the awake imaging approach described here are limited to target structures near the surface of the brain. As the approach is minimally invasive (to allow for long-term maintenance in the awake animal) and uses optical imaging (which capitalises on measuring light absorption and reflectance to calculate underlying haemodynamic changes), only cortical structures near the surface of the brain were targeted. Being limited to imaging the brain surface is appropriate in this case: the somatosensory cortex (specifically the whisker barrels) has been identified as an ideal model for investigating neurovascular coupling (Masamoto & Kanno, 2012; Zehendner et al., 2013); and imaging closer to the surface ensures there is a better spatial resolution.

Physiological effects of stress. An important consideration of work such as this is restraint-stress (Martin et al., 2013). Whilst the confounds associated with the use of anaesthesia have been avoided, there may be (neuro)physiological effects of stress. Previous work has shown that if the same animal is subject to training to accept the restraint regimen, then habituation occurs and indications of stress (e.g. vocalisations and resistance to handling) are effectively minimised (Martin et al., 2006; 2013). Future work may benefit from the inclusion of non-invasive monitoring of physiological indicators of stress (e.g. non-invasive pulse oximetry and blood pressure measurements).

3.5.6 Future Directions

The development of the awake imaging platform described here is a first step towards offering more comprehensive chronic awake imaging. The following thesis chapters will

look in more detail at the temporal profile and spatial extent of evoked and spontaneously occurring haemodynamic changes, with the later comparison of these with data from anaesthetised mice.

It is acknowledged that there are further developments which can be added to the awake imaging platform described, but that these go beyond the scope of this thesis. In future studies it would be advantageous to make concurrent neural recordings from the somatosensory cortex of the awake, head-fixed mice. Previous electrophysiological recordings made in this laboratory in the anaesthetised rodent used a 16 channel electrode, inserted into the active area through a burr hole which was created using a dental drill (refer to Berwick et al., 2008 for detailed methods). This technique of recording neural activity is an invasive method, which would not be suitable for later recovery of the animal. It may be more suitable to use alternative, less-invasive means to record the neural activity from the somatosensory cortex of the awake rodent, for instance by using genetically encoded voltage indicators (Knopfel, 2012; Carandini et al., 2015). It could be important to measure whisking (as well as locomotion), as it has been shown that rodents always whisk whilst walking (Arkley et al., 2014). The whiskers were not tracked in these experiments due to the limitations of the experimental set-up. It may also be beneficial to gain additional behavioural information from the awake mouse by creating a more naturalistic environment, or by varying the sensory stimuli presented during imaging sessions. Examples of such sensory variations include: changing the objects in the visual field as the animal moves and engages with the environment (Chen et al., 2013); varying the textures or positions of objects which the subjects comes into contact with (O'Connor et al., 2010); or adding different odorants (Smear et al., 2011). These limitations and future research avenues will be discussed in more detail in the next chapter (chapter 4).

A fundamental goal of neuroscience is to gain an understanding of the computations performed by the mammalian cortex, and to comprehend how such computations are modified in a behavioural context (Chen et al., 2013). The awake imaging platform developed here offers a base which can be used to glean a wealth of important extra information, not possible with the anaesthetised or awake limb-restricted preparations. The next chapter seeks to utilise the awake imaging platform to assess the effects of locomotion and whisker stimulation on the haemodynamic changes in the somatosensory cortex.

Chapter 4

Investigating haemodynamic changes in awake, head-fixed mice during whisker stimulation and spontaneous locomotion

4.1 Abstract

Recent investigations have used an awake preparation to study neural activity and haemodynamic responses in the mouse, due to the known effects of anaesthesia on neurovascular coupling. Whilst the brain physiology of an awake mouse remains unaltered by anaesthetic agents, other behavioural factors such as locomotion may affect underlying neurovascular coupling mechanisms. Here, 2-dimensional optical imaging spectroscopy was used to measure haemodynamic changes in the somatosensory cortex of awake mice (n=7). During imaging sessions mice were head-fixed atop of a spherical treadmill, whilst locomotion was tracked using an optical motion sensor. Locomotion was associated with an increase in the total blood volume in the whisker barrel region compared to stationary periods. The spatial extent of the blood volume changes during locomotion were globally spread throughout the exposed somatosensory cortex, compared to the spatial extent of blood volume changes to whisker stimulation (not sorted for locomotion) which were localised to the whisker barrel region. The interaction between locomotion and whisker stimulation was also assessed, and locomotion was sorted in ascending order from the 'least' to the 'most' locomotion during the whisker stimulation period. Haemodynamic responses in the whisker barrel region to whisker stimulation with the 'most' locomotion were significantly larger than haemodynamic responses to whisker stimulation with the 'least' locomotion. Spatially, whisker stimulation with 'most' locomotion showed a global increase in blood volume across the exposed cortex; whereas whisker stimulation with the 'least' locomotion showed a localised increase in blood volume centred on the whisker barrels, with a decrease in total blood volume in the region surrounding the whisker barrels. Locomotion had a clear effect on blood volume changes in the somatosensory cortex. Therefore experiments exploiting the benefits of the awake preparation for neurovascular research need to take into consideration the behavioural confounds the awake preparation also introduces.

4.2 Introduction

Neural activation leads to a localised increase in cerebral blood flow, volume and oxygenation (Ogawa et al., 1993). A detailed investigation into the relationship between neural activity and the consequential changes in the haemodynamic response has wide implications for research into brain physiology, and into the interpretation of data from functional brain mapping studies such as fMRI (Martin et al., 2002). The previous chapter (chapter 3) described the development of a novel method for optical imaging and locomotion tracking of awake, head-fixed mice. This imaging platform is useful as it allows for the chronic assessment of haemodynamic signals underlying neurovascular coupling, without the influence of anaesthesia. The current chapter implements this imaging platform to measure the haemodynamic changes in the somatosensory cortex (S1) of behaving, head-fixed mice during spontaneous locomotion and whisker stimulation.

4.2.1 The Effects of Anaesthesia on Neurovascular Coupling

Many previous studies of neurovascular coupling in the rodent whisker barrels have typically utilised *in vivo* animal preparations, in which the S1 is imaged whilst the subject is under anaesthesia (e.g. Berwick et al., 2008 [urethane]; Boorman et al., 2010 [urethane]; Devor et al., 2003 [urethane]; Martindale et al., 2003 [urethane]; Nakao et al., 2001 [alpha-chloralose]; Nielsen & Lauritzen, 2001 [alpha-chloralose]; Sharp, Shaw et al., 2015 [fentanyl-fluanisone/midazolam]; Sheth et al., 2003 [enflurane]; Ureshi et al., 2004 [alpha-chloralose]). Under anaesthesia it has been possible to utilise invasive techniques to uncover some of the temporal and spatial characteristics of neurovascular coupling. Recording electrodes can be directly inserted into the cortex of an anaesthetised animal to collect information regarding neural firing patterns. The insertion of multi-channel electrodes have been used in combination with 2-dimensional optical imaging (2D-OIS) to look at neurovascular events in fine detail: as centred on a single whisker barrel (Berwick et al., 2008); to uncover the role of the neural activity underpinning the negative BOLD response (Boorman et al., 2010); and to gain a better understanding of spontaneous fMRI

BOLD fluctuations (Bruyns-Haylett et al., 2013). Whilst it is clear that anaesthesia has much value by offering the researcher the option of using invasive neuroimaging techniques to acquire a high level of spatiotemporal detail, there are downsides to its use, namely due to the uncontrollable effects of anaesthesia on the brains physiology (Hildebrandt, Su & Weber, 2008; Masamoto & Kanno, 2012). Anaesthesia can affect the major properties of neurovascular coupling, such as the temporal dynamics of the neural and vascular responses (Hayton et al., 1999; Prakash et al., 2007; Sebel et al., 1986); and the spatial coordination of the vascular response with respect to the neurally derived map (Chen et al., 2001). The development of an unanaesthetised animal preparation would also be more homologous with human functional imaging, which is typically conducted with awake subjects.

These effects of anaesthesia on the neural and vascular responses of the brain ultimately alter the stability and reproducibility of neurovascular imaging (Masamoto & Kanno, 2012). This unreliability has provided the motivation to seek alternative imaging methods, which do not rely on the use of anaesthesia.

4.2.2 Measuring Neurovascular Coupling in Awake Subjects

The long-term monitoring of neurovascular coupling in the brain of healthy, behaving subjects allows for the characterisation of typical neuronal and haemodynamic responses both spontaneously and to external stimuli. Neuroimaging of awake mice usually involves the subjects being head-fixed atop of a treadmill (Dombeck et al., 2007); which keeps the cortex stable for imaging, but allows the animal to move to reduce any stress induced from complete physical restraint (Ayaz et al., 2013; Haider et al., 2013; Pisauro et al., 2013). Unlike in the anaesthetised preparation, the animal is free to run and whisk during such experimental imaging sessions, therefore researchers have also taken to measuring these behavioural variables in order to assess whether they have any additional effect on the neurovascular coupling response in the active cortex (Ayaz et al, 2013; Huo et al., 2014; Niell & Stryker, 2010; Saleem et al., 2013; Vinck et al., 2015).

4.2.2.1 Visual Cortex

The visual cortex (V1) has been a popular area for investigating neurovascular coupling using awake subjects (Ayaz et al, 2013; Haider et al., 2013; Niell & Stryker, 2010; Pisauro et al., 2013; 2016; Saleem et al., 2013; Vinck et al., 2015). In those studies which specifically consider the V1, the awake model is considered to be superior to the anaesthetised for receiving and interpreting visual inputs. In an awake animal there is an interaction between visual signals and locomotion, leading to the possibility that walking or resting whilst interacting with the environment may have different impacts upon area V1. There is now growing evidence for activity in area V1 being determined not only by light patterns which fall on the retina, but also by multiple non-visual factors such as spatial attention (McAdams & Reid, 2005), arousal levels and locomotion (Pisauro et al., 2016; Vinck et al., 2015), or impending reward (Schuler & Bear, 2006). Vision and locomotor behaviour are thought to interact, as successful navigation through the environment requires an accurate estimation of one's own direction and speed. Animals have been known to derive the speed estimate through the integration of optic flow (visual speed) with proprioceptive and locomotor systems (run speed) (Ayaz et al, 2013; Niell & Stryker, 2010).

In mice robust changes in the firing of V1 neurons have been linked with locomotion (Ayaz et al, 2013; Niell & Stryker, 2010; Saleem et al, 2013). Saleem and colleagues studied how visual and locomotion neuronal signals are combined in mouse V1, by assessing visual input which was controlled by or independent of locomotion (Saleem et al, 2013). Locomotion information was categorised as "stationary" or "running", and running periods were further sorted by running speed. It was confirmed that running affects neuronal firing in V1, even when there was no visual stimuli (lights were switched off and room was dark). The authors extended these findings to demonstrate that V1 neural responses varied smoothly and non-monotonically with run speed, highlighting that V1 neurons combine run speed and visual speed as a weighted sum, with weights varying across neurons, and most neurons attributing positive weights to visual and run speeds. Such results suggest the function of the mouse visual cortex extends beyond just vision. It seems that neocortical areas are not specific to a single function, and that neurons of even primary sensory cortices can respond to a wide range of multimodal stimuli and non-sensory features, such as locomotion (Saleem et al, 2013). Vinck and colleagues (2015) examined the distinct contributions of arousal and locomotion to V1 activity, by using extracellular neural recordings in combination with behavioural state monitoring. Substantial differences were found in V1 activity between rest periods and locomotor periods. They discovered that a lot of the change in V1 LFP power, spike-LFP phase-locking, and unit activity, as associated with

locomotion, were actually the result of increased arousal. Regular-spiking firing was increased in anticipation of locomotion and during movement, even when no visual stimulation was presented.

The relationships between locomotion and haemodynamic responses have also been investigated in V1 of the awake mouse using optical imaging (Pisauro et al., 2013). In these experiments, the haemodynamic responses to visual stimulation were not significantly altered by locomotion. These results were unexpected as physical exercise has been shown to increase cerebral blood flow (Querido & Sheel, 2007); and locomotion was previously shown to increase neural responses in V1 (Ayaz et al., 2013; Niell & Stryker, 2010), particularly for oscillations in the gamma range (30-80Hz; Niell & Stryker, 2010), which are associated with haemodynamic activity (Koch et al., 2009; Muthukumaraswamy et al., 2009). It is possible that the optical imaging techniques used were not sufficient to detect the effect of locomotion on visually-evoked haemodynamic responses, as functional hyperemia was not measured directly, but rather an intrinsic signal was measured which was only partially caused by a vascular component. Locomotion could potentially affect other aspects of the signals, or it may even only affect haemodynamic activity in different regions of the cortex.

The evidence linking vision and locomotion shows the two are well integrated, although more investigation is required into the potential effects of locomotion on the haemodynamic responses of V1. Thus, fully understanding complex cortical function in awake behaving animals is not as simple as applying an external stimuli (e.g. a light flash) and measuring the corresponding neuronal and haemodynamic changes. This also suggests that there may be interplay between locomotion and other cortical regions, for example the S1.

4.2.2.2 Somatosensory Cortex

The rodent S1 is frequently used in the investigation of neurovascular coupling, most likely due to the well-defined somatotopic mapping and highly concomitant blood supply from the whiskers to the whisker-barrel region (Woolsey et al., 1975). In contrast to the well-accepted view that locomotion affects neurovascular coupling responses in V1, equivalent research in S1 is limited and somewhat contradictory.

The reproducibility and variance of CBF responses to naturalistic whisker stimulation was evaluated in the barrel cortex of the awake, head-fixed mouse (Takuwa et al, 2011). CBF changes were monitored using laser Doppler flowmetry (LDF), alongside locomotion changes tracked using an optical motion sensor. Repeated longitudinal experiments over seven days showed reproducible evoked increases in CBF in response to whisker stimulation. This increase in blood flow was maintained regardless of variations in locomotion. The effect of locomotion in the absence of whisker stimulation, on CBF changes in the whisker barrels was not elucidated. Takuwa and colleagues further investigated the mechanisms underlying cerebral blood flow regulation in the awake mouse compared with the anaesthetised mouse using LDF (Takuwa et al, 2012). A haemodynamic response to whisker stimulation in the S1 was observed under both conditions using LDF. The increase in CBF to whisker stimulation in the awake condition was four times higher than in the anaesthetised condition, despite a relatively stable baseline CBF between the two conditions. Locomotion events were not considered, due to previous results showing differences between resting and moving periods were negligible (Takuwa et al, 2011).

In contrast to these results, which indicate the effect of locomotion on blood changes in the S1 are insignificant, Huo et al. (2014) found that during phases of locomotion there are distinct changes in haemodynamic and neural responses in the S1, when compared to resting periods. Intrinsic optical signal imaging revealed increases in cerebral blood volume (CBV) in hind- and fore- limb representations in the S1 during periods of movement as compared to rest periods. This increase in CBV in the S1 during locomotion was found to correlate with a strong increase in LFP recorded from the hind-limb area when compared to rest. The authors found a coupling between haemodynamic and neural activity in the S1 during locomotion despite no external stimulation; however this coupling was not preserved in the frontal lobe where they observed increases in gamma-band power during locomotion, but no distinct increases in CBV. Huo and colleagues further investigated the vascular mechanisms underlying the haemodynamic response to locomotion hind- and fore- limb representations in S1 of the awake mouse (Huo et al., 2015). The results showed that blood volume-related haemodynamic responses to locomotion could be divided into arterial and venous components, each with distinct spatial patterns. The pial arteries dilated strongly and rapidly in response to both short and long duration locomotion events. Once locomotion ceased, the arteries constricted back to baseline diameter within a few seconds. The dilations of the pial veins were only apparent during long duration locomotion

events due to their smaller amplitudes. The diameters of veins also took tens of seconds to return back to baseline following locomotion cessation.

Blood volume changes have been observed in the hind-limb representation of the S1 during locomotion (Huo, et al., 2014), however the whisker barrel region specifically was not investigated. Takuwa and colleagues focused on the whisker barrel region when investigating neurovascular coupling, but found no effect of locomotion on CBF changes (Takuwa et al, 2011; 2012). Further, there has been limited previous consideration of the interaction between locomotion and whisker stimulation in the whisker barrels of the S1, i.e. how locomotion may affect the stimulus-evoked haemodynamic response. In light of these inconsistencies, it will be important to use improved optical techniques with fine spatiotemporal detail to investigate the typical haemodynamic response in the whisker barrels of awake, head-fixed mice.

4.2.3 Aims

This chapter aims to apply the experimental set-up detailed in chapter 3 to examine the impact of locomotion on haemodynamic responses across S1 during spontaneous behaviour (i.e. no whisker stimulation), and during mechanical whisker stimulation.

Firstly, the effect of spontaneous locomotion on CBV changes in S1 will be considered. Next, to confirm the suitability of the imaging set-up for measuring CBV changes in the whisker barrel region, haemodynamic changes to whisker stimulation (regardless of locomotion) will be assessed. Finally, the CBV changes in S1 resulting from the interaction between locomotion and whisker stimulation will be investigated (to see if there is linear superposition of the Hbt responses to stimulation and locomotion).

4.3 Methods

The experiments detailed in this chapter follow the same protocol as the animal preparation described previously in chapters 2 (sections 2.2-2.4) and 3 (section 3.3). Briefly, the animal was anaesthetised and a thinned cranial window was created on the skull overlying the right S1, a head plate holder was then secured to the skull using dental cement. The animal was allowed at least one week for recovery from the surgical procedure, before being increasingly exposed to the experimental set-up in order to reduce stress from later head fixation. Once the subject was habituated to the experimental apparatus, it was head-fixed above a spherical treadmill whilst locomotion was monitored using an optical motion sensor, and CBV changes were measured using 2D-OIS. A mechanical whisker stimulator was placed on the contralateral side of the face from the thinned cranial window. During stimulation experiments the whiskers were stimulated for either 2 or 16 seconds across multiple trials, however for the spontaneous (no whisker stimulation) experiments the stimulation motor was switched off. Seven adult C57BL/6J mice were included in this specific study (24-40g, 2 male, 5 female; Harlan, UK), and all procedures were conducted in accordance with the Animals (Scientific Procedures) Act 1986. All data analysis was performed using MATLAB® (MathWorks). The data were statistically analysed using two-tailed paired t-tests. Bonferonni-adjusted α was applied to correct for multiple comparisons, with p levels for significance set at 0.05 before Bonferroni's correction for multiple comparisons.

4.4 Results

The following section reports the haemodynamic changes and locomotion events detected during both whisker stimulation and spontaneous (non-stimulation) experimental recordings.

4.4.1 Haemodynamic Responses during Spontaneous Locomotion

Neurovascular coupling is commonly investigated by evoking haemodynamic and neural responses through stimulation, however more recent work, especially using fMRI, has investigated spontaneous haemodynamic changes (see van den Heuvel & Hulshoff Pol (2010) for review). Here, haemodynamic responses driven by spontaneous locomotion in awake subjects will be investigated.

4.4.1.1 Detecting the Onset of Locomotion

To assess haemodynamic changes arising from locomotion, spontaneous locomotion events were first detected and extracted (i.e. onset and cessation of locomotion in time, Figure 4.1 A; see section 3.4.3 & 3.4.4 for a detailed description of the locomotion detector process). Once distinct locomotion events had been isolated, they were further separated by duration (short and long). The duration threshold was chosen by taking the average duration of locomotion across all events recorded (i.e. 6.3004 seconds). Locomotion lasting for periods below this threshold were classified as short, any above this threshold were deemed long (Figure 4.1 A). Haemodynamic data were then extracted for fixed time points

before and after the onset of each locomotion event, to assess the effect of locomotion on the haemodynamic changes in the S1 (Figure 4.1 B). For analysis of the temporal haemodynamic changes, the whisker barrel region was located using a separate whisker stimulation experiment**.** A region of interest was selected overlying the whisker barrel region in S1 (the selection process for this region of interest is described in detail in section 3.4.2), and the time series of haemodynamic changes generated.

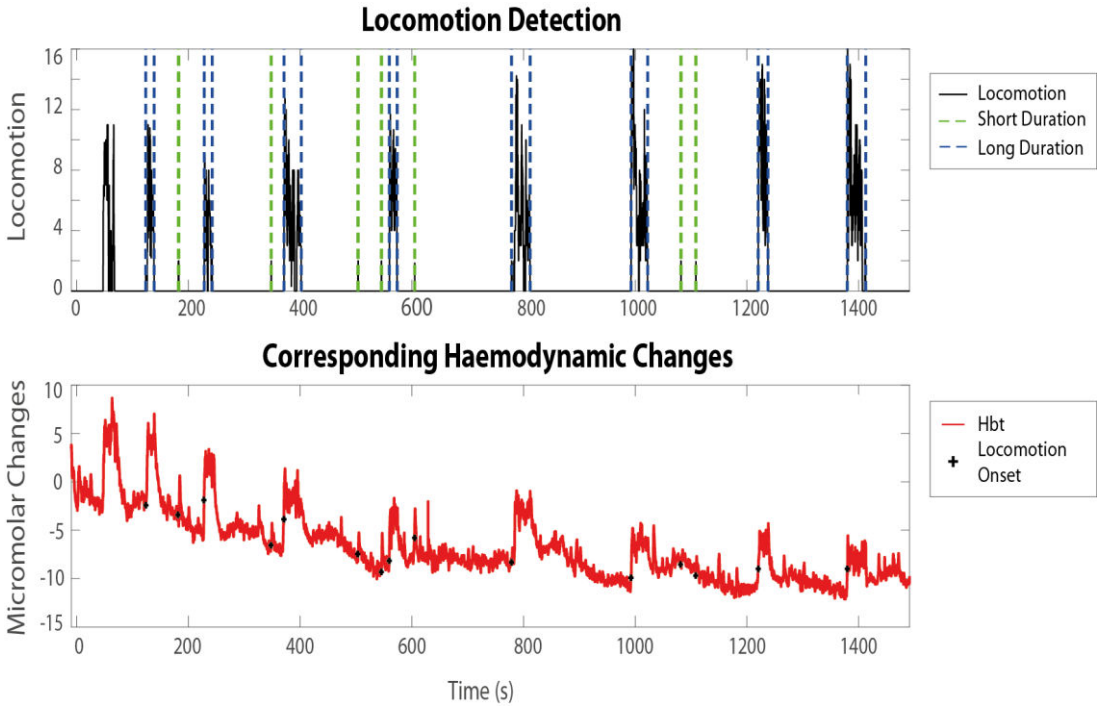

Figure 4.1 – ***Locomotion Detector with Corresponding Haemodynamic Changes in the Whisker Barrels***

A. *Time course of locomotion (distinct locomotion periods marked in black) across one representative spontaneous experimental recording session (no whisker stimulation). Locomotion periods are labelled according to duration; the short duration locomotion events are marked by green dotted lines, and the long duration locomotion events are contained within the blue dotted lines.* ***B.*** *Corresponding Hbt changes in the active whisker barrel region taken from the same representative experimental session. The onset of all detected locomotion events which occurred during the experimental session are marked with a black cross.*

4.4.1.2 Examining the Time Course of Haemodynamic Responses in the Somatosensory Cortex during Spontaneous Locomotion

Locomotion and haemodynamic data were extracted for fixed periods before and after the onset of each detected locomotion event. The temporal profile of locomotion and the concomitant haemodynamic changes occurring within the whisker barrels were then averaged across all experimental sessions and animals (Figure 4.2). An increase in Hbt and HbO_2, and a concomitant decrease in Hbr were observed following the onset of locomotion (Figure 4.2 C). Another interesting finding was that the haemodynamic responses within the whisker barrel region of S1 seemed to occur slightly before the onset of locomotion. To further understand the haemodynamic changes occurring during periods of locomotion, they were also investigated spatially.

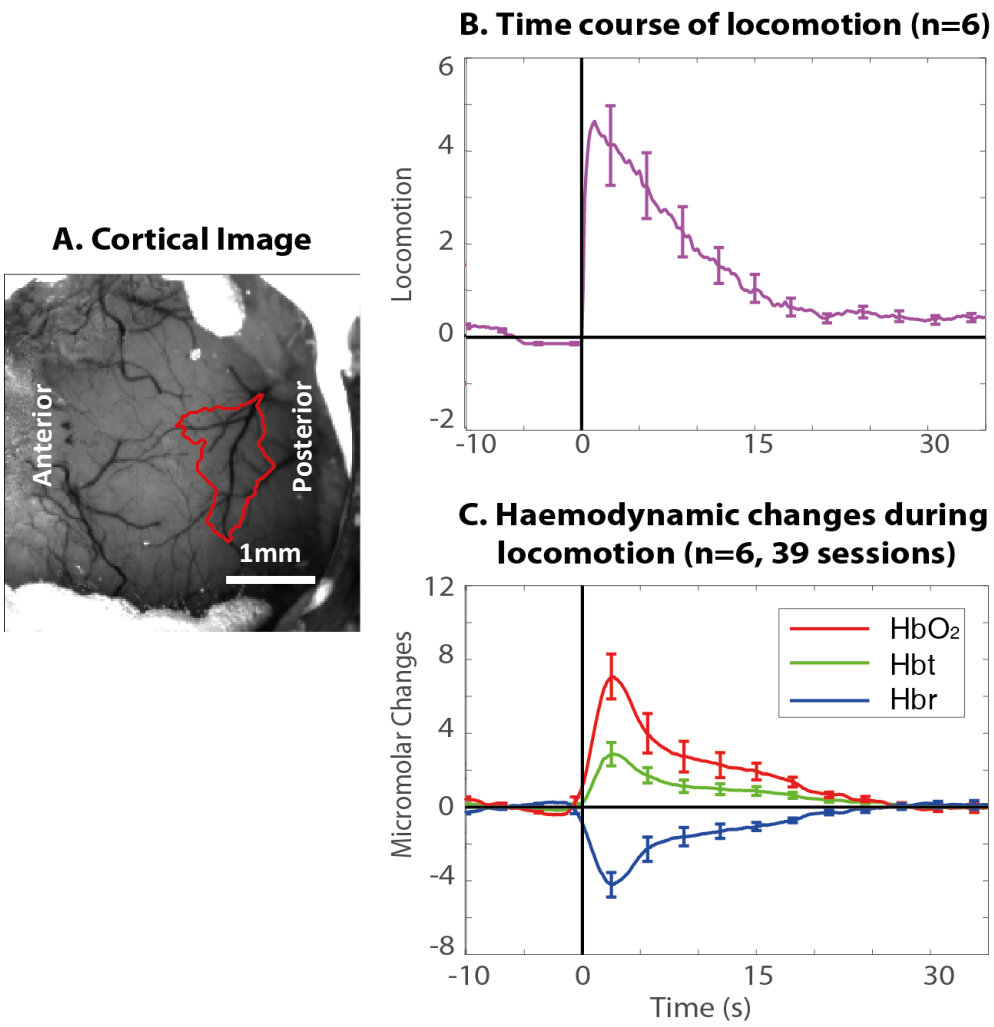

Figure 4.2 – Haemodynamic Responses occurring during periods of Locomotion

A. *Grayscale image of the cortex taken from one representative animal, with the region of interest marked in red centred over the whisker barrels.* ***B.*** *Time course of locomotion, extracted 10s before to 35s after the detected locomotion onset.* ***C.*** *Haemodynamic changes during detected periods of locomotion. Time courses were averaged across locomotion events and animals (n=6). Error bars represent SEM.*

4.4.1.3 Examining the Spatial Extent of Haemodynamic Responses across the Somatosensory Cortex during Spontaneous Locomotion

Spontaneous periods of locomotion were associated with increases in Hbt in the whisker barrels. The spatial spread of the haemodynamic responses were investigated across S1 for all subjects (Figure 4.3). The change in Hbt was averaged between 0 and 5 seconds after of the onset of locomotion, and spatial maps were generated. These spatial maps shall be referred to as 'Hbt response maps' throughout this chapter.

The onset of locomotion resulted in an increase in Hbt which was spread across most of the exposed S1 and recruited much of the surface vasculature (Figure 4.3 B). The time course of haemodynamic responses from individual subjects were the same as those previously described (averaged across all subjects, Figure 4.2). Spontaneous locomotion resulted in an overall increase in Hbt and HbO_2 in the whisker barrel region during locomotion, which decreased once locomotion ceased, with a concomitant decrease in Hbr in the whisker barrel region (Figure 4.3 C). Again, the onset of these haemodynamic responses occurred slightly before locomotion started.

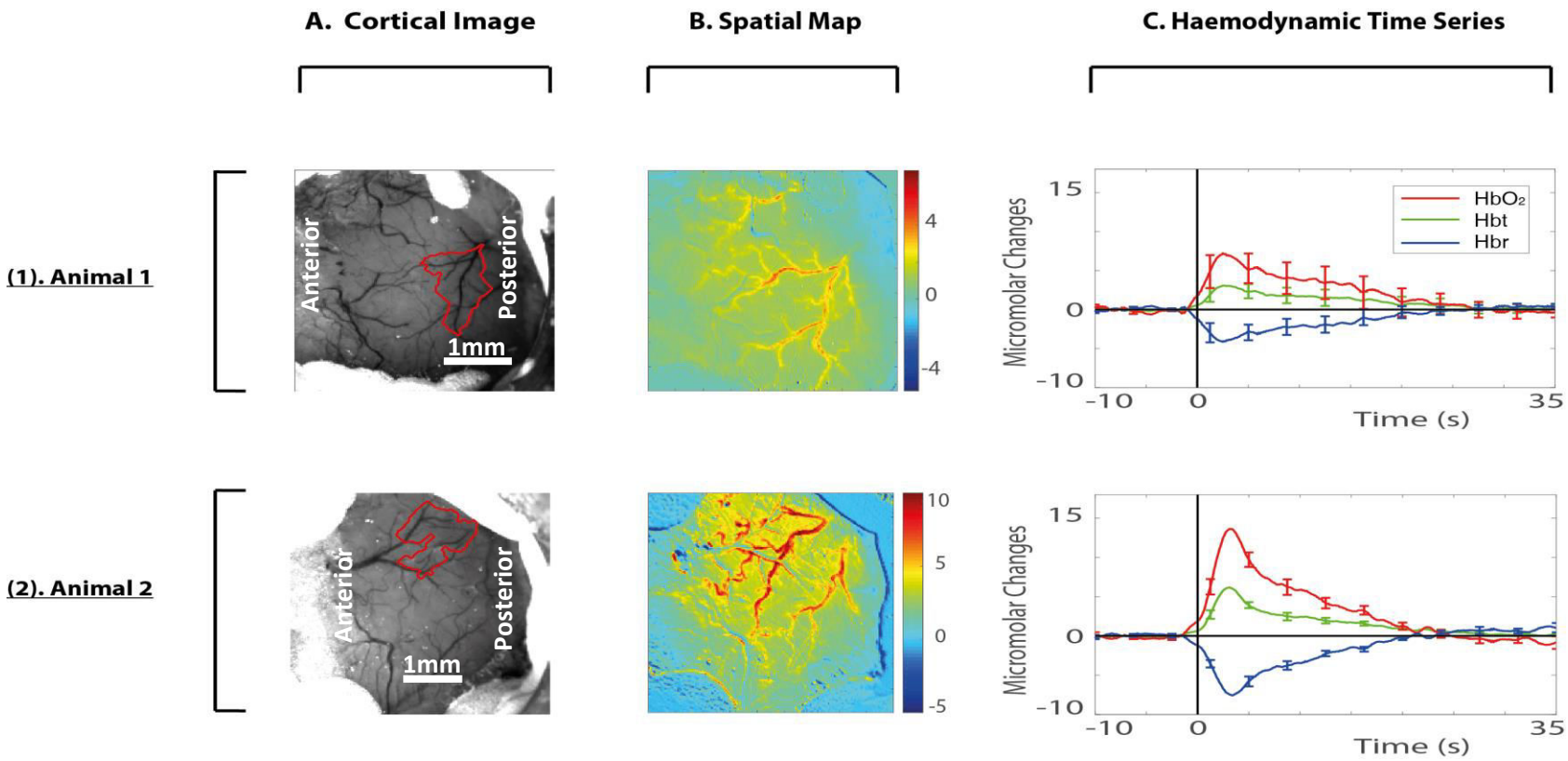

Figure 4.3 – The Spatial Extent and Temporal Profile of the Haemodynamic Response in S1 during Spontaneous Locomotion

A. *A representative image of the cortex taken for each example subject, with the whisker barrel region of interest (used to visualise the time series of the haemodynamic response) marked in red.* ***B.*** *A representative image of the cortex taken for each subject which shows the spatial extent of the Hbt response during the onset of locomotion.* ***C.*** *Time series of the average haemodynamic response across numerous sessions (n=6) for each subject during the onset of locomotion. Error bars represent SEM.*

4.4.1.4 Separating Spontaneous Locomotion Events by Duration

Once it was clear that locomotion altered haemodynamic responses within S1, locomotion was further explored by separating it by duration (long and short duration). The time course and Hbt response maps were then visualised for long and short duration locomotion.

The Hbt response maps showed that both short and long duration periods of locomotion also resulted in an increase in Hbt, which was spread across most of the exposed S1 and recruited much of the surface vasculature (Figure 4.4 B). The temporal profiles of the haemodynamic responses during short and long duration locomotion showed the expected increases in Hbt and HbO_2, with a concomitant decrease in Hbr (Figure 4.4 C). Haemodynamic responses during short duration locomotion showed a quicker return to baseline levels than during long duration runs, corresponding to the shorter duration locomotion events. The average area under the Hbt curve from the onset of locomotion until the end of the trial (i.e. 0 to 35 seconds) was assessed for both the short duration and long duration locomotion events across animals. The Hbt response during the short duration locomotion events (M=0.35µM, SD=0.40) returned to baseline levels significantly faster than the Hbt response during the long duration locomotion events (M=1.52µM, SD=0.58; $t(10)=4.03, p<0.01$**).

These results demonstrated that the onset of locomotion was tightly coupled with haemodynamic changes; as long duration locomotion events corresponded with long duration haemodynamic changes, and short duration locomotion events corresponded with short duration haemodynamic changes.

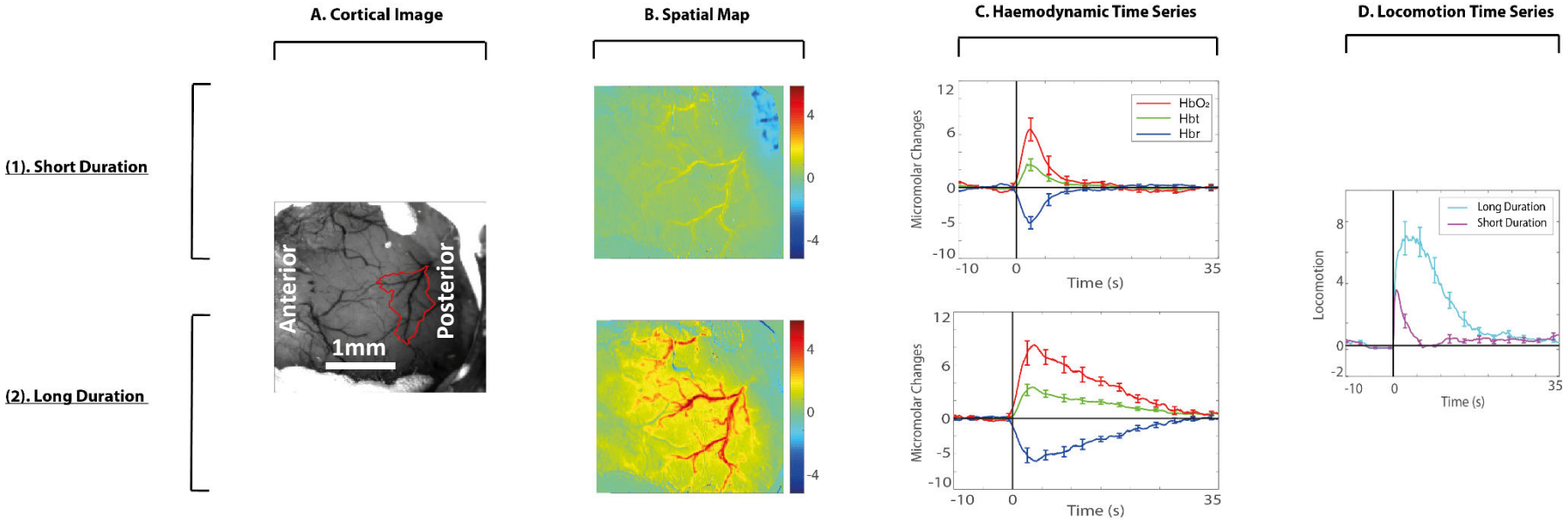

Figure 4.4 – The Spatial Extent and Temporal Profile of the Haemodynamic Response in the S1 during Short and Long Duration Locomotion Events

A. *A representative image of the cortex with the whisker barrel region of interest (used to visualise the time series of the haemodynamic response) marked in red.* ***B.*** *The spatial spread of the haemodynamic response averaged from 0-5 seconds after locomotion onset in one representative animal (animal 1 as presented in Figure 4.3) for:* ***(1)*** *a short duration; and* ***(2)*** *a long duration period of locomotion.* ***B.*** *The temporal profile of the haemodynamic response in the whisker barrels averaged across all subjects during:* ***(1)*** *short duration locomotion; and* ***(2)*** *long duration locomotion (n=6).****D.*** *The time course of short duration and long duration locomotion events averaged across all subjects (n=6). Error bars represent SEM.*

4.4.2 The Haemodynamic Responses during Whisker Stimulation

The previous section investigated the locomotion-evoked haemodynamic responses across S1 occurring during spontaneous (no stimulation) experiments. The following section examines stimulation-evoked haemodynamic responses, which can be spatially localised using whisker stimulation.

4.4.2.1 Examining the Time Course of Haemodynamic Responses in the Somatosensory Cortex during Whisker Stimulation

Mechanical whisker stimulation evoked increases in both Hbt and HbO_2, with a decrease in Hbr in the whisker barrel region, which returned to baseline levels following stimulus cessation (Figure 4.5). The 2s stimulation paradigm produced a short duration monophasic haemodynamic response (Figure 4.5 A), while the 16s stimulation paradigm produced a larger magnitude and longer duration haemodynamic response (Figure 4.5 B). The 16s response was characterised by an initial peak, followed by a secondary peak with increased magnitude. This temporal response profile was consistent with that previously seen to 16s whisker stimulation in awake rats (Martin et al., 2013b).

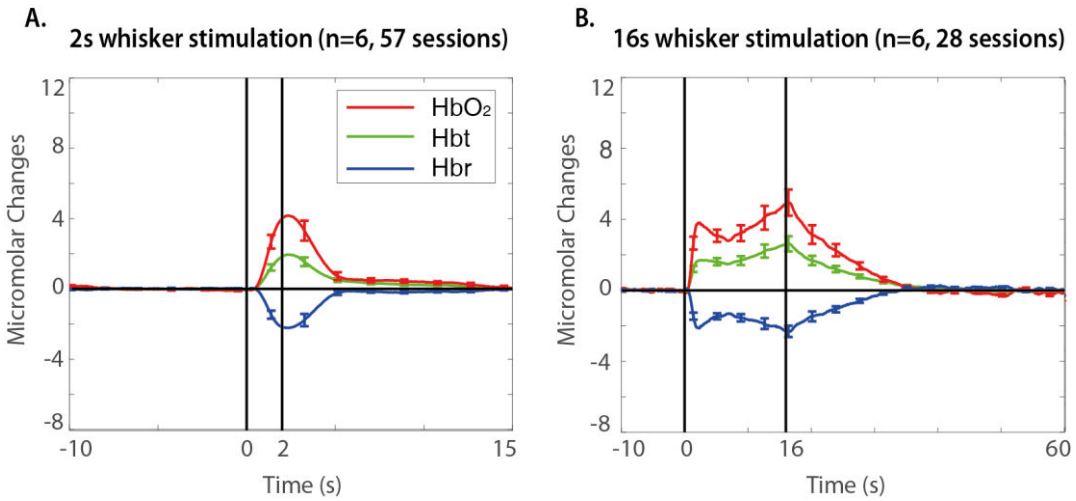

Figure 4.5 – Time series showing Stimulus-Evoked Haemodynamic Changes in the Whisker Barrel Region, averaged across multiple subjects

*Time series of cortical haemodynamic responses (Hb0, Hbt and Hbr) averaged across subjects, elicited by **A.** a 2s; and **B.** a 16s mechanical whisker stimulation (n=6). Error bars represent SEM.*

The time course of stimulus-evoked responses were compared to the spontaneous haemodynamic responses associated with locomotion (studied in section 4.4.1). The overall peak magnitude of the Hbt change during locomotion (n=6; M=3.05µM, SD=1.63, Figure 4.2) surpassed those seen in response to the mechanical whisker stimulation (n=6; 2s, M=1.96µM, SD=0.74, and 16s, M=2.67µM, SD=1.03), Figure 4.5), although the differences were non-significant.

4.4.2.2 Examining the Spatial Extent of Haemodynamic Responses across the Somatosensory Cortex during Whisker Stimulation

The spatial extent of the stimulus-evoked haemodynamic responses were investigated across the exposed cranial window for all subjects (Figure 4.6, shown for two representative animals). For both 2s and 16s mechanical whisker stimulation the Hbt response maps showed an increase in Hbt, with the greatest magnitude response localised to the whisker barrel region (Figure 4.6).

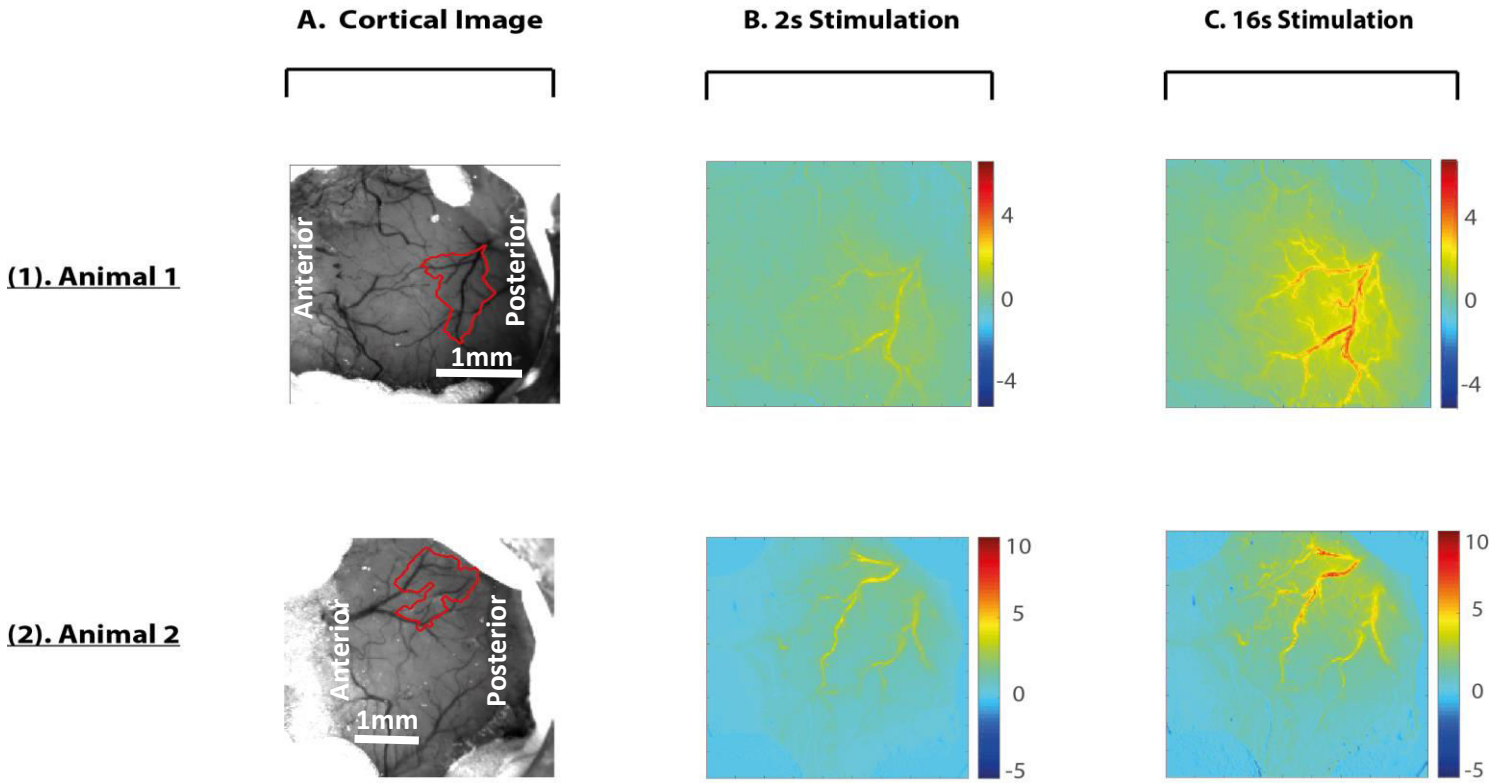

Figure 4.6 - The Spatial Extent of the Haemodynamic Response in the S1 during Whisker Stimulation

A. *Representative images of the cortex (animals 1 (1) & 2 (2) as seen in Figure 4.3), with the whisker barrel region of interest (used to visualise the time series of the haemodynamic response) marked in red. Hbt response maps from the onset of whisker stimulation for:* ***B.*** *a 2s, and* ***C.*** *a 16s whisker stimulation.*

The number of active pixels within the Hbt response maps were calculated for the 2s and 16s whisker stimulation, and compared to during spontaneous locomotion (Figure 4.7). The pixel analysis is described in detail in section 2.5.1.3.2. Briefly, a threshold was applied to images of the Hbt response during whisker stimulation or locomotion which detected the largest area of active pixels, and calculated the number of active pixels as a percentage of the Hbt response map over time.

The overall average percentage of active pixels within the Hbt response maps (Figure 4.7) during spontaneous locomotion (n=39 sessions; M=19.24%, SD=4.93) was greater than during 2s stimulation (n=57 sessions; M=18.56%, SD=2.83; t(10)=-0.30, p=1.55, ns) or 16s stimulation (n=28 sessions; M=14.13%, SD=1.75; t(10)=-2.40, p=0.07, ns), although these differences were not significant. The maximum number of active pixels recruited during locomotion (M=34.69%, SD=8.55) was less than the maximum recruited during 2s whisker stimulation (M=40.43%, SD=8.16; t(10)=1.19, p=0.52, ns), and greater than the maximum recruited during 16s whisker stimulation (M=27.14%, SD=5.01; t(10)=-1.86, p=0.18, ns), but again these differences were non-significant.

Previous research has shown that the time course of the Hbt response during 2s (shorter duration) whisker stimulation, will be smaller in peak magnitude than the time course of the Hbt response to 16s (longer duration) whisker stimulation (e.g. Berwick et al., 2005; Martindale et al., 2005). However, the differences in the spatial extent of the Hbt response between 2s and 16s whisker stimulation have not been previously investigated. Interestingly, both the overall average percentage of pixels recruited during 2s whisker stimulation (t(10)=3.26, p=0.02*), and the maximum peak of pixels recruited during 2s whisker stimulation (t(10)=3.40, p=0.014*), were significantly greater than during 16s whisker stimulation. It is also interesting to note that the number of active pixels recruited during the whisker stimulations, followed a similar temporal profile to the stimulus-evoked changes in blood volume seen in the active whisker region (i.e. the time course of haemodynamic responses in Figure 4.5). This indicates that the pattern of blood volume changes is closely mirrored in the spatial extent of the vasculature recruitment.

It is clear that the blood volume changes are closely coupled with locomotion and whisker stimulation. However, it is not yet known whether locomotion occurring during whisker stimulation could also have an effect the blood volume changes. The next stage of the

analysis will be to determine whether it is possible to distinguish between the input of locomotion and whisker stimulation on the haemodynamic response.

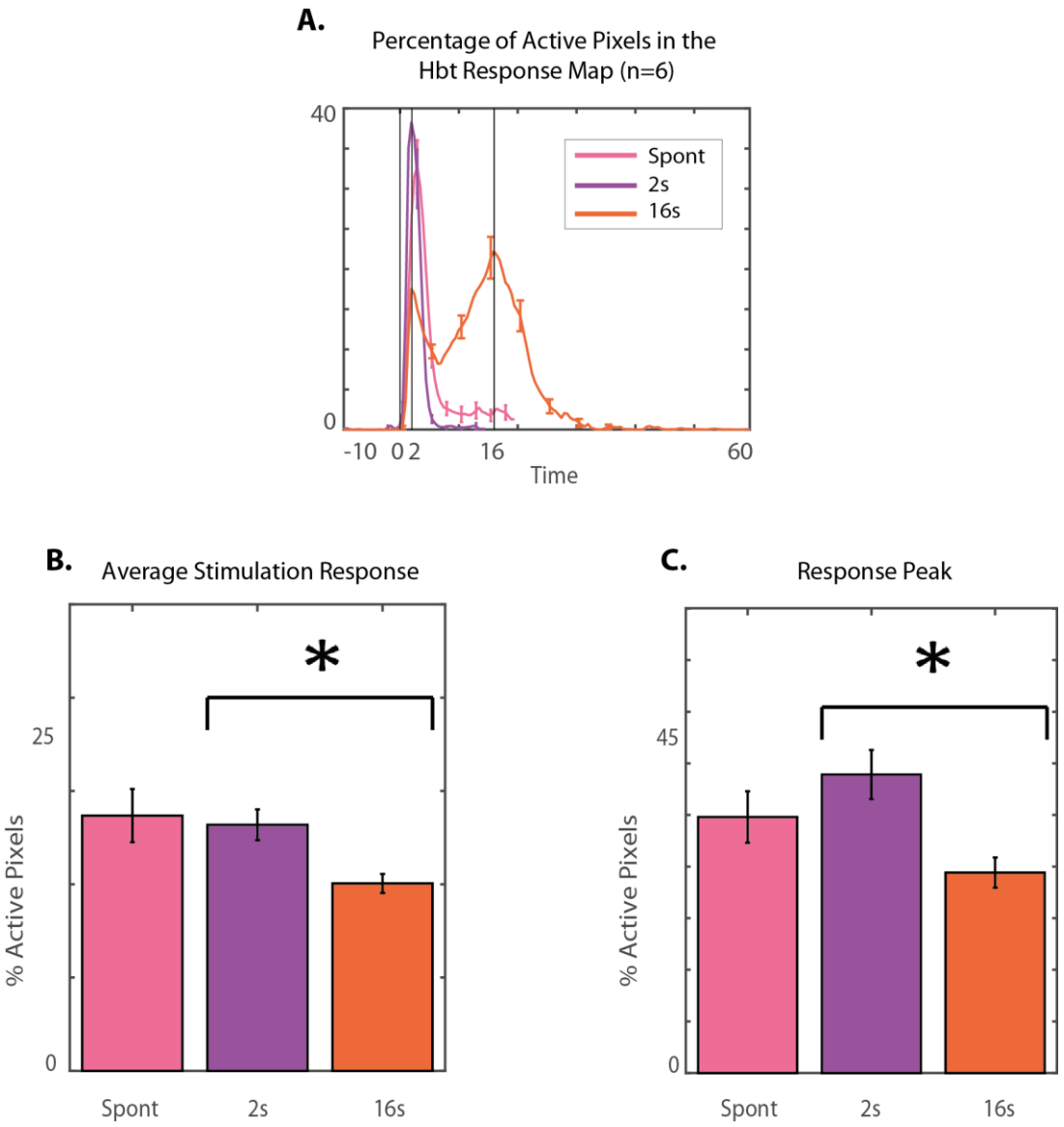

Figure 4.7 – *Active Pixels within the Hbt Response Maps during Spontaneous Locomotion and Whisker Stimulation*

The number of active pixels within the Hbt response maps during spontaneous locomotion, 2s whisker stimulation and 16s whisker stimulation (n=6). Error bars represent SEM.

4.4.3 Examining the Effect of the Interaction between Whisker Stimulation & Locomotion on the Haemodynamic Responses

Due to the strong effect of locomotion on the spontaneous haemodynamic response, it was important to assess whether locomotion interacted with whisker stimulation to alter the haemodynamic activity in S1. The basic comparisons of the Hbt response maps and the number of active pixels within these spatial maps (section 4.4.2, Figure 4.7), suggests that there may be an interaction between whisker stimulation and locomotion; this will be explored further in the following section.

4.4.3.1 Sorting Individual Whisker Stimulation Trials by Associated Locomotion occurring During the Stimulation Period

Locomotion was sorted into ascending order from the least to the most locomotion during the stimulation period for both 2s (Figure 4.8 A(1)) and 16s (Figure 4.8 B(1)) whisker stimulation experiments. The locomotion trials considered the 'least locomotion' were the bottom 25% of trials, and the locomotion trials considered the 'most locomotion' were the top 25% of trials. The least and the most locomotion trials during the stimulation period were then isolated, and the corresponding haemodynamic changes were visualised.

4.4.3.2 Examining the Time Course of Haemodynamic Responses in the Somatosensory Cortex during Whisker Stimulation Trials sorted by Locomotion

The haemodynamic responses during both 2s and 16s whisker stimulation experiments with the least locomotion (Figure 4.8 A(2) & Figure 4.8 B(2)) were smaller in magnitude, and returned back to baseline levels quicker following stimulation cessation, compared to the haemodynamic responses during 2s and 16s whisker stimulation with the most locomotion (Figure 4.8 A(3) & Figure 4.8 B(3)). A paired-samples t-test was conducted to statistically compare the Hbt responses during whisker stimulation for both the least and the most locomotion conditions. The average Hbt response was taken for 0 to 5 seconds in the 2s whisker stimulation; and for 0 to 20 seconds in the 16s whisker stimulation. There was a significant difference in the Hbt response between the least locomotion (M=0.60μM, SD=0.24) and most locomotion (M=2.05μM, SD=0.72) conditions for the 2s whisker stimulation ($t(5)=-6.10$, $p<0.01^{**}$). A significant difference was also found in the Hbt

response between the least locomotion (M=0.98μM, SD=0.38) and most locomotion (M=3.29μM, SD=1.33) conditions for the 16s whisker stimulation ($t(5)=-3.92$, $p<0.01$**). Overall, locomotion had a significant effect on the stimulus-evoked blood volume changes.

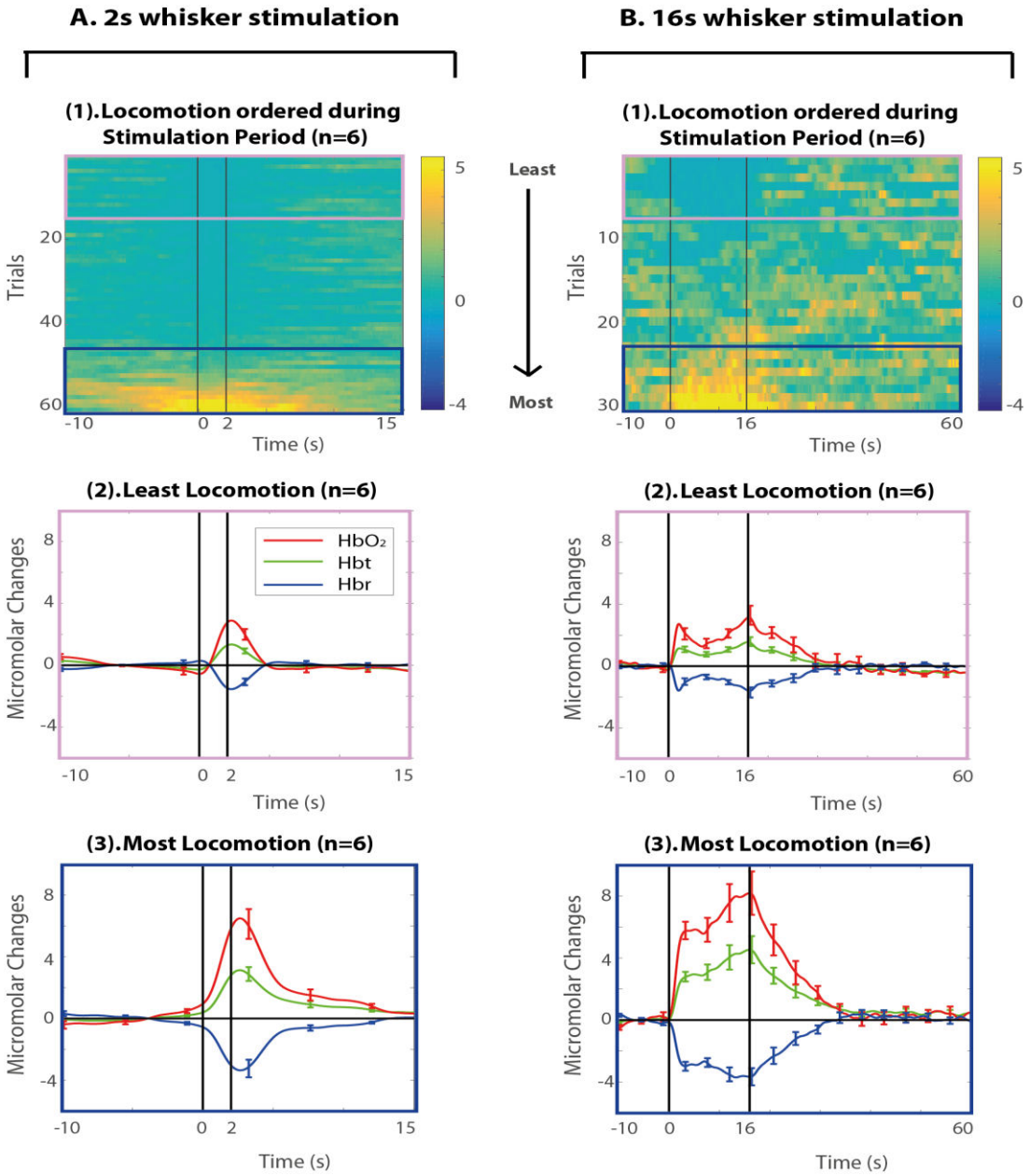

Figure 4.8 – The Temporal Profile of the Haemodynamic Response to Locomotion during Whisker Stimulation

(1) *Locomotion was sorted in ascending order from 'least' to 'most' locomotion during the whisker stimulation period across all experimental trials (locomotion was averaged across n=6 animals) for* ***A.*** *2s; and* ***B.*** *16s whisker stimulation. The corresponding temporal profile of the haemodynamic response in the whisker barrels was averaged across all subjects for the 25% trials with the:* ***(2)*** *least (light purple box); and* ***(3)*** *most (dark purple box) locomotion (for* ***A.*** *2s; and* ***B.*** *16s whisker stimulation (n=6)). Error bars represent SEM.*

4.4.3.3 Examining the Spatial Extent of Haemodynamic Responses in the Somatosensory Cortex during Whisker Stimulation Trials sorted by Locomotion

Spatial maps of the haemodynamic responses (Hbt, HbO_2 and Hbr) during whisker stimulation trials with the least and most locomotion were generated (Figure 4.9 & Figure 4.10, shown for two representative animals). For both 2s and 16s mechanical whisker stimulation with the least locomotion, an increase in Hbt was observed which was mainly localised to the whisker barrel region. However, the spatial extent of the Hbt response to whisker stimulation with the most locomotion was greater.

Next, all experimental sessions were considered in a spatial pixel analysis to statistically assess the spatial extent of the haemodynamic responses during whisker stimulation with the least and most locomotion (Figure 4.11).

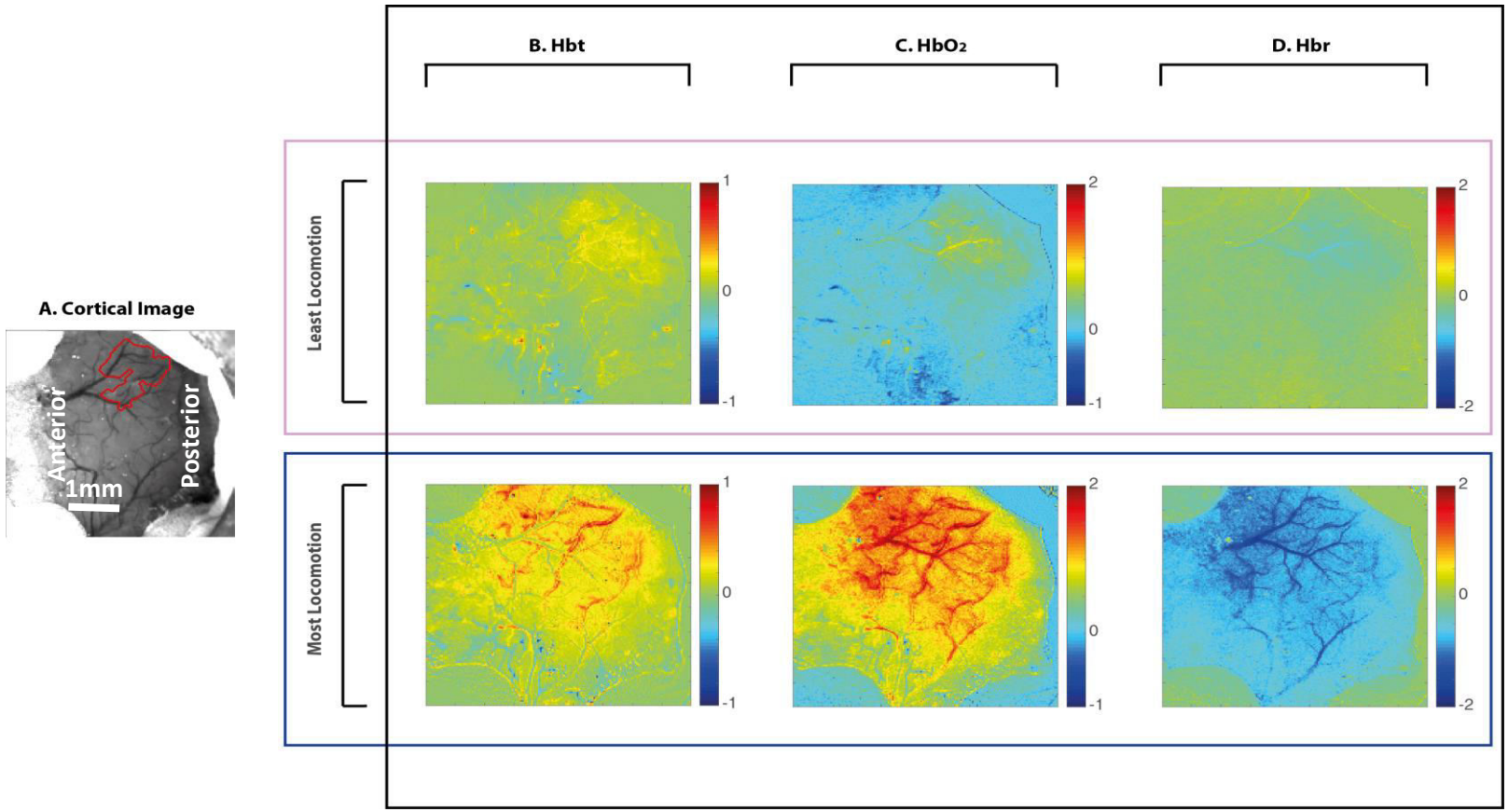

Figure 4.9 – The Spatial Extent of the Haemodynamic Response in the S1 during 2s Whisker Stimulation sorted by Least & Most Locomotion

A. *Representative images of the cortex (animal 2 as seen in Figure 4.3), with the whisker barrel region of interest marked in red. The spatial extent of the Hbt response was averaged from the onset of whisker stimulation until 5 seconds post stimulation onset for 2s whisker stimulation during the 25% of trials with the least locomotion (light purple), and the 25% of trials with the most locomotion (dark purple) (**B**. Hbt spatial map; **C**. HbO_2 spatial map; **D.** Hbr spatial map).*

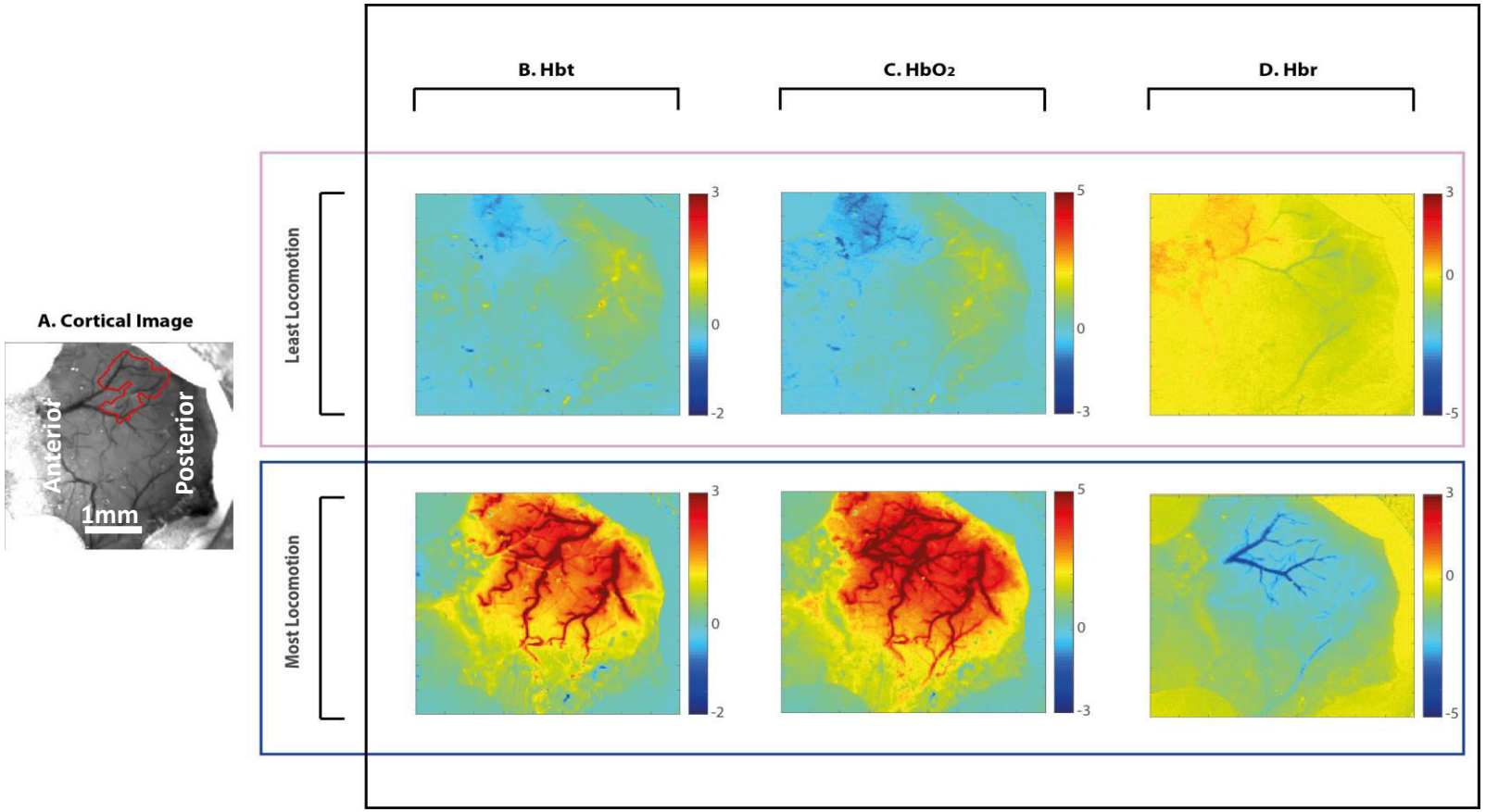

Figure 4.10 – The Spatial Extent of the Haemodynamic Response in the S1 during 16s Whisker Stimulation sorted by Least & Most Locomotion

A. *Representative images of the cortex (animal 2 as seen in Figure 4.3), with the whisker barrel region of interest marked in red. The spatial extent of the Hbt response was averaged from the onset of whisker stimulation until 5 seconds post stimulation onset for 16s whisker stimulation during the 25% of trials with the least locomotion (light purple), and the 25% of trials with the most locomotion (dark purple) (**B**. Hbt spatial map; **C**. HbO_2 spatial map; **D.** Hbr spatial map).*

The number of active pixels within the Hbt response maps was calculated for the 2s and 16s whisker stimulation during the least and most locomotion (Figure 4.11). The overall average percentage of active pixels within the Hbt response maps during 2s whisker stimulation (n=57 sessions) with the least locomotion (M=12.12%, SD=3.43) was significantly less than during 2s stimulation with the most locomotion (M=39.66%, SD=5.80; t(10)=-10.01, p=0.000003***). The maximum number of active pixels recruited during 2s whisker stimulation with the least locomotion (M=29.73%, SD=9.99) was also significantly lower than during 2s whisker stimulation with the most locomotion (M=56.89%, SD=6.26; t(10)=-5.64, p=0.0004***). Furthermore, the overall average percentage of active pixels within the Hbt response maps during 16s whisker stimulation (n=28 sessions) with the least locomotion (M=8.33%, SD=4.20) was significantly less than during 16s stimulation with the most locomotion (M=13.87%, SD=1.94; t(10)=-2.93, p=0.03*). Although the maximum number of active pixels recruited during 16s whisker stimulation with the least locomotion (M=19.71%, SD=6.25) was lower than during 16s whisker stimulation with the most locomotion (M=24.74%, SD=3.59; t(10)=-1.71, p=0.24, ns), this difference was non-significant. It is clear from this sorting of locomotion, that locomotion during the whisker stimulation affects the blood volume responses.

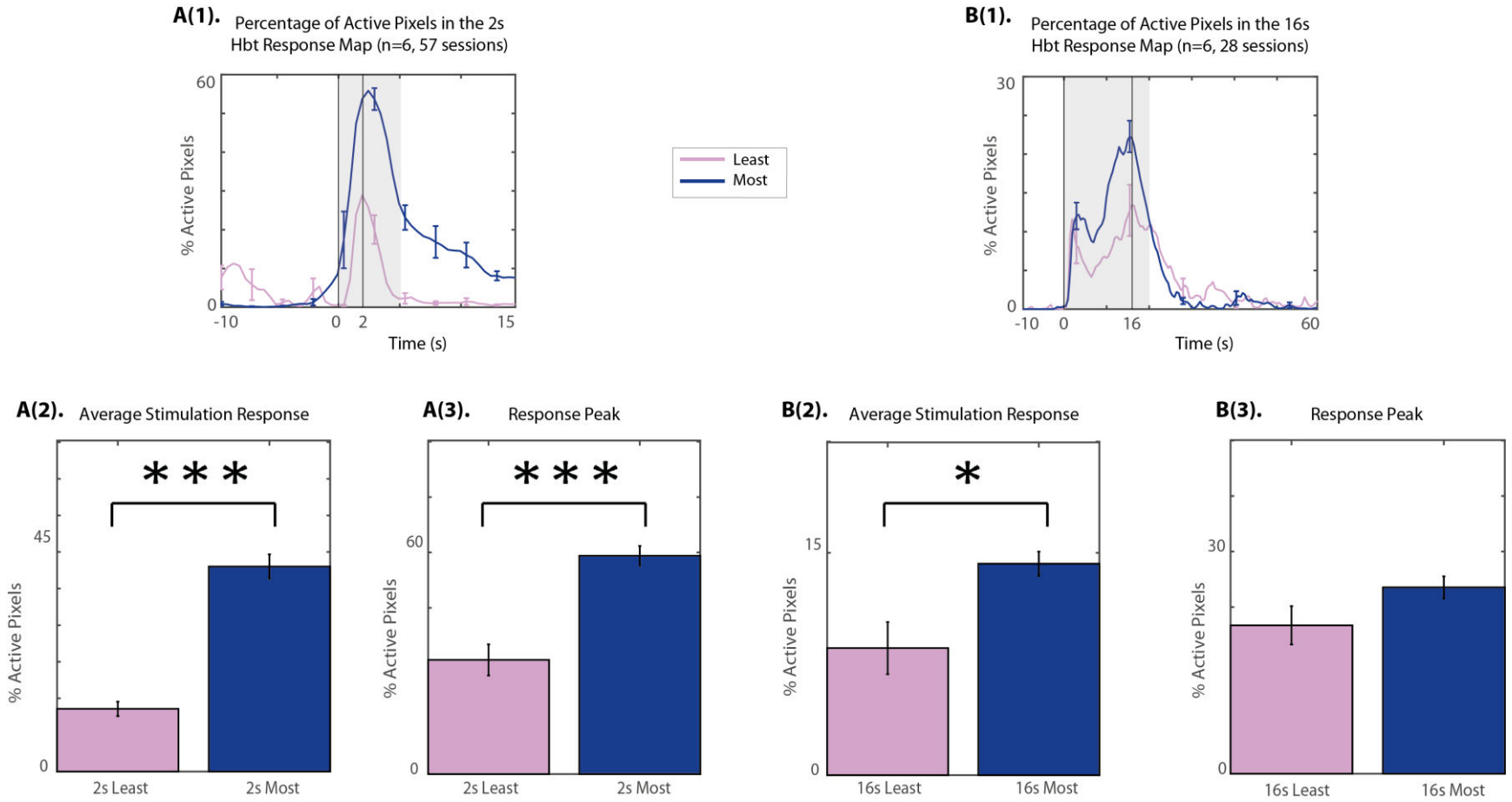

Figure 4.11 – Active Pixels within the Hbt Response Maps during Whisker Stimulation sorted by Locomotion

The active pixels within the Hbt response maps for were calculated both 2s and 16s whisker stimulation experiments (A(1) & B(1)) as: the average percentage of active pixels to stimulation (A(2) and B(2)), and the maximum number of active pixels during stimulation (A(3) & B(3); n=6) for whisker stimulation with the least locomotion (light purple) and whisker stimulations with the most locomotion (dark purple). Error bars represent SEM.

4.4.4 Investigation of the Linear Superposition of Locomotion-Evoked and Stimulus-Evoked Haemodynamic Responses

The magnitude of stimulus-evoked haemodynamic responses were altered when sorted by the co-occurring locomotion (Figure 4.11). This section assesses the contribution of either the whisker stimulation or locomotion in isolation. For isolating these contributions, a control condition was added, which could be used to remove the effects of sorting by locomotion (Figure 4.12).

To create the control condition, spontaneous (no stimulation) experiments were cut into trials which corresponded to the timing of the whisker stimulation experiments. The locomotion during these spontaneous experiments was sorted (in the same way as described in section 4.4.3.1, Figure 4.8) in ascending order from the 'least' to the 'most' locomotion during the corresponding 'stimulation period' (Figure 4.12 A(1) & Figure 4.12 B(1)). The haemodynamic changes during the 'least' (Figure 4.12 A(2) & Figure 4.12 B(2)) and 'most' (Figure 4.12 A(3) & Figure 4.12 B(3)) locomotion periods were then extracted.

The haemodynamic responses during the spontaneous experiments showed differences between the 'least' and 'most' locomotion trials. The haemodynamic responses during spontaneous experiments with the 'least' locomotion showed an overall decrease in HbO_2 and Hbt, with an increase in Hbr, which subsequently returned to baseline. This overall negative response (i.e. decrease in Hbt) was most likely an effect of sorting by locomotion, as there was a reduction in locomotion below baseline levels. The haemodynamic responses during spontaneous experiments with the 'most' locomotion during the 'stimulation period' showed an increase in HbO_2 and Hbt, with a decrease in Hbr, which returned to baseline.

In order to assess whether whisker stimulation and locomotion linearly sum to account for the overall changes observed in the Hbt response, the Hbt data for whisker stimulation and spontaneous experiments, sorted by 'least' and 'most' locomotion, were subjected to a series of subtractions (see sections 4.4.4.1 & 4.4.4.2). Following these subtractions, the resulting time series should show similar magnitudes and temporal profiles, if: a) the locomotion component is spontaneous in nature (i.e. not related to the stimulation); and b)

the stimulus-evoked Hbt component is not affected by the underlying spontaneous locomotion.

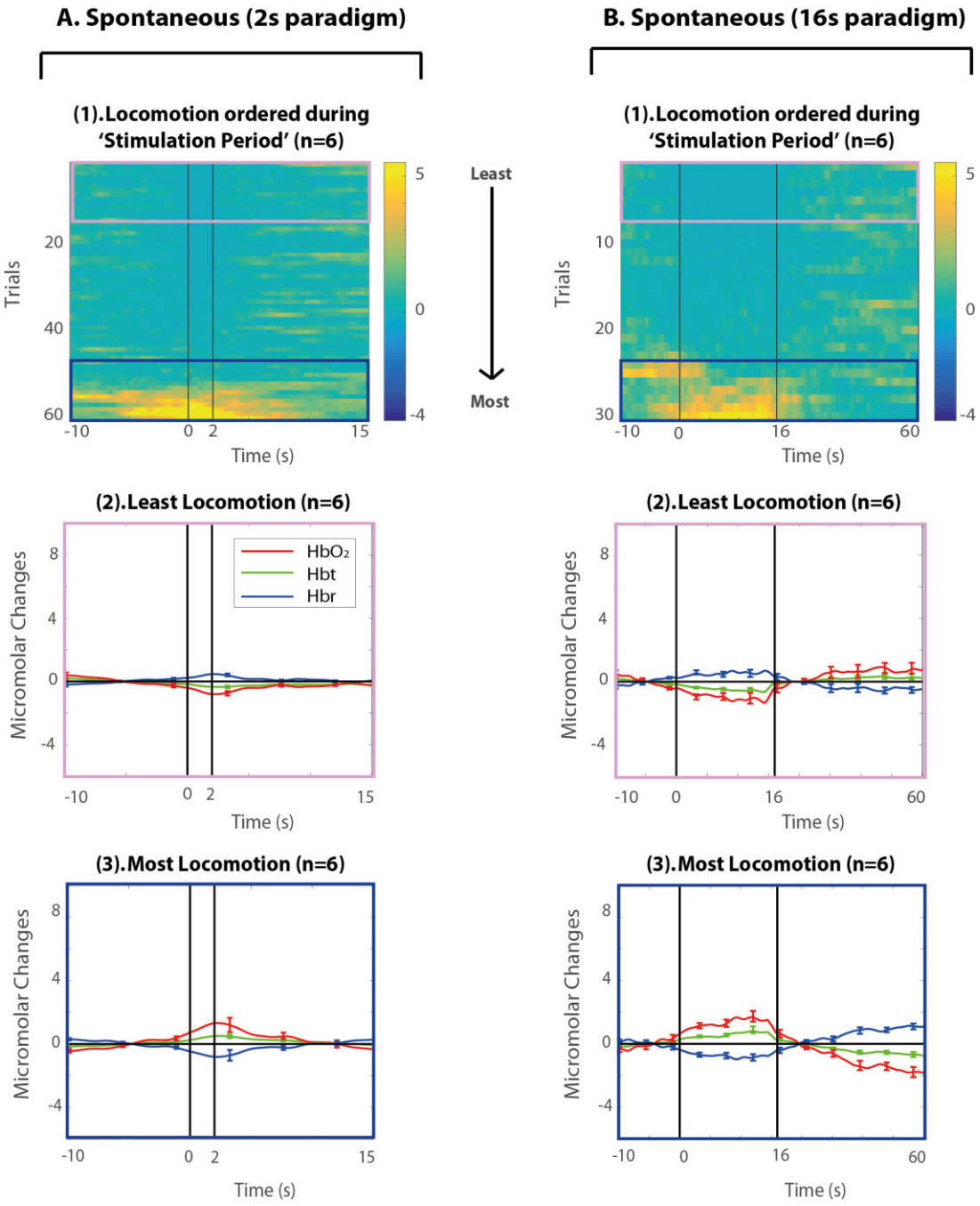

Figure 4.12 — The Temporal Profile of the Haemodynamic Response to Locomotion during Spontaneous (no stimulation) Recordings

(1) *Locomotion was sorted in ascending order from the least to most locomotion during the corresponding 'whisker stimulation period' across all experimental trials (n=6) for* ***A.*** *a 2s paradigm; and* ***B.*** *a 16s paradigm. The corresponding temporal profile of the haemodynamic response in the whisker barrels was averaged across all subjects for the 25%*

trials with the: ***(2)*** *least (light purple); and* ***(3)*** *most (dark purple) locomotion (n=6). Error bars represent SEM.*

4.4.4.1 Extracting and Investigating the Stimulus-Evoked Haemodynamic Component

To obtain the stimulus-evoked haemodynamic component, the effects of locomotion and sorting by locomotion were removed from the Hbt response (for 2s and 16s paradigms; Figure 4.13). This was achieved by producing two time series, where the effects of the 'least' and 'most' locomotion were subtracted and then compared.

The first ('most') time-series was generated by taking the stimulus-evoked Hbt responses with the 'most' locomotion and subtracting the spontaneous Hbt responses with the 'most' locomotion (for 2s and 16s paradigms; Figure 4.13 A & Figure 4.13 D). The second ('least') time-series was generated by taking the stimulus-evoked Hbt responses with the 'least' locomotion and subtracting the spontaneous Hbt responses with the 'least' locomotion (for 2s and 16s paradigms; Figure 4.13 B & Figure 4.13 E).

The two stimulus-evoked only time series generated were significantly different for both the 2s ($t(71)=5.81$, $p<0.001$***; Figure 4.13 C) and 16s ($t(100)=5.20$, $p<0.001$***; Figure 4.13 F) paradigms. This strongly suggests the time series were thus not linearly superimposed.

4.4.4.2 Extracting and Investigating the Locomotion-Evoked Haemodynamic Component

To obtain the locomotion-evoked haemodynamic component, the effects of whisker stimulation and sorting by locomotion were removed from the Hbt response (for 2s and 16s paradigms; Figure 4.14). This was achieved by producing two time series, where the effects of 'least' locomotion were subtracted from those of 'most' locomotion for both the whisker stimulation Hbt response and the spontaneous paradigm Hbt response. These subtractions remove either the effects of the whisker stimulation or of sorting by locomotion.

The first time series (removing the effects of whisker stimulation) was generated by taking the stimulus-evoked Hbt responses with the 'most' locomotion and subtracting the stimulus-evoked Hbt responses with the 'least' locomotion (for 2s and 16s paradigms; Figure 4.14 A & Figure 4.14 D). The second time series (removing the effects of sorting by

locomotion) was generated by taking the spontaneous Hbt responses with the 'most' locomotion and subtracting the spontaneous Hbt responses with the 'least' locomotion (for 2s and 16s paradigms; Figure 4.14 B & Figure 4.14 E).

The two locomotion-evoked only time series generated were significantly different for both the 2s ($t(88)=4.09$, $p<0.001$***; Figure 4.14 C) and 16s ($t(88)=6.06$, $p<0.001$***; Figure 4.14 F) paradigms. Thus, the time-series were not linearly superimposed.

The linear subtractions conducted (i.e. the stimulus-evoked and locomotion-evoked) resulted in significantly different time series. These results suggest that either there was an interaction of locomotion with the whisker stimulation (i.e. locomotion was not spontaneously occurring); and/or that the stimulus-evoked Hbt response was affected by spontaneous locomotion. These possible explanations will be discussed in more detail later (section 4.4.5).

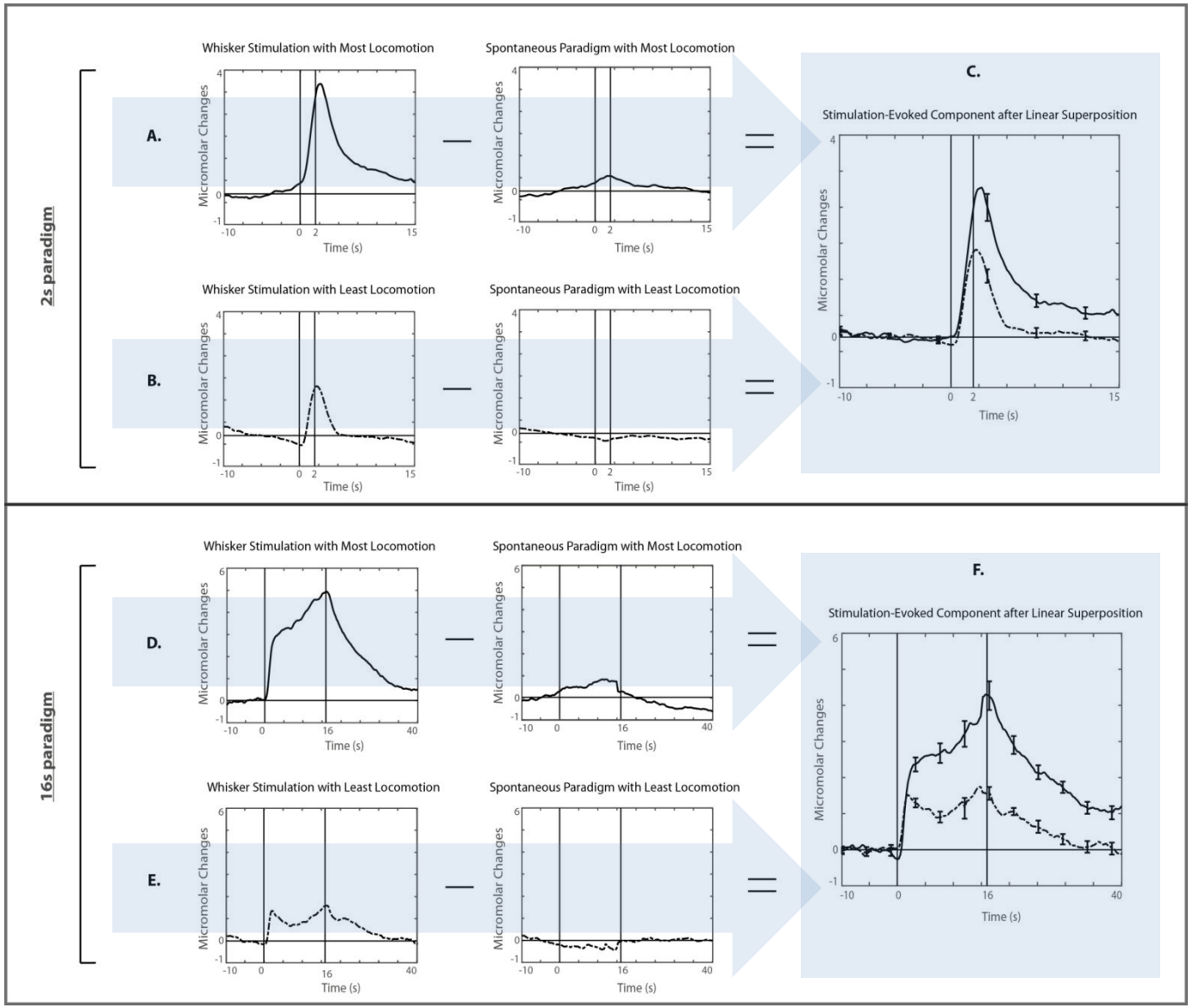

Figure 4.13 – Extracting and Investigating the Stimulus-Evoked Haemodynamic Component

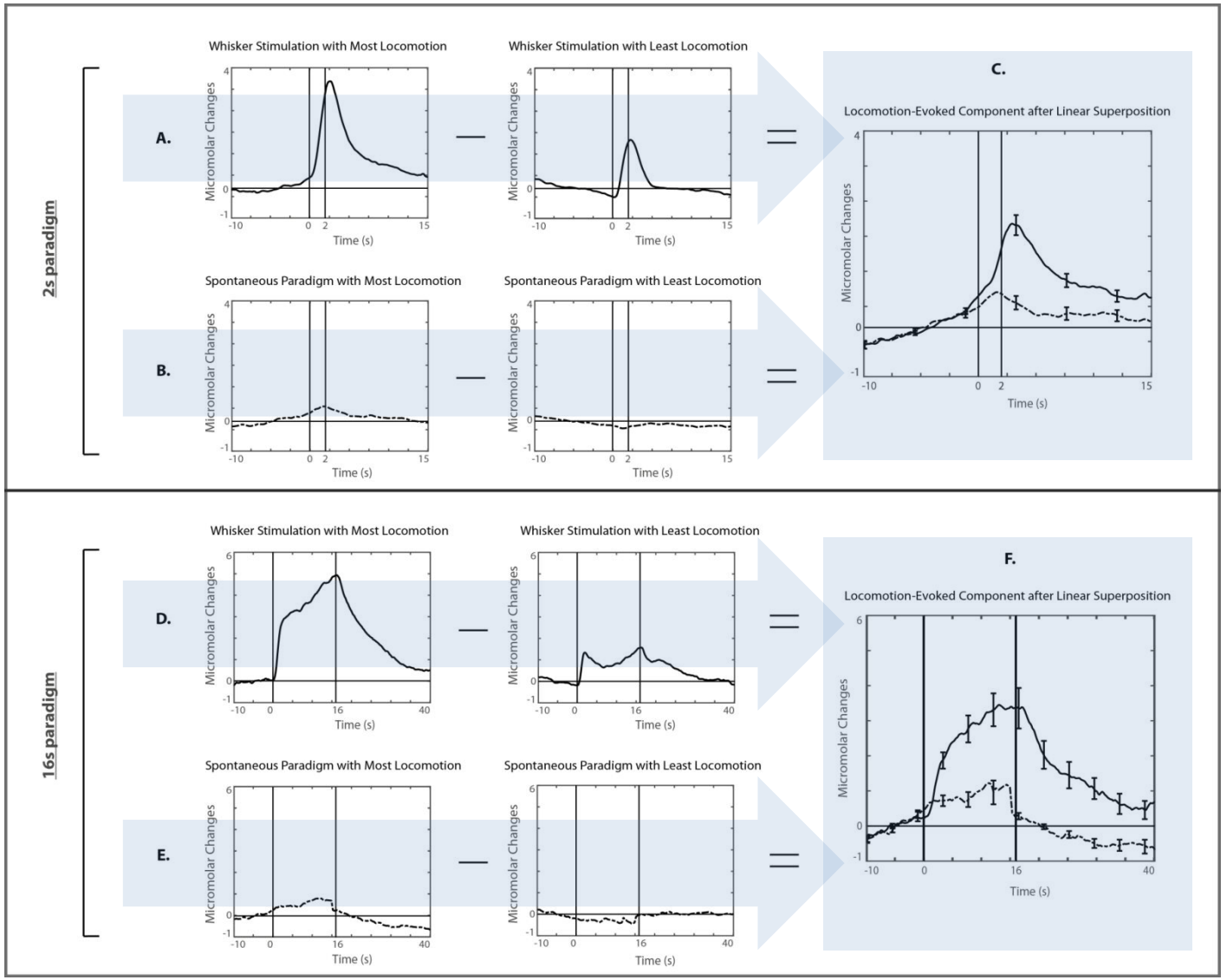

Figure 4.14 – Extracting and Investigating the Locomotion-Evoked Haemodynamic Component

4.4.5 Examining the Interaction between Stimulus-Evoked and Locomotion-Evoked Haemodynamic Changes

The locomotion and stimulus-evoked haemodynamic responses could not be linearly separated, which suggests a possible interaction between the two.

Two hypotheses were proposed to explain why the Hbt responses during whisker stimulation only (Figure 4.13) and the Hbt responses during locomotion in isolation (Figure 4.14) did not account for the entirety of the observed increases in the blood volume occurring within the whisker barrel region:

(1) **Hypothesis 1**: The whisker stimulation may alter the locomotion (i.e. the animal starts or stops locomotion in response to whisker stimulation);

(2) **Hypothesis 2:** The whisker stimulation may cause the animal to engage with a different behaviour, such as whisking (i.e. the animal starts or stops whisking during whisker stimulation).

These additional behaviours, which were not measured in the previous analysis, could account for additional variance in the haemodynamic responses.

4.5.4.1 Hypothesis 1: Whisker Stimulation alters Locomotion Behaviour

In order to assess the effects of locomotion and whisker stimulation on the haemodynamic activity in S1, the interaction between whisker stimulation (2s and 16s) and locomotion behaviour was categorised. There were three ways in which the whisker stimulation could alter the locomotion behaviour:

(1) Whisker stimulation correlated with the onset of locomotion;

(2) Whisker stimulation correlated with the offset of locomotion; or

(3) Locomotion events were unrelated to the whisker stimulation.

It is known from the previous analysis that locomotion affects the haemodynamic responses in the somatosensory cortex, thus it may be possible that these alternative locomotion behaviours (i.e. offset or onset of locomotion) could alter haemodynamic response profiles.

To categorise the possible interaction between whisker stimulation and locomotion behaviour a metric for the average locomotion during the pre-stimulus baseline period, and a metric for the average locomotion during the stimulation period, were extracted for each experimental session across the 6 animals (between 3-16 sessions were contributed by each animal). The metric for 'locomotion during the pre-stimulus baseline period' was subtracted from the metric for the 'locomotion during the stimulation period'. Positive results indicated an overall increase in locomotion from baseline during the stimulation period, whereas negative results indicated an overall decrease in locomotion from baseline during the stimulation period (Figure 4.15 & Figure 4.16).

To ascertain which locomotion behaviour (i.e. onset, offset, no change) the whisker stimulation correlated with at a 95% confidence level (i.e. significance level), a student's t inverse cumulative distribution function test was applied to find the standard mean error (SEM) of the 'locomotion and stimulation interaction' metric (for each experimental session; Figure 4.15 & Figure 4.16). The overall positive confidence interval results were categorised as whisker stimulation correlating with the onset of locomotion ((1), Figure 4.15 & Figure 4.16, *green*); the overall negative confidence interval results were categorised as whisker stimulation correlating with the cessation of locomotion ((2), Figure 4.15 & Figure 4.16, *red*); and confidence intervals which ranged from a negative result to a positive result (i.e. crossed zero) were categorised as locomotion events which were unrelated to the whisker stimulation ((3), Figure 4.15 & Figure 4.16, *yellow*).

This analysis demonstrated that in these experimental sessions the majority of locomotion events were not significantly related to the whisker stimulation (2s: 82.46%; 16s: 89.29%). This means that in general the whisker stimulation was likely not altering the locomotion behaviour, and so this explanation may not account for the variance seen in the Hbt responses after linear superposition.

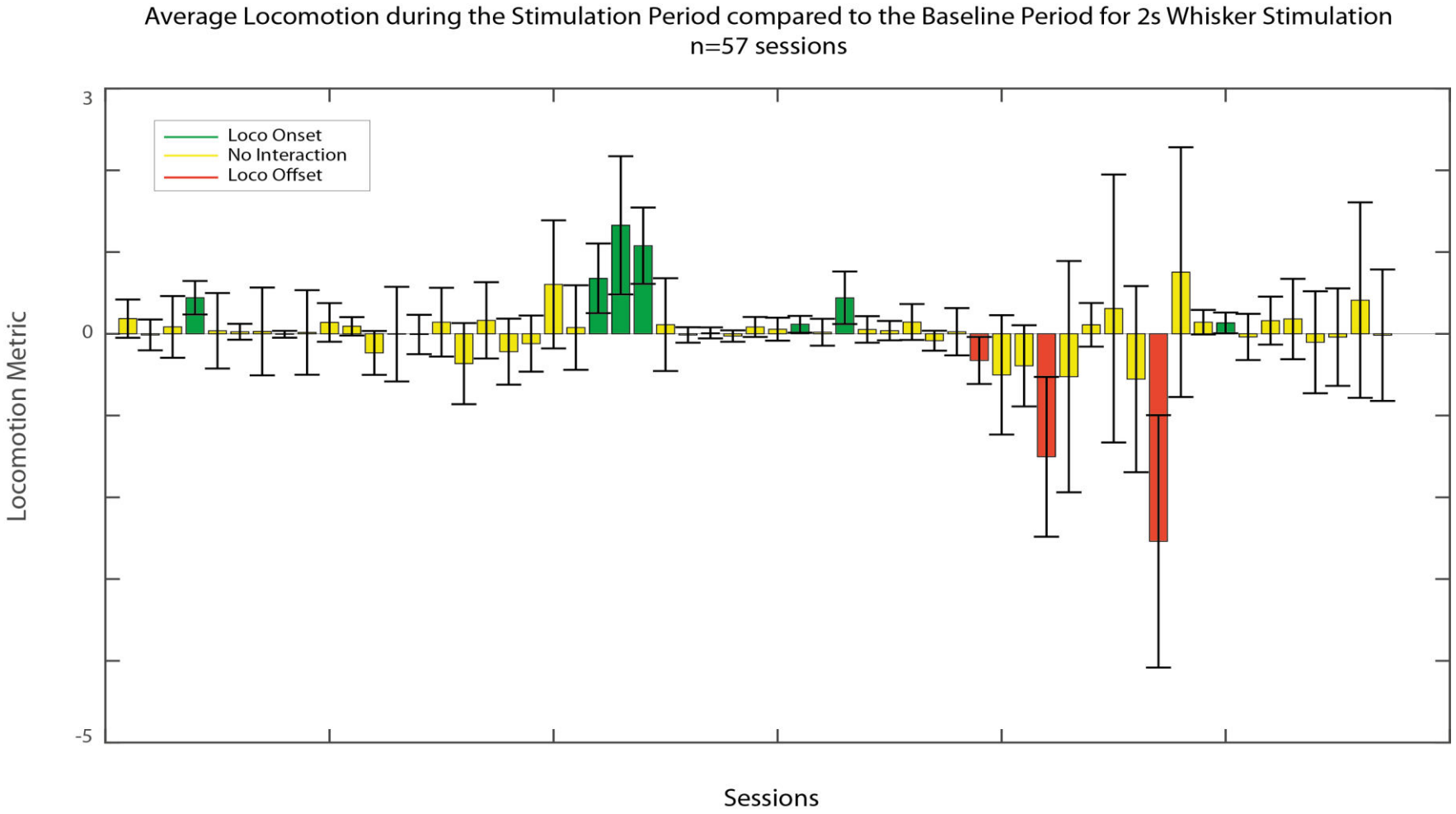

Figure 4.15 – The Average Locomotion during the Stimulation Period compared to the Baseline Period of 2s Whisker Stimulation (n=57 sessions)

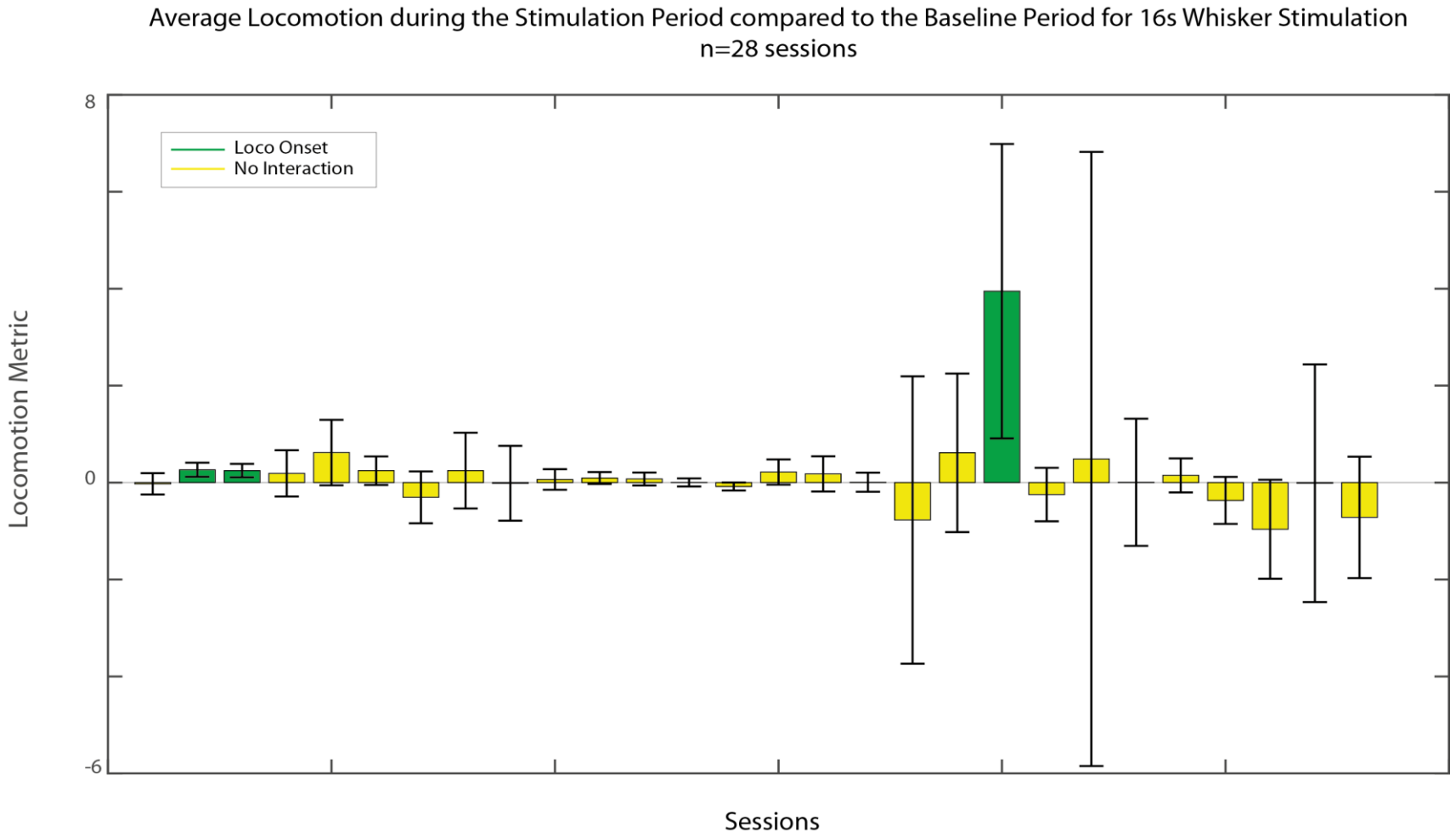

Figure 4.16 – The Average Locomotion during the Stimulation Period compared to the Baseline Period of 16s Whisker Stimulation (n=28 sessions)

4.5.4.2 Hypothesis 2: Natural Whisking Occurs throughout the Imaging Session

Another possible explanation for the variance in the Hbt responses, which could not be accounted for by whisker stimulation or spontaneous locomotion, is that the animal may or may not have been engaging with whisking. In these experiments, the haemodynamic responses in the whisker barrel region are measured, and so any natural whisking has the potential to alter these responses.

It is known that rodents whisk during locomotion (Arkley et al., 2014; Sofroniew et al., 2014); and this extends to head-fixed mice, which have been shown to whisk naturally when running on a spherical treadmill (Sofroniew & Svoboda, 2015). This means that the haemodynamic responses observed during locomotion, will likely also be affected by coexisting natural whisking.

Furthermore, rodents have been known use their mechanosensitive whiskers for a diverse range of tactile behaviours such as navigation, object recognition, and social interactions (Sofroniew & Svoboda, 2015). Rodents naturally live in dark conditions, meaning they rely most on their whiskers to sense the world around them. Due to rodents reliance on the diverse information which is collected using the whiskers, rhythmic whisking has actually been coupled to running speed, stepping, sniffing, and even ultrasonic vocalisations (Sofroniew & Svoboda, 2015). This means that not only will the subjects be whisking during locomotion, but they may also start or stop whisking during the whisker stimulation period.

Thus, it is important to simultaneously track the whiskers whilst imaging the haemodynamic changes in S1 and tracking locomotion. However, because whiskers move at considerable speed (up to 10,000 degrees per second) they must be imaged using a high-speed (1,000 frames per second) camera (Sofroniew & Svoboda, 2015). There was not a separate camera system available to track the whiskers in the Sheffield laboratory, as such the whisker movements could not be correlated with corresponding haemodynamic responses in S1 for these experiments.

4.5 Discussion

The awake mouse imaging platform (first described in chapter 3) provides a useful tool to study haemodynamic changes in S1 during locomotion. From this study it is clear that locomotion alters the haemodynamic response in S1 on a trial-by-trial basis, and so researchers using this model to study neurovascular coupling may wish to consider locomotion in their data analyses.

4.5.1 Results Summary

4.5.1.1 Characterisation of the Haemodynamic Responses during Spontaneous Locomotion

Locomotion and the corresponding haemodynamic responses in S1 were assessed for spontaneous experimental paradigms, in which no whisker stimulation was presented. Locomotion was extracted by detecting the onset and cessation of walking events. The haemodynamic responses were assessed in the whisker barrel region during these locomotion events.

Contrary to previous research (Takuwa et al., 2011; 2012), locomotion was found to cause an overall increase in Hbt and HbO_2, with a concurrent decrease in Hbr in the whisker barrel region of S1. The peak influx of Hbt and HbO_2 reached a higher magnitude in the whisker barrels during locomotion than during whisker stimulation. Further, haemodynamic responses to locomotion appeared to onset slightly before locomotion physically began. Previous work has shown that activity in S1 can precede voluntary movement (e.g. Hamada et al., 1999; Paz et al., 2003). However, this result would require further investigation before any firm conclusions could be drawn. For instance, future work could test mice on an automated treadmill, in which involuntary locomotion was induced. It would be expected in this case that the haemodynamic responses would be slightly delayed following the onset of involuntary locomotion (as seen in the whisker stimulation experiments).

The spatial extent of the haemodynamic responses during locomotion was also investigated. The onset of locomotion resulted in an increase in Hbt which was global, spreading across most of the exposed S1 and recruiting much of the surface vasculature.

The locomotion events were then further separated by duration (i.e. long and short duration). Long and short duration events showed increases in Hbt following the onset of locomotion, with responses to long duration events taking longer to return to baseline and reaching a greater magnitude than short duration runs. Locomotion was tightly coupled with haemodynamic changes. Spatially, both long and short duration runs showed global recruitment of the vasculature of the exposed S1.

4.5.1.2 Characterisation of the Haemodynamic Responses to Whisker Stimulation

Typical haemodynamic response profiles were observed to both 2 and 16 second mechanical whisker stimulation across subjects. The expected increases in Hbt and HbO_2, with the concomitant decrease in Hbr, were produced in the whisker barrels in response to the stimulations. The 2s stimulation produced a short duration monophasic haemodynamic response; whilst the 16s stimulation produced larger magnitude, longer duration haemodynamic responses characterised by initial and secondary response peaks. Spatially, for both 2s and 16s mechanical whisker stimulation, an increase in Hbt was observed which was largely centred on the 'active whisker region'.

The number of active pixels within the Hbt response maps were calculated for spontaneous locomotion, 2s and 16s whisker stimulation. The overall average percentage of active pixels in the Hbt response maps during spontaneous locomotion was larger than for 2s and 16s whisker stimulation. However, there were significantly more active pixels for 2s stimulation than for 16s stimulation, likely due to there being less variance in the number of active pixels in the Hbt response maps during 2s whisker stimulation. The absolute maximum number of active pixels (i.e. response peak) in these Hbt response maps was also significantly larger for 2s stimulation compared to 16s stimulation. This result is somewhat surprising, as the Hbt time course response was larger for 16s stimulation, which is typically tightly coupled with the spatial recruitment of vasculature. Spontaneous locomotion also showed a higher number of active pixels in the Hbt response maps compared to 16s whisker stimulation. Locomotion during whisker stimulation was not initially considered here, however it is possible that locomotion was confounding the haemodynamic responses observed during whisker stimulation.

4.5.1.3 Characterisation of the Haemodynamic Responses to Whisker Stimulation & Locomotion

Locomotion was sorted into ascending order from the 'least' to the 'most' locomotion during the stimulation period for both 2s and 16s whisker stimulation experiments. The corresponding haemodynamic changes were visualised during time points with the 'least' and 'most' locomotion. The haemodynamic responses during whisker stimulation experiments with the 'least' locomotion were significantly smaller in magnitude, and returned back to baseline levels quicker following stimulation cessation, compared to the haemodynamic responses during whisker stimulation with the 'most' locomotion.

Next, the spatial extent of the Hbt response maps during whisker stimulation with the 'least' and 'most' locomotion were visualised. For both 2s and 16s mechanical whisker stimulation with the 'least' locomotion an increase in Hbt was observed which was primarily localised to the whisker barrel region. However, the spatial extent of the Hbt response to whisker stimulation with the 'most' locomotion was more globally spread. Separating the whisker stimulation by 'least' and 'most' locomotion demonstrated that locomotion during the whisker stimulation period was confounding the haemodynamic responses.

4.5.1.4 Distinguishing between the Effects of Locomotion & Whisker Stimulation on Haemodynamic Responses

The next stage of the analysis was to assess whether locomotion and whisker stimulation accounted for the observed increases in Hbt. Analysis was performed to assess whether there was a linear relationship between the effects of whisker stimulation and spontaneous locomotion on the overall Hbt response within the whisker barrel region. The whisker stimulation responses were sorted for 'least' and 'most' locomotion, and the spontaneous (no stimulation) experiments were sorted in the same way. When the Hbt responses during whisker stimulation only and locomotion only were linearly superimposed, there were still significant differences in the Hbt responses, meaning that additional behavioural variables (not accounted for here) were potentially affecting the Hbt responses.

Subsequent analysis demonstrated that, on the whole, whisker stimulation did not alter locomotion behaviour (i.e. onset or offset). It was possible that whisker stimulation altered

whisking behaviour, although with the current experimental set-up this could not be ascertained.

4.5.2 Results Interpretation

The results of this chapter strongly indicate that during locomotion (with and without whisker stimulation), the increases in Hbt in S1 are more globally spread (Figure 4.9 & Figure 4.10). Here, the behavioural state of the subject (i.e. active locomotion versus rest) was shown to affect the Hbt response in the exposed somatosensory cortex. However, the neural circuits responsible for such modulations were not measured.

Previous work has demonstrated that increases in locomotion are closely correlated with increases in the neural activity of vasoactive intestinal peptide-expressing (VIP) interneurons (in V1, Fu et al., 2014; Pfeffer et al., 2013). The VIP interneuron is a specific type of GABAergic cortical interneuron, thought to mediate disinhibitory control in the cortex (Pi et al., 2013). The circuit by which VIP interneurons may enhance cortical excitation during locomotion is: VIP interneurons have been shown to preferentially inhibit somatostatin (SST) interneurons, which provide inhibitory input onto pyramidal cells (Fu et al., 2014; Pfeffer et al., 2013; Pi et al., 2013). This results in increased activity in the pyramidal cells during locomotion, which will likely require more oxygen and glucose, supplied by a concurrent increase in Hbt.

As well as observing global increases in Hbt during locomotion (with and without whisker stimulation), the results from this chapter also showed a more localised haemodynamic response during whisker stimulation with little or no locomotion (i.e. during rest). Interpreting these results using the disinhibition model, if the subject is not engaging in locomotion, then VIP interneurons will not be activated, meaning SST interneurons will inhibit pyramidal cell activity. This inhibition of pyramidal cell activity, will mean more localised neuronal firing centred on the whisker barrel region (i.e. in response to whisker stimulation), and as such more localised energy and glucose supplies (i.e. HbO_2 and Hbt increases).

4.5.3 Limitations of the Current Study

Whilst the approach developed and described in this and the previous chapter was: (A) a novel preparation within the Sheffield laboratory, and (B) helped towards resolving some of the discrepancies within the field of imaging the awake mouse S1, there are still a number of limitations.

Tracking Simultaneous Whisking. The results of this experiment indicate that the Hbt in the whisker barrels increases during locomotion periods compared with stationary periods. There is an underlying assumption that this increase in Hbt during locomotion in the whisker barrels is actually a result of the tight coupling between locomotion and whisking. As the rodent uses its whiskers to gain more information during exploratory behaviour, it is assumed that whilst walking the animal is concurrently whisking (Arkley et al., 2014; Sofroniew et al, 2014). Sofroniew and colleagues developed a tactile virtual reality system with which to quantify whisker-guided locomotion (Sofroniew et al, 2014). During running, mice moved their whiskers in a rhythmic fashion, and whisking was found to be closely linked with both running speed and running direction. There is a tight-coupling between locomotion and whisking, demonstrating the benefits of considering both locomotion and whisking when studying neurovascular coupling in the cortex of the awake behaving animal. Whisking was not considered for the purpose of this study, as the experimental techniques for tracking whisking were not available.

Concurrent Electrophysiological Recordings. The present study provides a narrowed view of neurovascular coupling in the awake behaving mouse during whisker stimulation and locomotion, as the vascular responses are considered in isolation. Neural and vascular activity are known to be tightly coupled, as the active brain relies on a constant source of energy and oxygen, which is supplied via cerebral blood flow (Roy & Sherrington, 1890; Cox et al., 1993). It is important to assess whether the changes in Hbt resulting from whisker stimulation or locomotion, are also reflected in the neural activity. Huo and colleagues found an increase in gamma-band power in the hind-limb area of the S1 during walking periods compared to stationary periods (Huo, Smith & Drew, 2014). It would be beneficial to expand on these findings to investigate local field potentials and multi-unit activity in the whisker barrel region of S1 during locomotion and rest.

The electrophysiology technique available in the Sheffield laboratory was deemed too invasive to use in the awake mouse preparation presented in this chapter. The available electrophysiology technique requires the drilling of a small hole through the skull and dura

overlying the whisker barrel region in S1. A multi-channel electrode is then inserted through this hole, into the underlying cortex. Due to the damage imposed from this particular technique on the skull and brain, and the required physical fixing, it was deemed to be not possible to employ these methods without anaesthesia, or to recover the animals following such procedures. Other experiments which have recorded neural activity chronically from the awake, behaving mouse have typically used less-invasive techniques such as two-photon fluorescence imaging (Andermann et al., 2013; Dombeck et al., 2007) or genetically encoded voltage indicators (Carandini et al., 2015; Chen et al., 2013; Knopfel, 2012).

Naturalistic Experimental Set-Up. For the experiments described in this chapter, the mice were head-fixed atop of a spherical treadmill. This set-up is not a reflection of the natural environment within which the subject freely explores their surroundings. However, in this case head fixation was a necessity for stable neuroimaging, as the cerebral vessels must remain physically static to record the underlying haemodynamic changes which occur during locomotion and whisker stimulation. Whilst the limitations of the optical imaging technique used here do not allow for free exploration, there are complimentary methods available which may create a slightly more naturalistic setting via virtual maze navigation. Head-fixed animals can be presented with virtual environments through which to navigate. The visual stimuli updates in real-time as the animal changes the speed and direction of its locomotion, as detected by the optical motion sensor (Dombeck et al., 2007; 2010; Harvey et al., 2009; 2012; Ravassard et al., 2013). This provides a framework in which virtual mazes can be presented, where locomotion serves as a readout for decision making (Chen et al., 2013).

Whilst recent advances in imaging technology have allowed routine measurement of the spatiotemporal dynamics of sensory processing in head-fixed animals (Ayaz et al, 2013; Dombeck et al., 2007; 2010; Huo et al., 2014; Niell & Stryker, 2010; Petersen et al., 2003; Saleem et al, 2013; Takuwa et al., 2011; 2012); it would be even more optimal to image cortical function in awake, non-head-fixed animals. Neural spiking activity has previously been recorded in freely behaving rodents using wire electrodes (O'Keefe & Dostrovsky, 1971; Hafting et al., 2005). Functional optical imaging in freely behaving rodents draws on the same idea, however microscopes must be fabricated which are small and light enough to be mounted onto the head of the animal without significantly altering its behaviour (Chen et al., 2013; Ziv et al., 2013). For example, fibre optic image bundles have been used

by Petersen and colleagues to image cortical spatiotemporal dynamics in freely moving mice (Ferezou et al., 2006). The excitation light for fluorescence imaging was brought to the cortical surface via these fibres, which were also able to detect emission. The researchers used this methodology in combination with voltage-sensitive dyes to detect spatiotemporal dynamics in supragranular layers of the cortex (layers 1-3), with millisecond temporal resolution and subcolumnar spatial resolution. A more recent study combined an integrated fluorescence microscope with a chronic microendoscopy mouse preparation to access deeper areas of the cortex (Barretto et al., 2011).

The possibility of imaging under freely moving conditions provides an opportunity to study cortical function under behavioural contexts usually constrained or precluded under the head-fixed condition, such as self-determined and social behaviour. Such naturalistic experimental set-ups allow researchers to create tasks which probe sensation and perception, and even aspects of cognition (Burgess et al., 2016; Bussey et al., 2012; Nithianantharajah et al., 2015).

Post-Experiment Histology. For the data presented here, it was not possible to gain complimentary cytochrome oxidase staining to confirm the location of the whisker barrels and adjacent regions. It was possible to localise the whisker barrel region by conducting whisker stimulations on the awake animal, and finding the active region; however it could be interesting to investigate visible structures within the remainder of the exposed S1. During locomotion the spatial extent of the haemodynamic response was global, spreading across the exposed S1 and recruiting surface vasculature from regions outside of the whisker barrels. It was possible that the fore- and hind- limb representations were receiving an influx of cerebral blood, as the limbs are recruited during movement; however it was not possible to confirm whether these regions were within the exposed S1 without cytochrome oxidase staining to confirm their exact locations.

4.5.4 Possible Future Directions

The awake imaging platform, described in this chapter and the previous chapter, could be improved with the addition of recording devices to track concurrent whisking and neuronal activity; and with the encompassment of further behavioural training.

Recent technological advances in neuroimaging have led to the development of minimally-invasive methods for concurrently measuring haemodynamic and neural activity *in vivo* (Svoboda & Yasuda, 2006). One such method is two-photon microscopy, which allows for the high-resolution imaging of intact neural and haemodynamic tissue through optical imaging. Using two-photon microscopy it would be possible to measure blood flow changes from the surface vasculature in S1, as well as concurrent calcium changes from multiple single neurons on the surface of S1 (e.g. O'Herron et al., 2016; Santisakultarm et al., 2016).

Furthermore, two-photon microscopy allows for the targeting of specific cell types, meaning pyramidal cells, VIP interneurons and/or SST interneurons could all be imaged. Targeting these different cell types would allow for the mechanisms involved in the disinhibitory circuit during locomotion or rest (with and without sensory stimulation) to be elucidated within S1 specifically. The addition of concurrent optogenetics would also allow for these interneurons to be turned on or off selectively with millisecond temporal precision (Boyden et al., 2005; Chow et al., 2010; Fenno et al., 2011; Han & Boyden, 2007), meaning the function of these cells could be further probed by looking at the resultant neuronal, haemodynamic or behavioural responses.

Whilst technological advances may allow for the more detailed investigation of neurovascular coupling in the awake, head-fixed mouse; it could also be important to introduce behavioural training to assess the effects of behavioural state (Fu et al., 2014; Gentet et al., 2012; Polack et al., 2013) and learned behaviours (Kvitsiani et al., 2013; Pinto & Dan., 2015; Sippy et al., 2015) on neurovascular responses. A key function of the brain is to interpret incoming sensory information in the context of learned associations, so as to guide adaptive behaviour (Sippy et al., 2015). In the experimental paradigm described here (whisker stimulation or spontaneous experiments), it could be interesting to train the animals to start or stop engaging in locomotion in response to a cue (e.g. light flash or sound). This way, the effects of starting or stopping locomotion during whisker stimulation may be better elucidated.

4.5.5 Conclusions

The novel awake imaging platform described is useful for assessing the effect of locomotion on the haemodynamic activity in the S1. The data indicates that locomotion has an effect on the underlying haemodynamic response profiles within S1. This experimental finding

may be vital for researchers using the awake imaging platform to study neurovascular coupling in S1, as locomotion events could have a significant effect on their data analyses. Especially when using a limited number of response trials.

Whilst the awake preparation described here was suitable for measuring the overall average haemodynamic responses to whisker stimulation; locomotion particularly confounded the haemodynamic responses on a trial by trial basis. To eliminate the effects of active behaviour on neurovascular coupling responses, and to allow for the invasive insertion of a multichannel electrode to collect concurrent neural measurements, for the next chapter (chapter 5) a novel 'modular' anaesthesia regime was developed and tested.

Chapter 5

Comparing the Haemodynamic Response Profiles of Anaesthetised and Awake Mice

5.1 Abstract

Neurovascular coupling is the process by which increases in neuronal activity are supplied by localised increases in cerebral blood flow. The neurovascular unit comprises the neurons, blood vessels, and supporting cells (e.g. astrocytes). Anaesthetics can influence any of the components of the neurovascular unit, e.g. by modulating neural processing or vascular reactivity; and the type and depth of the anaesthesia selected can have varying influence on these neurovascular responses. However, some experimental preparations require the use of anaesthesia, e.g. due to the application of high spatiotemporal resolution, invasive techniques. Thus, it will be important to establish a suitable anaesthesia regime to study neurovascular coupling in the mouse model. Currently an optimised anaesthetic protocol is still a matter of debate. Here, two dimensional optical imaging spectroscopy was applied to compare haemodynamic changes in awake (n=6) and anaesthetised (n=16) mice. The anaesthetised mice were sedated with a novel 'modular' anaesthetic regime combining inhalation and injectable anaesthetics. Under this novel regime, average stimulus-evoked haemodynamic responses were comparable between awake and anaesthetised subjects, both temporally and spatially. The novel anaesthetic combination detailed here minimised the impact of anaesthesia, which may have broad implications for neurovascular research which requires the use of anaesthesia.

5.2 Introduction

This chapter is based on the published study by Sharp, Shaw, et al. (2015). The Sharp, Shaw et al. (2015) study investigates the haemodynamic responses of anaesthetised and awake mice during 16s whisker stimulation under 100% oxygen and medical air. This thesis chapter will expand on this investigation, by assessing the haemodynamic responses of anaesthetised and awake mice during short (2s) and long (16s) duration stimulations under 100% oxygen.

Neurovascular coupling is an important avenue of research, due to its essential role in normal brain functioning. Neurovascular coupling is the process which links increases in brain activity with localised increases in cerebral blood flow (CBF) to meet the rising energy demands (Roy & Sherrington, 1890). This is an active process mediated by vasoactive signals (refer back to Figure 1.2), which cause an inflow of oxygenated haemoglobin (HbO_2) and concomitant decrease in deoxygenated haemoglobin (Hbr) (Attwell & Iadecola, 2002; Attwell et al., 2010). The stimulus-evoked haemodynamic responses last several seconds, and are thought to reflect the activity of local neurons (Heeger et al., 2000; Logothetis et al., 2001). As such, these haemodynamic changes are recorded in the blood oxygenation level-dependent (BOLD) functional magnetic resonance imaging (fMRI) signal, and used to make inferences about underlying neuronal responses (Buxton et al., 1997; 1998; Ogawa et al., 1990). Thus, studying the physiological mechanisms underlying neurovascular coupling has direct implications for the analysis and interpretation of fMRI data (Hillman, 2014). There is also accumulating evidence which shows that neurovascular coupling may be impaired in neurodegenerative disorders, meaning a comprehensive understanding of neurovascular coupling may lead to earlier diagnosis and improved therapeutic strategies (Iadecola, 2013; Nicolakakis & Hamel, 2011).

The studies which investigate neurovascular coupling in high spatiotemporal detail have typically employed anaesthetised *in vivo* animal models (Berwick et al., 2005; 2008; Boorman et al., 2010; 2015; Bruyns-Haylett et al., 2010; Harris et al., 2010; Kennerley et al., 2005; 2012; Slack et al., 2015), due to the invasive nature of the techniques applied. Whilst the use of anaesthesia minimises motion artefacts and eliminates induced stress, it also alters baseline brain physiology. Anaesthetics can influence the components of the neurovascular unit by modulating neural processing or vascular reactivity (for review see Masamoto & Kanno, 2011); and the type and depth of the anaesthesia selected has varying influence on these neurovascular responses (Masamoto et al., 2009; Schroeter et al., 2014; Schulte et al., 2006).The optimal anaesthetic protocol is still a matter of debate. Previous studies have demonstrated stimulus-evoked haemodynamic responses in a number of species under anaesthesia, although these responses were attenuated compared to those seen in awake subjects (Logothetis et al., 1999; Martin et al., 2006; 2013; Peeters et al., 2001; Pisauro et al., 2013). Studies investigating neurovascular coupling specifically in anaesthetised mice face challenges arising from the species sensitivity to anaesthetics, emphasized by the weak and inconsistent haemodynamic responses reported and low study numbers (Adamcszak et al., 2010; Ahrens & Dubowitz, 2001; Jonckers et al., 2014; Prakash et al., 2007; Schroeter et al., 2014). It will be an important step to establish an anaesthetic regime under which neurovascular responses strongly resemble those seen in the awake state, particularly due to availability of mouse models of neurodegenerative diseases.

The previous chapter (chapter 4) investigated haemodynamic responses in awake, head-fixed mice. Whilst the overall average stimulus-evoked haemodynamic responses were preserved, when assessing the responses on a trial-by-trial basis, locomotion was shown to have a profound influence. Further, it was not possible to gain neural data from the current preparation, as at the Sheffield laboratory, electrophysiological information is gained through the invasive insertion of a multichannel electrode. Thus, in order to avoid the confounds associated with locomotion, and to apply high spatiotemporal resolution invasive techniques to the detailed investigation of neurovascular coupling, there was a drive to develop a suitable anaesthetised preparation.

5.2.1 Aims

In the present study the haemodynamic response to short and long duration whisker stimulation was characterised in the anaesthetised and the awake mouse model. A novel 'modular' anaesthesia regime was developed (Cesarovic et al., 2012; Sharp, Shaw, et al., 2015), which combined injectable and volatile anaesthetics for prolonged anaesthetic depth during imaging, with limited adverse effects on the cerebral physiology. The stimulus-evoked responses in mice anaesthetised using this novel approach were then compared with the stimulus-evoked responses seen in the awake mouse.

5.3 Methods

The experiments performed in this chapter used the same protocol as the animal preparation described previously in chapter 2 (sections 2.2-2.4), and built on the methods furthered described in chapters 3 & 4 (as the same awake subjects were used in this analysis). The data from the awake subjects included in this chapter were all collected by Miss Kira Shaw. The data from the anaesthetised subjects were collected by Miss Kira Shaw and by Dr Paul Sharp.

Anaesthetised and awake mice were included in this study, and the same aseptic surgical procedure was conducted across both groups. All procedures were conducted in accordance with the Animals (Scientific Procedures) Act 1986. Briefly, the animal was anaesthetised and a thinned cranial window was created on the skull overlying the right somatosensory cortex. A headplate holder was secured to the skull using dental cement. The animal was allowed at least one week to recover from the surgical procedure, and during this time it was monitored daily to ensure there were no adverse effects from the surgery.

Following this recovery period, the haemodynamic responses of the anaesthetised group were recorded using two-dimensional optical imaging spectroscopy (2D-OIS). The subjects were anaesthetised with fentanyl-fluanisone (Hypnorm, Vetapharm Ltd), midazolam (Hypnovel, Roche Ltd) and water (1:1:2 by volume; 0.7 ml/kg, i.p.) maintained using isoflurane (0.5%) in 100% oxygen. The awake subjects were subject to a training period before imaging. During this training period subjects were increasingly exposed to the

experimental set-up to reduce stress from later head-fixation. Once habituated to the set-up, the haemodynamic responses of awake subjects were also monitored using 2D-OIS.

A mechanical whisker stimulator was placed on the contralateral side of the face from the exposed somatosensory cortex. The experimental paradigms consisted of short (2 second) and long (16 second) duration whisker stimulations across multiple trials. Six adult C57BL/6J mice were included in the awake group (1 male, 5 female; each animal contributed multiple sessions (3-16 sessions), which were averaged so that each awake subject contributed equally to the overall mean haemodynamic response); and sixteen C57BL/6J mice were included in the anaesthetised group (16 female; each animal contributed one session). All data analyses were performed using MATLAB (MathWorks).

5.4 Results

The following section reports stimulus-evoked haemodynamic changes in the awake state (n=6, multiple sessions) and the anaesthetised state (n=16). Both short duration (2s) and long duration (16s) mechanical whisker stimulation were delivered across multiple trials, and the spatial extent and time course of the haemodynamic responses were assessed.

5.4.1 Investigating the Spatial Extent of Haemodynamic Responses to Whisker Stimulation

First, the spatial extent of the haemodynamic response to 2s and 16s whisker stimulation was compared for awake and anaesthetised subjects. Previous work has shown the spatial profile of haemodynamic responses to be preserved under isoflurane anaesthesia (Pisauro et al., 2013).

5.4.1.1 Spatial Maps of the Stimulus-Evoked Haemodynamic Response in Awake & Anaesthetised Subjects

Spatial maps were generated to show the averaged haemodynamic response to stimulation. Haemodynamic response maps are averaged between 0 and 5 seconds from the onset of stimulation. The magnitude of the response is displayed as micromolar change from baseline elicited by whisker stimulation. In the spatial maps for the awake and

anaesthetised state, there were large increases in total blood volume (Hbt) and oxygenated haemoglobin (HbO_2) centred on the active whisker barrel region, with corresponding decreases in deoxygenated haemoglobin (Hbr) (Figure 5.1 & Figure 5.2).

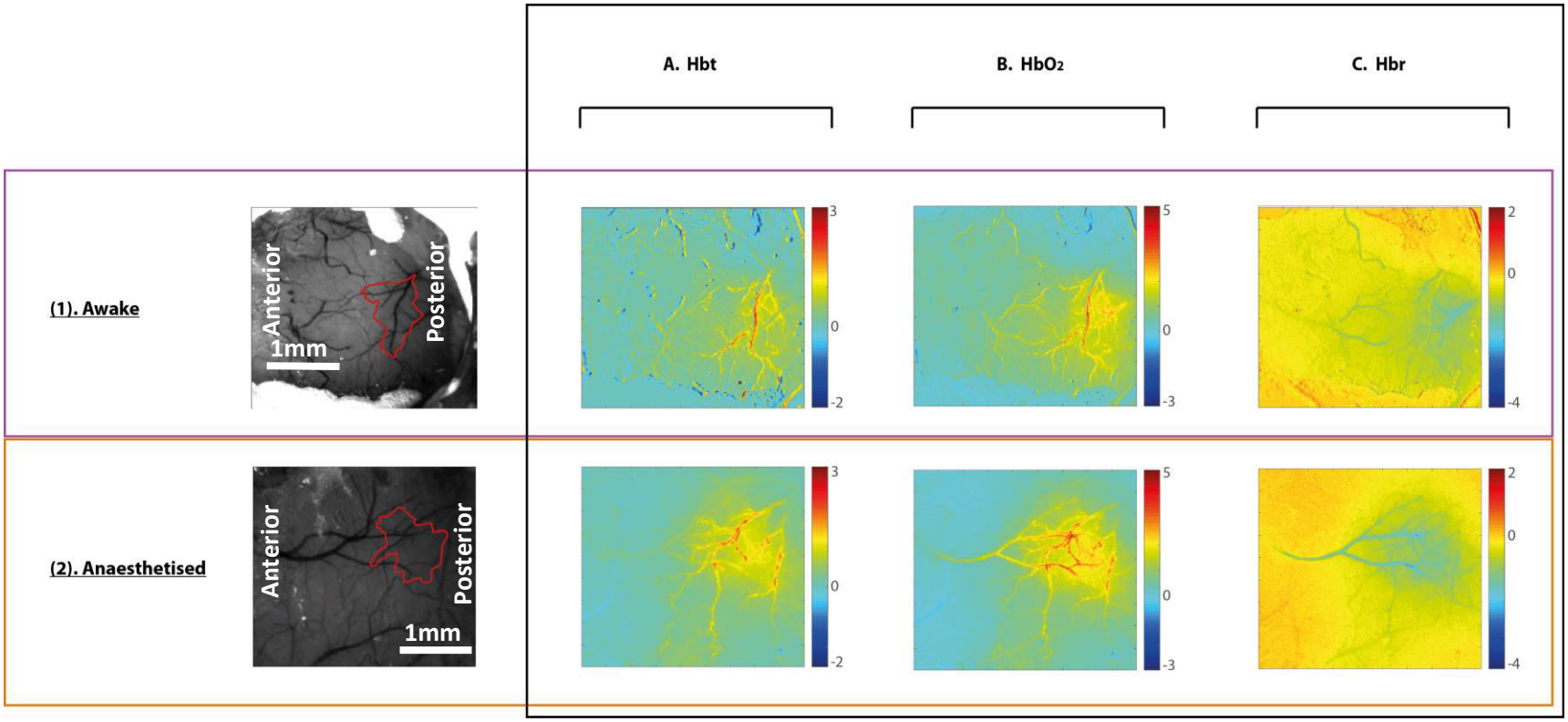

Figure 5.1 – Spatial Haemodynamic Responses evoked by 2s Whisker Stimulation

*A greyscale image of the cortex taken for a representative animal in the **(1)** awake, and **(2)** anaesthetised conditions, with the whisker barrel region marked in red. The spatial extent of the haemodynamic changes averaged from the onset of a 2s whisker stimulation until 5s post-stimulation onset are shown for these representative animals for **A.** Hbt, **B.** HbO_2, and **C.** Hbr.*

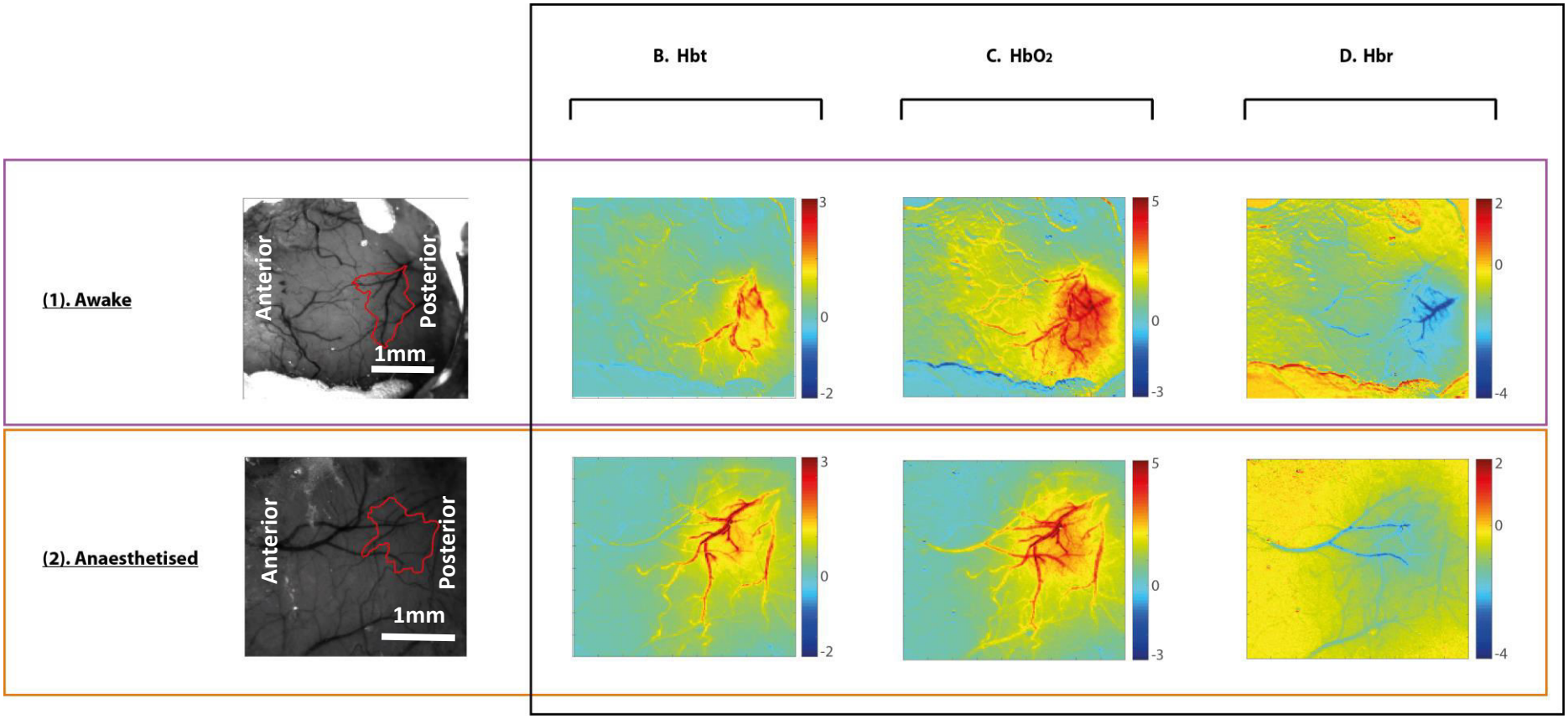

Figure 5.2 – Spatial Haemodynamic Responses evoked by 16s Whisker Stimulation

*A greyscale image of the cortex taken for a representative animal in the **(1)** awake, and **(2)** anaesthetised conditions, with the whisker barrel region marked in red. The spatial extent of the haemodynamic changes averaged from the onset of a 16s whisker stimulation until 5s post-stimulation onset are shown for these representative animals for **A.** Hbt, **B.** HbO_2, and **C.** Hbr.*

5.4.1.2 The Fraction of Active Pixels in Hbt Response Maps during Whisker Stimulation

The fraction of active pixels within the whole cranial window of each Hbt response map was calculated as a percentage (using the pixel analysis method detailed in section 2.5.1.3.2 & Figure 2.5) to allow for comparison of the spatial extent of the Hbt response between the awake and anaesthetised state for 2s (Figure 5.3 A) and 16s (Figure 5.3 B) whisker stimulation.

The percentage of active pixels within the Hbt response maps were calculated across time, and plotted as an average time series over the stimulation trial (Figure 5.3 A(1) & Figure 5.3 A(1)). The average spatial spread of the stimulus-evoked Hbt responses over the stimulation period (i.e. from 0 to 5s for 2s stimulation, and from 0 to 20s for 16s stimulation; (Figure 5.3 A(2) & Figure 5.3 A(2)), and the response peak (i.e. the maximum number of active pixels during the stimulation; Figure 5.3 A(3) & Figure 5.3 A(3)) were calculated and compared between the awake and anaesthetised subjects. Two-tailed t-tests were carried out to compare the spatial extent of Hbt responses between awake and anaesthetised subjects. Bonferonni corrections were made to account for multiple comparisons.

The spatial extent of the Hbt response to 2s whisker stimulation was comparable between awake and anaesthetised subjects. The average response over the stimulation period for awake (M=18.56%, SD=2.83) and anaesthetised (M=20.20%, SD=2.01) subjects (t(19)=-1.51, p=0.30, ns) showed no significant differences. The maximum spatial spread of the Hbt response during 2s whisker stimulation also showed no significant differences between awake (M=40.43%, SD=8.16) and adult (M=41.98%, SD=4.87) subjects (t(19)=-0.54, p=1.19, ns).

The spatial extent of the Hbt response during 16s whisker stimulation was also similar between awake and anaesthetised subjects. The maximum spatial spread of the Hbt response during 16s whisker stimulation showed no significant differences between awake (M=27.14%, SD=5.01) and adult (M=30.93%, SD=6.00) subjects (t(19)=-1.36, p=0.38, ns). Although, the average response over the stimulation period for awake (M=14.13%, SD=1.75) and anaesthetised (M=16.85%, SD=1.54) subjects (t(19)=-3.53, p=0.005**) did show significant differences, likely because of the more complex spatial area response profile seen in the awake state (Figure 5.3 B(1)).

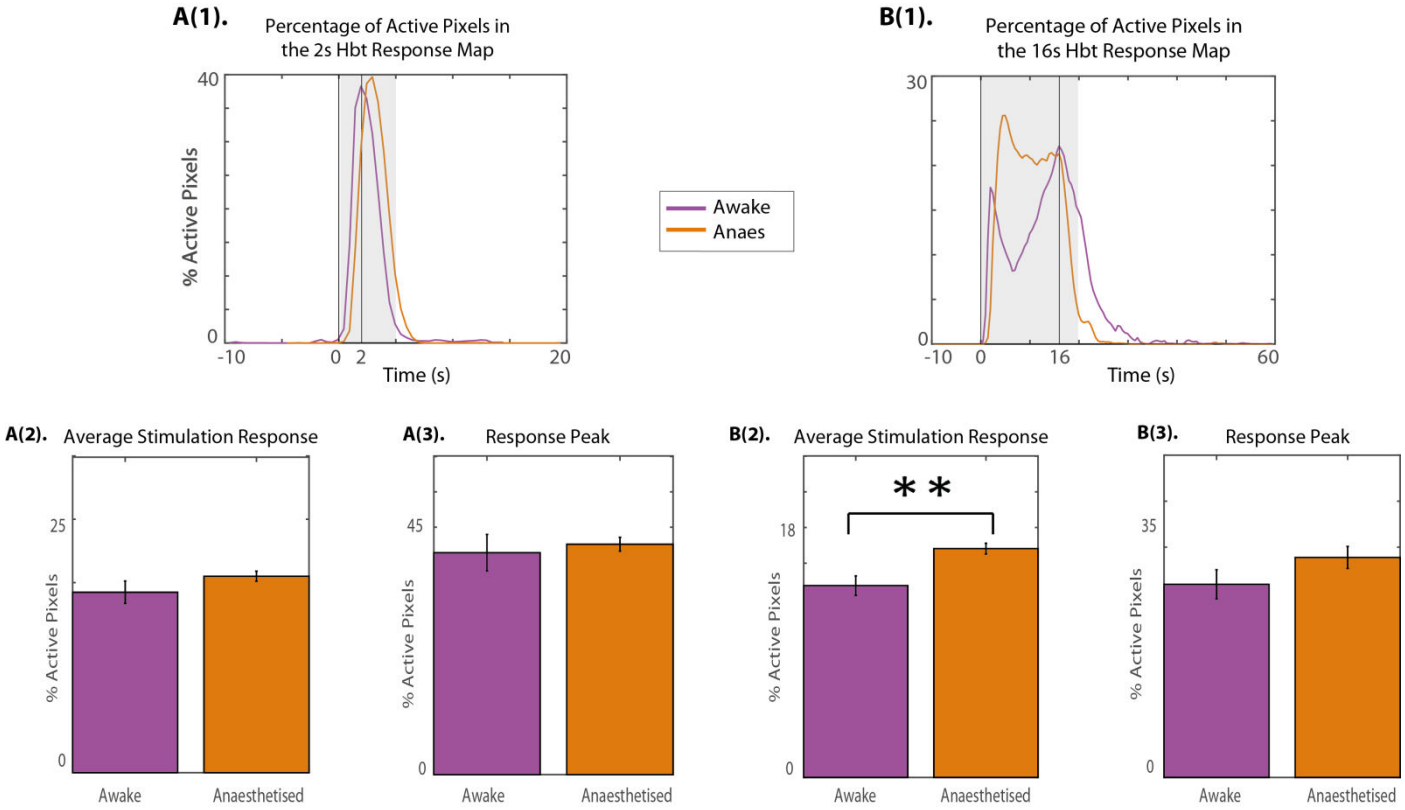

Figure 5.3 – Active Pixels within the Hbt Response Maps during Whisker Stimulation

(1) *The time course of the spatial extent of the active pixels, as a percentage of the Hbt response maps, during the* ***A.*** *2s whisker stimulation, and* ***B.*** *16s stimulation for awake (n=6, purple), and anaesthetised (n=16, orange) subjects The black lines (at* ***A.*** *0 & 2 seconds, and* ***B.*** *0 & 16 seconds) mark the stimulation period; the grey box marks the time window over which the average response over the time period was calculated. (****2****) Bar plots showing the average percentage of active pixels.* ***(3)*** *Bar plots showing the maximum percentage of active pixels. Data shown as mean ± S.E.M.*

5.4.2 Investigating the Temporal Profile of Haemodynamic Responses to Whisker Stimulation

As the spatial extent of stimulus-evoked haemodynamic responses were comparable between the awake and anaesthetised subjects, the time course of haemodynamic responses from the 'active whisker region' were assessed next. Previous work has shown the time course of haemodynamic responses to be slower and smaller in magnitude under anaesthesia as compared to in awake subjects (Logothetis et al., 1999; Martin et al., 2006; 2013; Peeters et al., 2001; Pisauro et al., 2013).

5.4.2.1 Visualising the Time Course of the Stimulus-Evoked Haemodynamic Responses in Awake and Anaesthetised Subjects

The haemodynamic responses to 2s whisker stimulation were characterised by monophasic increases in Hbt and HbO_2, and a corresponding decrease in Hbr for both the awake and anaesthetised preparations (Figure 5.4).

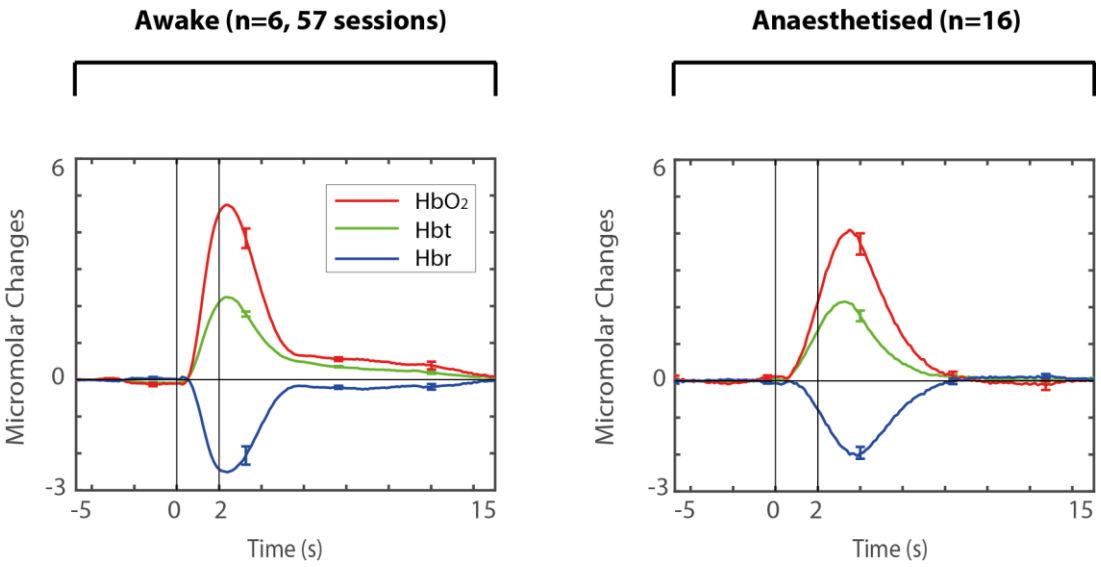

Figure 5.4 - Time Course of Haemodynamic Responses evoked by 2s Whisker Stimulation

The average haemodynamic responses (Hbt. HbO_2 & Hbr) evoked during 2s whisker stimulation are shown in the whisker barrel region for awake (n=6, 57 sessions) and anaesthetised (n=16) subjects. Error bars represent SEM.

The haemodynamic responses to 16s whisker stimulation were characterised by long duration increases in Hbt and HbO_2, with a concomitant decrease in Hbr for both the awake and anaesthetised preparations (Figure 5.5). In the awake state the 16s response profile was more complex, characterised by an initial peak, followed by a secondary peak with increased magnitude.

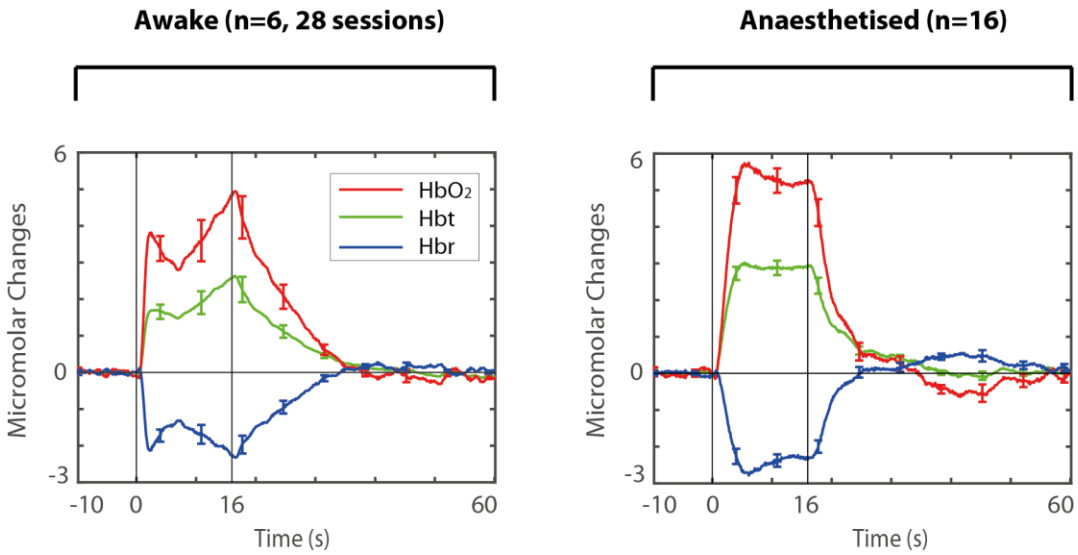

Figure 5.5 - Time Course of Haemodynamic Responses evoked by 16s Whisker Stimulation

The average haemodynamic responses (Hbt. HbO_2 & Hbr) evoked during 16s whisker stimulation are shown in the whisker barrel region for awake (n=6, 28 sessions) and anaesthetised (n=16) subjects. Error bars represent SEM.

5.4.2.2 Comparison of Awake and Anaesthetised Haemodynamic Response Profiles

The temporal characteristics of the Hbt response were assessed across awake and anaesthetised subjects for 2s (Figure 5.6) and 16s (Figure 5.7) whisker stimulations. Two-tailed t-tests were carried out to compare Hbt responses between awake and anaesthetised subjects. Bonferonni corrections were made to account for multiple comparisons. The average stimulation Hbt response was calculated from 0-5 seconds for 2s whisker stimulation; and from 0 to 20 seconds for 16s stimulation. The Hbt response peak was the maximum value of the micromolar changes in Hbt during this time period. As the onset of haemodynamic responses appeared to be slightly quicker in the awake state, the

time to 10% was also calculated by finding the time (in seconds) it took the Hbt response to reach 10% of the maximum peak.

Overall, no significant differences were found in the time course of stimulus-evoked Hbt responses between awake and anaesthetised subjects. For the 2s whisker stimulation: the average stimulation response for awake (M=1.22µM, SD=0.09) and anaesthetised (M=1.21µM, SD=0.32; t(19)=-0.07, p=2.83, ns); maximum response peak for awake (M=3.00µM, SD=0.004) and anaesthetised (M=3.03µM, SD=0.03; t(19)=1.92, p=0.21, ns); and time to 10% for awake (M=0.83µM, SD=0.07) and anaesthetised (M=0.99µM, SD=0.20; t(19)=1.70, p=0.32, ns) were similar (Figure 5.6).

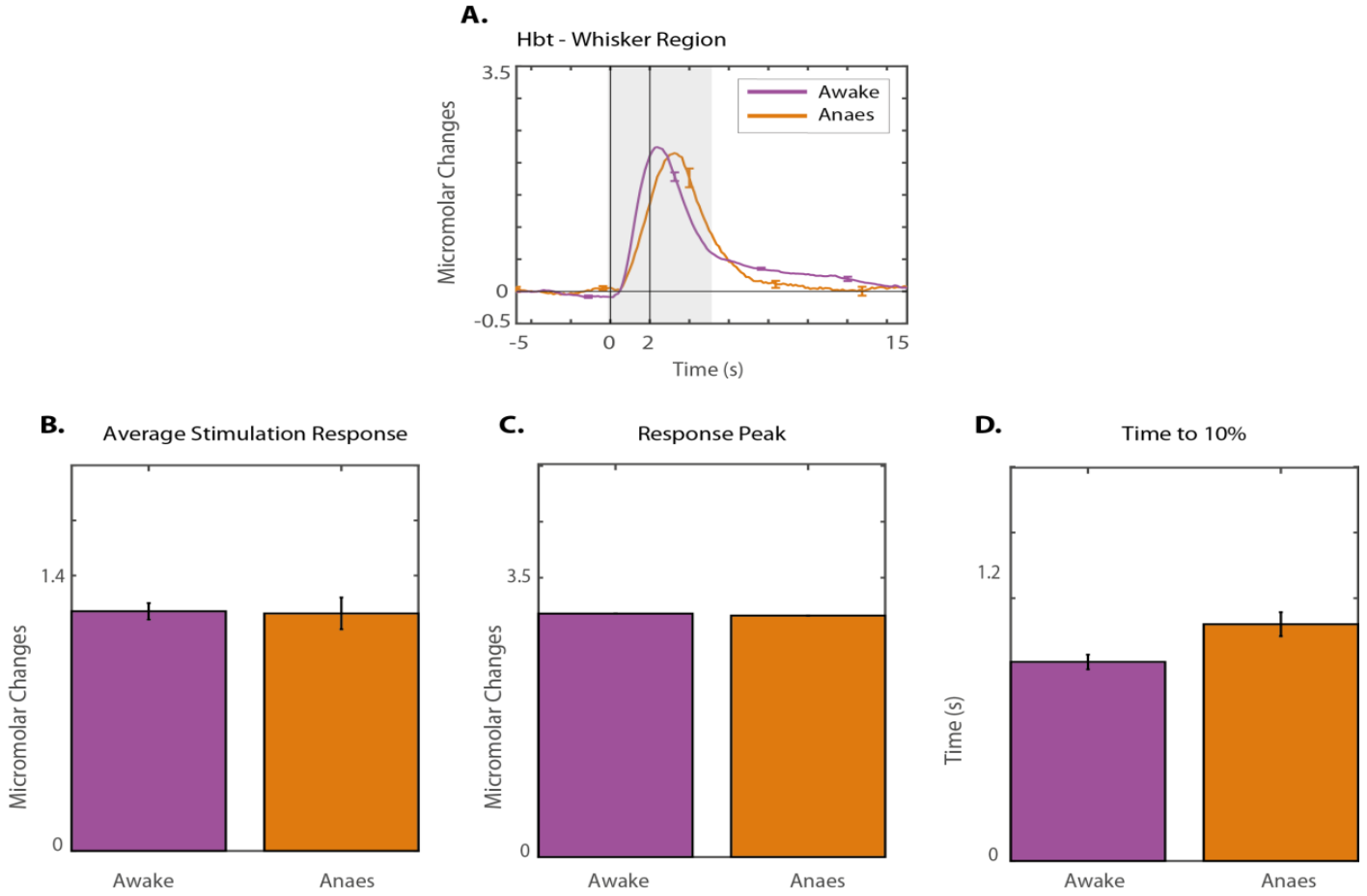

Figure 5.6 – Temporal Properties of the Haemodynamic Response to 2s Whisker Stimulation in Awake & Anaesthetised Mice

A. *The Hbt responses during 2s whisker stimulation from the whisker barrel region for awake (purple) and anaesthetised (orange) subjects.* ***B.*** *The average Hbt response to stimulation,* ***C.*** *the maximum response peak, and* ***D.*** *the time to reach 10% of the maximum peak, are visualised from for the awake and anaesthetised subjects. Error bars represent SEM.*

There were also no significant differences for the 16s whisker stimulation: as the average stimulation response for awake (M=1.80µM, SD=0.64) and anaesthetised (M=2.42µM, SD=0.65; t(20)=1.98, p=0.18, ns); maximum response peak for awake (M=3.06µM, SD=0.09) and anaesthetised (M=2.42µM, SD=0.65; t(20)=2.40, p=0.08, ns); and time to 10% for awake (M=0.94µM, SD=0.13) and anaesthetised (M=1µM, SD=0.45; t(20)=0.33, p=2.23, ns) were similar (Figure 5.7).

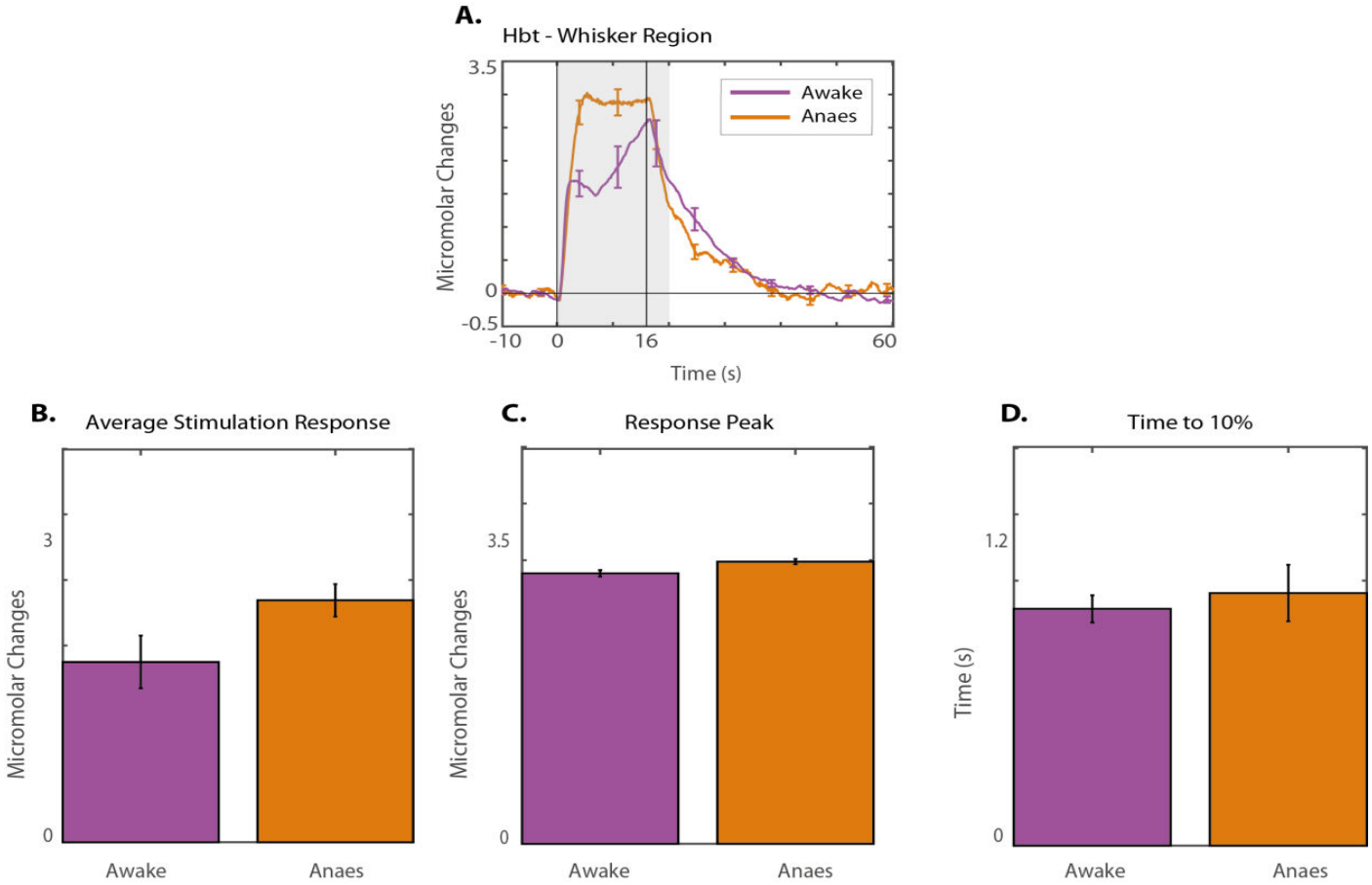

Figure 5.7 – Temporal Properties of the Haemodynamic Response to 16s Whisker Stimulation in Awake & Anaesthetised MiceA. *The Hbt responses during 16s whisker stimulation from the whisker barrel region for awake (purple) and anaesthetised (orange) subjects.* ***B.*** *The average Hbt response to stimulation,* ***C.*** *the maximum response peak, and* ***D.*** *the time to reach 10% of the maximum peak, are visualised from for the awake and anaesthetised subjects. Error bars represent SEM.*

5.5 Discussion

The current study investigated and compared haemodynamic responses to whisker stimulation in awake and anaesthetised mice using 2D-OIS.

5.5.1 Results Summary & Interpretation

The overall findings of this study indicate that the application of this novel 'modular' anaesthesia regime, i.e. with combined injectable and volatile anaesthetics, results in stimulus-evoked haemodynamic responses which are similar to those seen in the awake state. This result is in contrast to previous papers which showed that anaesthesia decreased the amplitude of haemodynamic responses in humans (Marcar et al., 2006; Qiu et al., 2008), primates (Chen et al., 2005; Goense & Logothetis, 2008; Shtoyerman et al., 2000), and rodents (Desai et al., 2011; Martin et al., 2006; Peeters et al., 2001; Pisauro et al., 2013).

5.5.1.1 Comparing the Spatial Extent of Stimulus-Evoked Haemodynamic Responses in Awake & Anaesthetised Subjects

Spatial maps of the stimulus-evoked haemodynamic responses were generated in representative animals for the awake and anaesthetised states. Both groups showed increases in Hbt and HbO_2 centred on the active whisker region, with concurrent decreases in Hbr, in response to stimulation. The overall spatial extent of these Hbt activations were assessed across all subjects, and stimulation was found to activate a comparable percentage of the exposed cranial window for awake and anaesthetised preparations. This finding is in agreement with Pisauro et al. (2013), who found anaesthesia did not influence the spatial extent of haemodynamic responses in mouse V1. Whilst Pisauro and colleagues showed no effect of their chosen anaesthesia on the spatial extent of haemodynamic responses, they showed there was a profound effect on the amplitude and temporal properties of haemodynamic responses, as such here the differences in the time courses of haemodynamic responses were examined next.

5.5.1.2 Comparing the Temporal Profile of Stimulus-Evoked Haemodynamic Responses in Awake & Anaesthetised Subjects

The time course of haemodynamic responses from the active whisker region were compared between awake and anaesthetised subjects. Haemodynamic responses to 2s whisker stimulation showed the expected monophasic increases in Hbt and HbO_2, with concomitant decreases in Hbr, in both awake and anaesthetised subjects (no significant differences). The average size, maximum peak, and time to 10% of the stimulus-evoked Hbt response were comparable between the awake and anaesthetised state. Although non-significant, the time to 10% was slightly slower for the anaesthetised condition (delayed by 0.06-0.16s), which is reflective of a slower onset time of the Hbt response. These delays in the onset of the haemodynamic response may be because inhalation anaesthetics (e.g. isoflurane) partially impair cerebral autoregulation (Engelhard & Werner, 2006; Hoffman et al., 1991; Strebel et al., 1995). However, the novel 'modular' anaesthesia regime applied here (and in Sharp, Shaw et al., 2015) can overcome some of the issues which affect the speed of the haemodynamic response, due to the combined use of inhalation and injectable anaesthetics. In particular, whilst inhalation anaesthetics have a vasodilatory effect (Hendrich et al., 2001; Van Hemelrijck et al., 1993), injectable anaesthetics have vasoconstrictive effects with well-preserved cerebral autoregulation (Engelhard & Werner, 2006; Strebel et al., 1995). Thus, this novel combination can potentially overcome the issues associated with using each type of anaesthetic in isolation.

Haemodynamic responses to 16s whisker stimulation showed increases in Hbt and HbO_2, with decreases in Hbr, in the awake and anaesthetised state. The average size, maximum peak, and time to 10% of the Hbt response were comparable between groups (no significant differences). Although non-significant, the average Hbt response to stimulation was slightly larger in the anaesthetised state, reaching maximum levels sooner, with the peak being sustained throughout stimulation. In the awake state however, a more complex temporal profile was observed in which the initial stimulus-evoked Hbt increase was followed by a secondary Hbt response peak. These differences in the temporal profile of the awake and anaesthetised haemodynamic responses to long duration stimulation were also shown in the study by Martin et al. (2013b); who speculated that the additional complexity of the awake haemodynamic response was likely driven by neurovascular or cerebrovascular factors, rather than by neuronal activity directly. Indeed, long duration stimulation has been suggested to interact more with astrocytes (Cauli & Hamel, 2010), and

so these different response profiles seen could reflect the effect of the anaesthesia on astrocytic signalling.

5.5.2 Conclusions

The findings of this study show that a balanced 'modular' anaesthetic regime can be used to minimise the impact of anaesthesia on the mechanisms underlying neurovascular coupling in mice. Whilst it is acknowledged that studying the anaesthetised brain can never fully reflect normal physiology, the optimisation of an anaesthesia protocol, under which neurovascular coupling mechanisms are mainly preserved, will be important in research which seeks to apply high spatiotemporal invasive methods. In particular, due to the availability of disease models in mice, the use of this anaesthesia regime may also aid in research which seeks to investigate the alterations of neurovascular coupling which are associated with disease. As neurodegenerative diseases may cause subtle changes to neurovascular coupling, the anaesthesia regime described here could allow for researchers to detect such small changes, which were potentially previously masked by unsuitable anaesthesia regimes or by locomotion.

The next chapter will apply this anaesthetic regime to study neurovascular coupling in development and ageing. Given that the haemodynamic responses observed in the anaesthetised subjects here were comparable to those seen in the awake state, a subset of these subjects will be used as the 'adult group' in the next chapter. This 'adult group' will represent the healthy neurovascular coupling response, to which the neurovascular responses seen in young and old subjects will be compared.

Chapter 6

A Mouse Model of Neurovascular Coupling during Development and Old Age

6.1 Abstract

Neural activity leads to localised changes in cerebral blood flow through a process termed neurovascular coupling. These haemodynamic changes are used in blood oxygen level dependent (BOLD) functional magnetic resonance imaging (fMRI) to infer underlying neuronal changes. Neurovascular coupling may be altered in development and during ageing due to structural and functional changes to the components of the neurovascular unit, although this is still being investigated. Here, 2-dimensional optical imaging spectroscopy and electrophysiology were employed to record haemodynamic and neural changes in the somatosensory cortex of young (n=5), adult (n=5) and old (n=5) anaesthetised mice in response to whisker stimulation or a carbogen challenge. Compared to the adult mice, haemodynamic responses to whisker stimulation were attenuated in the whisker barrel region of young and old mice. The young mice also showed negative haemodynamic responses (i.e. decreased blood volume) in the surrounding region adjacent to the whisker barrels during whisker stimulation. The corresponding neural changes during whisker stimulation were also assessed. Young mice showed increased stimulus-evoked local field potentials (LFP) responses compared to adult mice; whereas LFP responses in old mice compared to adult mice were attenuated during short duration stimulation, and comparable during long duration stimulation. The haemodynamic changes evoked by inspiration of carbon dioxide were reduced in young and old subjects compared to adult. Overall these findings indicate that neurovascular coupling is altered during development and old age, which may be caused by: changes to the balance of excitation and inhibition, reduced vascular reactivity, or impaired vasoactive signalling. As such, caution is needed when interpreting BOLD fMRI studies of development or ageing.

6.2 Introduction

The brain relies on a continuous and well-regulated blood supply matching its energetic needs, a process termed neurovascular coupling (Iadecola & Nedergaard, 2007). Neurovascular coupling critically depends on an intact functional network of neurons, vascular endothelial cells, and astrocytes (Attwell et al., 2010; Chen et al., 2014). In the healthy adult cortex, sensory processing results in an increase in cerebral blood flow (CBF) in activated sensory cortical areas, and a concomitant decrease in local levels of deoxyhaemoglobin which result in a positive BOLD signal (Kennerley et al., 2009; Zehendner et al., 2013). This BOLD signal is generated on the basis of the differential magnetic properties of deoxygenated and oxygenated haemoglobin. Thus, the BOLD signal measured using fMRI is thought to indirectly provide information on underlying neural activity in a non-invasive manner (Logothetis et al., 2001). The physiological basis for the interpretation of the BOLD signal with regard to the neural activity is based on neurovascular coupling (Attwell et al., 2010; Harris et al., 2011; Logothetis et al., 2001). Disruptions of neurovascular coupling occur in certain disorders of the central nervous system such as Alzheimer's disease, vascular dementia, and stroke (Barber, 2013; Iadecola, 2004; Girouard & Iadecola, 2006; Nicolakakis & Hamel, 2011). It is therefore important to gain a better understanding of the mechanisms which underlie neurovascular coupling in health and disease, with the aim of developing novel treatments to restore brain function.

Neurovascular coupling has been studied across the lifespan: in infants, adolescents, adults and the elderly. Even when studying neurovascular coupling in the healthy cortex however, there are confounds associated with the age of the subject. This chapter will briefly discuss the literature regarding neurovascular coupling in development (section 6.2.1) and ageing (section 6.2.2).

6.2.1 Neurovascular Coupling during Development

The developing brain undergoes many changes to the neurovascular unit, which have the potential to alter neuronal and/or haemodynamic responses. Neuronal development is incomplete at birth. There are changes to the cortical thickness, which reflect the excessive formation and selective deletion of synapses (Chan et al., 2002). There are also changes to the balance of excitation and inhibition, with a developmental switch of the neurotransmitter GABA from hyperpolarising to depolarising (Ben-Ari, 2002). Altering the

excitatory and inhibitory balance of the brain likely sharpens the neural responses a stimulus. The vasculature too continues to develop postnatally. Vascular volume increases have been found during development (Keep & Jones, 1990; Risser et al., 2009), which reduce the mean distance between the tissue and the nearest vessel. Astrocytic changes include differences in size and connectivity during development (Nixdorf-Bergweiler et al., 1994; Stichel et al., 1991), which may alter blood flow responses as caused by neuronal activation.

Such changes in blood volume fraction (and neurovascular signalling) can alter the BOLD signals observed experimentally and can cause problems in their interpretation (Harris et al., 2011). Indeed, previous work has shown conflicting results regarding NVC in the developing brain (e.g. Colonnese et al., 2008; Kozberg et al., 2013; Martin et al., 1999; Roche-Labarbe et al., 2014). Developmental studies investigating haemodynamic responses have shown both positive (Arichi et al., 2010; Cantlon et al., 2006; Liao et al., 2010; Marcar et al., 2004; Scapiro et al., 2004) and negative (Anderson et al., 2001; Born et al., 1998; 2000; Heep et al., 2009; Martin et al., 1999; Muramoto et al., 2002; Seghier et al., 2004; Yamada et al., 1997; 2000) BOLD signal responses within the same study population. These discrepancies are thought to arise from technical issues (e.g. the stimulus paradigms used or analysis techniques applied), differences in behavioural state, or from genuine existing physiological differences (Arichi et al., 2010). It is of upmost importance to resolve these contradictions in order to gain an improved understanding of the developing brain. Recent animal studies have attempted to employ invasive, high resolution techniques to investigate the neural and haemodynamic changes which occur in development (e.g. Colonnese et al., 2008; Kozberg et al., 2013; Zehender et al., 2013). Even when using animal models of development there are still some inconsistencies, although there is a general consensus that vasodilatory responses are altered in some way. The following chapter will attempt to address some of these inconsistencies by applying concurrent 2D-OIS and electrophysiology to measure NVC in a developing mouse.

6.2.2 Neurovascular Coupling during Ageing

To gain a complete understanding of the maturation of NVC across the life span, it will also be important to consider how NVC changes during old age. Reductions in grey and white matter volume have been shown in the aged brain (Sowell et al., 2003); with corresponding decreases in neuron count, dendrites and synapses in the cortex (Creasey & Rapoport,

1985; Huttenlocher, 1979; Jacobs & Scheibel, 1993; & Masliah et al., 1993). Ultimately, reductions in neuron numbers and connections will affect the brains processing efficiency and plasticity, thereby compromising learning. Cerebral blood vessels also undergo profound changes associated with ageing. For example, capillaries are thickened, pericytes degenerate, and endothelial cells are elongated with reduced numbers of mitochondria (Farkas & Luiten, 2001). Ageing is also thought to contribute to reduced levels of vasoactive messengers such as nitric oxide, which may promote endothelial dysfunction (Topcuoglu et al., 2009; Toth et al., 2015a; 2015b). Such profound structural and regulatory changes to the blood vessels during ageing have been associated with a reduction in resting CBF (Farkas & Luiten (2001); Kalaria, 2008), and attenuation of the stimulus-evoked CBF response (Iadecola et al., 2009; Panczel et al., 1999). It is generally agreed that there is hypertrophy of astrocytes in ageing (Peters, 2007); with a switch from astrocytes being neurotrophic to neurotoxic (Garcia-Matas et al., 2008; Jiang & Cadenas, 2014). These pathologies which alter NVC in ageing will affect the interpretation of fMRI studies which compare elderly patients to healthy adult patients. As such, inconsistencies have been found in ageing fMRI studies (Ances et al., 2009; D'Esposito et al., 2003).

Cognitive, motor, and sensory tasks have been linked with increases (Lee et al., 2011; Mattay et al., 2001); decreases (Buckner et al., 2000; Hesselman et al., 2001; Nyberg et al., 2010; Raemaekers et al., 2006; Ross et al., 1999; Tekes et al., 2005); and even no change (Aizenstein et al., 2004; Gazzeley & D'Esposito, 2005; Huettel et al., 2000; 2001) in the size of the positive BOLD response between young adults and old adults. These differences could result from the application of different data analysis techniques (Aizenstein et al., 2004; Ances et al., 2009), or from regionally-dependent alterations in the BOLD response during ageing (Bucker et al., 2000). The supplementary animal studies which investigated neurovascular coupling in old age in fine spatiotemporal detail are generally in agreement that blood flow responses are attenuated in ageing (Balbli et al., 2015; Jessen et al., 2015; Park et al., 2007; Toth et al., 2014a; 2014b; Tucsek et al., 2014). Some authors concluded that there was 'neurovascular uncoupling' as neuronal activity remained functionally intact (Tarantini et al., 2015), whereas others showed that there were also attenuations of the neuronal response in ageing (Jessen et al., 2015). Clearly, more work is required to investigate changes to neurovascular mechanisms associated with ageing. Such studies will be of prime importance in the treatment or prevention of age-related cognitive decline or diseases. The following thesis chapter will investigate neurovascular coupling in the old mouse by applying concurrent 2D-OIS and electrophysiological techniques.

6.2.3 Aims & Justifications for the Current Study

The current study aims to apply high spatial and temporal resolution techniques (optical imaging spectroscopy and multichannel electrode) to investigate neurovascular coupling (CBV and LFP) in the somatosensory cortex of young, adult, and old mice. Stimulus-evoked neuronal and haemodynamic changes were assessed to short and long duration whisker stimulations across age groups. The effects of carbogen by inhalation of CO_2 (delivered in 100% oxygen) were also assessed across age groups, as this is thought to induce nitric-oxide dependent vasodilation which is impaired in ageing. This appears to be the first study to apply the same high-resolution, invasive experimental techniques to study neurovascular coupling across both development and ageing. By studying neurovascular coupling at these time points, it may be possible to assess how it adapts and deteriorates throughout life.

The subjects included in this study were anaesthetised during imaging experiments. Anaesthesia was used to overcome the potential confounding effects of locomotion (chapter 4), as locomotion behaviour could include age-dependent alterations. Further to this, the multi-channel electrode technique applied here to measure electrophysiology was invasive and required subject sedation; and the selection of a suitable anaesthetic regime has previously been shown to result in haemodynamic responses comparable in magnitude to those seen in awake subjects (chapter 5; Sharp, Shaw, et al., 2015).

The 'young' mice included in this study were 8-12 weeks old, the 'adult' mice were ~6months of age, and the 'old' mice were all >19months.

Previous developmental studies have typically used younger mice (Colonnese et al., 2008; Kozberg et al., 2013; Zehender et al., 2013). These studies used mice <2weeks old; however, consistent findings from the studies employing high resolution optical imaging techniques have shown a decrease in stimulus-evoked CBF at this age (Kozberg et al., 2013; Zehender et al., 2013). C57BL/6J mice become sexually mature around 6-8 weeks postnatal, and the average age at first mating for this strain is 6.8 weeks (Silver, 1995). The developmental period between childhood and adulthood occurs when the capacity to reproduce is attained. The young mice selected for this study (8-12 weeks old) were thus thought to correspond to late adolescence. There are structural changes to the components of the neurovascular unit throughout childhood and adolescence, and so it will

be interesting to study functional changes in neurovascular coupling which occur in this period in between infancy (i.e. stimulus-evoked decreases in CBF) and mature adulthood (i.e. stimulus-evoked increases in CBF). The adult mice included within these experiments were ~6months old, as mice >3months old are considered to be adult (Harb et al., 2013). The old mice used for this study were >19 months; which is consistent with previous work that has shown age-related changes to neurovascular coupling can occur in mice from 8 months (Balbi et al., 2015), and 12 months (Balbi et al., 2015; Park et al., 2007). For the purposes of this study however, mice >12 months old were used, as Park et al. (2007) showed that carbon dioxide responses don't alter until much later (24 months). Thus, as a carbogen challenge is used here, it makes sense to look at older animals.

6.3 Methods

The methods detailed here expand upon those described in chapter 2 (sections 2.2-2.4).

6.3.1 Animal Subjects

Young (8-12 weeks, n=5), adult (~6months, n=5), and old (>19months, n=5) female C57BL/6J mice were used for these experiments (Charles River, UK). All animals were housed in a 12h light/dark cycle in 25°C temperatures. Food and water were made freely available.

6.3.2 Animal Surgery

All animal procedures performed were in accordance with the Animals (Scientific Procedures) Act 1986. Prior to surgery mice were anaesthetised with a mixture of fentanyl-fluanisone (Hypnorm, Vetapharm Ltd), midazolam (Hypnovel, Roche Ltd), and sterile water (1:1:2 by volume; 0.7-0.8ml/kg, i.p.). During surgery anaesthesia levels were maintained using isoflurane (0.5-0.8%) in 100% oxygen, and temperature was controlled using a homoeothermic blanket with a rectal probe (Harvard Apparatus) set at 37°C. The surgical procedures conducted here were the same as those detailed in section 2.2.2 for the recovery preparations. Briefly, a thinned cranial window was created overlying the right somatosensory cortex; and a stainless steel head plate was fixed to the skull with dental cement. The head plate acted as a holding device for all imaging experiments, to minimise possible motion artefacts. Mice were allowed at least one week for recovery before any imaging was performed.

6.3.3 Experimental Procedures

Following the recovery period, mice underwent two imaging sessions separated by at least one week. During the imaging experiments, mice were anaesthetised using the same combination of anaesthetics as during the surgical procedures, although the dose was reduced to 0.7ml/kg, and the isoflurane levels were slightly reduced (0.25-0.5%). The combination of these injectable (midazolam, fentanyl-fluanisone) and volatile (isoflurane) anaesthetics was chosen as, under their effect, mice have been shown to produce

hemodynamic responses of similar magnitude and speed as seen in the awake state (see chapter 5; Sharp, Shaw, et al., 2015).

The first imaging session used 2-dimensional optical imaging spectroscopy (2D-OIS) to measure haemodynamic activity only (refer to section 2.5.1.2 from main methods); and the second imaging session used 2D-OIS in combination with an electrode placement (refer to section 2.5.2.2 from main methods) to measure concurrent haemodynamic and neuronal activity. The haemodynamic data presented in this chapter were taken from the first imaging session in which only 2D-OIS recordings were made. 2D-OIS was used to provide spatial estimates of changes in the cortical oxyhaemoglobin (HbO_2), deoxyhaemoglobin (Hbr), and total haemoglobin (Hbt) concentrations across the cortical surface. The 16-channel electrode (Neuronexus Technologies) was placed in the parenchymal area of somatosensory cortex with the highest Hbt increase in response to whisker stimulation. Electrode placement allowed for the measurement of the electrical activity of the neurons within this activated whisker region.

6.3.4 Experimental Paradigms

All subjects underwent both whisker stimulation and spontaneous (no whisker stimulation) experiments. During whisker stimulation experiments a mechanical whisker stimulator was used, which deflected the whiskers for either 2s or 16s at 5Hz using a plastic T-bar attached to a stepper motor. Whiskers were deflected ~1cm in the rostro-caudal direction. Each 2s and 16s experiment consisted of multiple stimulus presentation trials (30 or 15, respectively) of 25s or 70s (respectively) to improve signal-to-noise. During spontaneous (no whisker stimulation) experiments the motor for the whisker stimulator was switched off, meaning the whiskers were not deflected. Spontaneous experiments followed the same format as the 2s whisker stimulation experiments, consisting of 30 trials which were each 25s in duration. Spontaneous experiments involved a carbogen challenge (under 100% oxygen) in which the middle 10 trials also encompassed 10% CO_2.

6.3.5 Selection of Regions of Interest (ROI) for 2D-OIS Data

The selection of the activated whisker region has been previously described in section 3.4.2. Briefly, 'activation' z-scores were calculated on a pixel-by-pixel basis, and the 2000 contiguous pixels having the maximum z-score were selected to form the 'whisker barrel

region' used in subsequent time-series analysis. An alternative surround region (set at 650-750 pixels) which did not overlap with the 'whisker region' was also selected from within the cortical window.

6.3.6 Data Analysis

All data analysis was performed using MATLAB® (MathWorks).

6.4 Results

The following section reports the haemodynamic and neuronal responses to whisker stimulation across three age categories (young, adult and old mice). The haemodynamic changes to a 10% CO_2 challenge (induced carbogen) were also assessed across these age categories. Throughout this chapter, the haemodynamic responses seen in the adult mice were taken as the baseline standard by which to compare the developmental (young) and old responses, as neurovascular coupling is said to be fully developed and relatively consistent in the healthy, adult model (Fox & Raichle, 2007; Kozberg & Hillman, 2016). The haemodynamic responses to whisker stimulation in healthy adult animals, under the anaesthesia regime employed here, were also previously compared and found to be comparable to those of awake adult subjects (chapter 5; Sharp, Shaw, et al., 2015).

6.4.1 Whisker Stimulation Responses

Both a short duration (2s) and long duration (16s) mechanical whisker stimulation were delivered across multiple trials under 100% oxygen. The spatial extent and the time course of the haemodynamic response to whisker stimulation was assessed across age matched groups.

6.4.1.1 Examining the Spatial Extent of the Haemodynamic Response to Whisker Stimulation

The spatial extent of the haemodynamic response to 2s (Figure 6.1) and 16s (Figure 6.2) whisker stimulation was compared (each of the age conditions: (1) young, (2) adult, and (3) old are shown for matched representative animals, Figure 6.1 & Figure 6.2). The spatial maps generated show the averaged haemodynamic responses to stimulation (haemodynamic response maps are averaged between 0 and 5 seconds from the onset of stimulation). The magnitude of the response is displayed as micromolar change from baseline elicited by whisker stimulation. For all age categories, within the whisker barrel region, there were increases in Hbt and HbO_2, with a concomitant decrease in Hbr. The young age group also showed decreases in Hbt and HbO_2 in the surround region during whisker stimulation (dark blue regions to the left of the whisker barrels, Figure 6.1(1) & Figure 6.2(1)).

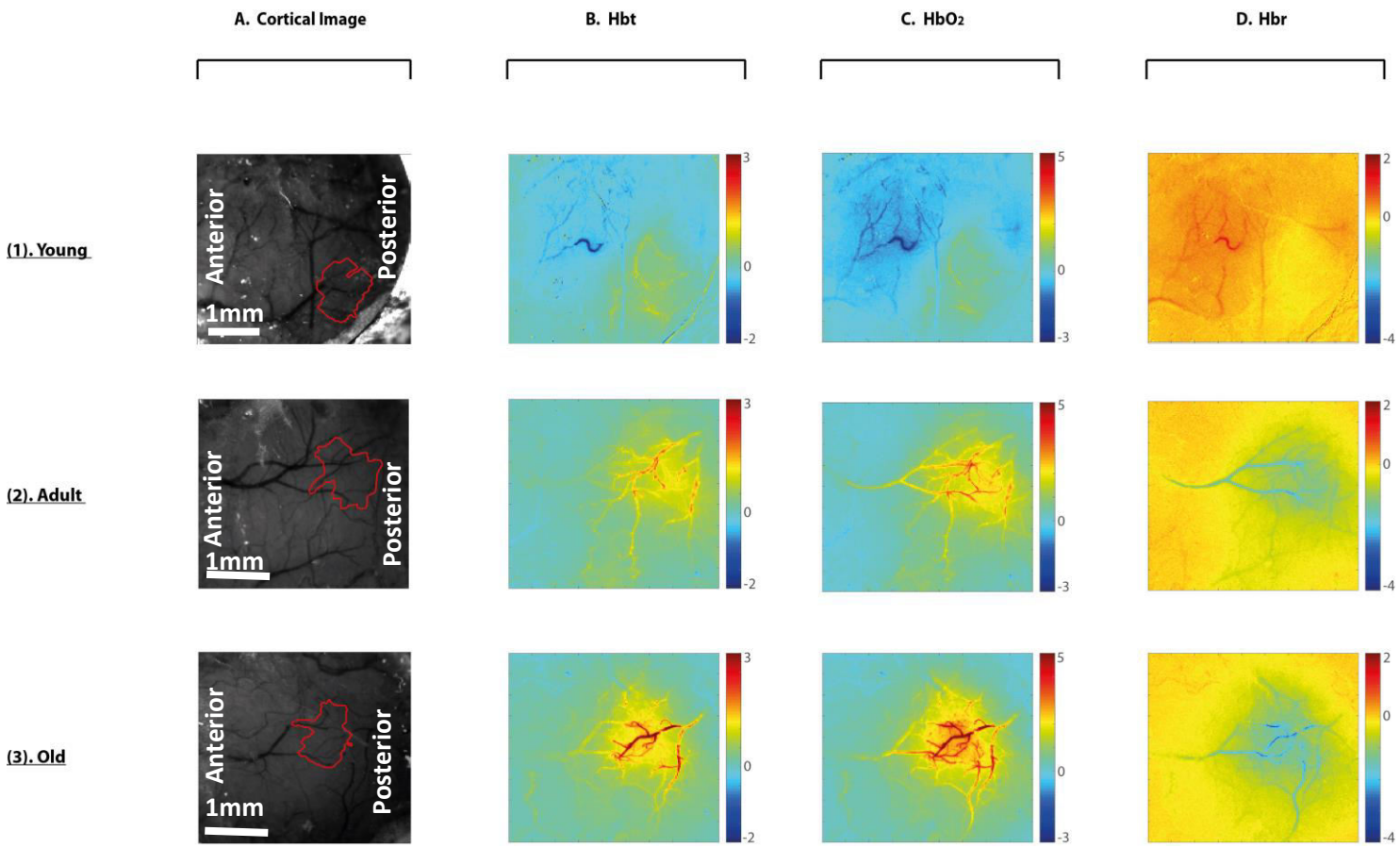

Figure 6.1 – Spatial Haemodynamic Responses evoked by 2s Whisker Stimulation

A. *An image of the cortex taken for a representative animal from each age category (**(1)** young, **(2)** adult, **(3)** old), with the whisker barrel region marked in red. The spatial extent of the haemodynamic changes averaged from the onset of a 2s whisker stimulation until 5s post-stimulation onset are shown for each of these representative animals for **B.** Hbt, **C.** HbO_2, and **D.** Hbr.*

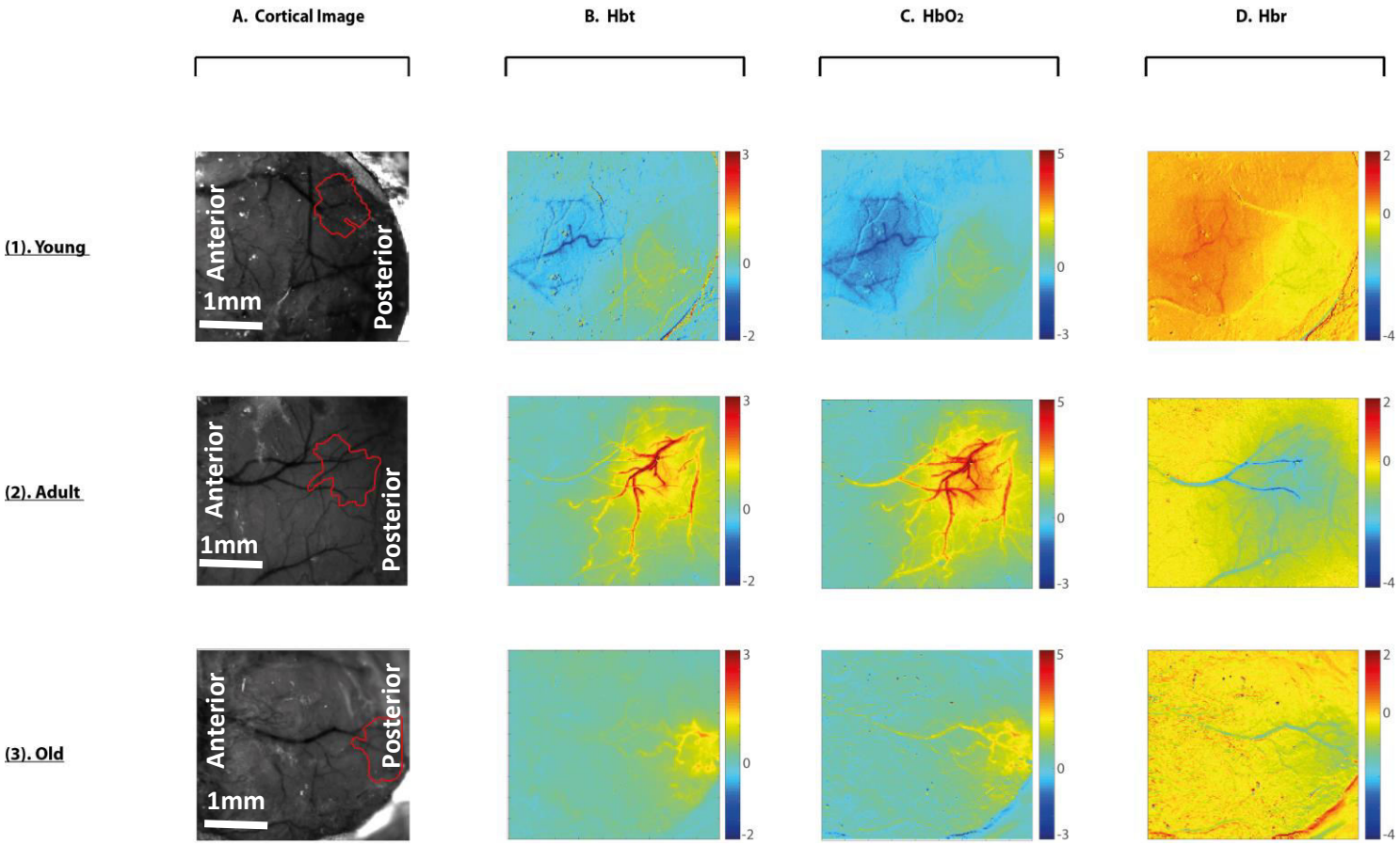

Figure 6.2 – Spatial Haemodynamic Responses evoked by 16s Whisker Stimulation

A. *An image of the cortex taken for a representative animal from each age category (**(1)** young, **(2)** adult, **(3)** old), with the whisker barrel region marked in red. The spatial extent of the haemodynamic changes averaged from the onset of a 16s whisker stimulation until 5s post-stimulation onset are shown for each of these representative animals for **B.** Hbt, **C.** HbO_2, and **D.** Hbr.*

6.4.1.2 Examining the Temporal Properties of the Haemodynamic Responses to Whisker Stimulation

The time course of the haemodynamic response to 2s (Figure 6.3) and 16s (Figure 6.4) whisker stimulation was averaged across subjects for each of the age conditions ((1) young, (2) adult, and (3) old). For all age groups there was an increase in Hbt and HbO_2, with a decrease in Hbr, in the whisker barrel region. For the young animals, a decrease in Hbt and HbO_2 was observed in the surround region, with a concomitant increase in Hbr ('negative surround'). This 'negative' response was not seen in the surround region for the adult or the old subjects; instead very small increases in Hbt were observed.

The temporal characteristics of the Hbt response were assessed across age groups for 2s (Figure 6.5) and 16s (Figure 6.6) whisker stimulations. Temporal dynamics were calculated using the time series data from the whisker region and the surround region. One-way ANOVAs were conducted to look for significant differences between Hbt responses to whisker stimulation across age groups. The average temporal Hbt response used for these comparisons was calculated from 0-5 seconds for 2s whisker stimulation; and from 0 to 20 seconds for 16s stimulation.

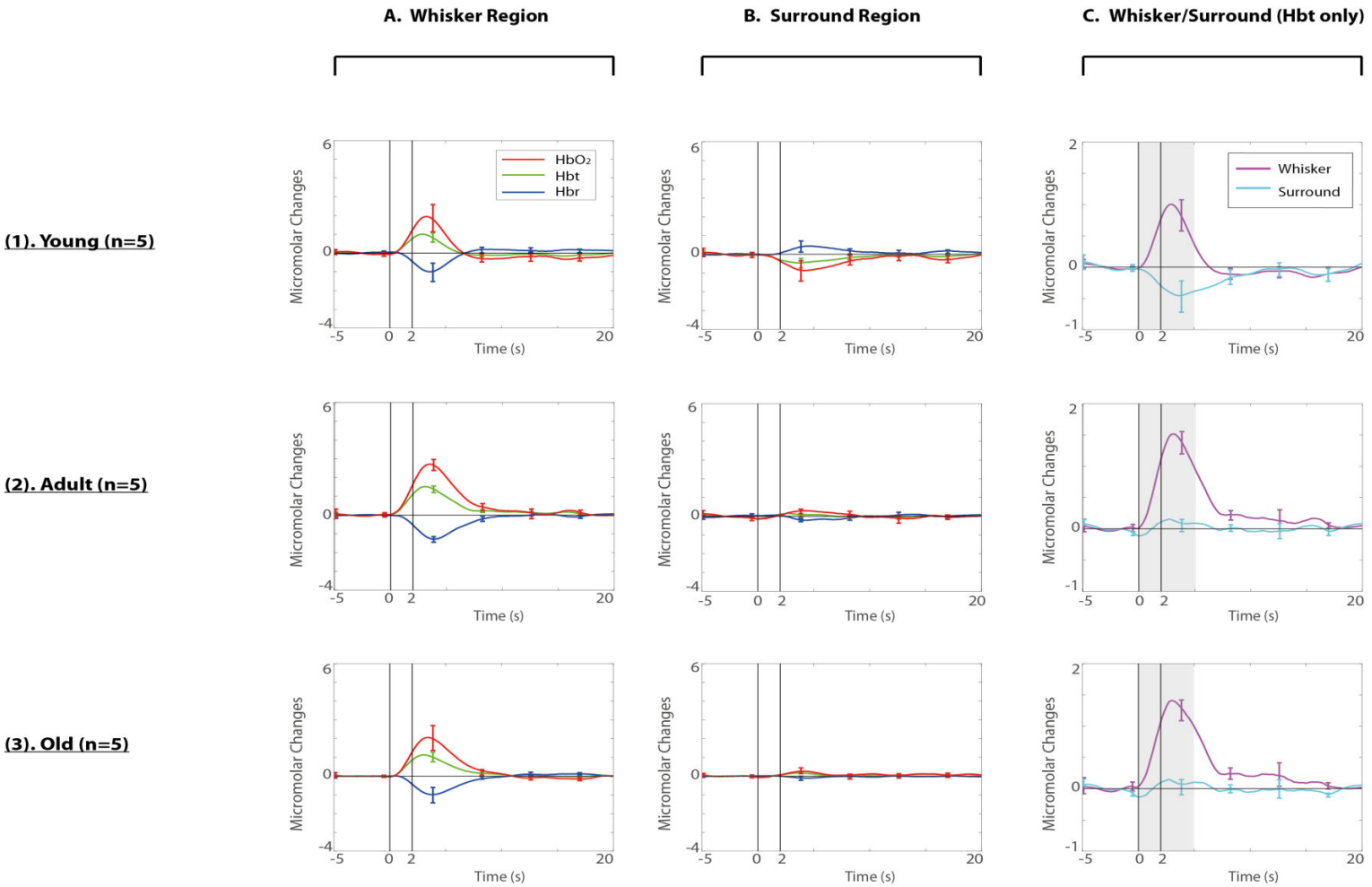

Figure 6.3 – The Time Course of Haemodynamic Responses evoked by a 2s Whisker Stimulation in the Whisker and Surround Regions

*The average haemodynamic responses (Hbt. HbO_2 & Hbr) evoked during 2s whisker stimulation are shown in **A.** the whisker barrel region, and **B.** the adjacent surround region (for **(1)** young, **(2)** adult, and **(3)** old subjects, n=5). **C.** The Hbt responses from both regions. Error bars represent SEM.*

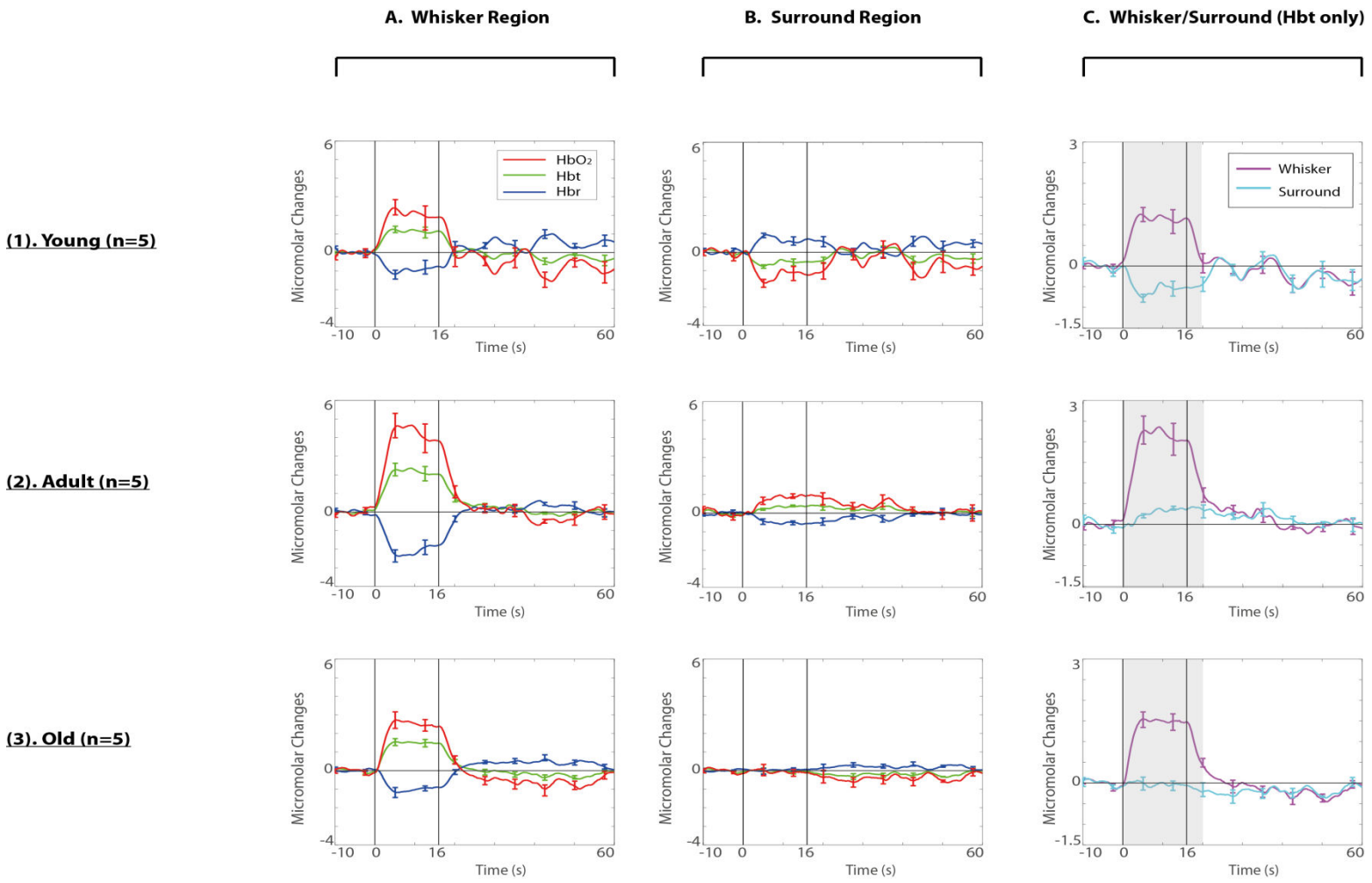

Figure 6.4 – The Time Course of Haemodynamic Responses evoked by a 16s Whisker Stimulation in the Whisker and Surround Regions

*The average haemodynamic responses (Hbt. HbO_2 & Hbr) evoked during 16s whisker stimulation are shown in **A.** the whisker barrel region, and **B.** the adjacent surround region (for **(1)** young, **(2)** adult, and **(3)** old subjects, n=5). **C.** The Hbt responses from both regions. Error bars represent SEM.*

There were no statistically significant differences between the average 2s stimulation-evoked Hbt responses in the whisker barrel region between young (M=0.60µm, SD=0.46), adult (M=0.99µm, SD=0.43) or old (M=0.73µm, SD=0.43) animals, as determined by a one-way ANOVA ($F(2,12)=1.35$, $p=0.30$). Although non-significant, there was a general trend for the average 2s-stimulation evoked Hbt response in the whisker barrels of adult subjects to be larger than those seen in both the young and adult animals (Figure 6.5 A, C).

There were significant differences between the average 2s stimulus-evoked Hbt responses in the surround barrel region between young (M=-0.30µm, SD=0.36), adult (M=0.06µm, SD=0.08), and old (M=0.08µm, SD=0.08) subjects, as determined by a one-way ANOVA ($F(2,12)=4.75$, $p=0.03$). A Tukey post hoc test revealed that the average 2s stimulus-evoked Hbt response in the surround region was significantly larger in the old animals compared to the young animals ($p=0.04$). Although non-significant, there was also a general trend for the average 2s-stimulation evoked Hbt response in the surround region of adult subjects to be larger than that seen in the young animals. The young subjects showed an overall negative Hbt response in the surround region during 2s whisker stimulation, whereas both the young and adult subjects showed a very slightly positive Hbt response (Figure 6.5 B, D).

There were significant differences between the average 16s stimulus-evoked Hbt responses in the whisker barrel region between young (M=0.96µm, SD=0.42), adult (M=1.80µm, SD=0.67), and old (M=1.24µm, SD=0.28) subjects, as determined by a one-way ANOVA ($F(2,12)=3.92$, $p=0.05$). A Tukey post hoc test revealed that the average 16s stimulus-evoked Hbt response in the whisker barrel region was significantly larger in the adult animals compared to the young animals ($p=0.04$). There were no significant differences between adult and old animals, although there was a general trend that the responses were smaller in the old animals (Figure 6.6 A, C).

There were significant differences between the average 16s stimulus-evoked Hbt responses in the surround region between young (M=-0.51µm, SD=0.18), adult (M=0.28µm, SD=0.11), and old (M=-0.05µm, SD=0.27) subjects, as determined by a one-way ANOVA ($F(2,12)=20.71$, $p<0.001$). A Tukey post hoc test revealed that the average 16s stimulus-evoked Hbt response in the surround region was significantly larger in the adult animals compared to the young animals ($p<0.001$), and the old animals ($p=0.05$) (Figure 6.6 B, D).

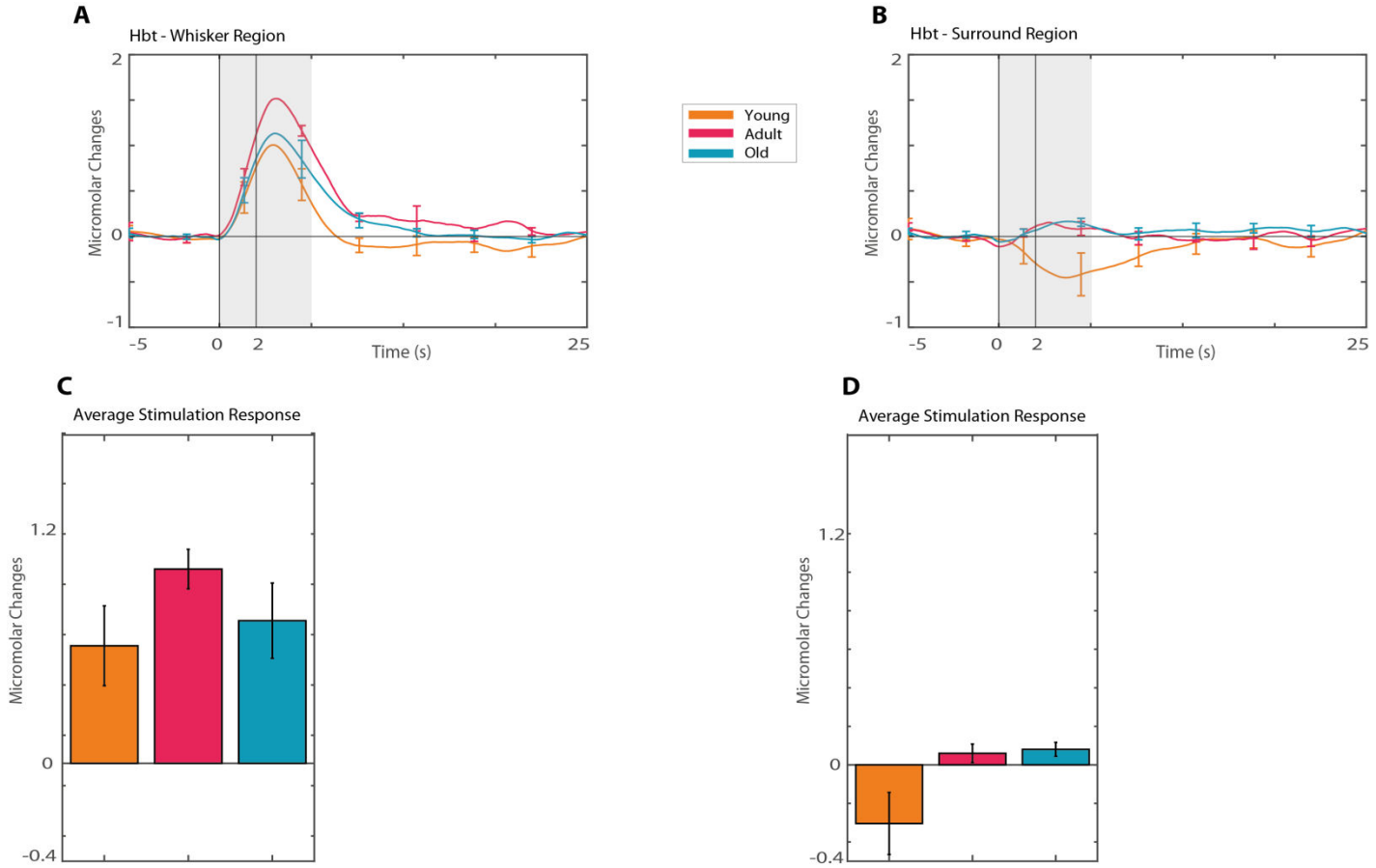

Figure 6.5 – Temporal Properties of the Haemodynamic Response to 2s Whisker Stimulation across Young, Adult & Old Mice

*The Hbt responses during 2s whisker stimulation from **A.** the whisker barrel region & **B.** the adjacent surround region for young (orange), adult (pink) and old (blue) subjects. The average Hbt response to stimulation and the maximum response peak are visualised from **C.** the whisker barrels, and **D.** the surround region for each of these age categories. Error bars represent SEM.*

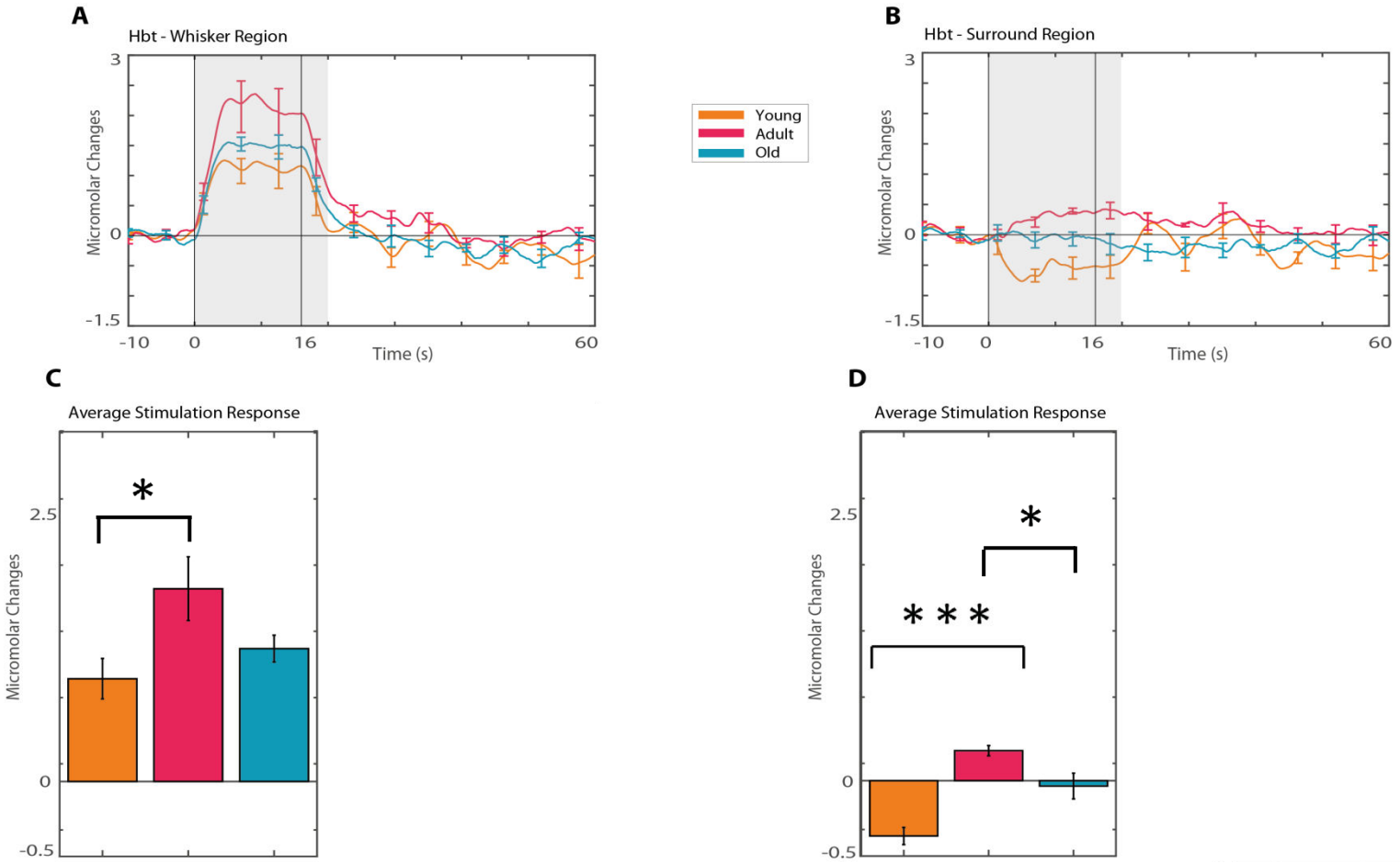

Figure 6.6 – Temporal Properties of the Haemodynamic Response to 16s Whisker Stimulation across Young, Adult & Old Mice

*The Hbt responses during 16s whisker stimulation from **A.** the whisker barrel region & **B.** the adjacent surround region for young (orange), adult (pink) and old (blue) subjects. The average Hbt response to stimulation and the maximum response peak are visualised from **C.** the whisker barrels, and **D.** the surround region for each of these age categories. Error bars represent SEM.*

6.4.1.3 Examining the Temporal Properties of the Neuronal Responses to Whisker Stimulation

Neural responses were also recorded from the whisker barrel region in response to sensory stimulation (2s or 16s). The neural data studied here, recorded using a 16-channel electrode, were averaged across the 4 channels from within the cortex with the greatest stimulus-evoked responses. The evoked neural activity recorded produced an individual LFP depolarisation to each of the individual stimuli within the stimulation train across all age categories (Figure 6.9 & Figure 6.10; i.e. 2s whisker stimulation at 5Hz was 10 stimulus trains; 16s whisker stimulation at 5Hz was 80 stimulus trains). Typical LFP responses in the healthy adult subjects generally demonstrated a profile of gradually decreasing responses to successive stimuli (Figure 6.7 B & Figure 6.9 B), which were associated with a large-magnitude positive haemodynamic response within this same whisker barrel region (Figure 6.3 A & Figure 6.5 A).

The temporal characteristics of the stimulus-evoked neural responses were assessed across age groups for 2s (Figure 6.9) and 16s (Figure 6.10) whisker stimulations. Temporal dynamics were calculated using the raw LFP data recorded from the whisker region. The initial depolarisation was calculated as the magnitude of the LFP response to the first stimulation pulse. The average neural response was calculated as the overall average depolarisation during the stimulation period (i.e. 0 to 2s, or 0 to 16s). One way ANOVAs were conducted on the average neural response data, in order to compare stimulus-evoked neuronal activity between age groups.

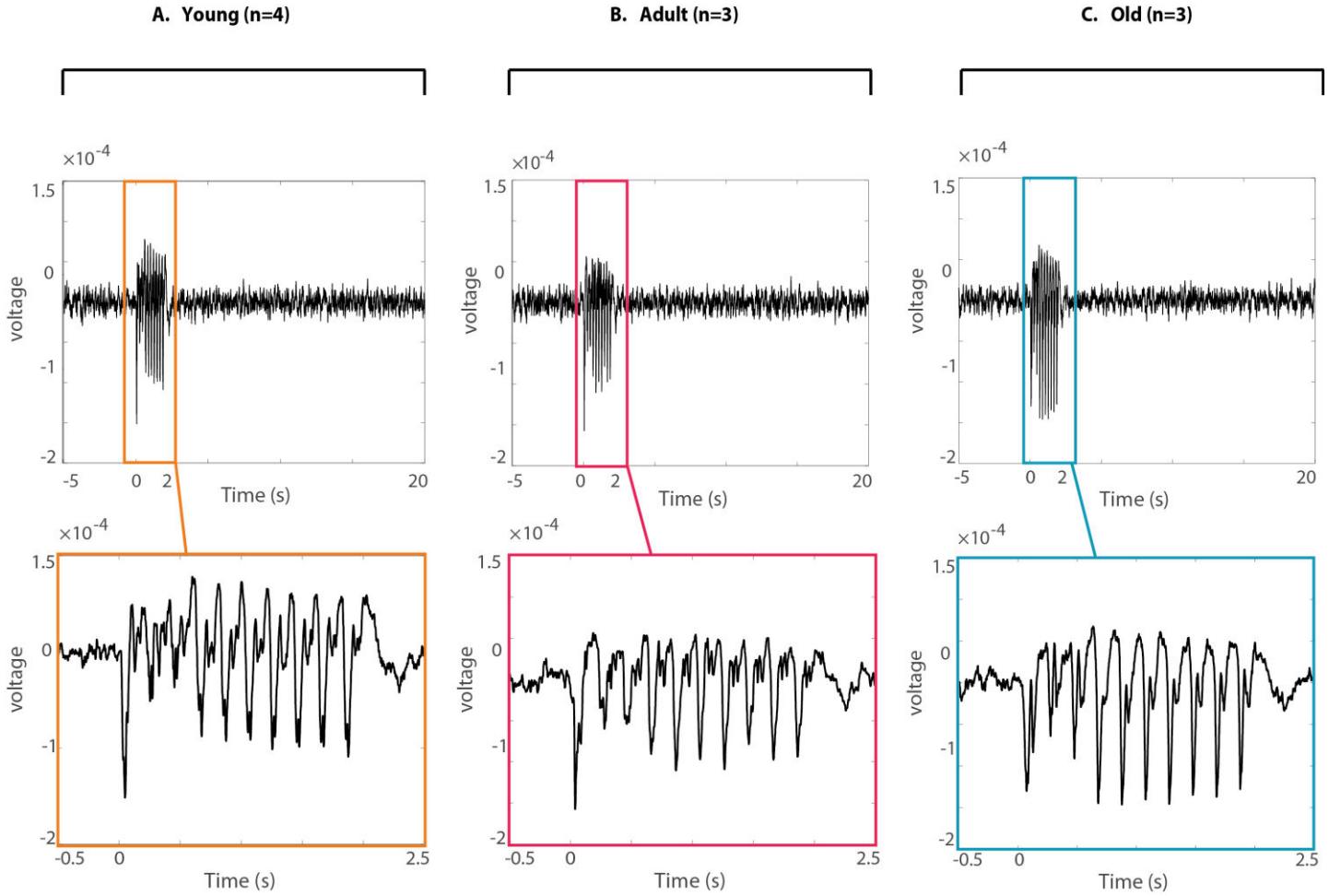

Figure 6.7 – The Time Course of the Neuronal Response evoked by 2s Whisker Stimulation across Young, Adult & Old Mice in the Whisker Barrel Region

*LFP neural responses recorded in the whisker barrels during a 2s whisker stimulation averaged across stimulation trials and electrode channels for **A.** young, **B.** adult, and **C.** old subjects.*

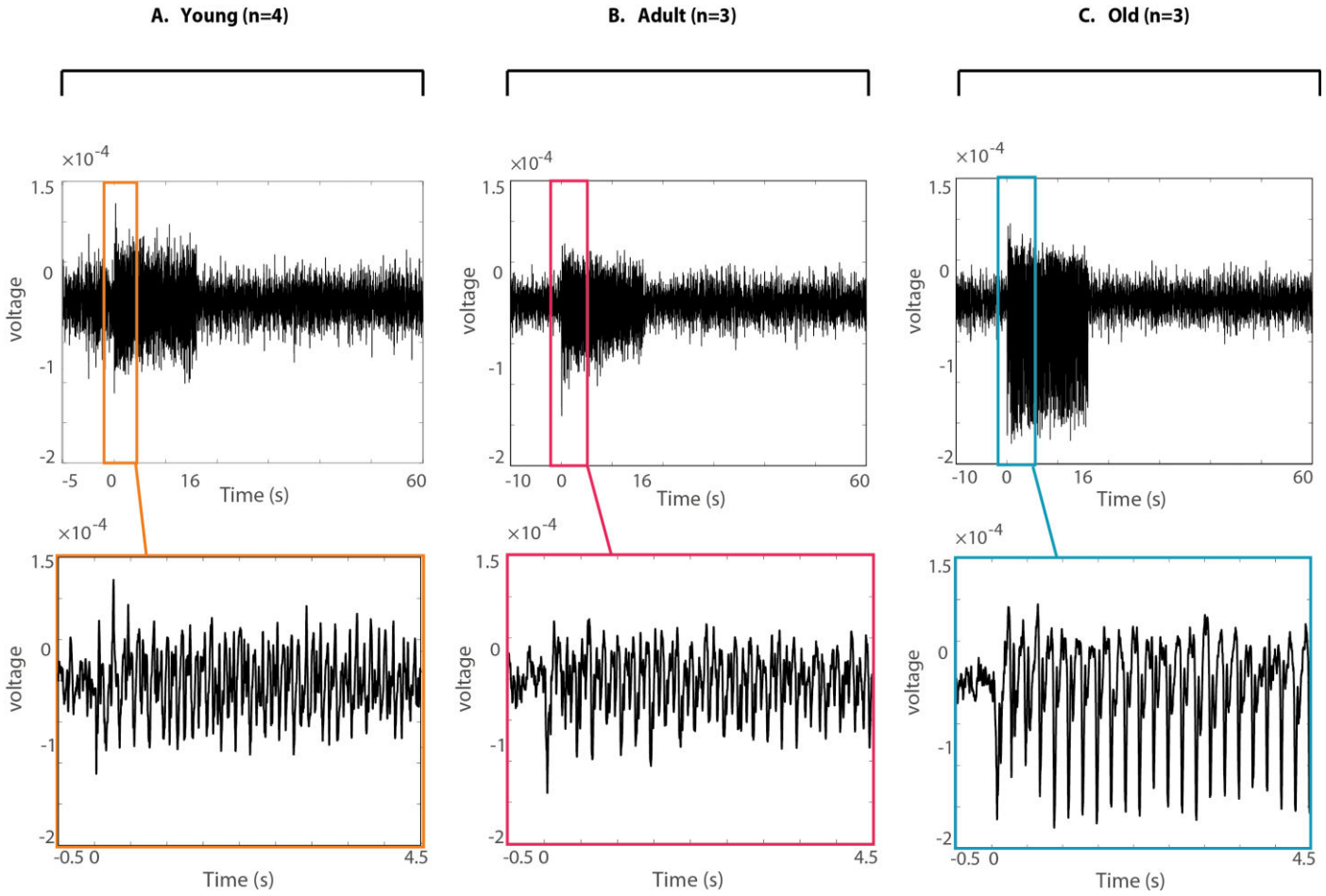

Figure 6.8 - The Time Course of the Neuronal Response evoked by 16s Whisker Stimulation across Young, Adult & Old Mice in the Whisker Barrel Region

LFP neural responses recorded in the whisker barrels during a 16s whisker stimulation averaged across stimulation trials and electrode channels for ***A.*** *young,* ***B.*** *adult, and* ***C.*** *old subjects.*

There were no statistically significant differences between the average 2s stimulation-evoked neuronal responses in the whisker barrel region between young ($M=-1.80e^{-4}v$, $SD=4.54e^{-5}$), adult ($M=-1.56e^{-4}v$, $SD=2.11e^{-5}$) and old ($M=-1.38e^{-4}v$, $SD=2.66e^{-5}$) animals, as determined by a one-way ANOVA ($F(2,7)=1.24$, $p=0.35$). Although non-significant, there was a general trend for the average 2s stimulus-evoked LFP responses be largest in the young subjects, then the adult subjects, and smallest in the old subjects (Figure 6.9 B).

There were also no statistically significant differences between the average 16s stimulation-evoked neuronal responses in the whisker barrel region between young ($M=-3.41e^{-4}v$, $SD=6.54e^{-5}$), adult ($M=-2.12e^{-4}v$, $SD=7.95e^{-5}$) and old ($M=-2.47e^{-4}v$, $SD=1.01e^{-4}$) animals, as determined by a one-way ANOVA ($F(2,7)=2.42$, $p=0.16$). Although non-significant, there was a general trend for the average 2s stimulus-evoked LFP responses be largest in the young subjects, then the old subjects, and smallest in the adult subjects (Figure 6.10 B).

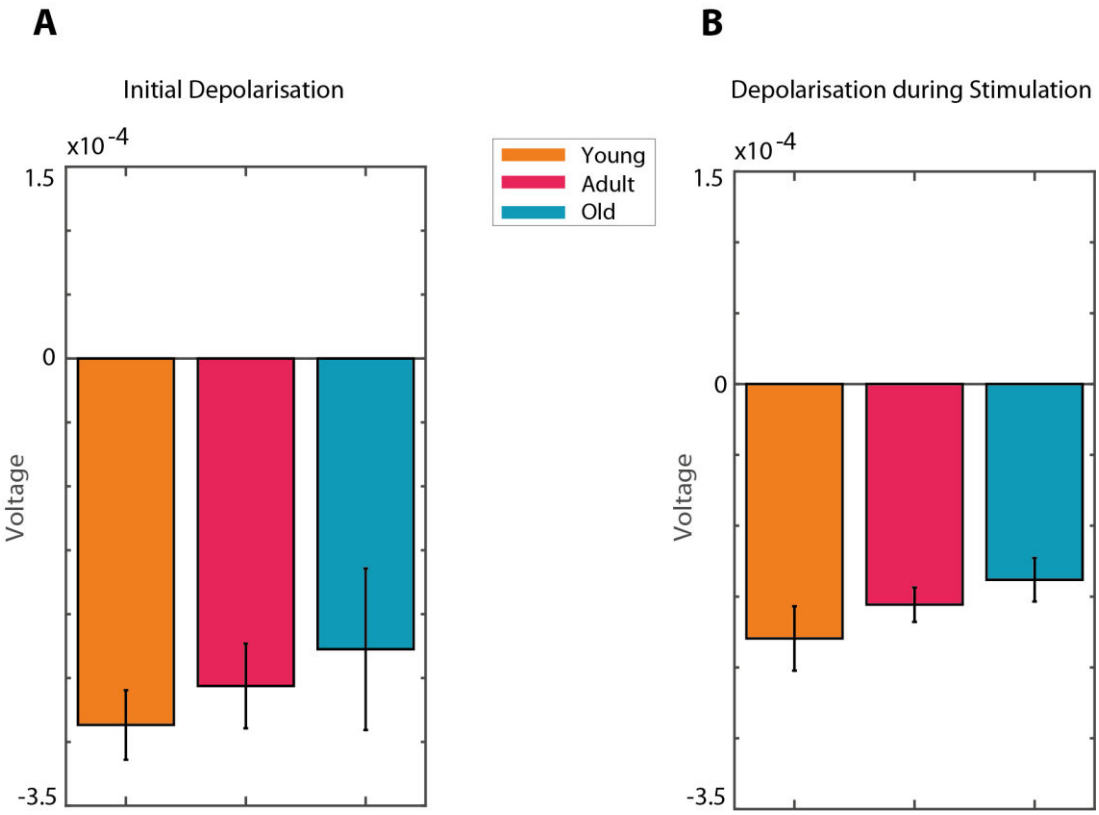

Figure 6.9 – Temporal Properties of the Neuronal Response to 2s Whisker Stimulation across Young, Adult & Old Mice

The LFP neural responses averaged across stimulation trials and electrode channels for ***A.*** *the initial depolarisation and* ***B.*** *the depolarisation during the entire stimulation for young (orange), adult (pink), and old (blue) subjects during a 2s whisker stimulation. Error bars represent SEM.*

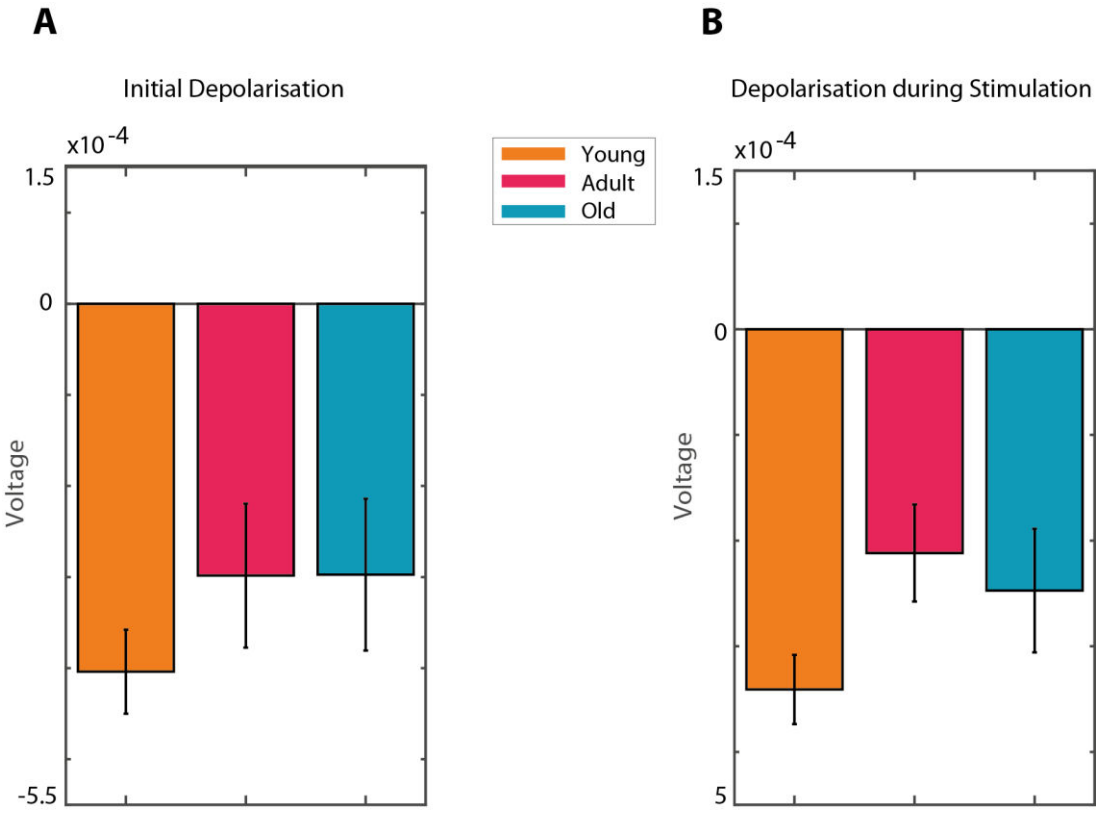

Figure 6.10 – Temporal Properties of the Neuronal Response to 16s Whisker Stimulation across Young, Adult & Old Mice

*The LFP neural responses averaged across stimulation trials and electrode channels for **A.** the initial depolarisation and **B.** the depolarisation during the entire stimulation for young (orange), adult (pink), and old (blue) subjects during a 16s whisker stimulation. Error bars represent SEM.*

6.4.1.4 Examining the Temporal Properties of Neurovascular Coupling during Whisker Stimulation

In order to compare neurovascular coupling across age groups within the whisker barrel region, a metric was taken for both the neural activity and for the haemodynamic responses. The neural activity metric was created by averaging the stimulus-evoked LFP depolarisations during the stimulation period; and the haemodynamic response metric was taken by averaging the area under the stimulus-evoked Hbt response curve. These metrics were taken on a trial-by-trial basis due to low animal numbers (the 2s stimulation experiments consisted of 30 trials; and the 16s stimulation experiments of 15 trials). A scatterplot was created to visualise the average stimulus-evoked Hbt and LFP responses across age groups (Figure 6.11). The spread of data points across the y axis showed variance in the LFP response, whereas the spread of data points across the x axis showed variance in the Hbt response. For the 2s whisker stimulation, the Hbt response looked similar between young and adult subjects, but the LFP depolarisations were larger in the young animals; the adult and old animals showed similar LFP depolarisations during the stimulation, but there was attenuation of the Hbt response within old animals (Figure 6.11 A). For the 16s whisker stimulation, the younger animals showed slightly smaller Hbt responses and larger LFP responses than the adult subjects; and the older animals showed a similar spread of Hbt responses and LFP responses to the adult animals (Figure 6.11 B).

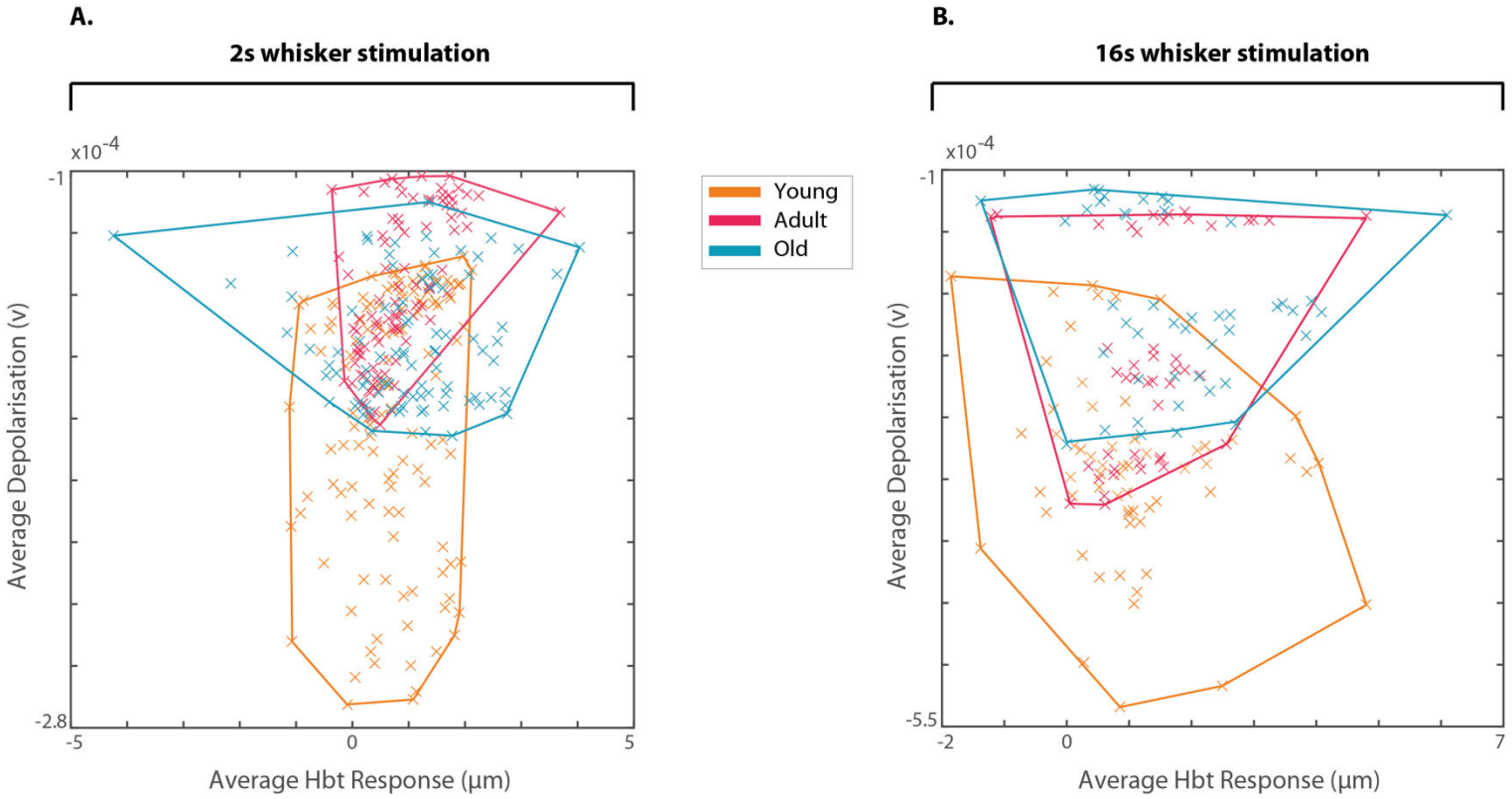

Figure 6.11 – Temporal Properties of Neurovascular Coupling during Whisker Stimulation for Young, Adult & Old Mice

A plot showing the LFP neural responses averaged across electrode channels for the depolarisation during the entire stimulation period, and the average Hbt response to stimulation, for young (orange), adult (pink), and old (blue) subjects.

6.4.2 Examining the Haemodynamic Responses during an Induced Carbogen Challenge

Haemodynamic changes were recorded (from the 'active whisker region') during a carbogen challenge, in the absence of whisker stimulation, as this allows the investigation of global changes in haemodynamics. The experimental paradigm consisted of 750 seconds under 100% oxygen, with the middle 250 seconds including 10% CO_2.

Following the onset of the carbogen challenge the young, adult and old subjects showed an increase in Hbt and HbO_2, with concomitant decreases in Hbr (Figure 6.12 A & B). The average temporal Hbt response was calculated by meaning the Hbt response from the onset of the carbogen challenge until the end of the experimental recording. A one-way ANOVA was conducted to compare the average temporal Hbt responses as induced by a carbogen challenge between young, adult and old subjects.

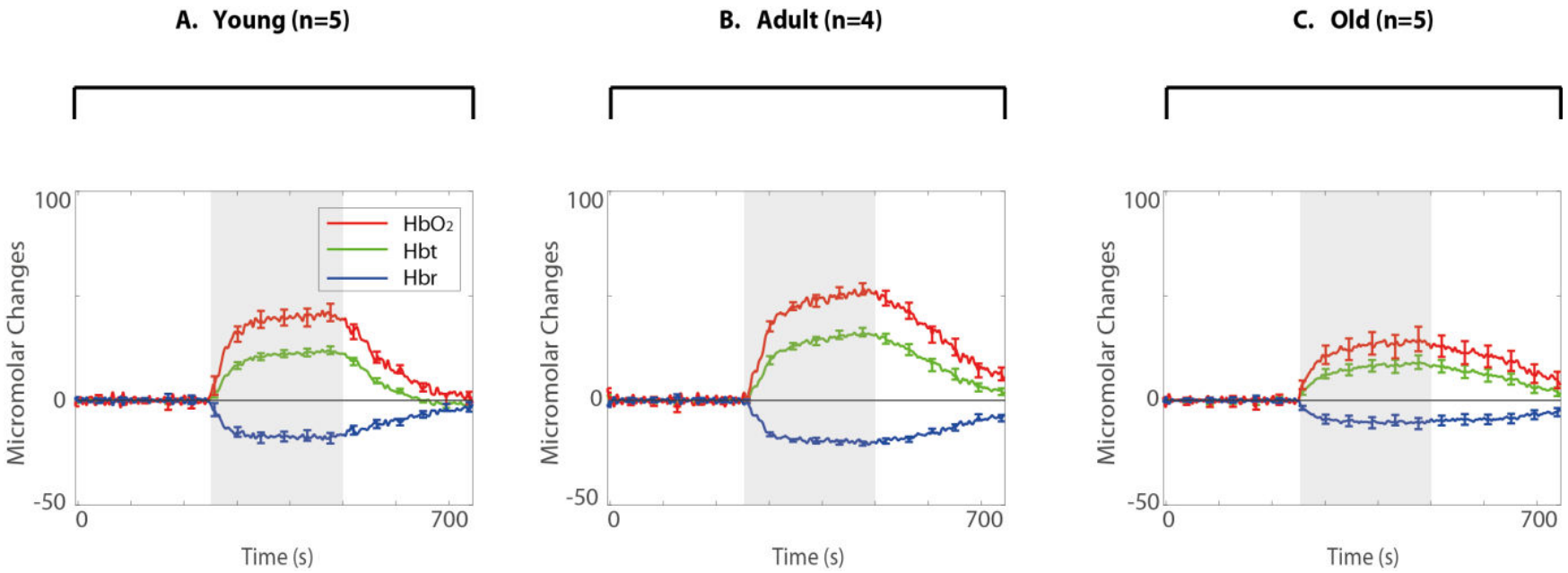

Figure 6.12 – Haemodynamic Responses during a Carbogen Challenge for Young, Adult & Old Mice

Continuous haemodynamic responses were recorded from the whisker barrel region over 750 seconds under 100% oxygen from ***A.*** *young,* ***B.*** *adult, and* ***C.*** *old subjects. The middle trials (from 250-500 seconds, outlined with a grey box) included the additional delivery of 10% CO_2. Error bars represent SEM.*

There were significant differences between the averaged temporal Hbt response following the onset of a carbogen challenge between the young (M= 11.98µm, SD= 2.31), adult (M= 19.91µm, SD= 3.34), and old (M=13.01µm, SD=5.13) subjects, as determined by a one-way ANOVA ($F(2,11)=5.5$, $p=0.02$). A Tukey post hoc test revealed that the increase in Hbt following the carbogen challenge was significantly larger in adult animals compared to young animals ($p<0.05$), and in adult animals compared to old animals ($p=0.05$).

Overall the increase in Hbt responses, as induced by carbogen challenge, were smaller in young and old subjects compared to healthy adult subjects. These findings will be dissected in more detail in the discussion section.

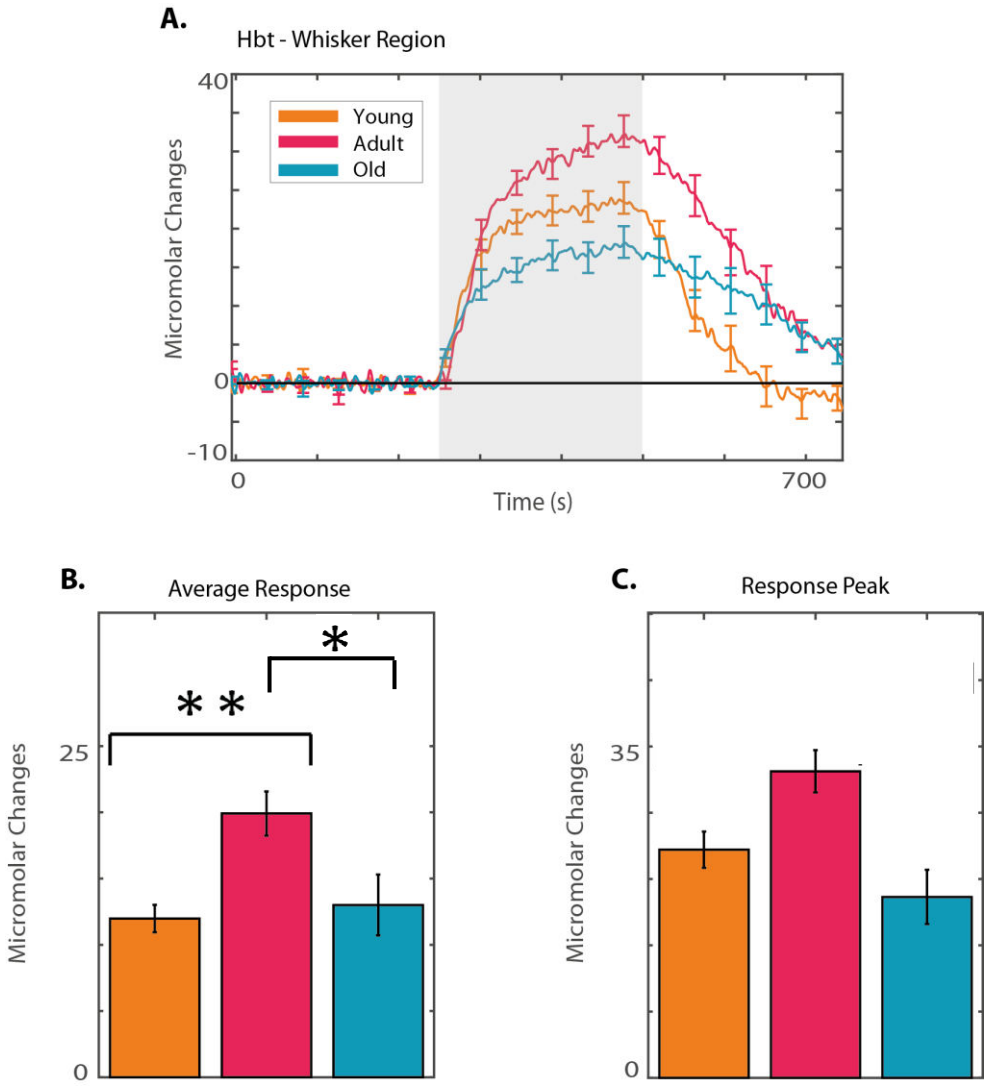

Figure 6.13 – Temporal Properties of the Haemodynamic Response to a Carbogen Challenge in Young, Adult & Old Mice

A. *The mean Hbt responses under 100% oxygen continuously recorded from the whisker barrel region for young (orange), adult (pink) and old (blue) subjects. During the middle of the recording 10% CO_2 was delivered (to induce a carbogen challenge, timing marked by the grey box).Temporal properties of the Hbt response which were measured were:* ***B.*** *The average Hbt response following CO_2 inspiration, and* ***C.*** *the maximum peak of the Hbt response. Error bars represent SEM.*

6.5 Discussion

Optical imaging spectroscopy and the insertion of a multi-channel electrode were applied to study neurovascular coupling during whisker stimulation or during a carbogen challenge in young, adult, and old mice.

6.5.1 Results Summary and Interpretation

6.5.1.1 Characterisation of the Haemodynamic Responses to Whisker Stimulation

There were no significant differences in the spatial extent of the stimulation-evoked Hbt responses between young, adult or old animals. This indicates that the evoked functional hyperemia was likely well-localised to the whisker barrel region across all age groups studied.

Mice in all age groups showed the expected stimulus-evoked increases in Hbt and HbO_2, with concomitant decreases in Hbr, which were centred on the whisker barrel region. Although non-significant, the increases in Hbt and HbO_2 and decreases in Hbr evoked by 2s whisker stimulation in the young and old animals were smaller than those seen in the adults. Significant differences in 16s stimulus-evoked Hbt responses were observed between young and adult animals, as the young subjects showed smaller evoked responses. There were no significant differences between Hbt responses in adult and old subjects as evoked by 16s whisker stimulation, however the responses were generally smaller in the old subjects.

Interestingly, young mice also showed a 'negative surround' region, in which the cortical area adjacent to the whisker barrels showed an overall decrease in Hbt and HbO_2, with increases in Hbr. The "negative surround" is commonly interpreted as reflecting either "vascular steal" or as an indicator of reduced excitatory or increased inhibitory neural activity (Boas et al., 2008; Boorman et al., 2010; Devor et al., 2008).

The haemodynamic response patterns seen in these young mice are perhaps reflective of the progressive maturation of neurovascular coupling (Arichi et al., 2012; Kozberg & Hillman, 2016), since the components of the neurovascular unit still undergo development postnatally (Harris et al., 2011). Functional hyperemia is still being honed during

adolescence (Harris et al., 2011), and so neurovascular coupling may not yet be at maximum efficiency. The results might be reflective of a transitional period from the negative BOLD response (NBR) to stimulation seen in infants (i.e. increased Hbr, with decreased Hbt and HbO_2 in the corresponding sensory region of the cortex), to the positive BOLD response (PBR) to stimulation seen in mature adults (i.e. decreased Hbr, with increased Hbt and HbO_2). The postnatal brain is a dynamic system that undergoes radical changes in neural connectivity and function, which extend well into childhood and adolescence (Kozberg & Hillman, 2016).

The existence and role of the NBR in the area of somatosensory cortex adjacent to the activated whisker barrel region has previously been investigated in rats in the Sheffield laboratory by Boorman and colleagues (Boorman et al., 2010; 2015). The authors speculated that the stimulus-evoked excitatory and inhibitory activity were greatest within the activated region, but that the inhibitory signals spread over a greater area than the excitatory signals (Boorman et al., 2010). This would produce net inhibition in surrounding regions. In line with this, a long-latency gamma-band neural marker (i.e. a decrease in gamma-band activity 300-2000ms post-stimulation) was shown to predict the negative haemodynamic responses seen in the surround region (Boorman et al., 2015). Previous studies have demonstrated that there are changes to the balance of excitation and inhibition in the developing brain (Akerman & Cline, 2007; Ben-Ari, 2002; Le Magueresse & Monyer, 2013), and the negative haemodynamic surround response observed in these studies may reflect underlying changes to local excitatory and inhibitory circuits during development.

The attenuated stimulus-evoked haemodynamic responses in old mice compared to adult mice is in agreement with previous work showing reduced CBF associated with ageing (Balbi et al., 2015; Fabiani et al., 2013; Jessen et al., 2015; Park et al., 2007; Toth et al., 2014a; 2014b; Tucsek et al., 2014; Zalatel et al., 2015). These findings may be indicative of underlying changes to the cerebral microvasculature (Farkas & Luiten, 2001; Iadecola et al., 2009; Park et al., 2007), which reduce the efficiency of neurovascular coupling.

6.5.1.2 Characterisation of the Neuronal Responses to Whisker Stimulation

The raw LFP responses to whisker stimulation in the whisker barrel region were also assessed for young, adult and old subjects. The evoked neural activity consistently

produced individual LFP depolarisation to each individual stimulus within the stimulation train; with the first depolarisation typically showing the largest response.

Although not significant, the neuronal response to short duration (2s) & long duration (16s) whisker stimulation showed larger depolarisations in young subjects compared to adult. Synaptic density increases have been found in development, before later synaptic pruning occurs in adulthood (Otsby et al., 2009; Paus et al., 2005; Shaw et al., 2008; Tamnes et al., 2010). It's possible that the larger LFP signals seen in the young mice compared to the adult are a result of higher synaptic density levels. The increased LFP responses to whisker stimulation in young animals may also reflect developmental changes to the GABAergic system. There is a developmental switch of GABA from depolarising to hyperpolarising (Ben-Ari, 2002), responsible for altering the excitatory to inhibitory balance of the brain and sharpening neuronal responses to stimulation (Sillito, 1975; Crook et al., 1998; Gabernet et al., 2005). In the mature adult brain, GABA is the primary inhibitory neurotransmitter, involved in the regulation of action potentials through membrane hyperpolarisation or the shunting of excitatory inputs. However, during development GABAergic synaptic transmission is excitatory, elevating intracellular Ca^{2+} concentration and triggering action potentials (Chen et al., 1996; Mueller et al., 1984; Obrietan and van den Pol, 1995). It is thought that such GABA-induced elevation of Ca^{2+} plays a critical role in the maturation of the nervous system, by promoting neuronal survival and differentiation (Ikeda et al. 1997; LoTurco et al. 1995; Marty et al. 1996); required to form, stabilise, and strengthen synaptic connections (Kirsch & Betz, 1998; Kneussel & Betz, 2000). Previous work from the Sheffield laboratory has demonstrated that the balance between neural excitation and inhibition can be investigated using these extracellular recordings (Zheng et al., 2012). Thus, the large depolarisations to whisker stimulation seen in the young subjects here may reflect higher levels of GABAergic-induced excitation, critical for strengthening synaptic connections during development and adolescence.

The LFP responses to 2s whisker stimulation in the old mice compared to the adult mice were generally attenuated; whilst the LFP responses to 16s whisker stimulation in old and adult mice were initially comparable, with slight increases in the overall average depolarisation throughout the stimulation in the old subjects. The attenuated LFP responses to short duration stimulation correspond with previous findings that neuronal activity is reduced in old age (Jessen et al., 2015; Nitish & Tong, 2004; Purdon et al., 2005; Thompson et al., 2008; West & Covell, 2001). This finding did not extend to long duration

stimulations, which have been suggested to interact more with astrocytic signalling. As the short and long duration neuronal responses have different neurovascular pathways, it is possible that they are affected differently by old age. Cauli & Hamel (2010) reviewed the relative timings of astrocytic and neuronal calcium responses to neuronal activity, suggesting that rapid calcium events reflect activation of ionotropic receptors expressed frequently on neurons, and slower calcium responses reflect the activation of metabotropic receptors expressed by neurons (and astrocytes). Perhaps the neurovascular events which occur during short duration stimulation (i.e. involving ionotropic neuronal receptors) are affected earlier in the ageing process (attenuated LFP responses); but the neurovascular events associated with long duration stimulation (i.e. metabotropic receptors on neurons) remain unaffected (LFP responses are comparable).

Neurovascular coupling was visualised across age conditions through a scatterplot of metrics representing neural and haemodynamic responses (Figure 6.13). The spread of data points across the y axis showed variance in the LFP response, whereas the spread of data points across the x axis showed variance in the Hbt response. From this scatterplot it appears that stimulation-evoked neurovascular coupling may be altered during development, as the spread of the haemodynamic and neural metrics for the young age condition appeared somewhat distinct to that for the adult age group (i.e. the younger animals showed slightly smaller Hbt responses and larger LFP responses than the adult subjects). However, from these results neurovascular coupling seemed more stable in old age. Specifically, neural responses looked similar in old age to those seen in the adult group, although haemodynamic responses appeared to show more variation in the old group (as the spread of the scatterplot was more wide-reaching for the Hbt metric compared to that seen in adults). Overall, there are trends which imply neurovascular coupling could be altered in both development and old age, although more investigations will be necessary before firm conclusions can be drawn.

6.5.1.3 Characterisation of the Haemodynamic Responses during an Induced Carbogen Challenge

Previous research has employed a hypercapnia challenge by inhalation of CO_2, which is thought to induce and maintain NO dependent vasodilation (Park et al., 2007). NO is

important for inducing vasodilation following neuronal activation (Lindauer et al., 1999). Here a carbogen challenge was presented, as the 10% CO_2 was inhaled under oxygen.

The increase in Hbt in response to the carbogen challenge was attenuated in young subjects compared to adult, and returned back to baseline levels quicker following the cessation of CO_2. This result is somewhat surprising as nitric oxide synthase (as found in GABAergic interneurons) occurs in increasingly higher densities throughout development (Downen et al., 1999; Eto et al., 2010; Ohyu & Takashima, 1998). Thus, if nitric oxide release causes vasodilation, it would be expected that more nitric oxide would mean greater increases of Hbt in response to a carbogen challenge in the young animals compared to the adult. As neurovascular coupling is still being honed in adolescence, it is possible that the vasoactive signalling between neurons and blood vessels has not yet reached maximum efficiency, and also that the vasodilator capacity of the vasculature itself is still developing.

The Hbt response to the carbogen challenge was also attenuated in the old subjects compared to adult. This result is in agreement with previous studies which showed that the increases in CBF induced by a hypercapnia challenge were reduced in old age (Park et al., 2007; Topcuoglu et al., 2009; Toth et al., 2015b; Zalatel et al., 2005). Previous studies, which measured NO, demonstrated that attenuated NO dependent vasodilation in ageing is thought to reflect deficiencies in neurovascular coupling, which increase the brain's susceptibility to vascular insufficiency and ischemic injury (Farkas & Luiten, 2001). It has also been shown that the vasculature itself can't respond as well in old age (e.g. due to increased stiffness, tortuosity, and narrowing of the vessels; Hajdu et al., 1990; Hutchins et al., 1996; Park et al., 2007).

6.5.2 Limitations of the Current Study

Whilst the study described here provides a useful model for studying neurovascular coupling in development, adulthood and ageing, there are a number of limitations.

Anaesthetised Preparation. Anaesthesia was used in these experiments, and has previously been shown to affect cerebral physiology (i.e. neural activity and vascular responsiveness;

Masamoto & Kanno, 2012). Any physiological changes resulting from the use of anaesthesia may also alter neurovascular coupling differently in the developing or old brain. This particular anaesthetic regime was employed as it was recently shown to produce similar stimulus-evoked haemodynamic responses to those seen in awake animals (chapter 5; Sharp, Shaw, et al., 2015); although the effects of this anaesthesia regime on neural activity, or different age categories, were not elucidated. However, as in previous animal studies investigating neurovascular coupling in development and ageing, anaesthesia was used (e.g. Kozberg et al., 2013; Park et al., 2007; Topcuoglu et al., 2009; Toth et al., 2015b; Zalatel et al., 2005; Zehender et al., 2013), as this allows for the application of invasive methods to gain high spatiotemporal detail about the mechanisms of neurovascular coupling. Future work may benefit from investigating neurovascular coupling in development and ageing using awake subjects; although the effects of locomotion would need to be controlled for (chapter 4).

Physiological Parameters. The current study did not control for age-related differences in baseline haemodynamic parameters (e.g. baseline CBF or CBV) or systemic blood pressure, which could vary with age (Behnke et al., 2005). For instance, previous work has shown that baseline CBF is reduced in old age; and when controlling for baseline CBF levels, there were no differences between old and adult subjects in the magnitude of the haemodynamic response to stimulation (Ances et al., 2009). Further, arterial pressure has been shown to be a determinant of blood flow and volume which could influence stimulus-induced haemodynamic changes (Boas et al., 2008). It would be beneficial in future work to control for baseline CBF levels, and to measure oxygen saturation or blood pressure using a pulse oximeter or other more accurate but invasive methods, such as an oxygen probe (due to the limited accuracy of pulse oximeter).

Low Sample Size. The subject numbers in each age group used in this study are low (n=5 for haemodynamic imaging sessions; and n=3 or 4 for electrophysiological recordings). A study with a low sample size has low statistical power, which means there is a reduced chance of detecting a true effect and of reproducing the results (Button et al., 2013). The current study has low numbers due to supply issues when recruiting the older animals (i.e. waiting for them to age), and sudden deaths from old age. It will be important going forward to gain larger sample sizes for each group, in order to generalise and interpret the findings with higher confidence.

6.5.3 Possible Future Directions

The study described in this chapter shows alterations in haemodynamic responses across different age groups. These significant differences between age groups did not extend to the stimulus-evoked LFP responses, which will likely require further investigation. In order to elucidate the mechanisms responsible for the differences observed it will be important to measure concurrent neural activity (i.e. pyramidal cells and interneurons), haemodynamic changes, and astrocytic activity over a larger cortical area (i.e. also encompassing the adjacent surround region). One set of mechanistic questions concerns the patterns of neuronal signals which lead to vasoactivity, for example what is the role of inhibitory versus excitatory cells in dilating or constricting blood vessels. Another set concerns the role of the astrocytes which surround the vasculature, i.e. are they mediators between neurons and vessels. And finally, how do such processes change in response to development or maturation of the nervous system? Two photon microscopy is a useful tool which allows researchers to measure from neurons, blood vessels and glial cells (such as astrocytes) concurrently (Svoboda & Yasuda, 2006). In the future, it may be useful to implement two photon microscopy to measure the different components of the neurovascular unit within young, adult and old subjects, giving a more detailed understanding of the experimental results. Future studies would also benefit from the inclusion of more animals to increase the sample size, and the measurement of baseline physiology (i.e. by adding an oxygen probe).

6.5.4 Conclusions

Overall, further work is needed to conclusively decide whether neurovascular coupling is altered during development and ageing. fMRI, a widely used clinical tool, relies on haemodynamic measurements as a proxy for neural activity. If there are certain periods of development and maturation in which neurovascular coupling is different to that seen in healthy adults, then standard analysis and interpretation of fMRI data may be misleading. A more comprehensive understanding of the normal stages of the maturation of neurovascular coupling could provide important new insights into the plasticity and

dynamism of the brain, but also may provide new biomarkers for the diagnosis and treatment of both developmental and age-associated disorders.

Chapter 7

Discussion

7.1 Abstract

In the previous chapters, two-dimensional optical imaging spectroscopy (2D-OIS) and electrophysiology were applied to investigate mouse models of neurovascular coupling in the awake and anaesthetised mouse. This chapter draws together the major findings of this thesis, and discusses the wider implications for the field of research. Practical limitations of the experimental set-up developed here will be addressed, and then future research plans outlined. Finally, the thesis conclusions will be stated.

7.1.1 Research Aims

The aims of the research outlined in this thesis were as follows:

1. To establish an experimental set-up to measure haemodynamic responses and locomotion in awake mice
2. To implement the awake mouse experimental set-up to investigate the effect and interaction of whisker stimulation and locomotion on haemodynamic responses
3. To test the suitability of a novel 'modular' anaesthetic regime by comparing stimulus-evoked haemodynamic responses between awake and anaesthetised mice
4. To implement the optimised anaesthesia regime to investigate changes in neurovascular coupling associated with development and ageing

The discussion will draw together the key findings and insights resulting from this work. Each aim will be examined in detail, and the relevant items from chapters 2-6 will be linked to these aims.

7.2 Principle Research Findings

The overall results of this experimental thesis are reviewed below.

7.2.1 Aim 1: To Establish an Experimental Set-Up for the Measurement of Haemodynamic Responses and Locomotion in Awake Mice

The procedure and experimental set-up for measuring haemodynamic changes and locomotion in awake, head-fixed mice was detailed in chapter 3. Many previous studies have employed the use of anaesthesia to investigate neurovascular coupling *in vivo*, typically due to the invasive nature of the techniques applied. However, to overcome the effects of anaesthesia on the neural and vascular physiology (Masamoto & Kanno, 2012), there has been a recent movement which favours the use of awake, behaving animals. For the experiments described in this thesis (chapter 4 & 5), the methods of Carandini and colleagues (Haider et al., 2013; Ayaz et al., 2013; Pisauro et al., 2013) were adapted for the imaging of awake mice. This experimental set-up involved head fixing a mouse atop of a spherical treadmill (Styrofoam ball) which rotated as the animal moved backwards/forwards. The movement of the rotating ball was detected with optical motion sensors, which provided information about the speed and direction of locomotion. A CCD camera concurrently recorded images of the cortex through a thinned cranial window overlying the somatosensory cortex. Haemodynamic responses were recorded using 2D-OIS during spontaneous (i.e. no whisker stimulation) or stimulus-evoked (i.e. whisker stimulation) experiments. The small mass of the mouse combined with the low friction environment of the spherical treadmill meant it was possible to conduct long-term imaging over numerous experimental sessions. Specifically, the quality of the thinned cranial window was found to be stable for up to 3 months using this experimental set-up, after which partial skull regrowth (which obscured imaging) was observed (Figure 3.3).

This experimental set-up proved suitable for the concurrent measurement of haemodynamic responses and locomotion, although motion artefacts arose from the movements of the head during running, which affected subsequent data analysis. Two approaches were applied to counteract these motion artefacts. First, a second holding arm was added to the experimental set-up for extra mechanical security; then post-processing image registration (MATLAB, image processing toolbox) was applied to the data, to align the multiple images taken within an experimental recording (Figure 3.7).

The development of this awake imaging platform was the first step towards offering more comprehensive and robust chronic awake imaging, and achieved the goals outlined in Aim 1. The next two experimental chapters (chapter 4 & 5) applied this imaging set-up to assess the time course and spatial extent of haemodynamic changes during whisker stimulation and spontaneous (no stimulation) experimental paradigms.

7.2.2 Aim 2: To Investigate the Effects and Interactions of Locomotion and/or Whisker Stimulation on Haemodynamic Responses in Awake Mice

The experimental set-up previously described (in chapter 3) was applied to measure haemodynamic changes in the awake mouse to whisker stimulation and/or locomotion (chapter 4). Recent studies have utilised awake mouse imaging to study neurovascular coupling to: overcome the confounds of anaesthesia, allow for long-term neuroimaging, and to encompass the effects of behavioural state or learning (Ayaz et al., 2013; Huo et al., 2014; Niell & Stryker, 2010; Saleem et al., 2015; Vinck et al., 2015). In comparison to the anaesthetised preparation, the awake experimental set-up allows the animal to run and whisk. As such, researchers have also taken to measuring these behavioural variables to assess whether they have any additional effect on neurovascular coupling (Ayaz et al., 2013; Huo et al., 2014; Niell & Stryker, 2010; Saleem et al., 2015; Vinck et al., 2015).

In mice, locomotion has been found to induce robust changes in the firing of neurons in the visual cortex (Ayaz et al., 2013; Neill & Stryker, 2011; Saleem et al., 2013); but no changes to the corresponding haemodynamic responses were observed (Pisauro et al., 2013). In the somatosensory cortex (S1) of mice, locomotion has been linked with increases in neural activity (Huo et al., 2014), with mixed results regarding the haemodynamic changes (increases: Huo et al., 2014; no changes: Takuwa et al., 2011; 2012). Here, it was thus hypothesized that whisker stimulation would cause increased haemodynamic activity in the

whisker barrel region; but that the effects of locomotion on haemodynamic responses would be negligible.

The time course of haemodynamic responses in the whisker barrel region of awake mice during spontaneous locomotion (with no stimulation) was actually shown to evoke increases in total blood volume (Hbt) and oxygenated haemoglobin (HbO_2), with concomitant decreases in deoxygenated haemoglobin (Hbr) (Figure 4.2). Hbt response maps were generated to assess the spatial extent of the haemodynamic changes during locomotion, which was found to cause Hbt increases recruiting much of the surface vasculature within exposed S1 (Figure 4.3). The onset of locomotion was tightly coupled with haemodynamic changes.

The time course of the haemodynamic responses in the active whisker region of awake mice during whisker stimulation was also shown to evoke increases in Hbt and HbO_2, with concomitant decreases in Hbr. As expected, the 2s stimulation paradigm produced a short duration monophasic haemodynamic response, whereas the 16s stimulation produced a larger magnitude and longer duration haemodynamic response (Figure 4.5). A pixel analysis was conducted to assess the number of active pixels during whisker stimulation and spontaneous locomotion. No significant differences were found in the spatial extent of the Hbt responses during 2s and 16s stimulation as compared to during spontaneous locomotion, confirming that both locomotion and whisker stimulation evoked similar haemodynamic changes in S1 (Figure 4.7). Interestingly, significant differences were found between the spatial extent of the 2s and 16s stimulation Hbt responses; with 2s stimulation showing a greater average change in the number of active pixels during stimulation, and a greater maximum peak in the number of active pixels.

As spontaneous locomotion and whisker stimulation were separately shown to drive haemodynamic responses, next the interaction of locomotion on the stimulus-evoked haemodynamic responses was elucidated. The whisker stimulation trials were sorted and grouped into the top (‘most’) and bottom (‘least’) 25% of trials, dependent on the average amount of locomotion occurring during the stimulation period (Figure 4.8). There were significant differences in the haemodynamic response profiles between ‘least’ and ‘most’ locomotion conditions, with stimulus-evoked haemodynamic changes during periods of ‘most locomotion’ showing significantly larger increases in Hbt for both stimulation durations. During ‘least locomotion’ trials the haemodynamic responses were more

localised and centred on the whisker barrels, whereas during 'most locomotion' trials the spatial extent of the haemodynamic response seemed more global (Figure 4.9 & 4.10). This was confirmed with pixel analysis revealing significant differences in the average percentage of active pixels during stimulation, and in the maximum peak percentage of active pixels, for both 2s and 16s stimulation paradigms during 'least' and 'most' locomotion (Figure 4.11). The trial 'sorting' suggested there was an interaction between locomotion and stimulus-evoked haemodynamic responses. To investigate this further, the locomotion and stimulus-evoked responses were isolated, to check for linear superposition of the responses.

A 'control condition' was used to remove the effects of 'trial sorting'. To create the 'control condition', spontaneous (no stimulation) experiments were sectioned into trials which corresponded to the timing of whisker stimulation experiments, and locomotion was sorted in the same way from least to most during the corresponding 'stimulation period' (Figure 4.12). After removing the effects of whisker stimulation and locomotion from the Hbt response, the resulting Hbt time series were not found to be comparable (Figure 4.13 & Figure 4.14), meaning the effects of locomotion and stimulation on the Hbt response could not be linearly superimposed. This suggests an interaction between locomotion and whisker stimulation. It was thus hypothesized that either locomotion was not spontaneously occurring, and was in some way related to the stimulus paradigm; or alternatively that additional behavioural variables (e.g. whisking) were affecting the responses. Analysis of the possible interaction suggested that locomotion was mainly unrelated to the period of whisker stimulation (Figure 4.15 & Figure 4.16). The current experimental platform does not allow for the concurrent tracking of spontaneous whisking behaviour (due to the multiple wavelengths of light required for 2D-OIS), and so the potential effects of whisking on haemodynamic responses in S1 could not be elucidated.

Contrary to the initial hypothesis (Aim 2), the experiments showed that locomotion alters haemodynamic responses in S1. Whilst the overall average stimulus-evoked haemodynamic responses show the 'normal' temporal profiles, when separating the experimental trials by 'least' and 'most' locomotion, locomotion was found to induce a larger stimulus-evoked haemodynamic response, which was spatially more global. Thus, studies which use an awake model to study neurovascular coupling may wish to consider locomotion in their data analyses, especially when relying on a limited number of stimulation trials or subjects.

Further, it was not possible to collect electrophysiological data using the awake experimental set-up, primarily due to the invasive nature of the multichannel electrode technique. Thus, because of the effects of locomotion on haemodynamic responses in S1 demonstrated here, and the necessity of collecting concurrent neural data when investigating neurovascular coupling, the next chapter sought to establish a suitable regime for studying neurovascular coupling in the anaesthetised mouse.

7.2.3 Aim 3: To Compare the Stimulus-Evoked Haemodynamic Responses of Awake Mice and Anaesthetised Mice under a Novel 'Modular' Anaesthetic Regime

To assess the suitability of a novel 'modular' anaesthetic regime, stimulus-evoked haemodynamic changes recorded using 2D-OIS from awake and anaesthetised subjects were compared (chapter 5). This thesis chapter was based on the publication by Sharp, Shaw et al., 2015. Previously, *in vivo* animal studies have used anaesthesia to minimise motion artefacts, reduce stress, and for the application of invasive high spatiotemporal techniques. Despite these benefits of using anaesthetics, there are issues arising from the effects of anaesthesia on brain physiology. Anaesthetics can influence the components of the neurovascular unit, e.g. by modulating neural processing or vascular reactivity (Masamoto & Kanno, 2011). The effect of anaesthesia on neurovascular coupling varies depending on the type and depth of anaesthesia selected. For instance, inhalation anaesthetics are said to have a vasodilatory effect (Hendrich et al., 2001; Van Hemelrijck et al., 1993) and impair the speed of autoregulation (Engelhard & Werner, 2006; Hoffman et al., 1991; Strebel et al., 1995); whereas injectable anaesthetics have vasoconstrictive effects with well-preserved cerebral autoregulation (Engelhard & Werner, 2006; Strebel et al., 1995). It would be advantageous to develop an anaesthetic regime which minimises these modulatory effects on neurovascular coupling, although the optimal anaesthetic protocol is still a matter of debate. Here, a novel 'balanced' anaesthetic regime which combined inhalation and injectable anaesthetics, was used to anaesthetise mice. Stimulus-evoked haemodynamic responses recorded from these anaesthetised mice were then compared the stimulus-evoked haemodynamic responses in awake mice.

During whisker pad stimulation increases in Hbt and HbO_2, with corresponding decreases in Hbr, were localised to the active whisker region across both awake and anaesthetised subjects. As hypothesized, the spatial extent of the haemodynamic responses were found to be comparable across the two groups. This finding was in agreement with previous work

which demonstrated that the spatial profile of haemodynamic responses was preserved under anaesthesia (Pisauro et al., 2013).

Two second whisker stimulation evoked monophasic increases in Hbt and HbO_2, with corresponding decreases in Hbr across both awake and anaesthetised groups. Sixteen second whisker stimulation evoked larger magnitude, longer duration increases in Hbt and HbO_2, with concomitant decreases in Hbr, across both experimental groups. Although, in the awake subjects, the 16s response profile was more complex, characterised by an initial peak, followed by a secondary peak with increased magnitude. As hypothesized, the awake and anaesthetised preparations were found to show similar response profiles (peak, time to 10%, and average magnitude of response) suggesting the novel 'modular' anaesthesia regime did not significantly alter haemodynamic activity in mice *in vivo*. This finding was in contrast to previous reports, in which the anaesthetic regime applied resulted in the time course of haemodynamic responses being slower and smaller in magnitude when compared to responses seen in awake subjects (Logothetis et al., 1999; Martin et al., 2006; 2013; Peeters et al., 2001; Pisauro et al., 2013).

Following the confirmation of similar haemodynamic responses, observed under the anaesthesia and awake regimes, the next chapter (chapter 6) sought to apply this anaesthetic combination to study neurovascular coupling in development and old age.

7.2.4 Aim 4: To Investigate Neurovascular Coupling in Development and Old Age

It is thought that neurovascular coupling is altered during development due to structural changes found to the components of the neurovascular unit (i.e. neurons, blood vessels, astrocytes). Postnatally there are increases in neurons (i.e. dendrite count, number of synapses; Chan et al., 2002), vasculature volume (Keep & Jones, 1990; Risser et al., 2009), and astrocyte population and connection numbers/densities (Nixdorf-Bergweiler et al., 1994; Stichel et al., 1991). These profound structural changes during development have been linked with functional changes in neurovascular coupling responses (Harris et al., 2011). Previous work has shown conflicting results using blood oxygen level dependent (BOLD) functional magnetic resonance imaging (fMRI) to study development, with both positive (Arichi et al., 2010; Cantlon et al., 2006; Liao et al., 2010; Marcar et al., 2004; Scapiro et al., 2004) and negative (Anderson et al., 2001; Born et al., 1998; 2000; Heep et al., 2009; Martin et al., 1999; Muramoto et al., 2002; Seghier et al., 2004; Yamaha et al.,

1997; 2000) BOLD signal responses observed within the same study population. It was possible the differences in the structure and function of vasculature during development could alter the BOLD signals observed experimentally, or that there were technical data analysis and interpretation issues. In an attempt to resolve these issues, recent animal studies have applied techniques with high spatiotemporal resolution to investigate neurovascular coupling during development in *in vivo* animal models. These studies have generally shown that haemodynamic responses are attenuated in development. Thus, it was hypothesized that stimulus-evoked neural and haemodynamic responses measured in this thesis (chapter 6), would also be attenuated in the developing brain.

Similar to during development, structural changes to the neurovascular unit have also been associated with ageing. For instance, there are reductions in neurons (grey matter volume, neuron count, dendrites and synapses, e.g. Creasey & Rapoport, 1985; Huttenlocher, 1979; Sowell et al., 2003); changes to cerebral blood vessels (i.e. thickened, tortuous capillaries, and pericyte degeneration; Farkas & Luiten, 2001); and hypertrophy of astrocytes (Peters, 2007). These profound structural changes associated with ageing, have been linked with a reduction in resting cerebral blood flow (Farkas & Luiten, 2001; Kalaria, 2008), which may affect the interpretation of BOLD fMRI studies. Indeed, inconsistencies have been shown in BOLD fMRI studies of the ageing population. Sensory tasks have been shown to cause increases (Lee et al., 2011; Mattay et al., 2001); decreases (Buckner et al., 2000; Hesselman et al., 2001; Nyberg et al., 2010; Raemekers et al., 2006; Ross et al., 1999; Tekes et al., 2005); and even no change (Aizenstein et al., 2004; Gazzeley & D'Esposito, 2005; Huettel et al., 2000; 2001) in the size of the positive BOLD response when compared to responses from healthy adults. These inconstancies may be due to different data analysis techniques, or regionally-specific alterations in the BOLD response. To resolve some of these issues recent animal studies have applied high resolution techniques to investigate neurovascular coupling in ageing *in vivo*. Generally, haemodynamic responses were attenuated in ageing (Balbi et al., 2015; Jessen et al., 2015; Park et al., 2007; Toth et al., 2014a; 2014b; Tucske et al., 2014); although there were mixed results regarding neural activity, with some studies showing it was preserved (i.e. 'neurovascular uncoupling', Tarantini et al., 2015), and others showing attenuated responses (Jessen et al., 2015). From the review of the literature, it was hypothesized that the stimulus-evoked neural and haemodynamic responses measured here (chapter 6), would also be attenuated in old age.

The spatial extent of haemodynamic responses evoked by whisker stimulation were comparable across all age groups (Figure 6.1 & Figure 6.2). Temporally, all age groups showed stimulus-evoked increases in Hbt and HbO_2, with concomitant decreases in Hbr in the whisker barrel region (Figure 6.3 & Figure 6.4). As expected, these haemodynamic responses were attenuated in the young and old mice compared to the adult mice (Figure 6.5). Interestingly, young subjects also showed a negative surround region, in which decreases in Hbt and HbO_2, and increases in Hbr, were observed (Figure 6.3 & Figure 6.4). This negative surround region was thought to reflect the transitional period from the negative BOLD response seen in infants to the positive BOLD response seen in mature adults (Harris et al., 2011).

Neuronal activity (LFPs) was also assessed for young, adult and old subjects (Figure 6.7 & Figure 6.8). Unexpectedly, young subjects showed larger stimulus-evoked depolarisations for both short and long duration stimulation than adult subjects, although these were non-significant (Figure 6.9 & Figure 6.10). There are changes to the GABAergic system in the developing brain, as GABA is mainly depolarising during development, this could increase the size of LFP responses (Ben-Ari, 2002). Old subjects showed smaller magnitude stimulus-evoked LFP neural activity compared to adult subjects during short duration (2s) whisker stimulation; although this attenuation was not observed during long duration (16s) whisker stimulation, where responses were comparable to adult subjects (Figure 6.9 & Figure 6.10). The short duration response to whisker stimulation is thought to depend on activation of ionotropic receptors expressed frequently on neurons; whereas the long duration response to whisker stimulation is thought to rely more on metabotropic receptors (Cauli & Hamel, 2010).

Finally, haemodynamic responses during an induced carbogen challenge (i.e. inhalation of 10% carbon dioxide (CO_2) in oxygen) were assessed (Figure 6.12). The induced carbogen challenge caused increases in Hbt and HbO_2, with decreases in Hbr, across all age groups. In the young and old subjects these increases in Hbt were attenuated compared to those in adult subjects (Figure 6.13). Previous research has shown that inhaling CO_2 is thought to induce nitric oxide dependent vasodilation (Toth et al., 2014b; 2015a), and so the attenuation of this response may reflect less efficient vasodilation in response to vasoactive messengers.

7.3 Results Interpretation and Implications

The primary driver of this thesis was to establish an experimental preparation for investigating neurovascular coupling in the mouse model in both an awake and anaesthetised state. For the following section the findings of this thesis will be reviewed in the context of the wider experimental field.

7.3.1 The Effects of Behavioural State when using an Awake Model

The head-fixed experimental preparation developed here (chapters 3 & 4), allowed the subjects to engage with locomotion or to remain stationary during imaging. Here, haemodynamic responses were shown to increase during periods of locomotion compared to during periods of rest. Such active (i.e. locomotion) versus passive (i.e. stationary) periods of behaviour may reflect different behavioural states, which may be underpinned by alterations in baseline cortical activity. Although neuronal population activity was not measured here directly (chapter 4), it is possible to reflect on the different cortical states, given the haemodynamic results observed, and in the context of previous literature.

7.3.1.1 State-Dependent Organisation of Cortical Activity

Previous research has shown that neurons in sensory areas not only depend on sensory input, but also rely on behavioural state (Erisken et al., 2014; Harris & Thiele, 2011; Ringach, 2009). These different states depend on the coordinated activity of several brainstem neuromodulatory nuclei which project diffusely throughout the brain (Steriade, 2004). Neuromodulators alter network activity by adjusting intrinsic membrane properties and synaptic weights of neurons (Wester & McBain, 2014). Recent awake experimental preparations have further complicated the picture, as cortical state may vary during wakefulness (Fu et al., 2014; Pfeffer et al., 2013; Pi et al., 2013).

In rodents, behavioural state is often dichotomised as passive (e.g. stationary) or active (e.g. locomotion), for instance by capitalising on experimental paradigms which measure locomotion (Ayaz et al., 2013; Keller et al., 2012; Neill & Stryker, 2010). In anaesthetised animals, the passive state has typically been associated with slow synchronous fluctuations, whereas the more active state has mostly been associated with desynchronised activity

(Harris & Thiele, 2011). Cortical states are not bimodal; the synchronised and desynchronised states likely represent two extremes of a continuum of states corresponding to fluctuations in neuronal population activity (Harris & Thiele, 2011). These fluctuations in neural activity can also correlate, at least partially, with ongoing behaviours such as whisking and locomotion (Crochet & Petersen, 2006; Ferezou et al., 2007; Poulet & Petersen, 2008; Neill & Stryker, 2010). Indeed, previous studies have shown that cortical activity becomes desynchronised in head-fixed mice during whisking or ball-running (Crochet & Petersen, 2006; Poulet & Petersen, 2008; Neill & Stryker, 2010). In awake animals, the desynchronised state is thought to occur when the animal is alert or vigilant (i.e. during locomotion or whisking), and the synchronised state when the animal is quiescent or drowsy (Harris & Thiele, 2011; Lee & Dan, 2012). However, as no neural data were collected for the awake experiments conducted here, this cannot be concluded for certain. Although, through the process of neurovascular coupling, it is likely that these state-dependent variations in neural activity will also be reflected in the haemodynamic responses.

7.3.1.2 Potential Mechanisms Controlling Cortical State

Changes of brain state have been linked to changes in the brain's excitatory/inhibitory balance (Bazhenov et al., 2002; Hill & Tononi, 2005), with powerful inhibition being a salient feature of awake cortical responses (Haider et al., 2013). Inhibitory neurons are thought to play an essential role in the behavioural state-dependent modulation of sensory processing (Buia & Tiesinga, 2008). As such, the correlations in state-dependent neural firing seen across neuronal populations may not require direct synaptic connections, but rather may arise from shared excitatory or inhibitory inputs (Gerstein & Perkel, 1969). Indeed, neighbouring pyramidal cells display such correlated activity due to their large numbers of shared inputs. One potential inhibitory circuit which projects onto pyramidal neurons in the cortex comprises of the vasoactive intestinal peptide-expressing (VIP) interneurons and the somatostatin (SST) interneurons. VIP interneurons are thought to mediate disinhibitory control in the cortex (Pi et al., 2013), and thus this circuit is typically referred to as the disinhibition model (see Figure 7.1).

Previous work has demonstrated that increases in locomotion are closely correlated with increases in the neural activity of VIP interneurons in V1 (Fu et al., 2014; Pfeffer et al., 2013). In this active, awake desynchronised state the VIP interneurons have been shown to

preferentially inhibit SST interneurons, which themselves provide inhibitory input onto pyramidal cells, resulting in increased pyramidal cell (PC) activity during locomotion (i.e. VIP → SST → PC circuit; Fu et al., 2014; Pfeffer et al., 2013; Pi et al., 2013; Figure 7.1 A). This increased activity in the pyramidal cells during locomotion will likely require more oxygen (O_2) and glucose, supplied by a corresponding increase in haemodynamic activity, through the process of neurovascular coupling. Conversely, during rest (in the awake synchronised state), the VIP interneurons are not active (Haider et al., 2013); meaning SST interneurons will provide inhibitory input onto pyramidal cells (Figure 7.1 B).

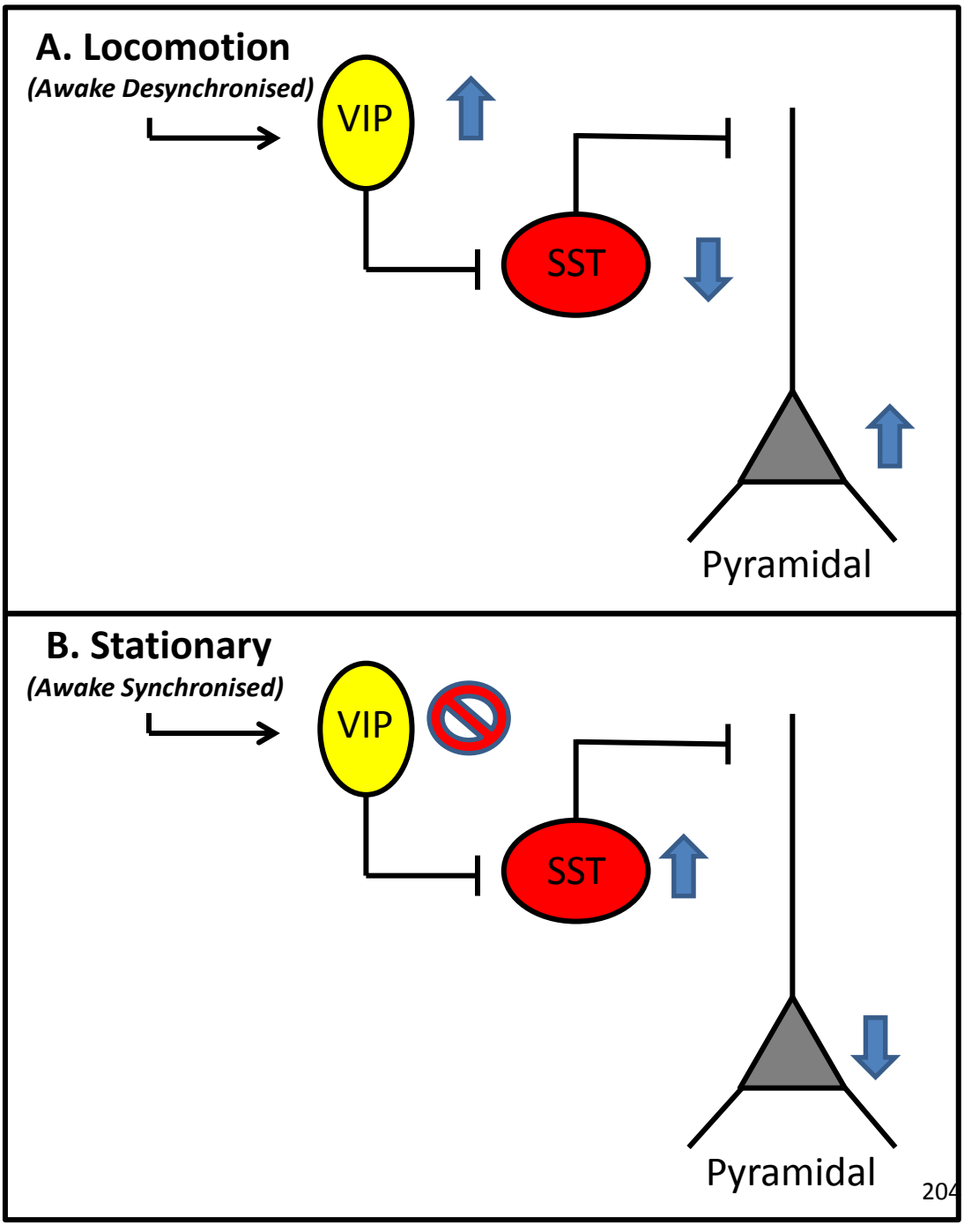

Figure 7.1 – The Disinhibition Model (adapted from Pfeffer et al., 2013; & Figure 4.17)

7.3.1.3 Interpreting the Experimental Results in the Context of Cortical State and the Disinhibition Model

For the experiments conducted in chapter 4, haemodynamic responses and locomotion were measured with the addition of a sensory stimulus (i.e. whisker stimulation). Here, the haemodynamic responses to whisker stimulation were sorted by whether the subject was walking or resting during the sensory stimulation. During locomotion, regional stimulus-evoked haemodynamic responses were increased, and there were also corresponding global increases in surrounding haemodynamic activity (Figures 4.8, 4.9 & 4.10). In line with the theories of inhibitory control, these global increases in haemodynamic activity during locomotion may reflect increased VIP interneuron activity and pyramidal cell activity. During the sensory stimulations with the least walking (i.e. stationary), more localised increases in the haemodynamic responses were observed. These results can be interpreted using the disinhibition model. If the subject is stationary (i.e. not engaging with locomotion) during whisker stimulation, then VIP interneurons will not be active, meaning the SST interneurons will be actively inhibiting the surrounding pyramidal cell activity (which has not directly been evoked by the sensory stimulation). This inhibition of surrounding pyramidal cell activity, results in more localised neuronal firing (i.e. centred on the whisker barrel region in response to whisker stimulation), which accordingly should require only localised energy and glucose supplies (i.e. HbO_2 and Hbt increases).

The role of the effects of locomotion on surround suppression, must be conceptualised in terms of survival (Krishnamurthy et al., 2015). The more global activations seen during locomotion (Fu et al., 2014; Pfeffer et al., 2013; Pi et al., 2013) may mean that a greater number of salient inputs can be detected and assessed at once. In the real world, locomotion is behaviour which typically represents running towards a prey or away from a predator. As the VIP-mediated disinhibition of pyramidal cell activity is proportional to the speed of locomotion (Fu et al., 2014), it is possible this process could promote the detection of salient stimuli within the environment (Krishnamurthy et al., 2015).

During the more quiescent, passive state however, it has been suggested that saliency maps are constructed to tailor attention for further processing (Krishnamurthy et al., 2015). Specifically, the focused neural activity within the stimulus field, with the suppression of surrounding neural activity, may serve to increase the saliency of the stimulus-evoked response (Bisley & Goldberg, 2010; Itti & Koch, 2001). The different behavioural needs of active versus quiescent animals can be used to explain why it might be beneficial to the stationary animal to enhance responses to sudden punctuate stimuli. In the passive, stationary animal the fine details of ongoing continuous sensory stimuli are of less relevance, meaning it is acceptable to filter them out and allow the cortex to exhibit endogenously generated patterns (Harris & Thiele, 2011). On the other hand, a more punctuate stimulus, such as an unexpected sound or touch (e.g. whisker stimulation), may signal the need for an immediate behavioural response (Harris & Thiele, 2011).

7.3.1.4 Suggestions of a 'Negative Surround Region' during Sensory Stimulation

A further experimental finding, which was not reported in the results section of chapter 4, showed the possibility of a 'negative surround region', during sensory stimulation when the animal was stationary (i.e. increased Hbr, decreased Hbt; Figure 7.2). This finding was not reported in the results section of the main experimental chapter (chapter 4), as the potential confounding effects of 'trial sorting' could not be confidently eliminated. Whilst the data may be suggestive of a negative surround region (possibly resulting from increased inhibitory SST activity), a different experimental paradigm or analysis method would be required to make any firm conclusions. For instance, a larger thinned cranial window would be beneficial, as it would be possible to record data from a larger region, to find how far the 'negative surround' extended.

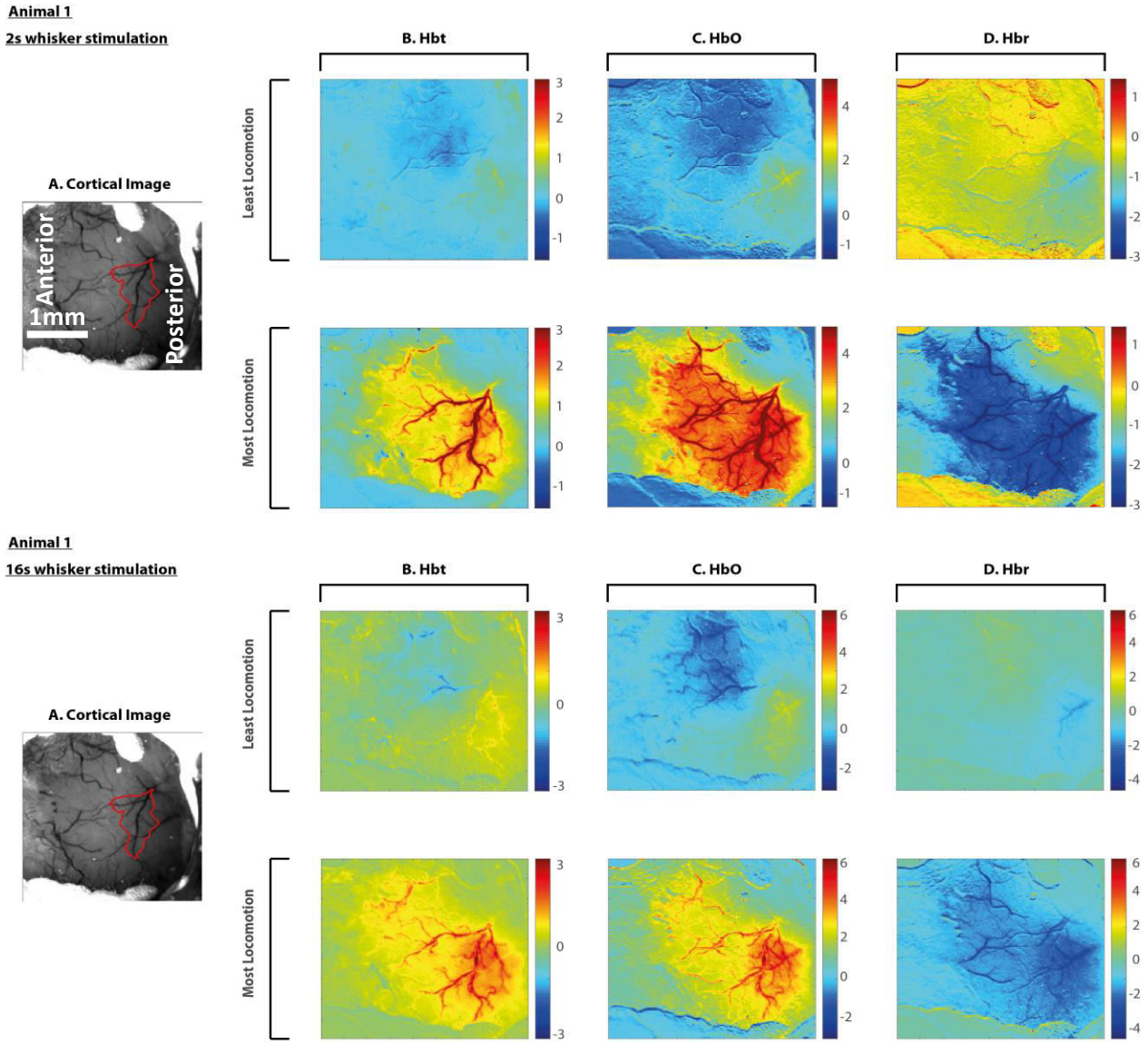

Figure 7.2 – Spatial Maps showing Stimulus-Evoked Haemodynamic Responses sorted by Least & Most Locomotion

If in fact the negative surround region observed (i.e. increased Hbr, decreased Hbt) was reflective of inhibitory SST activity, it would be because the haemodynamic responses were mirroring the underlying neural activity. Indeed, previous work has shown that the presence of SST interneurons can induce inhibition during sensory stimulation, resulting in a decrease in the overall activity levels of the network, with a corresponding increase in the size of the stimulus field (Adesnik et al., 2012; Krishnamurthy et al., 2015).

Through the techniques applied in this thesis so far (i.e. 2D-OIS and the insertion of a multichannel electrode), it was not possible to record directly from VIP or SST interneurons. As such, the mechanisms underlying the haemodynamic responses observed during cortical or behavioural state changes could not specifically be elucidated. Modern techniques like optogenetics may help to resolve the involvement of the different neurovascular components in cortical state and information processing. Optogenetics allows researchers to specifically target cells of interest (e.g. interneurons) which express channelrhodopsin-2 (ChR2), by activating them with light (Boyden et al., 2005; Deisseroth et al., 2006).

Optogenetics data has recently been collected by Dr Paul Sharp at the University of Sheffield. In these experiments, haemodynamic responses were recorded using 2D-OIS in anaesthetised mice to a 2s whisker stimulation. The mice used in these experiments had selective expression of ChR2 in somatosensory SST interneurons. The optogenetic activation of SST cells was thought to mimic the effect of the quiescent behavioural state in awake mice. Here, haemodynamic responses were measured in response to whisker stimulation alone (i.e. without the optogenetic manipulation of SST cells), and to whisker stimulation with the concurrent activation of inhibitory SST cells (Figure 7.3). During whisker stimulation alone, increased haemodynamic responses to whisker stimulation were found in the active whisker barrel region, with minimal haemodynamic changes in the surrounding regions. However, during whisker stimulation with concurrent activation of SST interneurons, increases in haemodynamic activity were observed in the active whisker region, with corresponding decreases of the haemodynamic response in surrounding regions. This result demonstrates that the activation of SST interneurons during stimulation is a plausible mechanism by which to explain the localised increases in haemodynamic activity seen in the quiescent state, with corresponding decreased haemodynamic responses in the surround region.

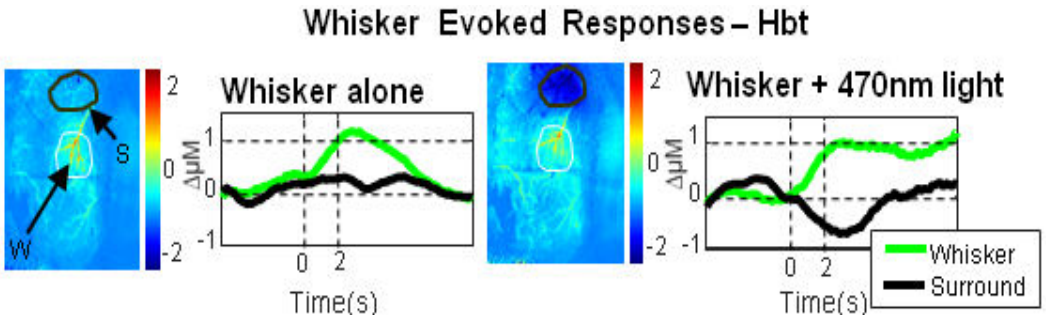

Figure 7.3 – Stimulation-Evoked Haemodynamic Responses With and Without the Optogenetic Manipulation of SST Interneurons

7.3.1.5 Conclusions

From this discussion it is clear that the use of an awake mouse model may be confounded by behavioural state. The experiments conducted in this thesis only measured haemodynamic changes, meaning the complex mechanisms underlying these haemodynamic changes could only be speculated upon. The limitations, and hence possible future directions, which arise from implementing this narrowed view of neurovascular coupling, will be further discussed in sections 7.4 & 7.5.

As such, whilst the awake preparation described here was suitable for measuring the overall average haemodynamic responses to whisker stimulation; locomotion particularly confounded the haemodynamic responses on a trial by trial basis. To eliminate the effects of behavioural state (i.e. active or quiescent) on neurovascular coupling responses, and to allow for the invasive insertion of a multichannel electrode to collect concurrent neural measurements, a novel 'modular' anaesthesia regime was tested (chapter 5).

7.3.2 The Importance of Selecting a Suitable Anaesthesia Regime for Mice

A novel 'balanced' anaesthetic regime was developed, which resulted in comparable stimulus-evoked haemodynamic responses (averaged across multiple trials) between awake and anaesthetised animals (chapter 5). The selection of an optimal anaesthetic regime, under which neurovascular coupling is mainly preserved, has wide implications for BOLD fMRI and studies of neurodegenerative diseases. The interpretation of fMRI data

depends on a detailed understanding of neurovascular coupling, as haemodynamic changes form the basis of the BOLD fMRI signal, and are used as a correlate for neural activity. Moreover, there is accumulating evidence that neurovascular coupling may be impaired in ageing and in certain neurodegenerative diseases, e.g. Alzheimer's disease (Iadecola, 2004; Zlokovic, 2011). As such, a detailed understanding of how neurovascular coupling is affected by age or disease, may inform diagnoses and treatments. Thus, elucidating the physiological mechanisms underlying neurovascular coupling is currently an active area of research; and the use of a 'balanced' anaesthesia regime, as described in this thesis, may aid with these research avenues.

7.3.3 Alterations to Neurovascular Coupling during Development and Old Age

The anaesthesia regime (as tested in chapter 5 and in Sharp, Shaw et al., 2015) was applied to study neurovascular coupling in young, adult, and old mice (chapter 6). Haemodynamic changes were measured using 2D-OIS, and cortical neural activity measured through the insertion of a multichannel electrode. Overall, age-dependent differences in haemodynamic responses were found; although further investigation will be needed to determine whether there are any neuronal changes associated with age. It is likely that through development and old age there are structural and functional changes to the components of the neurovascular unit (i.e. neurons, inhibitory/excitatory control, astrocytes, blood vessels, vasoactive messengers); and so investigating these age-related changes to neurovascular coupling will be critical for the treatment and prevention of age-related functional impairments.

Indeed, many clinical imaging studies have been conducted with infants and young children; however considerable variability has been reported in the findings, likely due to differences in neurovascular coupling within the developing population (Arichi et al., 2010; Seghier et al., 2006).Understanding physiological changes to the developing brain may help towards resolving these reported discrepancies. Through the application of highly detailed invasive neuro-imaging methods in rodent models, advancements have been made towards elucidating the underlying mechanisms responsible for the developmental changes to neurovascular coupling. For example, negative stimulus-evoked haemodynamic responses have been shown in newborn rats (Kozberg et al., 2013; Zehender et al., 2013), which switches to a positive haemodynamic response in later development (Zehender et al., 2013). This developmental transition of the haemodynamic response profile could help

towards explaining the discrepancies seen in clinical BOLD fMRI results, whose interpretation relies heavily on the vascular changes. Furthering our knowledge of neurovascular coupling during development is critical for an improved understanding of neonatal brain development, with implications for the development, treatment and management of neonatal neurological conditions.

Discrepancies have also been shown in the clinical imaging studies conducted in an older population. For instance, in older human subjects BOLD responses to different sensory tasks were found to be increased, decreased, or similar to the responses seen in healthy adult subjects (Aizenstein et al., 2004). It is possible that ageing causes regionally-dependent changes in neurovascular coupling, which may account for these discrepancies. Further, an age-related decline in resting CBF or cerebral metabolism may confound the interpretation of BOLD fMRI results. Again, it will be important to apply high resolution neuro-imaging techniques to investigate the underpinnings of neurovascular coupling in old age in fine detail. As such, recent investigations using rodents have shown stimulus-evoked and hypercapnia-induced haemodynamic responses to be attenuated in S1 of old mice compared to healthy, adult mice (Park et al., 2007; Toth et al., 2014a; 2014b; Tucsek et al., 2014); as well as, attenuated neural firing in old mice (Jessen et al., 2015).

7.3.3.1 Behavioural Correlates of Age-Dependent Alterations in Neurovascular Coupling

For the study conducted in chapter 6, attenuated haemodynamic responses were found in both young and old mice compared to adult mice. However, compared to the neuronal responses seen in adult subjects, in young animals there was increased stimulus-evoked firing, and in old subjects there was decreased stimulus-evoked firing. It would be interesting to see whether the effect of these alterations of neurovascular coupling in development and old age were associated with any impact upon cognitive functioning. As such, behavioural experiments were conducted by Dr Kamar Ameen-Ali at the University of Sheffield, in which young and old mice were tested on a behavioural apparatus to measure short term and long term memory performance (*unpublished results*; Figure 7.4; experimental apparatus described in: Ameen-Ali et al., 2012). The young mice used in these behavioural experiments were the littermates of the young mice used in chapter 6 (aged 6-8 weeks); and the old mice used in these behavioural experiments were the same as those used in chapter 6 (behaviourally tested at age 18 months). Briefly, the old mice showed a decline in both short-term and long-term memory, as their performance on a spontaneous

object recognition task was impaired compared to young mice. The enhanced memory performance seen in the young mice may be reflective of the developmental changes to the GABAergic system (Ben-Ari, 2002), or the synaptic density increases observed in development (Otsby et al., 2009; Paus et al., 2005; Shaw et al., 2008; Tamnes et al., 2010). These changes help towards altering the excitatory to inhibitory balance of the brain, sharpening neuronal responses (Crook et al., 1998; Gabernet et al., 2005; Sillito, 1975). The reduced memory performance seen in the old animals on the other hand, is potentially reflective of the reductions in grey matter volume (Sowell et al., 2003), neuron count (Creasey & Rapoport, 1985), dendrites (Jacobs & Scheibel, 1993), or synapses (Huttenlocher, 1979; Masliah et al., 1993) seen in ageing. These findings demonstrated that the changes in neurovascular coupling observed in the young and old mice, may be correlated with cognitive memory performance.

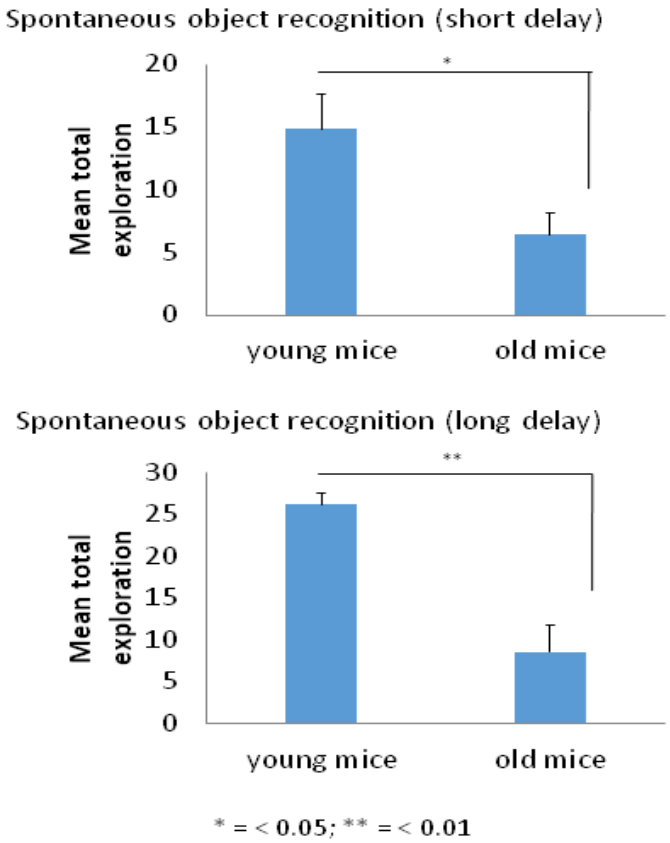

Figure 7.4 – The Performance of Young and Old Mice on a Spontaneous Object Recognition Task to Assess Short-Term and Long-Term Memory

7.3.3.2 Age-Associated Alterations to the Mechanisms of Neurovascular Coupling

As well as assessing the behavioural correlates of alterations to neurovascular coupling, it will also be important to elucidate the specific mechanisms which may be involved in the neurovascular decline observed in old age. Investigation of the potential mechanisms underlying neurovascular decline, and subsequently reduced cognitive performance, may help towards treatment to reduce or stop the age-associated deterioration. Indeed, recent work in rodents has attributed the reductions in the evoked haemodynamic responses to age-dependent alterations in the nitric oxide (NO) signalling pathway (Toth et al., 2014b; 2015a; 2015b).Specifically, old age was associated with a decline in circulating insulin-like growth factor 1 (IGF-1), which impaired cerebral vascular endothelial function, via the elevation of NADPH oxidase-derived reactive oxygen species (ROS), leading to a breakdown of NO (Toth et al., 2014b; 2015a). As NO is an important vasoactive messenger in the communication between neurons, astrocytes and blood vessels, any age-dependent alterations to its production and activities may affect neurovascular coupling. Advancements in the knowledge of the cerebral physiological changes associated with ageing may lead to potential treatments to restore neurovascular coupling in the elderly. Indeed, since the discovery of reduced NO signalling in ageing, Resveratrol (3,4',5-trihydroxystilbene), which increases the levels of endothelium-derived NO, has successfully been used to combat reduced CBF in ageing mice (Toth et al., 2014a). This is an example how advancing the understanding of neurovascular coupling during ageing, may eventually lead to improvements in the treatment of age-related physiological decline. Further studies of the mechanisms of neurovascular coupling in old subjects can be used to investigate additional treatment avenues. With an ever-ageing population, the discovery of such physiological changes and appropriate treatments may have wider implications for the management of cognitive decline and other age-related conditions.

7.4 Limitations

Whilst the experiments conducted for this thesis have important implications for the investigation of neurovascular coupling in the mouse model; because of the novelty of the preparations described, there are still a number of limitations which will need to be addressed, an overview of these will be given in the following section.

7.4.1 A Limited View of Neurovascular Coupling in the Awake, Head-Fixed Mouse Experimental Preparation

The awake imaging experimental preparation described in chapters 3 & 4 was restricted by the limitations of the experimental set-up. For instance, the subjects were head-fixed atop of a spherical treadmill, which does not entirely reflect a real-world context, and may induce additional stress. There were also limited measurements of the intrinsic physiological and extrinsic behavioural parameters of interest. Indeed, whilst haemodynamic responses and locomotion were monitored here, it would have also been beneficial to consider simultaneously recording neuronal activity and whisking behaviour. Previous studies of awake rodents have demonstrated the importance of measuring these additional variables (e.g. Arkley et al., 2014; Ayaz et al., 2013; Huo et al., 2014; Niell & Stryker, 2010; Sofroniew et al., 2014). In order to gain a complete understanding of neurovascular coupling, it is somewhat limited to only measure the haemodynamic responses, as it is in fact the neural activity which drives these responses (Iadecola, 2004). Furthermore, the awake animal's behavioural state (i.e. quiet, whisking, or locomotion) will affect this underlying neurovascular activity (Harris & Thiele, 2011). Methods for encompassing the measurement of these additional variables into the awake mouse preparation will be discussed in section 7.5.1, where the possible future research avenues will be elaborated upon.

7.4.2 A Limited View of Neurovascular Coupling in the Anaesthetised Mouse Experiments of Ageing and Development

The anaesthetised mouse preparation which was used to investigate the effects of development and ageing on neurovascular coupling in chapter 6 could be improved by encompassing the additional measurement of intrinsic physiological mechanisms of interest. For instance, the previous literature indicates that there are age-dependent changes to the components of the neurovascular unit (i.e. neurons, astrocytes, blood vessels; for reviews see D'Esposito et al., 2003; Harris et al., 2011). Further, these neurovascular changes are transitionary throughout the lifespan. Whilst the haemodynamic and neural activity were monitored in these experiments, it could be interesting to chronically measure neuronal, haemodynamic and astrocytic activity. Longitudinal measurements of the components of the neurovascular unit would require the application of slightly less invasive techniques (e.g. two-photon imaging), which will be discussed in more detail in section 7.5.2, where the possible future research avenues will be expanded upon.

7.5 Future Directions

Future research will seek to further elucidate the underlying cerebral mechanisms which link the neural activity and haemodynamic responses seen in the healthy awake, and anaesthetised mouse preparations described here. It will also be of interest to further study exactly how these mechanisms are altered during development and ageing.

7.5.1 Developing an Experimental Preparation for Investigating Neurovascular Coupling in the Awake, Behaving Mouse

Rodents are the most frequently studied model organisms of mammalian neuronal function and behaviour (Schwarz et al., 2010). In order to capitalise on the full potential of the awake imaging experimental platform, it would be optimal to track a multitude of relevant physiological and behavioural variables. The head-fixed rodent preparation allows for the research of different levels of observation, such as the cellular/molecular and the behavioural level. By tracking a wide range of parameters, the experimental set-up may best mimic a real-world setting. Whilst the current study (chapters 3 & 4) tracked locomotion behaviour, it would also be optimal to encompass measurements of whisking behaviour (e.g. Arkley et al., 2014; Sofroniew et al., 2014). Furthermore, future work would benefit from recording neuronal, as well as haemodynamic, responses.

Studying the Mechanisms of Neurovascular Coupling

Recent technological advances in neuroimaging have led to the development of minimally-invasive methods for concurrently measuring neural and haemodynamic activity *in vivo* (Svoboda & Yasuda, 2006). One such method is two-photon microscopy, which allows for the measurement of blood flow changes from the surface vasculature, as well as the concurrent calcium related changes from surface neurons (e.g. pyramidal cells, VIP interneurons, or SST interneurons) and astrocytes (e.g. O'Herron et al., 2016; Santisakultarm et al., 2016). Targeting these different cell types would allow for the mechanisms involved in the disinhibitory circuit during awake active (e.g. locomotion, whisking) and awake passive (e.g. quiescent, stationary) behavioural states (with and without sensory stimulation) to be elucidated. Indeed, the 'head-fixed behaving rodent' is said to be well-suited for the analysis of cellular, subcellular and molecular processes, and their relationship to sensorimotor and/ or cognitive processes. As such, measuring neurovascular coupling responses, as separated by behavioural state, would allow for

researchers to gain a more comprehensive picture of how the brain functions under more cognitively-realistic scenarios.

Perceptual & Cognitive Tasks

With the development of an awake preparation, it is also possible to introduce more extensive behavioural training to gain an even richer understanding of how the brain functions during adaptation and learning. The combination of head-fixation and behavioural training, allows for superior precision in both stimulus application and behavioural assessment (Schwarz et al., 2010). Rodents have an excellent learning capacity, and a rich behavioural repertoire. As such, a multitude of behavioural approaches can be used to study the function of neurovascular coupling at different hierarchical levels (e.g. sensorimotor, perceptual, or cognitive). To specifically extend the experiments conducted for this thesis, it could be of interest to train the mice to stop or start engaging with locomotion in response to sensory whisker stimulation. This would allow for the effects of behavioural state on incoming sensory cues to be better elucidated, as a key function of the brain is to interpret incoming sensory information in the context of learned associations in order to guide adaptive behaviour (Sippy et al., 2015).

Outlook

The potential of this experimental set-up in the Sheffield laboratory has wide reaching implications, which as of yet have not been fully exploited. Pioneering studies have thus far used awake, head-fixed mice to successfully study whisker and licking movements (Bryant et al., 2009; Crochet & Petersen, 2006; Poulet & Petersen, 2008), locomotion within a virtual environment (Dombeck et al., 2007; 2012; Harvey et al., 2009), and the effects of behavioural state on inhibitory control (Adesnik et al., 2012; Fu et al., 2014; Pfeffer et al., 2013; Pi et al., 2013). Future work would seek to build upon the findings of this thesis (i.e. locomotion alters haemodynamic activity in somatosensory cortex), and the pre-existing pioneering work studying head-fixed rodents (Adesnik et al., 2012; Ayaz et al., 2013; Crochet & Petersen, 2006; Dombeck et al., 2007; 2010; Fu et al., 2014; Huo et al., 2014; Niell & Stryker, 2010; Pfeffer et al., 2013; Pi et al., 2013; Poulet & Petersen, 2008; Saleem et al., 2013), to gain more information on the interface between behaviour and its neuronal and haemodynamic correlates.

7.5.2 Developing an Experimental Preparation for Investigating Neurovascular Coupling in Development and Ageing

It is well-established that there are changes to neurovascular coupling across the lifespan (D'Esposito et al., 2003; Harris et al., 2011). These structural and functional alterations to the neurons and the vasculature have previously caused issues in the interpretation of the BOLD fMRI data collected in developmental and ageing clinical populations (Aizenstein et al., 2004; Arichi et al., 2010). As such, for this thesis an *in vivo* rodent preparation, which applied invasive, high resolution techniques, was employed to gain a detailed understanding of neurovascular coupling in young and old mice. Whilst simultaneous recordings of the haemodynamic and neuronal activity were made, the experiments performed were acute, due to the particularly invasive procedure used to collect electrophysiological data (i.e. the insertion of a multichannel electrode).

Future work could benefit from the chronic measurement of neurovascular coupling, to assess the onset timings of the age-associated changes to cerebral physiology. For instance, in development it has been suggested that there is a switch from negative to positive stimulus-evoked haemodynamic responses (Kozberg et al., 2013; Zehender et al., 2013). Monitoring neurovascular coupling longitudinally in a developmental population (e.g. from birth to adolescence) would allow researchers to track this transition of functional hyperaemia over time, and to assess whether this transition was also reflected in the neural firing. Furthermore, attenuations in neuronal and vascular reactivity have been reported in old age (Balbi et al., 2015; Jessen et al., 2015; Park et al., 2007; Toth et al., 2014a; 2014b; Tucsek et al., 2014), and so longitudinal studies could also seek to monitor the progression of neurovascular decline.

Studying the Mechanisms of Neurovascular Coupling

Two-photon microscopy is minimally invasive, meaning it would be possible to chronically monitor the transition in neurovascular activity during development or ageing using this technique. Further, two photon imaging allows for the concurrent measurement of blood flow responses, neuronal calcium firing, and astrocytic calcium firing; as such, each of these components of the neurovascular unit could be assessed. Another interesting avenue to pursue would be to evaluate the involvement of different vasoactive messengers. For instance, specific synthase inhibitors (e.g. the NO synthase inhibitor $_{L}$-NAME) could be used to try and elucidate the mechanisms associated with cognitive decline or enhancement,

thus providing potential treatment avenues. It will be important to pursue potential treatments which may help to stop or slow down the debilitating cognitive decline often seen in older patients.

7.6 Final Conclusions

This thesis has demonstrated the value of employing an *in vivo* mouse model to gain a detailed understanding of neurovascular coupling. Understanding the physiological processes underlying brain function is critical for the interpretation of brain imaging techniques, and for understanding and treating certain neurodegenerative diseases or age-related cognitive decline.

The findings of this thesis, and the future research which can be conducted using the methodology it describes, will thus provide important insights which will aid in the investigation of the links between neural activity and haemodynamic responses *in vivo*. The work conducted in Sheffield which investigates neurovascular coupling in the mouse model is still ongoing (Sharp, Shaw, et al., 2015), and indeed other laboratories are also pursuing similar research avenues (e.g. Adesnik et al., 2012; Ayaz et al., 2013; Crochet & Petersen, 2006; Dombeck et al., 2007; 2010; Fu et al., 2014; Huo et al., 2014; Niell & Stryker, 2010; Pfeffer et al., 2013; Pi et al., 2013; Poulet & Petersen, 2008; Saleem et al., 2013).

It is the hope that mouse models of neurovascular coupling will provide a good stepping stone to study how behaviour, disease, and ageing can affect the brains physiology and function. Ultimately, the long-term goals described here (and elsewhere) are to gain a deeper understanding of neurovascular coupling, to best comprehend how the brain intrinsically processes information in everyday life.

References

Adamczak, J. M., Farr, T. D., Seehafer, J.U., Kalthoff, D. & Hoehn, M. (2010). High field BOLD response to forepaw stimulation in the mouse. *NeuroImage, 51*, 704–712.

Adesnik, H., Bruns, W., Taniguchi, H., Huang, Z. J., & Scanziani, M. (2012). A neural circuit for spatial summation in visual cortex. *Nature, 490(7419),* 226-231.

Ahrens,E.T. & Dubowitz,D.J. (2001). Peripheral somatosensory fMRI in mouse at 11.7 T. *NMR Biomed. 14,* 318–324.

Aizenstein, H. J., Clark, K. A., Butters, M. A., Cochran, J., Stenger, V. A., Meltzer, C. C., Reynolds, C. F., & Carter, C. S. (2004). The BOLD hemodynamic response in healthy aging. *Journal of Cognitive Neuroscience, 16*, 786–793.

Akerman, C. J., & Cline, H. T. (2007). Refining the roles of GABAergic signaling during neural circuit formation. *Trends in Neuroscience, 30,* 382-389.

Ameen-Ali, K. E., Eacott, M. J., & Easton, A. (2012). A new behavioural apparatus to reduce animal numbers in multiple types of spontaneous object recognition paradigms in rats. *Journal of Neuroscience Methods, 211(1),* 66-76.

Ances, B. M., Liang, C. L., Leontiev, O., Perthen, J. E., Fleisher, A. S., Lansing, A. E., & Buxton, R. B. (2009). Effects of ageing on cerebral blood flow, oxygen metabolism, and blood oxygenation level dependent responses to visual stimulation. *Human brain mapping, 30(4)*, 1120-1132.

Andermann, M. L., Gilfoy, N. B., Goldey, G. J., Sachdev, R. N., Wolfel, M., McCormick, D. A., Reid, R. C., & Levene, M. J. (2013). Chronic cellular imaging of entire cortical columns in awake mice using microprisms. *Neuron, 80 (4),* 900-913.

Anderson, A. W., Marois, R., Colson, E. R., Peterson, B. S., Duncan, C. C., Ehrenkranz, R. A., Schneider, K. C., Gore, J. C., & Ment, L. R. (2001). Neonatal auditory activation detected by functional magnetic resonance imaging. *Magnetic Resonance Imaging, 19,* 1-5.

Arichi, T., Fagiolo, G., Varela, M., Melendez-Calderon, A., Allievi, A., Merchant, N., Tusor, N., Counsell, S. J., Burdet, E., Beckmann, C. F., & Edwards, A. D. (2012). Development of BOLD signal hemodynamic responses in the human brain. *NeuroImage, 63(2),* 663-673.

Arichi, T., Moraux, A., Melendez, A., Doria, V., Groppo, M., Merchant, N., Combs, S., Burdet, E., Larkman, D. J., Counsell, S. J., Beckmann, C. F., & Edwards, A. D. (2010). Somatosensory cortical activation identified by functional MRI in preterm and term infants. *NeuroImage, 49,* 2063-2071.

Arkley, K. P., Grant, R. A., Mitchinson, B., & Prescott, T. J. (2014). Strategy change in vibrissal active sensing during rat locomotion. *Current Biology, 24,* 1507-1512.

Attwell, D., Buchan, A. M., Charpak, S., Lauritzen, M., Macvicar, B. A., & Newman, E. A. (2010). Glial and neuronal control of brain blood flow. *Nature, 468,* 232-243.

Attwell, D., & Iadecola, C. (2002). The neural basis of functional brain imaging signals. *Trends in neurosciences, 25(12),* 621-625.

Attwell, D., & Laughlin, S. B. (2001). An energy budget for signalling in the grey matter of the brain. *Journal of Cerebral Blood Flow & Metabolism, 21*, 1133-1145.

Ayata, C., Ma, J., Meng, W., Huang, P., & Moskowitz, M. A. (1996). L-NA-sensitive rCBF augmentation during vibrissal stimulation in Type III nitric oxide synthase mutant mice. *Journal of Cerebral Blood Flow & Metabolism, 16(4)*, 539-541.

Ayaz, A., Saleem, A. B., Scholvinck, M. L., & Carandini, M. (2013). Locomotion controls spatial integration in mouse visual cortex. *Current Biology, 23*, 890-894.

Ba, A. M., Guiou, M., Pouratian, N., Muthialu, A., Rex, D. E., Cannestra, A. F., Chen, J. W. Y., & Toga, A. W. (2002). Multiwavelength optical intrinsic signal imaging of cortical spreading depression. *Journal of Neurophysiology, 88,* 2726-2735.

Balbi, M., Ghosh, M., Longden, T. A., Vega, M. J., Gesierich, B., Hellal, F., Lourbopoulos, A., Nelson, M. T., & Plesnila, N. (2015). Dysfunction of mouse cerebral arteries during early ageing. *Journal of Cerebral Blood Flow & Metabolism, 35,* 1445-1453.

Barber, P. A. (2013). Magnetic resonance imageing of ischemia viability thresholds and the neurovascular unit. *Sensors, 13*, 6981–7003.

Barnes, C., & Burke, S. (2006). Neural plasticity in the ageing brain. *Nature Reviews Neuroscience, 7(1)*, 30–40.

Barretto, R. P., Ko, T. H., Jung, J. C., Wang, T. J., Capps, G., Waters, A. C., Ziv, Y., Attardo, A., Recht, L., & Schnitzer, M. J. (2011). Time-lapsed imaging of disease progression in deep brain areas using fluorescence microendoscopy. *Nature Medicine, 17,* 223-228.

Bazhenov, M., Timofeev, I., Steriade, M., & Sejnowski, T. J. (2002). Model of thalamocortical slow-wave sleep oscillations and transitions to activated States. *Journal of Neuroscience, 22*, 8691–8704.

Behnke, B. J., Delp, M. D., Dougherty, P. J., Musch, T. I., & Poole, D. C. (2005). Effects of aging on microvascular oxygen pressures in rat skeletal muscle*. Respiratory physiology & neurobiology, 146(2)*, 259-268.

Bekar, L. K., Wei, H. S., & Nedergaard, M. (2012). The locus coeruleus-norepinephrine network optimizes coupling of cerebral blood volume with oxygen demand. *Journal of Cerebral. Blood Flow & Metabolism, 32*, 2135–2145.

Ben-Ari, Y., (2002). Excitatory actions of gaba during development: the nature of the nurture*. Nature Reviews Neuroscience, 3,* 728–739.

Berciano, M. T., Andres, M. A., Calle, E., & Lafarga, M. (1995). Age-induced hypertrophy of astrocytes in rat supraoptic nucleus: a cytological, morphometric, and immunocytochemical study. *The Anatomical Record, 243(1),* 129-144.

Bernardo, K. L., McCasland, J. S., Woolsey, T. A., & Strominger, R. N. (1990). Local intra- and interlaminar connections in mouse barrel cortex. *Journal of Comparative Neurology, 291(2),* 231-255.

Berwick, J., Johnston, D., Jones, M., Martindale, J., Redgrave, P., McLoughlin, N., Schiessel, I., & Mayhew, J. E. W. (2005). Neurovascular coupling investigated with two-dimensional optical imaging spectroscopy in rat whisker barrel cortex. *European Journal of Neuroscience, 22(7),* 1655-1666.

Berwick, J., Johnston, D., Jones, M., Martindale, J., Martin, C., Kennerley, A. J., Redgrave, P., & Mayhew, J. E. W. (2008). Fine detail of neurovascular coupling revealed by spatiotemporal analysis of the haemodynamic response to single whisker stimulation in rat barrel cortex. *Journal of Neurophysiology, 99(2)*, 787-798.

Berwick, J., Martin, C., Martindale, J., Jones, M., Johnston, D., Zheng, Y., Redgrave, P., & Mayhew, J. (2002). Hemodynamic response in the unanesthetized rat: intrinsic optical imaging and spectroscopy of the barrel cortex. *J Cereb Blood Flow Metab, 22(6)*, 670-679.

Bisley, J. W., & Goldberg, M. E. (2010). Attention, intention, and priority in the parietal lobe. *Annual Review of Neuroscience, 33*, 1.

Biswal, B. B. (2012). Resting state fMRI: A personal history. *NeuroImage, 62(2),* 938-944.

Boas, D., Jones, S., Devor, A., Huppart, T. &, Dale, A. (2008). A vascular anatomical network model of the spatio-temporal response to brain activation. *NeuroImage, 40*, 1116–1129.

Boorman, L. W. (2009). *The haemodynamic and neural generators of the negative BOLD response in rat somatosensory cortex.* (Unpublished doctoral thesis). University of Sheffield, Sheffield, UK.

Boorman, L., Harris, S., Bruyns-Haylett, M., Kennerley, A., Zheng, Y., Martin, C., Jones, M., Redgrave, P., & Berwick, J. (2015). Long-Latency Reductions in Gamma Power Predict Hemodynamic Changes That Underlie the Negative BOLD Signal. *Journal of Neuroscience, 35(11),* 4641-4656.

Boorman, L., Kennerley, A. J., Johnston, D., Jones, M., Zheng, Y., Redgrave, P., & Berwick, J. (2010). Negative blood oxygen level dependence in the rat: a model for investigating the role of suppression in neurovascular coupling. *Journal of Neuroscience, 30*, 4285-4294.

Bonin, V., Histed, M. H., Yurgenson, S., & Reid, R. C. (2011). Local diversity and fine-scale organization of receptive fields in mouse visual cortex. *Journal of Neuroscience, 31,* 18506-18521.

Born, P., Leth, H., Miranda, M. J., Rostrup, E., Stensgaard, A., Peitersen, B., Larsson, H. B., & Lou, H. C. (1998). Visual activation in infants and young children studied by functional magnetic resonance imaging. *Pediatric Research, 44,* 578-583.

Born, A. P., Miranda, M. J., Rostrup, E., Toft, P. B., Peitersen, B., Larsson, H. B., & Lou, H. C. (2000). Functional magnetic resonance imaging of the normal and abnormal visual system in early life. *Neuropediatrics, 31(1)*, 24–32.

Bouchard, M. B., Chen, B. R., Burgess, S. A., & Hillman, E. M, C. (2009). Ultra-fast multispectral optical imaging of cortical oxygenation, blood flow, and intracellular calcium dynamics. *Optics Express, 17(18),* 15670-15678.

Boyden, E. S., Zhang, F., Bamberg, E., Nagel, G., & Deisseroth, K. (2005). Millisecond-timescale, genetically targeted optical control of neural activity. *Nature Neuroscience, 8*, 1263–1268.

Bruyns-Haylett, M. F. (2013). *An investigation of spatiotemporal variations in rsfMRI BOLD signal at a single cortical location*. (Unpublished doctoral thesis). University of Sheffield, Sheffield, UK.

Bruyns-Haylett, M., Harris, S., Boorman, L., Zheng, Y., Berwick, J., & Jones, M. (2013). The resting-state neurovascular coupling relationship: rapid changes in spontaneous neural activity in the somatosensory cortex are associated with haemodynamic fluctuations that resemble stimulus-evoked haemodynamics. *European Journal of Neuroscience, 38(6),* 2902-2916.

Bryant, J. L., Roy, S., & Heck, D. H. (2009). A technique for stereotaxic recordings of neuronal activity in awake, head-restrained mice. *Journal of Neuroscience Methods, 178(1),* 75-79.

Buckner, R. L., Snyder, A. Z., Sanders, A. L., Raichle, M. E., & Morris, J. C. (2000). Functional brain imaging of young, non-demented, and demented older adults. *Journal of Cognitive Neuroscience, 12(2),* 24–34.

Buia, C. I., & Tiesinga, P. H. (2008). Role of interneuron diversity in the cortical microcircuit for attention. *Journal of Neurophysiology, 99(5),* 2158-2182.

Burgess, C. P., Steinmetz, N., Lak, A., Zatka-Haas, P., Ranson, A., Wells, M., Schroeder, S., Jacobs, E. A. K., Reddy, C. B., Soares, S., Linden, J. F., Paton, J. J., Harris, K. D., & Carandini, M. (2016). High-yield methods for accurate two-alternative visual psychophysics in head-fixed mice. *bioRxiv*. Advance online publication. doi: 10.1101/051912.

Burns, S. P., Xing, D., & Shapley, R. M. (2010). Comparisons of the dynamics of LFP and MUA signals in macaque visual cortex, *Journal of Neuroscience, 30(41),* 13739-13749.

Bussey, T., et al. (2012). New translational assays for preclinical modelling of cognition and schizophrenia: the touchscreen method for mice and rats. *Neuropharmacology, 62,* 1191-1203.

Button, K. S., Ioannidis, J. P., Mokrysz, C., Nosek, B. A., Flint, J., Robinson, E. S., & Munafo, M. R. (2013). Power failure: why small sample size undermines the reliability of neuroscience. *Nature Reviews Neuroscience, 14(5),* 365-376.

Buxton, R. B., & Frank, L. R. (1997). A model for the coupling between cerebral blood flow and oxygen metabolism during neural stimulation. *Journal of Cerebral Blood Flow & Metabolism, 17,* 64-72.

Buxton, R. B., Uludağ, K., Dubowitz, D. J., & Liu, T. T. (2004). Modeling the hemodynamic response to brain activation. *NeuroImage, 23*, (Suppl 1) pp. S220–233.

Buxton, R. B., Wong, E. C. & Frank, L. R. (1998). Dynamics of blood flow and oxygenation changes during brain activation: the balloon model. *Magn Reson. Med., 39*, 855–864.

Cang, J., Kalatsky, V. A., Lowel, S., & Stryker, M. P. (2005). Optical imaging of the intrinsic signal as a measure of cortical plasticity in the mouse. *Visual Neuroscience, 22 (5),* 685-691.

Cantlon, J. F., Brannon, E. M., Carter, E. J., & Pelphrey, K. A. (2006). Functional Imaging of Numerical Processing in Adults and 4-y-Old Children. *PLoS Biol, 4*, e125.

Carandini, M., Shimaoka, D., Rossi, L, F., Sato, T, K., Benucci, A., & Knopfel, T. (2015). Imaging the awake visual cortex with a genetically encoded voltage indicator. *The Journal of Neuroscience, 35(1)*, 53-63.

Carmignoto, G., & Gomez-Gonzalo, M. (2010). The contribution of astrocyte signalling to neurovascular coupling. *Brain Research Reviews, 63*, 138-148.

Catania, M. V., Landwehrmeyer, G. B., Testa, C. M., Standaert, D. G., Penney Jr., J. B., & Young, A. B. (1994). Metabotropic glutamate receptors are differentially regulated during development. *Neuroscience, 61*, 481–495.

Cauli, B., & Hamel, E. (2010). Revisiting the role of neurons in neurovascular coupling. *Frontiers in Neuroenergetics, 2*, 9.

Cauli, B., Tong, X., Rancillac, A., Serluca, N., Lambolez, B., Rossier, J., & Hamel, E. (2004). Cortical GABA interneurons in neurovascular coupling: relays for subcortical vasoactive pathways. *Journal of Neuroscience, 24*, 8940–8949.

Cavallotti, D., Cavallotti, C., Pescosolido, N., Iannetti, G. D., & Pacella, E. (2001). A morphometric study of age changes in the rat optic nerve. *Ophthalmologica. 215*, 366-*371*.

Cesarovic, N., Jirkof, P., Rettich, A., Nicholls, F. & Arras, M. (2012). Combining sevoflurane anesthesia with fentanyl-midazolam or s-ketamine in laboratory mice. *J. Am. Assoc. Lab Anim Sci., 51*, 209–218.

Chan, W. Y., Lorke, D. E., Tiu, S. C., & Yew, D. T. (2002). Proliferation and apoptosis in the developing human neocortex. *The Anatomical Record, 267,* 261-276.

Chapin, J. K., & Lin, C. S. (1984). Mapping the body representation in the S1 cortex of anaesthetised and awake rats. *Journal of Comparative Neurology, 229,* 199-213.

Chen, J. L., Andermann, M. L., Keck, T., Xu, N-L., & Ziv, Y. (2013). Imaging neuronal populations in behaving rodents: paradigms for studying neural circuits underlying behavior in the mammalian cortex. *The Journal of Neuroscience, 33 (45),* 17631-17640.

Chen, B. R., Bouchard, M. B., McCasline, A. F. H., Burgess, S. A., & Hillman, E. M. C. (2011). High speed vascular dynamics of the haemodynamic response. *Neuroimage, 54(2),* 1021-1030.

Chen, L. M., Friedman, R. M., Ramsden, B. M., LaMotte, R. H., & Roe, A. W. (2001). Fine-scale organisation of S1 (area 3b) in the squirrel monkey revealed with intrinsic optical imaging. *Journal of Neurophysiology, 86*, 3011-3029.

Chen, L. M., Friedman, R. M., & Roe, A. W. (2005). Optical imaging of SI topography in anesthetized and awake squirrel monkeys. *The Journal of Neuroscience, 25(33),* 7648-7659.

Chen, B. R., Kozberg, M. G., Bouchard, M. B., Shaik, M. A., & Hillman, E. M. (2014). A critical role of the vascular endothelium in functional neurovascular coupling in the brain. *Journal of the American Heart Association, 3,* e000787.

Cheng, G., Trombley, P. Q., & van den Pol, A. N. (1996). Excitatory actions of GABA in developing rat hypothalamic neurones. *Journal of Physiology, 494,* 451-464.

Chiang, L. K., Dunn, A. E., (2000). Cardiology. In G. K., Siberry, &, R., Iannone, (Ed.), *The Harriet Lane Handbook: A Manual for Pediatric House Officers* (pp. 175-178). St. Louis: Mosby.

Chow, B. Y., Han, X., Dobry, A. S., Qian, X., Chuong, A. S., Li, M., Henninger, M. A., Belfort, G. M., Lin, Y., Monahan, P. E., & Boyden, E. S. (2010). High-performance genetically targetable optical neural silencing by light-driven proton pumps. *Nature, 463*, 98–102.

Collins, D. M., McCullough, W. T., & Ellsworth, M . L. (1998). Conducted vascular responses: communication across the capillary bed. *Microvascular Research, 56,* 43-54.

Colonnese, M. T., Phillips, M. A., Constantine-Paton, M., Kaila, K., & Jasanoff, A. (2008). Development of hemodynamic responses and functional connectivity in rat somatosensory cortex. *Nature Neuroscience, 11*, 72–79.

Cope, M., & Delpy, D. (1988). System for long-term measurement of cerebral blood and tissue oxygenation on newborn infants by near infra-red transillumination. *Medical and Biological Engineering and Computing, 26,* 289-294.

Cox, S. B., Woolsey, T. A., & Rovainen, C. M. (1993). Localized Dynamic Changes in Cortical Blood Flow With Whisker Stimulation Corresponds to Matched Vascular and Neuronal Architecture of Rat Barrels. *Journal of cerebral blood flow and metabolism, 13(6),* 899-913.

Creasey, H., & Rapoport, S. I. (1985). The aging human brain. *Annals of neurology, 17(1)*, 2-10.

Crook, J.M., Kisvárday, Z.F., & Eysel, U.T. (1998). Evidence for a contribution of lateral inhibition to orientation tuning and direction selectivity in cat visual cortex: reversible inactivation of functionally characterized sites combined with neuroanatomical tracing techniques. *European Journal of Neuroscience, 10*, 2056–2075.

Crochet, S., & Petersen, C. C. (2006). Correlating whisker behavior with membrane potential in barrel cortex of awake mice. *Nature Neuroscience, 9(5),* 608-610.

D'Esposito, M., Deouell, L. Y., & Gazzaley, A. (2003). Alterations in the BOLD fMRI signal with ageing and disease: a challenge for neuroimageing. *Nature Reviews Neuroscience, 4(11)*, 863-872.

Desai, M., Kahn, I., Knoblich, U., Bernstein, J., Atallah, H., Yang, A., ... & Boyden, E. S. (2011). Mapping brain networks in awake mice using combined optical neural control and fMRI. *Journal of Neurophysiology, 105(3),* 1393-1405.

Deisseroth, K., Feng, G., Majewska, A. K., Miesenböck, G., Ting, A., & Schnitzer, M. J. (2006). Next-generation optical technologies for illuminating genetically targeted brain circuits. The *Journal of Neuroscience, 26(41),* 10380-10386.

Devor, A., Dunn, A. K., Andermann, M. L., Ulbert, I., Boas, D. A., & Dale, A. M. (2003). Coupling of total hemoglobin concentration, oxygenation and neural activity in rat somatosensory cortex. *Neuron, 39 (2),* 353-359.

Devor, A., Tian, P., Nishimura, N., Teng, I. C., Hillman, E. M., Narayanan, S. N., Ulbert, I., Boas, D. A., Kleinfeld, D., & Dale, A. M. (2007). Suppressed neuronal activity and concurrent arteriolar vasoconstriction may explain negative blood oxygenation level-dependent signal. *Journal of Neuroscience, 27*, 4452-4459.

Di, S., Baumgartner, C., & Barth, D. S. (1990). Laminar analysis of extracellular field potentials in rat vibrissa/barrel cortex. *Journal of Neurophysiology, 63,* 832–840.

Diamond, M. C., Johnson, R. E., & Gold, M. W. (1977). Changes in neuron number and size and glial number in the young, adult and aging rat medial occipital cortex. *Behavioral Biology, 20,* 409-*418*.

Devor, A., Hillman, E. M. C., Tian, P., Waeber, C., Teng, I. C., Ruvinskaya, L., Shalinsky, M. H., Zhu, H., Haslinger, R. H., Narayanan, S. N., et al., (2008). Stimulus-induced changes in blood flow and 2-deoxyglucose uptake dissociate in ipsilateral somatosensory cortex. *Journal of Neuroscience, 28,* 14347–14357.

Dombeck, D. A., Harvey, C. D., Tian, L., Looger, L. L., & Tank, D. W. (2010). Functional imaging of hippocampal place cells at cellular resolution during virtual navigation. *Nature Reviews Neuroscience, 13,* 1433-1440.

Dombeck, D. A., Khabbaz, A. N., Collman, F., Adelman, T. L., & Tank, D. W. (2007). Imaging large scale neural activity with cellular resolution in awake mobile mice. *Neuron, 56 (1),* 43-57.

Downen, M., Zhao, M. L., Lee, P., Weidenheim, K. M., Dickson, D. W., & Lee, S. C. (1999). Neuronal nitric oxide synthase expression in developing and adult human CNS. *Journal of Neuropathology & Experimental Neurology, 58*, 12–21.

Drew P. J., Shih, A. Y., Driscoll, J. D., Knutsen, P. M., Blinder, P., Davalos, D., Akassoglou, K., Tsai, P. S., & Kleinfeld, D. (2010). Chronic optical access through a polished and reinforced thinned skull. *Nature Methods, 7*, 981–984

Du, C., Tully, M., Volkow, N. D., Schiffer, W. K., Yu, M., Luo, Z., Koretsky, A. P., & Benveniste, H. (2009). Differential effects of anaesthetics on cocaine's pharmacokinetic and pharmacodynamic effects in brain. *European Journal of Neuroscience, 30,* 1565-1575.

Einevoll, G. T., Pettersen, K. H., Devor, A., Ulbert, I., Halgren, E., & Dale, A. M. (2007). Laminar population analysis: estimating firing rates and evoked synaptic activity from multielectrode recordings in rat barrel cortex. *Journal of Neurophysiology, 97*, 2174–2190.

Enager, P., Piilgaard, H., Offenhauser, N., Kpcharyan, A., Fernandes, P., Hamel, E., & Lauritzen, M. (2009). Pathway-specific variations in neurovascular and neurometabolic coupling in rat primary somatosensory cortex. *Journal of cerebral blood flow and metabolism, 29,* 976-986.

Engelhard, K., & Werner, C. (2006). Inhalational or intravenous anesthetics for craniotomies? Pro inhalational. *Current Opinion in Anesthesiology, 19(5),* 504-508.

Erisken, S., Vaiceliunaite, A., Jurjut, O., Fiorini, M., Katzner, S., & Busse, L. (2014). Effects of locomotion extend throughout the mouse early visual system. *Current Biology, 24(24)*, 2899-2907.

Eto, R., Abe, M., Kimoto, H., Imaoka, E., Kato, H., Kasahara, J., & Araki, T. (2010). Alterations of interneurons in the striatum and frontal cortex of mice during postnatal development. International *Journal of Developmental Neuroscience, 28*, 359–370.

Fabiani, M., Gordon, B. A., Madin, E. L., Pearson, M. A., Brumback-Peltz, C. R., Low, K. A., McAuley, E., Sutton, B. P., Kramer, A. F., & Gratton, G. (2013). Neurovascular coupling in normal ageing: a combined optical, ERP and fMRI study. *NeuroImage, 85,* 592-607.

Faraci, F. M., & Heistad, D. D. (1998). Regulation of the cerebral circulation: role of endothelium and potassium channels. *Physiology Reviews, 78,* 53-97.

Farkas, E., & Luiten, P. G. (2001). Cerebral microvascular pathology in ageing and Alzheimer's disease. *Progress in Neurobiology, 64,* 575-611.

Fenno, L., Yizhar, O., & Deisseroth, K. (2011). The development and application of optogenetics. *Annual Review of Neuroscience, 34*, 389–412.

Ferezou, I., Bolea, S., & Petersen, C. C. H. (2006). Visualizing the cortical representation of whisker touch: voltage-sensitive dye imaging in freely moving mice. *Neuron, 50 (4),* 617-629.

Ferezou, I., Haiss, F., Gentet, L. J., Aronoff, R., Weber, B., & Petersen, C. C. (2007). Spatiotemporal dynamics of cortical sensorimotor integration in behaving mice. *Neuron, 56(5)*, 907-923.

Fields, R.D. (2008). White matter matters. *Scientific American, 298*, 42–49.

Filosa, J. A., Bonev, A. D., Straub, S. V., Meredith, A. L., Wilkerson, M. K., Aldrich, R. W., & Nelson, M. T. (2006). Local potassium signalling couples neuronal activity to vasodilation in the brain. *Nature Reviews Neuroscience, 9,* 1397-1403.

Filosa, J. A., Morrison, H. W., Iddings, J. A., Du, W., & Kim, K. J. (2016). Beyond neurovascular coupling, role of astrocytes in the regulation of vascular tone. *Neuroscience, 323*, 96-109.

Flück, D., Beaudin, A. E., Steinback, C. D., Kumarpillai, G., Shobha, N., McCreary, C. R., & Poulin, M. J. (2014). Effects of ageing on the association between cerebrovascular responses to visual stimulation, hypercapnia and arterial stiffness. *Frontiers in Physiology, 5(*49*),* 1389-1420.

Fox, M. D., & Raichle, M. E. (2007). Spontaneous fluctuations in brain activity observed with functional magnetic resonance imaging. *Nature Reviews Neuroscience, 8*, 700–711.

Fu, Y., Tucciarone, J. M., Espinosa, S., Sheng, N., Darcy, D. P., Nicoll, R. A., Huang, Z. J., & Stryker, M . P. (2014). A cortical circuit for gain control by behavioural state. *Cell, 156 (6),* 1139-1152.

Gabernet, L., Jadhav, S.P., Feldman, D.E., Carandini, M., Scanziani, M. (2005). Somatosensory integration controlled by dynamic thalamocortical feed-forward inhibition. *Neuron, 48*, 315–327.

Garcia-Matas, S., Gutierrez-Cuesta, J., Coto-Montes, A., Rubio-Acero, R., Diez-Vives, C., Camins, A., Pallas, M., Sanfeliu, C., & Cristofol, R. (2008). Dysfunction of astrocytes in senescence-accelerated mice SAMP8 reduces their neuroprotective capacity. *Aging Cell, 7,* 630–640.

Gazzaley, A., & D'Esposito, M. (2005). BOLD functional MRI and cognitive ageing. *Cognitive neuroscience of ageing: Linking cognitive and cerebral ageing*, UK: Oxford University Press.

Gentet, L. J., Kremer, Y., Taniguchi, H., Huang, Z. J., Staiger, J. F., & Petersen, C.C.H. (2012). Unique functional properties of somatostatin-expressing GABAergic neurons in mouse barrel cortex. *Nature Neuroscience, 15*, 607–612.

Gerrits, R. J., Stein, E. A., & Greene, A. S. (2001). Anesthesia alters NO-mediated functional hyperemia. *Brain Research, 907,* 20-26.

Gerstein, G. L., & Perkel, D. H. (1969). Simultaneously recorded trains of action potentials: analysis and functional interpretation. *Science, 164(3881),* 828-830.

Girouard, H., & Iadecola, C. (2006). Neurovascular coupling in the normal brain and in hypertension, stroke, and Alzheimer disease. *Journal of Applied Physiology, 100 (1),* 328-35.

Goense, J, B, M., & Logothetis, N, K. (2008). Neurophysiology of the BOLD fMRI signal in awake monkeys. *Current Biology, 18(9),* 631-640.

Goldstein, S., & Reivich, M. (1991). Cerebral blood flow and metabolism in aging and dementia. *Clinical Neuropharmacology, 14(1)*, S34–S44.

Gordon, R. J., Mulligan, S. J., & MacVicar, B. A. (2007). Astrocyte control of the cerebrovasculature. *Glia, 55,* 1214-1221.

Gorelick, P. B., Scuteri, A., Black, S. E., Decarli, C., Greenberg, S. M., Iadecola, C., Launer, L. J., Laurent, S., Lopez, O. L., Nyenhuis, D., Petersen, R. C., Schneider, J. A., Tzourio, C., Arnett, D. K., Bennett, D.A., Chui, H. C., Higashida, R. T., Lindquist, R., Nilsson, P. M., Roman, G. C., Sellke, F. W., & Seshadri, S. (2011) Vascular contributions to cognitive impairment and dementia: a statement for healthcare professionals from the american heart association/ american stroke association. *Stroke, 42*, 2672–2713.

Greenberg, D. S., & Kerr, J. N. (2009). Automated correction of fast motion artifacts for two-photon imaging of awake animals. *Journal of Neuroscience Methods, 176,* 1-15.

Guo, Z. V., Hires, A., Nuo, L., O'Connor, D. H., Komiyama, T., Ophir, E., Huber, D., Bonardi, C., Morandell, K., Gutnisky, D., Peron, S., Xu, N-L., Cox, J., & Svoboda, K. (2014). Procedure for Behavioural Experiments in Head-Fixed Mice. *PLoS ONE, 9(6),* e101397.

Hafting, T., Fyhn, M., Molden, S., Moser, M. B., & Moser, E. I. (2005). Microstructure of a spatial map in the entorhinal cortex. *Nature, 436,* 801-806.

Haider, B., Hausser, M., & Carandini, M. (2013). Inhibition dominates sensory responses in the awake cortex. *Nature, 493,* 97-100.

Hall, C., et al. (2014). Capillary pericytes regulate cerebral blood flow in health and disease. *Nature, 508,* 55-60.

Han, X., & Boyden, E. S. (2007). Multiple-color optical activation, silencing, and desynchronization of neural activity, with single-spike temporal resolution. *PLoS One, 2*, e299.

Hansen, L. A., Armstrong, D. M., & Terry, R. D. (1987). An immunohistochemical quantification of fibrous astrocytes in the aging human cerebral cortex. *Neurobiology of Aging, 8(1)*, 1-6.

Harel, N., Lee, S. P., Nagaoka, T., Kim, D. S., & Kim, S. G. (2002). Origin of negative blood oxygenation level-dependent fMRI signals. *Journal of Cerebral Blood Flow & Metabolism, 22*, 908 –917.

Harris, J. J., Jolivet, R., & Attwell, D. (2012). Synaptic energy use and supply. *Neuron, 75*, 762–777.

Harris, S., Jones, M., Zheng, Y., & Berwick, J. (2010). Does neural input or processing play a greater role in the magnitude of neuroimaging signals. *Front Neuroenergetics, 2*, ii.

Harris, J. J., Reynell, C., & Attwell, D. (2011). The physiology of developmental changes in BOLD functional imaging signals. *Developmental cognitive neuroscience, 1(3),* 199-216.

Harris, K. D., & Thiele, A. (2011). Cortical state and attention. *Nature Reviews Neuroscience, 12(9)*, 509-523.

Harvey, C. D., Collman, F., Dombeck, D. A., & Tank, D. W. (2009). Intracellular dynamics of hippocampal place cells during virtual navigation. *Nature, 461,* 941-946.

Hayama, T., Noguchi, J., Watanabe, S., Takahashi, N., Hayashi-Takagi, A., Ellis-Davies, G. C., et al. (2013). GABA promotes the competitive selection of dendritic spines by controlling local Ca2+ signaling. *Nature Neuroscience, 16*, 1409–1416.

Hayton, S. M., Kriss, A., & Muller, D. P. (1999). Comparison of the effects of four anaesthetic agents on somatosensory evoked potentials in the rat. *Laboratory Animals, 33,* 243-251.

Heeger DJ, Huk AC, Geisler WS, Albrecht DG. (2000). Spikes versus BOLD: what does neuroimaging tell us about neuronal activity*? Nature Neuroscience, 3*, 631–633.

Heep, A., Scheef. L., Jankowski, J., Born, M., Zimmermann, N., Sival, D., Bos, A., Gieseke, J., Bartmann, P., Schild, H., & Boecker, H. (2009). Functional magnetic resonance imaging of the sensorimotor system in preterm infants. *Pediatrics, 123(1)*, 294–300.

Hendrich, K. S., Kochanek, P. M., Melick, J. A., Schiding, J. K., Statler, K. D., Williams, D. S., ... & Ho, C. (2001). Cerebral perfusion during anesthesia with fentanyl, isoflurane, or

pentobarbital in normal rats studied by arterial spin-labeled MRI. *Magnetic resonance in medicine, 46(1)*, 202-206.

Herman, P., Sanganahalli, B. G., Blumenfeld, H., Rothman, D. L., & Hyder, F. (2013). Quantitative basis for neuroimaging of cortical laminae with calibrated functional MRI. *Proceedings of the National Academy of Sciences USA, 110,* 15115–15120.

Hesselmann, V., Weber, O. Z., Wedekind, C., Krings, T., Schulte, O., Kugel, H., ... & Lackner, K. J. (2001). Age related signal decrease in functional magnetic resonance imageing during motor stimulation in humans. *Neuroscience letters, 308(3)*, 141-144.

Hildebrandt, I. J., Su, H., & Weber, W. A. (2008). Anaesthesia and other considerations for in vivo imaging of small animals. *ILAR Journal, 49 (1),* 17-26.

Hill, S., & Tononi, G. (2005). Modeling sleep and wakefulness in the thalamocortical system. *Journal of Neurophysiology, 93(3),* 1671-1698.

Hillman, E. M. (2014). Coupling mechanism and significance of the BOLD signal: a status report. *Annual Reviews Neuroscience, 37,* 161-181.

Hillman, E. M., Devor, A., Bouchard, M. B., Dunn, A. K., Krauss, G. W., Skoch, J., Bacskai, B. J., Dale, A. M., & Boas, D. A. (2007). Depth-resolved optical imaging and microscopy of vascular compartment dynamics during somatosensory stimulation. *Neuroimage, 35,* 89-104.

Hoffman, W. E., Edelman, G., Kochs, E., Werner, C., Segil, L., & Albrecht, R. F. (1991). Cerebral autoregulation in awake versus isoflurane-anesthetized rats. *Anesthesia & Analgesia, 73(6),* 753-757.

Horiuchi, T., Dietrich, H. H., Hongo, K., & Dacet Jr, R. G. (2002). Mechanism of extracellular K^+-induced local and conducted responses in cerebral penetrating arterioles. *Stroke, 33,* 2692-2699.

Howarth, C. (2014). The contribution of astrocytes to the regulation of cerebral blood flow. *Frontiers in Neuroscience, 8,* 103.

Huo, B-X., Gao, Y-R., & Drew, P. J. (2015). Quantitative separation of arterial and venous cerebral blood volume increases during voluntary locomotion. *NeuroImage, 105,* 369-379.

Huo, B-X., Smith, J. B., & Drew, P. J. (2014). Neurovascular coupling and decoupling in the cortex during voluntary locomotion. *The Journal of Neuroscience, 34 (33),* 10975-10981.

Huttenlocher, P. R. (1990). Morphometric study of human cerebral cortex development. *Neuropsychologia, 28(6)*, 517-527.

Huttenlocher, P. R., de Courten, C., Garey, L. J., & Van der Loos, H. (1982). Synaptogenesis in human visual cortex—Evidence for synapse elimination during normal development. *Neuroscience Letters, 33,* 247–252.

Iadecola, C. (2004). Neurovascular regulation in the normal brain and in Alzheimer's disease. Nature Reviews Neuroscience, 5(5), 347-360.

Iadecola, C. (2013). The pathobiology of vascular dementia. *Neuron, 80,* 844-866.

Iadecola, C., Park, L., & Capone, C. (2009). Threats to the mind: ageing, amyloid & hypertension. *Stroke, 108,* 533-638.

Iadecola, C., & Nedergaard, M. (2007). Glial regulation of the cerebral microvasculature. *Nature Neuroscience, 10,* 1369-1376.

Itti, L., & Koch, C. (2001). Computational modelling of visual attention. *Nature Reviews Neuroscience, 2(3),* 194-203.

Ikeda, Y., Nishiyama, N., Saito, H., & Katsuki, H. (1997). GABAA receptor stimulation promotes survival of embryonic rat striatal neurons in culture. *Developmental Brain Research, 98*, 253–258.

Ito, H., Kanno, I., Ibaraki, M., Hatazawa, J., & Miura, S. (2003). Changes in human cerebral blood flow and cerebral blood volume during hypercapnia and hypocapnia measured by positron emission tomography. *Journal Cerebral Blood Flow & Metabolism, 23*, 665-670.

Jacobs, B., & Scheibel, A. B. (1993). A quantitative dendritic analysis of Wernicke's area in humans. I. Lifespan changes. *Journal of Comparative Neurology. 327*, 383–396.

Jessen, S. B., Mathiesen, C., Lind, B. L., & Lauritzen, M. (2015). Interneuron Deficit Associates Attenuated Network Synchronization to Mismatch of Energy Supply and Demand in Aging Mouse Brains. *Cerebral Cortex, 26(9),* bhv261.

Johns, M., Giller, C., German, D., & Liu, H. (2005). Determination of reduced scattering coefficient of biological tissue from a needle-like probe. *Optics Express, 13(13),* 4828-4842.

Jonckers, E., Delgado y Palacios, R., Shah, D., Guglielmetti, C., Verhoye, M., & Linden, A. (2014). Different anesthesia regimes modulate the functional connectivity outcome in mice. *Magnetic Resonance in Medicine, 72(4),* 1103-1112.

Jones, E. G. (1970). On the mode of entry of blood vessels into the cerebral cortex. *Journal of Anatomy, 106,* 507-520.

Jones, M. (2002). *Optical imaging spectroscopy and laser Doppler flowmetry in rodent barrel cortex: the haemodynamic response to whisker stimulation hypercapnia.* (Unpublished doctoral thesis). University of Sheffield, Sheffield, UK.

Jones, M., Berwick, J., Hewson-Stoate, N., Gias, C., & Mayhew, J. (2005). The effect of hypercapnia on the neural and hemodynamic responses to somatosensory stimulation. *Neuroimage, 27(3),* 609-623.

Jones, M., Berwick, J., Johnston, D., & Mayhew, J. (2001). Concurrent optical imaging spectroscopy and laser-Doppler flowmetry: the relationship between blood flow, oxygenation, and volume in rodent barrel cortex. *Neuroimage, 13(6 Pt 1)*, 1002-1015.

Jones, M., Devonshire, I. M., Berwick, J., Martin, C., Redgrave, P., & Mayhew, J. (2008). Altered neurovascular coupling during information-processing states. *Eur J Neurosci, 27(10)*, 2758-2772.

Joutel, A., Monet-Lepretre, M., Gosele, C., Bacon-Menguy, C., Hammes, A., Schmidt, S., et al. (2010). Cerebrovascular dysfunction and microcirculation rarefaction precede white matter lesions in a mouse geetc model of cerebral ischemic small vessel disease. *Journal of Clinical Investigations, 120,* 433-445.

Kalaria, R. N. (2008). Linking cerebrovascular defense mechanisms in brain ageing and Alzheimer's disease. *Neurobiology of Ageing, 30(9),* 1512-1514.

Kalisch, R., Elbel, G. K., Gossl, C., Czisch, M., & Auer, D. P. (2001). Blood pressure changes induced by arterial blood withdrawal influence bold signal in anesthesized rats at 7 Tesla: implications for pharmacologic mri. *NeuroImage, 14(4),* 891-898.

Karen, T., Morren, G., Haensse, D., Bauschatz, A. S., Bucher, H. U., & Wolf, M. (2008). Hemodynamic response to visual stimulation in newborn infants using functional near-infrared spectroscopy. *Human Brain Mapping, 29(4),* 453-460.

Karniski, W. (1992). The late somatosensory evoked potential in premature and term infants I. Principle Component Topograhpy. *Electroencephalography and Clinical Neurophysiology, 84(1),* 32-43.

Karniski, W., Wyble, L., Lease, L., & Blair, R.C. (1992). The late somatosensory evoked potential in premature and term infants II. Topography and latency development. *Electroencephalography and Clinical Neurophysiology, 84(1)*, 44–54.

Keep, R. F., & Jones, H. C. (1990). Cortical microvessels during brain development: a morphometric study in the rat. *Microvascular Research, 40*, 412–426.

Keller, G. B., Bonhoeffer, T., & Hübener, M. (2012). Sensorimotor mismatch signals in primary visual cortex of the behaving mouse. *Neuron, 74(5),* 809-815.

Kennerley, A. J., Berwick, J., Martindale, J., Johnston, D., Papadakis, N., & Mayhew, J. E. (2005). Concurrent fMRI and optical measures for the investigation of the hemodynamic response function. *Magnetic Resonance in Medicine, 54(2)*, 354-365.

Kennerley, A. J., Berwick, J., Martindale, J., Johnston, D., Zheng, Y., & Mayhew, J. E. (2009). Refinement of optical imaging spectroscopy algorithms using concurrent BOLD and CBV fMRI. *NeuroImage, 47(4),* 1608-1619.

Kennerley, A. J., Harris, S., Bruyns-Haylett, M., Boorman, L., Zheng, Y., Jones, M., & Berwick, J. (2012). Early and Late Stimulus-Evoked Cortical Hemodynamic Responses Provide Insight into the Neurogenic Nature of Neurovascular Coupling. *Journal of Cerebral Blood Flow & Metabolism, 32(3),* 468-480.

Kirsch, J., & Betz, H. (1998). Glycine-receptor activation is required for receptor clustering in spinal neurons. *Nature, 392*, 717–720.

Kitaura, H., Uozumi, N., Tohmi, M., Yamazaki, M., Sakimura, K., Kudoh, M., Shimizu, T., & Shibuki, K. (2007). Roles of nitric oxide as a vasodilator in neurovascular coupling of mouse somatosensory cortex. *Neuroscience Research, 59,* 160-171.

Kneussel, M., & Betz, H. (2000). Clustering of inhibitory neurotransmitter receptors at developing postsynaptic sites: the membrane activation model. *Trends in Neuroscience, 23,* 429–435.

Knopfel, T. (2012). Genetically encoded optical indicators for the analysis of neuronal circuits. *Nature Reviews Neuroscience, 13*, 687–700.

Koch, S. P., Werner, P., Steinbrink, J., Fries, P., & Obrig, H. (2009). Stimulus-induced and state-dependent sustained gamma activity is tightly coupled to the hemodynamic response in humans. *Journal of Neuroscience, 29*, 13962–13970.

Kocharyan, A., Fernandes, P., Tong, X. K., Vaucher, E., & Hamel, E. (2008). Specific subtypes of cortical GABA interneurons contribute to the neurovascular coupling response to basal forebrain stimulation. *Journal of Cerebral Blood Flow & Metabolism, 28,* 221-231.

Kourtzi, Z., Augath, M., Logothetis, N.K., Movshon, J.A. & Kiorpes, L. (2006). Development of visually evoked cortical activity in infant macaque monkeys studied longitudinally with fMRI. *Magnetic Resonance Imaging, 24*, 359–366.

Kozberg, M. G., Chen, B. R., DeLeo, S. E., Bouchard, M. B., & Hillman, E. M. C. (2013). Resolving the transition from negative to positive blood oxygen level-dependent responses in the developing brain. *Proceedings of the National Academy of Science USA, 110*, 4380–4385.

Kozberg, M. G., & Hillman, E. M. C. (2016). Neurovascular coupling and energy metabolism in the developing brain. *Progress in Brain Research, 225*, 213-42.

Krishnamurthy, P., Silberberg, G., & Lansner, A. (2015). Long-range recruitment of Martinotti cells causes surround suppression and promotes saliency in an attractor network model. *Frontiers in Neural Circuits, 9*, 60.

Kvitsiani, D., Ranade, S., Hangya, B., Taniguchi, H., Huang, J. Z., & Kepecs, A. (2013). Distinct behavioural and network correlates of two interneuron types in prefrontal cortex. *Nature, 498*, 363–366.

Lauritzen, M. (2005). Reading vascular changes in brain imaging: is dendritic calcium the key? *Nature Reviews Neuroscience, 6,* 77-85.

Lauritzen, M., Jørgensen, M. B., Diemer, N. H., Gjedde, A., & Hansen, A. J. (1982). Persistent oligemia of rat cerebral cortex in the wake of spreading depression. *Annals of Neurology, 12(5),* 469-474.

Lauronen, L., Nevalainen, P., Wikstrom, H., Parkkonen, L., Okada, Y., & Pihko, E. (2006). Immaturity of somatosensory cortical processing in human newborns. *NeuroImage, 33(1),* 195–203.

Le Magueresse, C., & Monyer, H. (2013). GABAergic interneurons shape the functional maturation of the cortex. *Neuron 77*, 388–405.

Lee, S. H., & Dan, Y. (2012). Neuromodulation of brain states. *Neuron, 76(1)*, 209-222.

Lee, Y., Grady, C. L., Habak, C., Wilson, H. R., & Moscovitch, M. (2011). Face processing changes in normal ageing revealed by fMRI adaptation. *Journal of cognitive neuroscience, 23(11)*, 3433-3447.

Legatt, A. D., Arezzo, J., & Vaughan Jr, H. G. (1980). Averaged multiple unit activity as an estimate of phasic changes in local neuronal activity: effects of volume-conducted potentials. *Journal of Neuroscience Methods, 2,* 203-217.

Levin, J. M., Frederick, B., Ross, M. H., Fox, J. F., von Rosenberg, H. L., et al. (2001). Influence of baseline hematocrit and hemodilution on BOLD fMRI activation. *Magnetic Resonance Imaging, 19*, 1055–1062.

Liao, S. M., Gregg, N. M., White, B. R., Zeff, B. W., Bjerkaas, K. A., Inder, T. E., & Culver, J. P. (2010). Neonatal hemodynamic response to visual cortex activity: high-density nearinfrared spectroscopy study. *Journal of Biomedical Optics, 15*, 1–9.

Lin, A. L., Fox, P. T., Hardie, J., Duong, T. Q., & Gao, J. H. (2010). Nonlinear coupling between cerebral blood flow, oxygen consumption, and ATP production in human visual cortex. *PNAS, 107,* 8446-8451.

Lincoln, D. W. (1969). Correlation of unit activity in the hypothalamus with EEG patterns associated with the sleep cycle. *Experimental Neurology, 24,* 1-18.

Lindauer, U., Megow, D., Matsuda, H., & Dirnagl, U. (1999). Nitric oxide: a modulator, but not a mediator, of neurovascular coupling in rat somatosensory cortex. *American Journal of Physiology, 277(2, pt 2),* H799-811.

Lindauer, U., Royl, G., Leithner, C., Kuhl, M., Gold, L., Gethmann, J., Kohl-Bareis, M., Villringer, A., & Dirnagl, U. (2001). No evidence for early decrease in blood oxygenation in rat whisker cortex in response to functional activation. *Neuroimage, 13 (6),* 988-1001.

Lindauer, U., et al. (2010). Neurovascular coupling in rat brain operates independent of haemoglobin deoxygenation. *Journal of Cerebral Blood Flow & Metabolism, 30,* 757-768.

Liu, X., Li, C., Falck, J. R., Roman, R. J., Harder, D. R., & Koehler, R. C. (2008). Interaction of nitric oxide, 20-HETE, and EETs during functional hyperemia in whisker barrel cortex. *American Journal of Heart and Circulatory Physiology, 295,* H619-H631.

Loessner, A., Alavi, A., Lewandrowski, K. U., Mozley, D., Souder, E., & Gur, R. E. (1995). Regional cerebral function determined by FDG-PET in healthy volunteers: Normal patterns and changes with age. *Journal of Nuclear Medicine, 36,* 1141–1149.

Logothetis, N. K., Guggenberger, H., Peled, S. & Pauls, J. (1999). Functional imaging of the monkey brain. *Nature Neuroscience, 2*, 555–562.

Logothetis, N. K., Pauls, J., Augath, M., Trinath, T., & Oeltermann, A. (2001). Neurophysiological investigation of the basis of the fMRI signal. *Nature, 412,* 150-157.

Logothetis, N. K., & Wandell, B. A. (2004). Interpreting the BOLD signal. *Annual Review of Physiology, 66,* 735-769.

Long, J. M., Kalehua, A. N., Muth, N. J., Calhoun, M. E., Jucker, M., Hengemihle, J. M., Ingram, D. K., & Mouton, P. R. (1998). Stereological analysis of astrocyte and microglia in aging mouse hippocampus. *Neurobiology of Aging, 19(5),* 497-503.

LoTurco, Owens, D. F., Heath, M. J., Davis, M. B., & Kriegstein, A. R. (1995). GABA and glutamate depolarize cortical progenitor cells and inhibit DNA synthesis. *Neuron, 15*, 1287–1298.

Lovick, T. A., Brown, L. A., & Key, B. J. (1999). Neurovascular relationships in hippocampal slices: physiological and anatomical studies of mechanisms underlying flow-metabolism coupling in intraparenchymal microvessels. *Neuroscience, 92,* 47-60.

Ma, J., Ayata, C., Huang, P. L., Fishman, M. C., & Moskowitz, M. A. (1996). Regional cerebral blood flow response to vibrissal stimulation in mice lacking type I NOS gene expression. *American Journal of Physiology, 270*, 1085-1090.

Madhusudan, A., Sidler, C., & Knuesel, I. (2009). Accumulation of reelin-positive plaques is accompanied by a decline in basal forebrain projection neurons during normal aging. *European Journal of Neuroscience, 30*, 1064–1076.

Makani, S., & Chesler, M. (2010). Rapid rise of extracellular pH evoked by neural activity is generated by the plasma membrane calcium ATPase. *Journal of Neurophysiology, 103,* 667-676.

Marcar, V. L., Schwarz, U., Martin, E., & Loenneker, T. (2006). How Depth of Anesthesia Influences the Blood Oxygenation Level–Dependent Signal from the Visual Cortex of Children. *American Journal of Neuroradiology, 27(4),* 799-805.

Marcar, V. L., Strassle, A. E., Loenneker, T., Schwarz, U., & Martin, E. (2004). The Influence of Cortical Maturation on the BOLD Response: An fMRI Study of Visual Cortex in Children. *Pediatric Research, 56*, 967–974.

Marchal, G., Rioux, P., Petit-Taboue, M. C., Sette, G., Travere, J. M., Le Poec, C., Courtheoux, P., Derlon, J. M., & Baron, J. C. (1992). Regional cerebral oxygen consumption, blood flow, and blood volume in healthy human aging. *Archives of Neurology, 49,* 1013–1020.

Marshall, P. J., Bar-Haim, Y., & Fox, N. A. (2002). Development of the EEG from 5 months to 4 years of age. *Clinical Neurophysiology 113*, 1199–1208.

Martin, C., Berwick, J., Johnston, D., Zheng, Y., Martindale, J., Port, M., Redgrave, P., & Mayhew, J. (2002). Optical imaging spectroscopy in the unanaesthetised rat. *Journal of Neuroscience Methods, 120(1)*, 25-34.

Martin, E., Joeri, P., Loenneker, T., Ekatodramis, D., Vitacco, D., et al. (1999). Visual processing in infants and children studied using functional MRI. *Pediatric Research, 46*, 135–140.

Martin, C. J., Kennerley, A. J., Berwick, J., Port, M., & Mayhew, J. E. W. (2013a). Functional MRI in conscious rats using a chronically implanted surface coil. *Journal of Magnetic Resonance Imaging, 38(3)*, 739-744.

Martin, C., Martindale, J., Berwick, J., & Mayhew, J. (2006). Investigating neural-hemodynamic coupling and the hemodynamic response function in the awake rat. *Neuroimage, 32(1)*, 33-48.

Martin, C., Zheng, Y., Sibson, N. R., Mayhew, J. E. W., & Berwick, J. (2013b). Complex spatiotemporal haemodynamic response following sensory stimulation in the awake rat. *NeuroImage, 66,* 1-8.

Martindale, J., Berwick, J., Martin, C., Kong, Y., Zheng, Y., & Mayhew, J. (2005). Long Duration Stimuli and Nonlinearities in the Neural–Haemodynamic Coupling. *Journal of Cerebral Blood Flow & Metabolism, 25(5),* 651-661.

Marty, S., Berninger, B., Carroll, P., & Thoenen, H. (1996). GABAergic stimulation regulates the phenotype of hippocampal interneurons through the regulation of brain-derived neurotrophic factor. *Neuron, 16,* 565–570.

Masamoto, K., Fukuda, M., Vazquez, A. & Kim, S. G. (2009). Dose-dependent effect of isoflurane on neurovascular coupling in rat cerebral cortex. *European Journal of Neuroscience, 30*, 242–250.

Masamoto, K., & Kanno, I. (2012). Anesthesia and the quantitative evaluation of neurovascular coupling. *Journal of Cerebral Blood Flow & Metabolism, 32*, 1233-1247.

Masamoto, K., Obata, T., & Kanno, I. (2010). Intracortical microcirculatory change induced by anesthesia in rat somatosensory cortex. *Advanced Experimental Medical Biology, 662,* 57-61.

Masliah, E., Mallory, M., Hansen, L., DeTeresa, R., & Terry, R. D. (1993). Quantitative synaptic alterations in the human neocortex during normal aging. *Neurology, 43,* 192-197.

Mattay, V. S., Fera, F., Tessitore, A., Hariri, A. R., Das, S., Callicot, J. H., & Weinberger, D. R. (2002). Neurophysiological correlates of age-related changes in human motor function. *Neurology, 58*, 630–635.

Mayhew, J., Johnston, D., Berwick, J., Jones, M., Coffey, P., & Zheng, Y. (2000). Spectroscopic analysis of neural activity in the brain: increased oxygen consumption following activation of barrel cortex. *NeuroImage, 12,* 664-675.

McAdams, C. J., & Reid, R. C. (2005). Attention modulates the responses of simple cells in monkey primary visual cortex. *Journal of Neuroscience, 25 (47),* 11023-11033.

McQuail, J. A., Bañuelos, C., LaSarge, C. L., Nicolle, M. M., & Bizon, J. L. (2012). $GABA_B$ receptor GTP-binding is decreased in the prefrontal cortex but not the hippocampus of aged rats. *Neurobiology of Aging, 33*, 1124.e1–1124.e12.

Meek, J. H., Firbank, M., Elwell, C. E., Atkinson, J., Braddick, O., & Wyatt, J. S., 1998. Regional hemodynamic responses to visual stimulation in awake infants. *Pediatric Research, 43*, 840–843.

Metea, M. R., & Newman, E. A. (2006). Glial cells dilate and constrict blood vessels: a mechanism of neurovascular coupling. *Journal of Neuroscience, 26,* 2862-2870.

Mitzdorf, U. (1987). Properties of the evoked potential generators: current source-density analysis of visually evoked potentials in the cat cortex. *The International Journal of Neuroscience, 33,* 33-59.

Mueller, A. L., Taube, J. S., & Schwartzkroin, P. A. (1984). Development of hyperpolarizing inhibitory postsynaptic potentials and hyperpolarizing response to gamma-aminobutyric acid in rabbit hippocampus studied in vitro. *Journal of Neuroscience, 4,* 860–867.

Mulligan, S. J., & MacVicar, B. A. (2004). Calcium transients in astrocyte endfeet cause cerebrovascular constrictions. *Nature, 431,* 195-199.

Muramoto, S., Yamada, H., Sadato, N., Kimura, H., Konishi, Y., Kimura, K., Tanaka, M., Kochiyama, T., Yonekura, Y., & Ito, H. (2002). Age-dependent change in metabolic response to photic stimulation of the primary visual cortex in infants: functional magnetic resonance imaging study. *Journal of Computer Assisted Tomography, 26,* 894-901.

Muthukumaraswamy, S. D., Edden, R. A., Jones, D. K., Swettenham, J. B., Singh, & K. D. (2009). Resting GABA concentration predicts peak gamma frequency and fMRI amplitude in response to visual stimulation in humans. Proceedings of National Academy og Science USA, *106*, 8356–8361.

Nakamura, K., Terasako, K., Toda, H., Miyawaki, I., Kakuyama, M., Nishiwada, M., Hatano, Y., & Mori, K. (1994). Mechanisms of inhibition of endothelium-dependent relaxation by halothane, isoflurane, and sevoflurane. *Canadian Journal of Anesthesia, 41,* 340-346.

Nakao, Y., Itoh, Y., Kuang, T. Y., Cook, M., Jehle, J., & Sokoloff, L. (2001). Effects of anesthesia on functional activation of cerebral blood flow and metabolism. *Proceedings of the National Academy of Sciences of the United States of America, 98 (13),* 7593-7598.

Nicolakakis, N., & Hamel, E. (2011). Neurovascular function in Alzheimer's disease patients and experimental models. *Journal of Cerebral Blood Flow & Metabolism, 31*, 1354–1370.

Niwa, K., Araki, E., Morham, S. G., Ross, M. E., & Iadecola, C. (2000). Cyclooxygenase-2 contributes to functional hyperaemia in whisker-barrel cortex. *Journal of Neuroscience, 20,* 763-770.

Neill, C. M., & Stryker, M. P. (2008). Highly selective receptive fields in mouse visual cortex. *Journal of Neuroscience, 28,* 7520-7536.

Neill, C. M., & Stryker, M. P. (2010). Modulation of visual responses by behavioural state in mouse visual cortex. *Neuron, 65,* 472-479.

Nielsen, A. N., & Lauritzen, M. (2001). Coupling and uncoupling of activity-dependent increases of neuronal activity and blood flow in rat somatosensory cortex. *Journal of Physiology, 553 (3),* 773-785.

Nithianantharajah, J., et al. (2015). Bridging the translational divide: identical cognitive touch screen testing in mice and humans carrying mutations in a disease-relevant homogolous gene. *Scientific Reports, 5,* 14613.

Nitish, V. T., & Tong, S. (2004). Advances in Quantitative Electroencephalogram analysis methods. *Annual Review of Biomedical Engineering, 6*, 453-95.

Nixdorf-Bergweiler, B. E., Albrecht, D., & Heinemann, U. (1994). Developmental changes in the number, size, and orientation of GFAP-positive cells in the CA1 region of rat hippocampus. *Glia, 12*, 180–195.

Nizar, K., Uhlirova, H., Tian, P., Saisan, P. A., Cheng, Q., Reznichenko, L., et al. (2013). In vivo stimulus-induced vasodilation occurs without IP3 receptor activation and may precede astrocytic calcium increase. *Journal of Neuroscience, 33*, 8411–8422.

Nyberg, L., Salami, A., Andersson, M., Eriksson, J., Kalpouzos, G., Kauppi, K., ... & Nilsson, L. G. (2010). Longitudinal evidence for diminished frontal cortex function in ageing. *Proceedings of the National Academy of Sciences*, *107*(52), 22682-22686.

O'Connor, D. H., Clack, N. G., Huber, D., Komiyama, T., Myers, E. W., & Svoboda, K. (2010) Vibrissa-based object localization in head-fixed mice. *J Neurosci., 30*, 1947–1967.

O'Herron, P., Chhatbar, P. Y., Levy, M., Shen, Z., Schramm, A. E., Lu, Z., & Kara, P. (2016). Neural correlates of single-vessel haemodynamic responses in vivo. *Nature, 534*, 378-382.

O'Keefe, J., & Dostrovsky, J. (1971). The hippocampus as a spatial map. Preliminary evidence from unit activity in the freely-moving rat. *Brain Research, 34,* 171-175.

Obrietan, K., & van den Pol, A. N. (1997). GABA activity mediating cytosolic Ca2+ rises in developing neurons is modulated by cAMP-dependent signal transduction. *Journal of Neuroscience, 17*, 4785–4799.

Ogawa, S., Lee, R. M., & Barrere, B. (1993). The sensitivity of magnetic resonance image signals of a rat brain to changes in the cerebral venous blood oxygenation. *Magnetic Resonance in Medicine, 29*, 205–210.

Ogawa, S., Lee, T. M., Kay, A. R., & Tank, D. W. (1990). Brain magnetic resonance imageing with contrast dependent on blood oxygenation. *Proceedings of the National Academy of Sciences*, *87*(24), 9868-9872.

Ohyu, J., & Takashima, S. (1998). Developmental characteristics of neuronal nitric oxide synthase (nNOS) immunoreactive neurons in fetal to adolescent human brains. *Developmental Brain Research, 110*, 193–202.

Oski, F. A., Brugnara, C., & Nathan, D. G. (1998). A diagnostic approach to the anemic patient. In D. G., Nathan & S. H., Oski (Eds.), *Hematology of Infancy and Childhood* (pp. 3375–376). Philadelphia: W.B. Saunders Company.

Ostby, Y., Tamnes, C. K., Fjell, A. M., Westlye, L. T., Due-Tonnessen, P., & Walhovd, K. B. (2009). Heterogeneity in subcortical brain development: A structural magnetic resonance imageing study of brain maturation from 8 to 30 years. *Journal of Neuroscience, 29,* 11772-11782.

Pakkenberg, B., Pelvig, D., Marner, L., Bundgaard, M. J., Gundersen, H. J. G., Nyengaard, J. R., & Regeur, L. (2003). Aging and the human neocortex. *Experimental Gerontology, 38,* 95-99.

Panczel, G., Daffertshofer, M., Ries, S., Spiegel, D., & Hennerici, M. (1999). Age and stimulus dependency of visually evoked cerebral blood flow responses. *Stroke, 30,* 619-623.

Park, L., Anrather, J., Girouard, H., Zhou, P., & Iadecola, C. (2007). Nox2-derived reactive oxygen species mediate neurovascular dysregulation in the ageing mouse brain. *Journal of Cerebral Blood Flow & Metabolism*, *27*(12), 1908-1918.

Paus, T. (2005). Mapping brain maturation and cognitive development during adolescence. *Trends in Cognitive Science, 9,* 60–68.

Pawela, C. P., Biswal, B. B., Hudetz, A. G., Schulte, M. L., Li, R., Jones, S. R., Cho, Y. R., Matloub, H. S., & Hyde, J. S. (2009). A protocol for use of medetomidine anesthesia in rats for extended studies using task-induced BOLD contrast and resting-state functional connectivity. *NeuroImage, 46,* 1137-1147.

Pawlik, G., Rackl, A., & Bing, R. J. (1981). Quantitative capillary topography and blood flow in the cerebral cortex of cats: an in vivo microscopic study. *Brain Research, 208(1),* 35-58.

Pi, H. J., Hangya, B., Kvitsiani, D., Sanders, J. I., Huang, Z. J., & Kepecs, A. (2013). Cortical interneurons that specialize in disinhibitory control. *Nature, 503(7477),* 521-524.

Pike, A. A., & Marlow, N. (2000). The role of cortical evoked potentials in predicting neuromotor outcome in very preterm infants. *Early Human Development, 57*, 123–135.

Pisauro, M. A., Dhruc, N. T., Carandini, M., & Benucci, A. (2013). Fast haemodynamic responses in the visual cortex of the awake mouse. *The Journal of Neuroscience, 33 (46),* 18343-18351.

Peeters, R. R., Tindemans, I., De Schutter. E. & Van der Linden, A. (2001). Comparing BOLD fMRI signal changes in the awake and anesthetized rat during electrical forepaw stimulation. *Magnetic Resonance Imaging, 19*, 821–826.

Perea, G., & Araque, A. (2005). Properties of synaptically evoked astrocyte calcium signal reveal synaptic information processing by astrocytes. *Journal of Neuroscience, 25,* 2192-2203.

Peters A. (2007). The Effects of Normal Aging on Nerve Fibers and Neuroglia in the Central Nervous System. In Riddle, D. R., (Ed.). Brain Aging: Models, Methods, and Mechanisms. Boca Raton (FL): CRC Press/Taylor & Francis.

Peters, A., Sethares, C., & Luebke, J. I. (2008). Synapses are lost during aging in the primate prefrontal cortex. *Journal of Neuroscience, 152(4),* 970-981.

Petersen, C. C. H., Hahn, T. T. G., Mehta, M., Grinvald, A., & Sakmann, B. (2003). Interaction of sensory responses with spontaneous depolarization in layer 2/3 barrel cortex. *Proceedings of the National Academy of Sciences of the United States of America, 100 (23),* 13638-13643.

Pfeffer, C. K., Xue, M., He, M., Huang, Z .J., & Scanziani, M. (2013). Inhibition of inhibition in visual cortex: the logic of connections between molecularly distinct interneurons. *Nature Neuroscience, 16*, 1068–1076.

Pi, H-J., Hangya, B., Kvitsiani, D., Sanders, J. I., Huang, Z. J., & Kepecs, A. (2013). Cortical interneurons that specialize in disinhibitory control. *Nature, 503*, 521–524.

Pinto, L., & Dan, Y. (2015). Cell-type-specific activity in prefrontal cortex during goal-directed behaviour. *Neuron, 87*, 437–450.

Pisauro, M. A., Benucci, A., & Carandini, M. (2016). Local and global contributions to hemodynamic activity in mouse cortex. *Journal of Neurophysiology, 115 (6),* 2931-2936.

Pisauro, M. A., Dhruv, N. T., Carandini, M., & Benucci, A. (2013). Fast haemodynamic responses in the visual cortex of the awake mouse. *The Journal of Neuroscience, 33 (46),* 18343-18351.

Polack, P. O., Friedman, J., & Golshani, P. (2013). Cellular mechanisms of brain state-dependent gain modulation in visual cortex. *Nature Neuroscience, 16*, 1331–1339.

Poulet, J. F., & Petersen, C. C. (2008). Internal brain state regulates membrane potential synchrony in barrel cortex of behaving mice. *Nature, 454(7206),* 881-885.

Powers, W. J., Hirsch, I. B., & Cryer, P. E. (1996). Effect of stepped hypoglycaemia on regional cerebral blood flow response to physiological brain activation. *American Journal of Physiology, 270,* H554-H559.

Prakash, N., Biag, J. D., Sheth, S. A., Mitsuyama, S., Theriot, J., Ramachandra, C., & Toga, A. W. (2007). Temporal profiles and 2-dimensional oxy-, deoxy-, and total-haemoglobin somatosensory maps in rat versus mouse cortex. *Neuroimage, 37 Suppl 1,* S27-S36.

Purdon, P. L., Pavone, K. J., Akeju, O., Smith, A. C., Sampson, A. L., Lee, J., Zhou, D. W., Solt, K., & Brown, E. N. (2015). The Ageing Brain: Age-dependent changes in the electroencephalogram during propofol and sevoflurane general anaesthesia. *British Journal of Anaesthesia, 115,* 46-57.

Puro, D. G. (2007). Physiology and pathobiology of the pericyte-containing retinal microvasculature: new developments. *Microcirculation, 14,* 1-10.

Querido, J. S., & Sheel, A. W. (2007). Regulation of cerebral blood flow during exercise. *Sports Medicine, 37 (9),* 765-782.

Qiu, M., Ramani, R., Swetye, M., Rajeevan, N., & Constable, R. T. (2008). Anesthetic effects on regional CBF, BOLD, and the coupling between task-induced changes in CBF and BOLD: An fMRI study in normal human subjects. *Magnetic Resonance in Medicine, 60(4),* 987-996.

Raemaekers, M., Vink, M., van den Heuvel, M. P., Kahn, R. S., & Ramsey, N. F. (2006). Effects of aging on BOLD fMRI during prosaccades and antisaccades. *Journal of Cognitive Neuroscience, 18,* 594-603.

Ravassard, P., Kees, A., Willers, B., Ho, D., Aharoni, D., Cushman, J., Aghajan, Z. M., & Mehta, M. R. (2013). Multisensory control of hippocampal spatiotemporal selectivity. *Science, 340,* 1342-1346.

Reuss, S., Schaeffer, D. F., Laages, M. H., & Riemann, R. (2000). Evidence for increased nitric oxide production in the auditory brain stem of the aged dwarf hamster (Phodopus sungorus): an NADPH-diaphorase histochemical study. *Mechanisms of Ageing & Development, 112*, 125–134.

Ringach, D. L. (2009). Spontaneous and driven cortical activity: implications for computation. *Current Opinion in Neurobiology, 19(4)*, 439-444.

Risser, L., Plouraboue, F., Cloetens, P., & Fonta, C. (2009). A 3D-investigation shows that angiogenesis in primate cerebral cortex mainly occurs at capillary level. *International Journal of Developmental Neuroscience, 27*, 185–196.

Roche-Labarbe, N., Fenoglio, A., Radhakrishnan, H., Kocienski-Filip, M., Carp, S. A., Dubb, J., Boas, D. A., Grant, P. E., & Franceschini, M. A. (2014). Somatosensory evoked changes in cerebral oxygen consumption measured non-invasively in premature neonates*. NeuroImage, 85(1)*, 279-286.

Rosazza, C., & Minati, L. (2011). Resting-state brain networks: literature review and clinical applications. *Neurological Sciences, 32 (5),* 773-785.

Ross, M. H., Yurgelun-Todd, D. A., Renshaw, P. F., Maas, L. C., Mendelson, J. H., Mello, N. K., Cohen, B. M., & Levin, J. M. (1997). Age-related reduction in functional MRI response to photic stimulation. *Neurology. 48*, 173–176.

Rothwell, P. M., Coull, A. J., Silver, L. E., Fairhead, J. F., Giles, M. F., Lovelock, C. E., Redgrave, J. N., Bull, L. M., Welch, S. J., Cuthbertson, F. C., Binney, L. E., Gutnikov, S. A., Anslow, P., Banning, A. P., Mant, D., & Mehta, Z. (2005). Population-based study of event-rate, incidence, case fatality, and mortality for all acute vascular events in all arterial territories (Oxford Vascular Study). *Lancet, 366,* 1773-1783.

Roy, C. S., & Sherrington, C. S. (1890). On the regulation of the blood-supply of the brain. *The Journal of Physiology, 11*, 85-158.

Ruiz, O., Lustig, B. R., Nassi, J. J., Cetin, A., Reynolds, J. H., Albright, T. D., Callaway, E. M., Stoner, G. R., & Roe, A. W. (2013). Optogenetics through windows on the brain in the nonhuman primate. *Journal of Neurophysiology, 110(6)*, 1455–1467.

Sánchez-Zuriaga, D., Marti-Gutierrez, N., De La Cruz, M. A., & Peris-Sanchis, M. R. (2007). Age-related changes of NADPH-diaphorase-positive neurons in the rat inferior colliculus and auditory cortex. *Microscopy Research Techniques, 70,* 1051–1059.

Saleem, A. B., Ayaz, A., Jeffrey, K. J., Harris, K. D., & Carandini, M. (2013). Integration of visual motion and locomotion in mouse visual cortex. *Nature Neuroscience, 16*, 1864-1869.

Santisakultarm, T. P., Kersbergen, C. J., Bandy, D. K., Ide, D. C., Choi, S-H., & Silva, A. C. (2016). Two-photon imaging of cerebral hemodynamics and neural activity in awake and anesthetized marmosets. *Journal of Neuroscience Methods, 271,* 55-64.

Schapiro, M. B., Schmithorst, V. J., Wilke, M., Byars, A. W., Strawsburg, R. H., & Holland, S. K. (2004). BOLD-fMRI signal increases with age in selected brain regions in children. *Neuroreport, 15(17),* 2575–2578.

Schmidt, S., Redecker, C., Bruehl, C., & Witte, O. W. (2010). Age-related decline of functional inhibition in rat cortex. *Neurobiology of Aging, 31*, 504–511.

Schroeter, A., Schlegel, F., Seuwen, A., Grandjean, J. & Rudin, M. (2014). Specificity of stimulus-evoked fMRI responses in the mouse: the influence of systemic physiological

changes associated with innocuous stimulation under four different anesthetics. *NeuroImage, 94*, 372–384.

Schulte, M. L. & Hudetz, A. G. (2006). Functional hyperemic response in the rat visual cortex under halothane anesthesia. *Neuroscience Letters, 394*, 63–68.

Schummers, J., Yu, H., & Sur, M. (2008). Tuned responses of astrocytes and their influence on hemodynamic signals in the visual cortex. *Science, 320*, 1638–1643.

Schwarz, C., Hentschke, H., Butovas, S., Haiss, F., Stüttgen, M. C., Gerdjikov, T. V., ... & Waiblinger, C. (2010). The head-fixed behaving rat—procedures and pitfalls. *Somatosensory & Motor Research, 27(4),* 131-148.

Sebel, P. S., Ingram, D. A., Flynn, P, J., Rutherfoord, C. F., & Rogers, H. (1986). Evoked potentials during isoflurane anaesthesia. *British Journal of Anaesthesia, 58,* 580-585.

Seghier, M. L., Lazeyras, F., Zimine, S., Maier, S. E., Hanquinet, S., Delavelle, J., Volpe, J. J., & Huppi, P. S. (2004). Combination of event-related fMRI and diffusion tensor imaging in an infant with perinatal stroke*. NeuroImage. 21(1),* 463–472.

Seghier, M. L., Lazeyras, F., & Huppi, P.S. (2006). Functional MRI of the newborn. *Seminars in Fetal & Neonatal Medicine, 11*, 479–488.

Sharp, P. S., Shaw, K., Boorman, L., Harris, S., Kennerley, A. J., Azzouz, M., & Berwick, J. (2015). Comparison of stimulus-evoked cerebral haemodynamics in the awake mouse and under a novel anaesthetic regime. *Scientific Reports, 5,* 12621.

Shaw, P., Kabani, N. J., Lerch, J. P., Eckstrand, K., Lenroot, R., Gogtay, N., Greenstein, D., Clasen, L., Evans, A., Rapoport, J.L., Giedd, J. N., & Wise, S. P. (2008). Neurodevelopmental trajectories of the human cerebral cortex. *Journal of Neuroscience, 28*, 3586–3594.

Sheth, S., Nemoto, M., Guiou, M., Walker, M., Pouratian, N., Toga, A. W. (2003). Evaluation of coupling between optical intrinsic signals and neuronal activity in rat somatosensory cortex. *NeuroImage, 19 (3),* 884-894.

Shmuel, A., Yacoub, E., Pfeuffer, J., Van de Moortele, P. F., Adriany, G., Hu, X., & Ugurbil, K. (2002). Sustained negative BOLD, blood flow and oxygen consumption response and its coupling to the positive response in the human brain. *Neuron, 36*,1195–1210.

Shtoyerman, E., Arieli, A., Slovin, H., Vanzetta, I., & Grinvald, A. (2000). Long-term optical imaging and spectroscopy reveal mechanisms underlying the intrinsic signal and stability of cortical maps in V1 of behaving monkeys. *The Journal of Neuroscience, 20(21),* 8111-8121.

Shuler, M. G., & Bear, M. F. (2006). Reward timing in the primary visual cortex. *Science, 311,* 1606-1609.

Sicard, K., Shen, Q., Brevard, M. E., Sullivan, R., Ferris, C. F., King, J. A., & Duong, T. Q. (2003). Regional cerebral blood flow and BOLD responses in conscious and anesthetized rats under basal hypercapnic conditions: implications for functional MRI studies. *Journal of Cerebral Blood Flow & Metabolism, 23,* 472-481.

Sillito, A.M. (1975). The contribution of inhibitory mechanisms to the receptive field properties of neurones in the striate cortex of the cat. *Journal of Physiology, 250*, 305–329.

Silva, A. C., Lee, S. P., Iadecola, C., & Kim, S. G. (2000). Early temporal characteristics of cerebral blood flow and deoxyhaemoglobin changes during somatosensory stimulation. *Journal of Cerebral Blood Flow & Metabolism, 19,* 871-879.

Silver, L. M. (1995). *Mouse Genetics: concepts and applications.* Oxford University Press, Oxford.

Sippy, T., Lapray, D., Crochet, S., & Petersen, C. C. H. (2015). Cell-type-specific sensorimotor processing in striatal projection neurons during goal-directed behavior. *Neuron, 88*. 298-305.

Sirotin, Y. B., Hillman, E. M. C., Bordier, C., & Das, A. (2009). Spatiotemporal precision and haemodynamic mechanism of optical point spreads in alert primates. *PNAS, 106 (43),* 18390-18395.

Slack, R., Boorman, L., Patel, P., Harris, S., Bruyns-Haylett, M., Kennerley, A., ... & Berwick, J. (2016). A novel method for classifying cortical state to identify the accompanying changes in cerebral hemodynamics. *Journal of neuroscience methods, 267,* 21-34.

Slovin, H., Arieli, A., Hildesheim, R., & Grinvald, A. (2002). Long-term voltage-sensitive dye imaging reveals cortical dynamics in behaving monkeys. *Journal of Neurophysiology, 88,* 3421-3438.

Smear, M., Shustermann, R., O'Connor, R., Bozza, T., & Rinberg, D. (2011). Perception of sniff phase in mouse olfaction. *Nature, 479,* 397-400.

Sofroniew, N. J., Cohen, J. D., Lee, A. K., Svoboda, K. (2014). Natural Whisker-Guided Behaviour by Head-Fixed Mice in Tactile Virtual Reality. *The Journal of Neuroscience, 34(29)*, 9537-9550.

Sorond, F. A., Hurwitz, S., Salat, D. H., Greve, D. N., & Fisher, N. D. (2013). Neurovascular coupling, cerebral white matter integrity, and response to cocoa in older people. *Neurology, 81,* 904-909.

Sowell, E. R., Peterson, B. S., Thompson, P. M., Welcome, S. E., Henkenius, A. L., & Toga, A. W. (2003). Mapping cortical change across the human life span. *Nature Neuroscience, 6(3),* 309–15.

Spear, L. P., & Brake, S. C. (1983). Periadolescence: age-dependent behavior and psychopharmacological responsivity in rats. *Developmental Psychobiology, 16,* 83-109.

Stanley, E. M., Fadel, J. R., & Mott, D. D. (2012). Interneuron loss reduces dendritic inhibition and GABA release in hippocampus of aged rats. *Neurobiology of Aging, 33*, 431.e1–431.e13.

Stefanova, I., Stephan, T., Becker-Bense, S., Dera, T., Brandt, T., & Dieterich, M. (2013). Age-related changes of blood-oxygen-level-dependent signal dynamics during optokinetic stimulation. *Neurobiology of Ageing, 34,* 2277-2286.

Steriade, M. (2004). Acetylcholine systems and rhythmic activities during the waking–sleep cycle. *Progress in Brain Research, 145*, 179-196.

Stichel, C. C., Muller, C. M., & Zilles, K. (1991). Distribution of glial fibrillary acidic protein and vimentin immunoreactivity during rat visual cortex development. *Journal of Neurocytology, 20* , 97–108.

Strebel, S., Lam, A., Matta, B., Mayberg, T. S., Aaslid, R., & Newell, D. W. (1995). Dynamic and static cerebral autoregulation during isoflurane, desflurane, and propofol anesthesia. *The Journal of the American Society of Anesthesiologists, 83(1)*, 66-76.

Svoboda, K., & Yasuda, R. (2006). Principles of Two-Photon Excitation Microscopy and Its Applications to Neuroscience. *Neuron, 50(6),* 823-839.

Szymanski, F. D., Rabinowitz, N. C., Magri, C., Panzeri, S., & Schnupp, J. W. (2011). The laminar and temporal structure of stimulus information in the phase of field potentials of auditory cortex. *Journal of Neuroscience, 31*, 15787–15801.

Takata, N., Nagai, T., Ozawa, K., Oe, Y., Mikoshiba, K., & Hirase, H. (2013). Cerebral blood flow modulation by basal forebrain or whisker stimulation can occur independently of large cytosolic Ca2+ signaling in astrocytes. *PLoS One, 8*, e66525.

Takuwa, H., Autio, J., Nakayama, H., Matsuura, T., Obata, T., Okada, E., Masamoto, K., & Kanno, I. (2011). Reproducibility and variance of a stimulation-induced haemodynamic response in barrel cortex of awake behaving mice. *Brain Research, 1369*, 103-111.

Takuwa, H., Matsuura, T., Obata, T., Kawaguchi, H., Kanno, I., & Ito, H. (2012). Haemodynamic changes during somatosensory stimulation in awake and isoflurane-anaesthetised mice measured by laser Doppler flowmetry. *Brain Research, 1472*, 107-112.

Tamnes, C. K., Ostby, Y., Fjell, A. M., Westlye, L. T., Due-Tønnessen, P., & Walhovd, K. B. (2010). Brain maturation in adolescence and young adulthood: regional age-related changes in cortical thickness and white matter volume and microstructure. *Cerebral Cortex, 20*, 534–548.

Tarantini, S., Hertelendy, P., Tucsek, Z., Valcarcel-Ares, M. N., Smith, N., Menyhart, A., Farkas, E., Hodges, E. L., Towner, R., Deak, F., Sonntag, W. E., Csiszar, A., Ungvari, Z., & Toth, P. (2015). Pharmacologically-induced neurovascular uncoupling is associated with cognitive impairment in mice. *Journal of Cerebral Blood Flow & Metabolism, 35,* 1871–1881.

Tekes, A., Mohamed, M. A., Browner, N. M., Calhoun, V. D., & Yousem, D. M. (2005). Effect of age on visuomotor functional MR imaging. *Academic Radiology, 12*, 739–745.

Thévenaz, P., Ruttimann, U. E., & Unser, M. (1998). A pyramid approach to subpixel registration based on intensity. *IEEE Trans Image Process, 7,* 27-41.

Thompson, T., Steffert, T., Ros, T., Leach, J., & Gruzelier, J. (2008). *EEG applications for sport and performance. Methods, 45*, 279-88.

Tieman, S. B., Mollers, S., Tieman, D. G., & White, J. (2004). The blood supply of the cat's visual cortex and its postnatal development. *Brain Research, 998*, 100–112.

Topcuoglu, M. A., Aydin, H., & Saka, E. (2009). Occipital cortex activation studied with simultaneous recordings of functional transcranial Doppler ultrasound (fTCD) and visual evoked potential (VEP) in cognitively normal human subjects: effect of healthy ageing. *Neuroscience Letters, 452,* 17-22.

Toth, P., Tarantini, S., Tucsek, Z., Ashpole, N. M., Sosnowska, D., Gautam, T., Ballabh, P., Koller, A., Sonntag, W. E., Csiszar, A., & Ungvari, Z. I. (2014a). Resveratrol treatment rescues neurovascular coupling in aged mice: role of improved cerebromicrovascular endothelial function and down-regulation of NADPH oxidase. *American Journal of Heart & Circulatory Physiology, 306,* H299-H308.

Toth, P., Tucsek, Z., Tarantini, S., Sosnowska, D., Gautam, T., Mitschelen, M., Koller, A., Sonntag, W., Csiszar, A., & Ungvari, Z. (2014b). IGF-1 Deficiency Impairs Cerebral Myogenic Autoregulation in Hypertensive Mice. *Journal of Cerebral Blood Flow & Metabolism, 34(12),* 1887-1897.

Toth, P., Tarantini, S., Ashpole, N. M., Tucsek, Z., Milne, G. L., Valcarcel-Ares, N. M., Menyhart, A., Farkas, E., Sonntag, W. E., Csiszar, A., & Ungvari, Z. (2015a). IGF-1 deficiency impairs neurovascular coupling implications for cerebromicrovascular ageing. *Ageing Cell, 14,* 1034-1044.

Toth, P., Tarantini, S., Davila, A., Valcarcel-Ares, M. N., Tucsek, Z., Varamini, B., Ballabh, P., Sonntag, W. E., Baur, W. E., Baur, J. A., Csiszar, A., & Ungvari, Z. (2015b). Purinergic glio-endothelial coupling during neuronal activity: role of $P2Y_1$ receptors and eNOS in functional hyperemia in the mouse somatosensory cortex. *American Journal of Physiology, 309(11),* 1837-1845.

Tucsek, Z., Toth, P., Tarantini, S., Sosnowska, D., Gautam, T., Warrington, J. P., Giles, C. B., Wren, J. D., Koller, A., Ballabh, P., Sonntag, W. E., Ungvari, Z., & Csiszar, A. (2014). Aging Exacerbates Obesity-induced Cerebromicrovascular Rarefaction, Neurovascular Uncoupling, and Cognitive Decline in Mice. *The Journal of Gerontology, 71(9),* 1-14.

Ureshi, M., Matsuura, T., & Kanno, I. (2004). Stimulus frequency dependence of the linear relationship between local cerebral blood flow and field potential evoked by activation of rat somatosensory cortex. *Neuroscience Research, 48 (2),* 147-153.

van den Heuvel, M. P., & Hulshoff Pol, H. E. (2010). Exploring the brain network: A review on resting-state fMRI functional connectivity. *European Neuropsychopharmacology, 20 (8),* 519-534.

van den Pol, A. N., Romano, C., & Ghosh, P. (1995). Metabotropic glutamate receptor mGluR5 subcellular distribution and developmental expression in hypothalamus. *Journal of Comparative Neurology, 362*, 134–150.

Van der Zee, P., 1992. “Measurement and modelling of the optical properties of human tissue in the near infrared”. Ph.D Thesis, UCL, 218–221.

Van Hemelrijck, J., Verhaegen, M., & Van Aken, H. (1993). Cerebral effects of inhalational anaesthetics. *Baillière's clinical anaesthesiology, 7(4)*, 1035-1055.

Vanhatalo, S., & Lauronen, L. (2006). Neonatal SEP - back to bedside with basic science. *Seminars in Fetal & Neonatal Medicine, 11*, 464–470.

Vansetta, I., & Grinvald, A. (2008). Coupling between neuronal activity and microcirculation: implications for functional brain imaging. *Human Frontier Science Program Journal, 2,* 79-98.

Vaucher, E., & Hamel, E. (1995). Cholinergic basal forebrain neurons project to cortical microvessels in the rat: electron microscopic study with anterogradely transported *Phaseolus vulgaris* leucogglutinin and choline acetyltransferase immunocytochemistry. *Journal of Neuroscience, 15*, 7427-7441.

Vinck, M., Batista-Brito, R., Knoblich, U., & Cardin, J. A. (2015). Arousal and locomotion make distinct contributions to cortical activity patterns and visual encoding. *Neuron, 86 (3),* 740-754.

Volterra, A., & Meldolesi, J. (2005). Astrocytes, from brain glue to communication elements: the revolution continues. *Nature Reviews Neuroscience, 6,* 626-640.

Wang, X., Lou, N., Xu, Q., Tian, G. F., Peng, W. G., Han, X., et al. (2006). Astrocytic Ca2+ signaling evoked by sensory stimulation in vivo. *Nature Neuroscience, 9,* 816–823.

Wang, X., Takano, T., & Nedergaard, M. (2009). Astrocytic Calcium Signaling: Mechanism and Implications for Functional Brain Imaging. *Methods in Molecular Biology, 489, I93-109.*

Weber, B., Keller, A. L., Reichold, J., & Logothetis, N. K. (2008). The microvascular system of the striate and extrastriate visual cortex of the macaque. *Cerebral Cortex, 18*, 2318–2330.

West, R., & Covell, E. (2001). Effects of ageing on event-related neural activity related to prospective memory. *Neuroreport, 12(13),* 2855-2858.

Wester, J. C., & McBain, C. J. (2014). Behavioral state-dependent modulation of distinct interneuron subtypes and consequences for circuit function. *Current Opinion in Neurobiology, 29,* 118-125.

Woolsey, T. A., Welker, C., & Schwartz, R. H. (1975). Comparative anatomical studies of the Sml face cortex with special reference to the occurrence of “barrels” in layer IV. *Journal of Comparative Neurology, 164 (1)*, 79–94.

Xing, D., Yeh, C. I., Burns, S., & Shapley, R. M. (2012). Laminar analysis of visually evoked activity in the primary visual cortex. *Proceedings of the National Academy of Science USA, 109,* 13871–13876.

Yamada, H., Sadato, N., Konishi, Y., Kimura, K., Tanaka, M., Yonekura, Y., & Ishii, Y. (1997). A rapid brain metabolic change in infants detected by fMRI. *Neuroreport, 8,* 3775-3778.

Yamada, H., Sadato, N., Konishi, Y., Muramoto, S., Kimura, K., Tanaka, M., Yonekura, Y., Ishii, Y., & Itoh, H. (2000). A milestone for normal development of the infantile brain detected by functional MRI*. Neurology, 55(2),* 218–223.

Yamaguchi, T., Kanno, I., Uemura, K., Shishido, F., Inugami, A., Ogawa, T., Murakami, M., & Suzuki, K. (1986). Reduction in regional cerebral metabolic rate of oxygen during human aging. *Stroke. 17*, 1220–1228.

Zaletel, M., Strucl, M., Pretnar-Oblak, J., & Zvan, B. (2005). Age-related changes in the relationship between visual evoked potentials and visually evoked cerebral blood flow velocity response. *Functional Neurology, 20,* 115-120.

Zehendner, C. M., Tsohataridis, S., Luhmann, H. J., & Yang, J. W. (2013). Developmental Switch in Neurovascular Coupling in the Immature Rodent Barrel Cortex. *PLoS ONE, 8(11)*, e80749.

Zhang, S., & Murphy, T. H. (2007). Imaging the impact of cortical microcirculation on synaptic structure and sensory-evoked haemodynamic responses in vivo. PLoS Biology, 5 (5), e119, doi:10.1371/journal.pbio.0050119.

Zheng, Y., Luo, J. J., Harris, S., Kennerley, A., Berwick, J., Billings, S. A., & Mayhew, J. (2012). Balanced excitation and inhibition: Model based analysis of local field potentials. *NeuroImage, 63(1),* 81-94.

Ziv, Y., Burns, L. D., Cocker, E. D., Hamel, E. O., Ghosh, K. K., Kitch, L. J., Gamal, A. E., & Schnitzer, M. J. (2013). Long-term dynamics of CA1 hippocampal place codes. *Nature Neuroscience, 16(3),* 264-266.

Zlokovic, B. V. (2011). Neurovascular pathways to neurodegeneration in Alzheimer's disease and other disorders. *Nature Reviews Neuroscience, 12(12)*, 723-738.

Zonta, M., et al. (2003). Neuron-to-astrocyte signalling is central to the dynamic control of brain microcirculation. *Nature Neuroscience, 6,* 43-50.